

THE EFFECT OF SPEED OF COMPRESSION  
ON THE PROPERTIES OF COMPACTS

BY

SIMON DAVID BATEMAN BSc., MRPharmS.

A thesis submitted to the Council  
for National Academic Awards in  
partial fulfilment of the  
requirements for the degree of  
DOCTOR OF PHILOSOPHY.

October 1988

School of Pharmacy  
Liverpool Polytechnic

THE FOLLOWING MATERIAL HAS NOT BEEN DIGITISED AT THE REQUEST OF THE AWARDING UNIVERSITY;

ARTICLES IN THE REAR COVER

TO

MELANIE

For her continual support,  
understanding and encouragement.

## ACKNOWLEDGEMENTS

My thanks are due to the following:

Dr P. Smeaton for assistance with and tuition of machine code programming and for writing the data transfer routines.

Dr D. Clegg for writing the fortran data analysis program.

Mr N. Solomans and Mr M. Hill of E.S.H. Testing LTD for technical advice, and assistance with mechanical, hydraulic and electrical engineering regarding the Compression Simulator.

The Liverpool Polytechnic Mechanical Engineering Department for helpful advice and use of their facilities.

The Liverpool Polytechnic Computer Services Department for guidance on data transfer.

Mrs A. Simpson for technical assistance.

Mr P. Drew and The Boots Co PLC for kindly supplying samples of an ibuprofen and paracetamol granulation for use in this investigation.

De Melkindustrie Veghel bv for the gift of DCL-30 lactose

I am grateful for the guidance and encouragement given to me by my supervisors Prof.M.H.Rubinstein of Liverpool School of Pharmacy, and Dr P. Wright of Fisons Pharmaceutical Division.

## ABSTRACT

### The Effect of Speed of Compression on The Properties of Compacts

Simon David Bateman

A high speed hydraulic press has been developed into a computer controlled high speed compression Simulator, capable of reproducing displacement time profiles seen on any production tableting machine. The system has been validated to monitor punch displacements to  $\pm 12\mu\text{m}$  and loads to  $\pm 0.05\%$  of full scale. Confidence in the results obtained using the Simulator were enhanced by comparison with other operational Simulators. The established Simulator was then used to investigate the effects of compression on ibuprofen.

Ibuprofen was found to consolidate mainly by plastic deformation with a lesser contribution from the melting of asperities. A significant amount of pressure induced melting and subsequent fusion bonding occurred at higher pressures. Ibuprofen was found to be sensitive to the magnitude and rate of application of the compression pressure. The extent of plastic flow exhibited by ibuprofen during compression was found to decrease as the compression speed increased. Lamination and capping of ibuprofen compacts at high compression speeds was considered to be due to a combination of air entrapment and the inability of the compact to withstand the stresses of decompression.

When ibuprofen was mixed with a second material and compressed, the consolidation mechanism and properties of the compacts formed were found to follow complex relationships. The relationships were dependant on the proportion of each material and the speed of compression. For ibuprofen microcrystalline cellulose mixtures positive interactions were considered to occur due to bonding between the two materials. For ibuprofen and lactose mixtures the interactions observed were considered to be a balance between the plastic deformation by the ibuprofen relieving the applied load preventing the critical force required for fracture of the lactose being attained, and the lactose fragments bearing the applied load reducing plastic flow by ibuprofen.

The Simulator was then employed to investigate different aspects of tableting machine design. A simple ibuprofen microcrystalline cellulose mixture and a commercial ibuprofen formulation were compressed to a constant load and then to a constant thickness and the properties of the compacts compared. Tablets prepared under a constant maximum applied load, with fill weights varied over the B.P uniformity of weight limits, had relatively constant disintegration times and radial tensile strengths. This was considered an advantage over the tablets prepared to a constant thickness which showed considerable variation under the same conditions.

The second aspect of tableting machine design to be investigated was the use of relatively high precompression pressures using a commercially available paracetamol granulation. The maximum compression pressure exerted during the tableting cycle was found to be the major factor contributing to the tensile strength of the tablets. The use of a second compression either before or after the main compression was found to produce a significant increase in tablet tensile strength. The greater the magnitude of the second compression, the greater its effect on tensile strength. The contribution of a second compression towards the tablet tensile strength was attributed to the effective increase in dwell time it generated. The orientation of the greater and lesser compression pressures during tableting was found to influence the tablet tensile strength. Stronger tablets resulted if the greater pressure was exerted first. This was considered to be a function of temperature increases within the tablet and the disruptive effects of the second compression.

## INDEX

	Page Number
Title page	i
Dedication	ii
Acknowledgments	iii
Abstract	iv
Index	v
List of figures	ix
List of Tables	xiii
1. Introduction	
1.1 Compression and Consolidation of Powders	1
1.1.1 The Compaction Process	1
1.1.2 Die Filling	2
1.1.3 Transitional Rearrangement	4
1.1.4 Deformation	5
1.1.5 The Elastic Effect	6
1.1.6 The Plastic Effect	7
1.1.7 The Brittle Effect	9
1.1.8 Bonding	12
1.1.9 Recovery	16
1.2 Interpretation of Compaction Data	20
1.2.1 Energy Involved in Compaction	20
1.2.2 Stress relaxation	23
1.2.3 Radial Versus Axial Compaction Cycles	24
1.2.4 Force Volume Relationships	26
1.3 Post Compression Assessments	31
1.3.1 Tablet Strength	31
1.3.2 Friability	34
1.3.3 Disintegration and Dissolution	34

1.4	Factors Effecting Compaction	35
1.4.1	Material Properties	35
1.4.2	Crystal Form	36
1.4.3	Particle Size	37
1.4.4	Particle Shape	40
1.4.5	Effect of Moisture	41
1.5	Environmental Factors	43
1.5.1	Humidity	43
1.5.2	Temperature	44
1.6	Machine Variables	45
1.6.1	Compression Force	46
1.6.2	Precompression	48
1.6.3	Tooling	49
1.6.4	Time Displacement Profiles	51
1.6.5	Speed of Compression	52
1.7	Investigative Equipment	57
1.7.1	Instrumented Single Punch Machines	57
1.7.2	Instrumented Rotary Machines	58
1.7.3	Physical Testing Machines	58
1.7.4	Compression Simulators	59
1.8	Conclusions	60
2.1	The High Speed Hydraulic Press	62
2.1.1	The Load Frame	62
2.1.2	The Hydraulic Power Supply	62
2.1.3	The Electronic Console	66
2.1.4	Displacement Closed Loop Feed-Back Method of Actuator Control	68
2.2	Commissioning	72
2.2.1	Design and Installation of the Die Holder and Measurement LVDTs	72

2.2.2	Alignment of the Actuators	74
2.2.3	Static Control and Response Optimisation	75
2.2.4	Microcomputer Control of the Press	76
2.2.5	Acquisition and Transfer of Data	80
2.3	Validation	83
2.3.1	Measurement of Displacement	
	Remote Calibration of the $\pm 10\text{mm}$ Measurement LVDTs	83
2.3.2	Insitu Calibration of the $\pm 10\text{mm}$ LVDTs	84
2.3.3	Calibration of the $\pm 25\text{mm}$ Control LVDTs	90
2.3.4	Measurement of Applied Load	92
2.3.5	Load Calibration of the Transient Recorder	95
2.3.6	Determination of the Punch and Load Frame Distortion	96
2.4	Computers and Software	99
2.4.1	Microcomputer control of the High Speed Press	99
2.4.2	Calibration of the Digital to Analogue Card Output	102
2.4.3	Validation of the Transfer of Data From the Transient Recorder to the Apple IIe and to the Dec 20 Mainframe	103
2.4.4	Software to be used for Analysis of Compaction Data	106
2.4.5	The High Speed Compression Simulator	115
3	Materials and Methods	118
3.1	Materials	118
3.2	Characterisation of Materials	122
3.2.1	True Density Determinations	122
3.2.2	Moisture Content Determination	125
3.2.3	Particle Size Analysis	126
3.2.4	Alpine Air Jet Sieving to Obtain Size Fractions of Powders	130
3.2.5	Electron Microscopy of Materials	131
3.2.6	Measurement and Pretreatment of Tooling	132

3.3	Preparation of Compacts	140
3.4	Characterisation of Compacts	141
3.4.1	Radial Tensile Strength	141
3.4.2	Disintegration Test	143
3.4.3	Electron Microscopy of Compacts	143
4.1	A Comparative Investigation of Compression Simulators	144
5.1	The Effect of Speed of Compression on Ibuprofen	151
5.1.1	The Effect of Pressure	156
5.1.2	The Effect of Speed	162
6.1	The Effect of speed of Compression on Ibuprofen, Avicel and Lactose Mixtures	175
6.1.1	The Effect of speed of Compression on Ibuprofen, Avicel Mixtures	182
6.1.2	The Effect of speed of Compression on Ibuprofen, Lactose Mixtures	200
7.1	Investigation of Compact Properties Prepared by Compression to Constant Thickness and to Constant load	215
8	Pre-compression	244
8.1	Investigation of Compact Properties Prepared Using Combinations of Pre-compression and Main-compression.	244
9.1	Conclusions	267
10.1	Recommendations For Future Work.	271
	References	272
	Appendix	280

## List of Figures

Figure Number	Title	Page Number
1.1a	Typical Force Displacement Curve for a First Compression.	21
1.1b	Typical Force Displacement Curve for a Recompression.	21
1.2a	Pressure Cycle for a Perfect Elastic Body.	25
1.2b	Pressure Cycle for a Body with Constant Yield Stress in Shear.	25
1.2c	Pressure Cycle for a Mohr's Body.	25
1.2d	Schematic Representation of the Heckel Equation.	28
1.2e	Heckel Plot for Type A Behaviour.	29
1.2f	Heckel Plot for Type B Behaviour.	29
1.2g	Heckel Plot for Type C Behaviour.	29
2.1a	Diagrammatic Representation of The High Speed Hydraulic Press.	63
2.1b	The Load Frame.	64
2.1c	The Hydraulic Power Supply.	65
2.1d	The Electronic Control Console and Microcomputer.	65
2.1e	Servo valve in the Closed Loop Configuration.	69
2.1f	Cross Section Through a Servo valve.	69
2.2a	Upper Load cell, Die and LVDT Support with Guide Rail.	73
2.2b	Lower Load cell, Spacer Ring and LVDT Support.	73
2.2c	Displacement/Time Traces For the Upper and Lower Actuators.	77
2.2d	Differential Displacement Potential Divider.	82
2.2e	Mean Punch Force Circuit.	82
2.3a	Non Linearity of The Upper and Lower 10mm LVDTs Before Optimisation	85
2.3b	Non Linearity of The Upper and Lower 10mm LVDTs After Optimisation	86
2.3c	Upper and Lower $\pm 10$ mm LVDT Displacement Ranges	87
2.3d	Non Linearity of The 10mm LVDT Punch Separation System	89

Figure Number	Title	Page Number
2.3e	Non Linearity of The Upper and Lower 25mm Displacement Control LVDTs	91
2.3f	Distortion During Loading and Unloading	98
2.4a	Manesty "F" Machine Displacement Profile	100
2.4b	The 6522 Parallel Interface Used to Down Load Data	104
2.4c	Force Displacement Model	106
2.4d,e,f	Triangular Force Displacement Models Atest1-3	108-110
2.4g,h,i	Force Displacement Model Atest4-6	112-114
2.4j	Diagrammatic Representation of the Simulator	117
3.2a	Particle Size Range Distribution for Ibuprofen as Determined Using the Coulter Counter	129
3.2b	SEM at Magnification X35 of Ibuprofen Crystals	133
3.2c	SEM at Magnification X1000 of Ibuprofen Crystals	133
3.2d	SEM at Magnification X100 of Ibuprofen Granulation	134
3.2e	SEM at Magnification X500 of Ibuprofen Granulation	134
3.2f	SEM at Magnification X35 of Paracetamol Granulation	135
3.2g	SEM at Magnification X500 of Paracetamol Granulation	135
3.2h	SEM at Magnification X100 of Microcrystalline Cellulose	136
3.2i	SEM at Magnification X500 of Microcrystalline Cellulose	136
3.2j	SEM at Magnification X100 of $\alpha$ -Anhydrous Lactose DCL-30	137
3.2k	SEM at Magnification X500 of $\alpha$ -Anhydrous Lactose DCL-30	137
3.2l	SEM at Magnification X500 of Magnesium Stearate	138
3.4	Instron Testing Machine Fitted with the Instrumented Upper Punch Connected to the Transient Recorder	142
4.1a	Heckel Plot of Tabletose from the Liverpool Polytechnic Compaction Simulator	146
5.1a	Pressure-Time Profile for a Rotary Machine	152
5.1b	Scanning Electron Micrograph of Ibuprofen Compact Upper Punch Contact Surface Compressed @22mm/s 400MPa	157
5.1c	Heckel Plot of Ibuprofen Compressed to High Pressure at Slow Speed	161
5.1d	Scanning Electron Micrograph of Ibuprofen Fractured Compact Edge Compressed @22mm/s 400MPa	157

Figure Number	Title	Page Number
5.1e	Ibuprofen Compact Compressed at 22mm/s up to 60MPa	163
5.1f	Ibuprofen Compact Compressed at 144mm/s up to 60MPa	163
5.1g	Ibuprofen Compact Compressed at 647mm/s up to 60MPa	164
5.1h	Ibuprofen Compact Compressed at 1123mm/s up to 60MPa	164
5.1i	Scanning Electron Micrograph of Ibuprofen Compact Upper Punch Contact Surface Compressed @22mm/s 60MPa	165
5.1j	Scanning Electron Micrograph of Ibuprofen Fractured Compact Edge Compressed @22mm/s 60MPa	165
5.1k	Scanning Electron Micrograph of Ibuprofen Fractured Compact Edge Compressed @1123mm/s 60MPa	166
5.1l	Tensile Strength of Ibuprofen Compacts Compressed at Increasing Speeds	168
5.1m	The Effect of Compression Speed on the Mean Yield Pressure of Ibuprofen	171
5.1n	Extent of Particle Rearrangement Db Versus Compression Speed for Ibuprofen	173
6.1a	The Effect of Compression Speed on the Mean Yield Pressure of Ibuprofen/Avicel Mixtures	190
6.1b	The Effect of Compression Speed on the Extent of Particle Rearrangement for Ibuprofen Avicel Mixtures	192
6.1c	The Effect of Compression Speed on the Tablet Tensile Strength for Ibuprofen/Avicel Mixtures	194
6.1d	The Effect of Compression Speed on the Net Energy of Ibuprofen/Avicel Mixtures	195
6.1e	The Effect of Compression Speed on the Elastic Recovery of Ibuprofen/Avicel Mixtures	197
6.1f	The Effect of Compression Speed on the Mean Yield Pressure of Ibuprofen/Lactose Mixtures	207
6.1g	The Effect of Compression Speed on the Extent of Particle Rearrangement for Ibuprofen Lactose Mixtures	208
6.1h	The Effect of Compression Speed on the Tablet Tensile Strength for Ibuprofen/Lactose Mixtures	210
6.1i	The Effect of Compression Speed on the Elastic Recovery of Ibuprofen/Lactose Mixtures	211
6.1j	The Effect of Compression Speed on the Net Energy of Ibuprofen/Lactose Mixtures	212

Figure Number	Title	Page Number
7.1a	Graph of Applied Force Versus Tablet Weight for an Ibuprofen Granulation Compressed to a Constant Thickness and a Constant Force	225
7.1b	Graph of Applied Force Versus Tablet Weight for an Ibuprofen Avicel 1:1 Mixture Compressed to a Constant Thickness and a Constant Force	226
7.1c	Graph of Tablet Weight Versus Tablet Weight for an Ibuprofen Granulation Compressed to a Constant Thickness and to a Constant Force	228
7.1d	Graph of Tablet Thickness Versus Tablet Weight for an Ibuprofen Avicel 1:1 Mixture Compressed to a Constant Thickness and to a Constant Force	229
7.1e	Graph of Radial Tensile Strength Versus Tablet Weight for an Ibuprofen Granulation Compressed to Constant Thickness and a Constant Force	231
7.1f	Graph of Radial Tensile Strength Versus Tablet Weight for an Ibuprofen Avicel Mixture Compressed to a Constant Thickness and to a Constant Force	233
7.1g	Scanning Electron Micrograph of Ibuprofen Avicel Mixture 1:1	234
7.1h	Scanning Electron Micrograph of Ibuprofen Avicel Mixture 1:1 Upper Punch Contact Surface	234
7.1i	Graph of Disintegration Time Versus Tablet Weight for an Ibuprofen Avicel 1:1 Mixture Compressed to Constant Thickness and to a Constant Force	237
7.1j	Graph of Disintegration Time Versus Tablet Weight for an Ibuprofen Granulation Compressed to Constant Thickness and to a Constant Force	238
8.1a	Simulator Control Profile for Pre and Main-compression	247
8.1b	Radial Tensile Strength Versus Main-compression Pressure For a Paracetamol Formulation	256
8.1c	Radial Tensile Strength Versus Compression Pressure for a Paracetamol Formulation with a Single and Double Compression	258
8.1d	Radial Tensile Strength Versus Maximum Compression Pressure for a Paracetamol Formulation	261
8.1e	Radial Tensile Strength Versus Main-compression Pressure for a Paracetamol Formulation with Varying Pre-compression Pressure	262
8.1f	Radial Tensile Strength for a Paracetamol Formulation Prepared with varying Pre and Main-compression Pressures	264

List of Tables

Table Number	Title	Page Number
2.3a	Displacement Error for the $\pm 10$ mm Measurement LVDTs	84
2.3b	Transient Recorder Displacement Data Output Calibrations	88
2.3c	Calibration of the Upper and Lower Load Cell Outputs Via the Servogor Plotter	93
2.3d	Loading and Unloading Calibrations For the Upper Load Cell Using a Pre-calibrated Test Load Cell	94
2.3e	Transient Recorder Load Data Output Calibrations	95
2.3f	Distortion of the Hydraulic Press	97
2.4a	Cycle Times and Displacements for the Actual and Control "F" Machine Profiles Executed at Variable Output Rates	101
2.4b	Area Under the Compression and Decompression Curves for Profiles Atest1-3 Derived by Manual Calculation and Using the Energy Program	111
2.4c	Area Under the Compression and Decompression Curves for Profiles Atest4-6 Derived by Manual Calculation and Using the Energy Program	111
3.2a	Typical Calibration Values for the Small and Large Stainless Steel Spheres	123
3.2b	True Densities of Powders as Determined Using the Beckman 930 Air Comparison Pycnometer	124
3.2c	Percentage Moisture Contents of Materials	125
3.2d	Powder Size Fraction Distributions Determined Using the Alpine Air Jet Sieve	131
3.2e	Dimensions of the 12.5mm Flat Faced Tooling	139
4.1a	High Speed Compression Simulator Specifications	144
4.1b	Heckel Analysis Results	147
4.1c	SK&F Mean Yield Pressure Analysis Before and After Correction for Distortion	149
5.1a	Heckel Analysis for Ibuprofen Compressed Between 22mm/s and 1700mm/s	170
6.1a	Ibuprofen Avicel Mixtures Compressed at 25mm/s Showing the Elastic Recovery, Heckel Parameters, Tablet Tensile Strength and the Net Energy of Compression	182
6.1b	Ibuprofen Avicel Mixtures Compressed at 380mm/s Showing the Elastic Recovery, Heckel Parameters, Tablet Tensile Strength and the Net Energy of Compression	183

Table Number	Title	Page Number
6.1c	Ibuprofen Avicel Mixtures Compressed at 1100mm/s Showing the Elastic Recovery, Heckel Parameters, Tablet Tensile Strength and the Net Energy of Compression	184
6.1d	Ibuprofen Lactose Mixtures Compressed at 25mm/s Showing the Elastic Recovery, Heckel Parameters, Tablet Tensile Strength and the Net Energy of Compression	200
6.1e	Ibuprofen Lactose Mixtures Compressed at 380mm/s Showing the Elastic Recovery, Heckel Parameters, Tablet Tensile Strength and the Net Energy of Compression	201
6.1f	Ibuprofen Lactose Mixtures Compressed at 1100mm/s Showing the Elastic Recovery, Heckel Parameters, Tablet Tensile Strength and the Net Energy of Compression	202
7.1a	B.P Uniformity of Tablet Weight	217
7.1b	The Maximum Force, Minimum Punch Separation, Disintegration Time and Tensile Strength for Tablets Prepared from an Ibuprofen Granulation Compressed to a Constant Force	220
7.1c	The Maximum Force, Minimum Punch Separation, Disintegration Time and Tensile Strength for Tablets Prepared from an Ibuprofen Granulation Compressed to a Constant Thickness	221
7.1d	The Maximum Force, Minimum Punch Separation, Disintegration Time and Tensile Strength for Tablets Prepared from an Ibuprofen Avicel Mixture Compressed to a Constant Force	222
7.1b	The Maximum Force, Minimum Punch Separation, Disintegration Time and Tensile Strength for Tablets Prepared from an Ibuprofen Avicel Mixture Compressed to a Constant Thickness	223
8.1a-f	Pre and Main-compression Pressures and Contact Times for a Paracetamol Formulation	249-254

## 1. INTRODUCTION

### 1.1 Compression and Consolidation of Powders

A powder is a solid-gas system composed of individual particles randomly interspersed with air spaces. In the case of pharmaceutical powders the particles are of varying sizes and shapes. These complex systems are difficult to characterise in terms of fundamental properties. The behaviour of the bulk powder and the individual particles are of importance when investigating any aspect of tableting.

A tablet may be formed by the compression of a powder mass between two punches within the confines of a die into a single coherent unit. The ability of a powder to decrease in volume under an applied pressure is its compressibility, which occurs as a result of displacement of the gaseous phase. Coincidental with this process is consolidation which is an increase in the mechanical strength of the material resulting from particle-particle interactions. Hence the compaction of a powder is the compression and consolidation of a powder into a tablet of specified strength.

#### 1.1.1 The Compaction Process

The compaction process was initially defined in three stages with reference to metal powders by Seelig and Wulff (1946) i) packing of particles ii) elastic and plastic deformation iii) cold working and fragmentation. The same stages occur using pharmaceutical powders and have been extended and subdivided by many workers, these stages may be summarised as follows:-

1. Transitional Repacking: Under low pressure the particles flow with respect to each other, the smaller particles filling the voids between the larger particles. The density of the powder bed is increased.

2. Deformation at Points of Contact: As the applied pressure increases deformation occurs. The type of deformation will be characteristic of the material being compressed. Both elastic and plastic deformation may take place increasing the contact area and forming potential bonding areas.

3. Fragmentation: Under higher pressure the deformed particles may fragment, generating fresh clean surfaces that are potential bonding areas. The fragments will infiltrate the remaining voids to further increase the densification.

4. Bonding: Under pressure the new surfaces formed by deformation and or fragmentation will make contact with other surfaces. Intermolecular interactions may then take place at the points of contact.

5. Deformation of the Solid Body: Further increasing the applied pressure consolidates the bonded solid by plastic and or elastic deformation.

6. Ejection: Removal of the upper punch relieves the axial pressure on the compact but a radial pressure due to the die remains. This allows the elastic axial recovery of the compact to take place. The compact is then ejected and the radial die wall pressure removed. This permits lateral elastic recovery. During this stage the compact volume increases.

Some of the research concerning these and further stages of compaction , which are of importance in the tableting event will be discussed below.

#### 1.1.2 Die Filling

The first factor with an influence on the compaction event is the actual filling of the die. In a single punch tableting machine the die is filled by passing a feed shoe containing the powder over the die space. This method relies on gravity to form a uniform powder bed. For

multi-station rotary tableting machines which operate at higher speeds, a feed frame spreads the powder over a large area to provide time for the dies to fill. In many rotary tableting machines the speed of the die table is such that the time of a die under the feed frame is too short to allow consistent gravity filling of the die. This, combined with the effects of centripetal force may result in improper filling of the die. Consequently mechanised feeders have been developed to force the powder into the die.

Ridgway-Watt (1981) employed Holographic Interferometry to study tablet relaxation. The die was filled with Avicel in normal, conical, and wedge shaped packings which were then compressed. The resulting tablets showed surface movements reflecting the initial packing shape. Wedge shaped packings have been demonstrated to occur in rotary presses through the combined action of the feed mechanism and centripetal force. Conical packing may occur when manually filling the die of an Instron press often used in research. Packing of the die has been shown to have a significant effect on the resulting tablet and thus is an important consideration in compression experimental design.

The initial porosity of the powder bed is determined by the shape, size distribution, and surface characteristics of particles and the manner in which they are deposited. Kolbuszewski (1950) studying sands found, that a low velocity of fall leads to a high porosity, irrespective of deposition intensity. A high velocity of fall was found to produce low porosity at low deposition intensities, but higher porosity at higher intensities.

Woodhead and Newton (1983) assessed the variability of porosity within a powder bed using a  $\gamma$ -Ray attenuation technique. It was demonstrated that both the overall porosity and the local porosity were dependant on particle properties and deposition method. The most uniform bed was produced by the deposition of multiple even layers. In

many cases the central areas were found to have the lowest porosity. Woodhead, Chapman and Newton (1983) extended this study to include the effects of vibration. Vertical vibration was found significantly more effective than horizontal vibration in terms of the degree of consolidation achieved. An optimum frequency and amplitude range was identified and shown to be dependant on particle size. Vibration in both planes would be expected to be present on a tableting machine and will have an effect on the powder bed prior to compression. The porosity of the initial powder bed has an effect on the properties of the compact and will be discussed later.

The effect of initial bulk density on the compression behaviour of lactose and sodium chloride was investigated by Sheikh-Salem and Fell (1981). Tight (tapped) and loose (non-tapped) packings of these materials were prepared and compressed. Compression data obtained were subjected to analysis by the equations of Kawakita (1956), Heckel (1961a,b), and Cooper & Eaton (1962). The Heckel constants K and A (see later) were found to be independent of initial packing. This would tend to indicate that if it is difficult to control the initial die packing then Heckel analysis should be used.

### 1.1.3 Transitional Rearrangement

De Blaey (1972) using an instrumented tableting machine indicated that for unlubricated powder samples, force transmission to the lower punch remained at zero until a certain value of applied pressure had been exceeded. This suggests that the applied pressure is initially used to overcome interparticular friction and cohesion. The magnitude of the pressure required to cause sliding, and thereby slippage and rearrangement will depend on the particle size, shape and surface characteristics. York (1978) showed that the degree of particle rearrangement taking place during compression increased as the

particle size of the powder decreased. This was explained by the increased number of contact points per unit area and higher interparticular cohesive forces existing at zero pressure which opposed dense packing conditions. Powders composed of spherical particles were found to pack densely when placed in the die and exhibit little movement under applied pressure.

Gerritsen and Stemerding (1980) proposed a crackling mechanism for certain types of powder. Under low pressures soft highly compressible elastic materials can experience sudden decreases in volume accompanied by the sound of crackling. It was proposed that this phenomena could be explained as follows. Each particle in a powder bed has unique contact conditions, on compression the forces applied to these contacts will vary considerably. When a particle-particle contact somewhere in the bed fails, the particle will move into a more stable position. This could mean that neighbouring particles loose stability and also start to move. This may trigger a chain reaction that leads to restacking of a large proportion of sample causing a rapid reduction in volume. This phenomenon was observed for potato starch and powdered milk however it could be the mechanism for other pharmaceutical materials.

As the applied pressure increases further relative movement of particles becomes impossible. A further increase in pressure will induce particle deformation, fragmentation or both. The dominating mechanism will depend on the properties of the material involved, both mechanisms result in a further decrease in porosity and increase in particle contact.

#### 1.1.4 Deformation

When any solid body is subjected to opposing forces, there is a finite change in its geometry. The relative amount of deformation

produced by such a force is a quantity called strain and the nature of the force will determine the type of strain. It may take the form of tensile, shear or compressive strain. For example if a solid rod is compressed by forces at each end to cause a reduction in length of  $\Delta H$  from an unloaded length of  $H_0$ , then the compressive strain ( $Z$ ) is given by the equation:

$$Z = \Delta H / H_0$$

The ratio of the force  $F$  required to produce this strain to the area  $A$  over which it acts is the stress ( $\sigma$ ):

$$\sigma = F / A$$

True analogous behaviour to a solid body should not be expected due to the air spaces present in powder masses. If on removal of the force, the deformation is to a large extent spontaneously reversible, then the deformation is said to be elastic. For other powdered solids an elastic limit or yield point is reached, at pressures beyond this point, permanent deformation is produced. Consolidation for such materials is by plastic deformation and or viscous flow of the particles, which are squeezed into the remaining void spaces. This mechanism predominates for materials with shear strength less than the tensile strength. If the shear strength is the greater then particles will tend to fracture; the smaller fragments will then tend to fill the remaining voids. This mechanism predominates for hard brittle materials and is called brittle fracture.

### 1.1.5 The Elastic Effect

Under initial low compression pressures materials may behave according to Hooke's law:

$$\text{Stress} = E \times \text{Strain}$$

Where  $E$  represents Young's Modulus which describes the stiffness of a material ie the resistance to strain. This behaviour is analogous with

that of a spring under increasing load. The elongation of the spring is proportional to the applied load and is totally reversible, that is if the load is removed the spring returns to its original length. However if the yield point of the material is exceeded further, elongation will result which is not reversible but permanent. The Modulus can be estimated by measurement of the slope of the stress-strain curve in the elastic region. Values have been determined by flexure testing of rectangular beams Church and Kennerley (1983). For porous materials the Young's modulus may be described by the Spriggs equation (1961):

$$E_p = E^{(1-bp)}$$

Where  $E_p$  is the specimen Young's Modulus at porosity  $p$ , and  $b$  is a material constant. This relationship was utilised by Kerridge and Newton (1986) to determine the Young's modulus for some pharmaceutical materials. The higher the value of Young's Modulus the greater the stress required to strain the inter-molecular bonds. Potassium chloride composed of strong ionic bonds was shown to have a higher modulus than covalently bonded aspirin molecules. This fundamental parameter allows a comparative measure of the elasticity of materials under stress.

#### 1.1.6 The Plastic Effect

Plastic deformation of a material may be as described by Houwink (1958); a plastic gliding process of total internal structural elements or a pressure of fluidity, as proposed by O'Neil and Greenwood (1932).

Hardman and Lilley (1970) utilised a direct method to provide evidence for compaction mechanisms. Scanning electron micrographs of materials before and after compaction were used to distinguish between the plastic deformation of sodium chloride and the extensive

fragmentation of sucrose. Coal was found to have intermediate behaviour exhibiting some fragmentation combined with plastic deformation of small fragments or regions of large particles. This technique was improved by Krycer, Pope, and Hersey (1982). A scanning electron microscope was modified to observe the compression of individual crystals, the event was recorded using a television video tape. It was demonstrated that potassium chloride exhibits near-ideal plastic flow under pressure, while lactose monohydrate compacts by brittle fracture. This method although direct is not representative of conventional tableting in terms of the magnitude and rate of application of the compressive force, while the images were often difficult to interpret.

An alternative approach to demonstrate the compaction mechanism was to instrument a tableting machine. Carless and Leigh (1974) monitored the axial pressure in relation to the radial die wall pressure. It was proposed that the resulting compression cycles could be used to identify particle rearrangement, elastic deformation and yielding of the material. The "pressure of fluidity" theory was favoured by these workers as tablets compressed to the yield pressure indicated that plastic flow or crushing had been confined mainly to interparticulate regions. The yield pressure its self was shown to increase as the particle size of sucrose crystals decreased. This could have been due to i) the increased number of contact points and hence larger area of contact which would facilitate the transmission of applied forces, or ii) increased shear stresses at the die wall.

An instrumented tableting machine was also used by David and Augsburg (1977), to illustrate the time dependant nature of plastic deformation. Compression dwell times were artificially increased upto twenty seconds. Tablet strengths were seen to increase with dwell time for microcrystalline cellulose and compressible starch due to extended

plastic flow producing more surface contact for interparticulate bonding. Increasing the duration of the compression cycle did not result in significant changes in the strength of sugar or lactose tablets. This indicated that plastic deformation was not the mode of consolidation for these materials.

Cole, Rees and Hersey (1975) employed particle size analysis to confirm plastic deformation was the method of consolidation for sodium chloride and potassium chloride. For such ionic crystalline materials it was suggested that plastic flow was achieved by repeated dislocations of the simple cubic lattice structure.

Irrespective of the behaviour of larger particles of a material, small particles may deform plastically by a process known as microsquashing. Asperities that are sheared off irregular particles could also behave in this way. Microsquashing has been proposed as an important factor in the achievement of sufficient area of contact between coal particles during the briquetting process Gregory (1962). Thus the particle shape and proportion of fine powder present may influence the consolidation mechanism.

#### 1.1.7 The Brittle Effect

Fragmentation processes are governed by the theories of Griffith (1920). In order for a crack growth to occur the energy stored at the tip of a crack must just exceed the energy required to form the two new surfaces resulting from the propagation of the crack. The energy stored at the tip of a crack is a function of the dimensions of the crack, brittle fracture may result from crack propagation from a flaw that concentrates the stress imposed during compression.

Hard brittle materials such as lactose monohydrate are most likely to consolidate by brittle fracture. Under pressure a brittle material will fracture, the broken particles may then realign and the

freshly generated surfaces may be subjected to intermolecular interaction at points of contact. The resulting compact strength will depend on the extent of particle breakage and the limits placed on particle interaction. This was demonstrated by Van Kamp, Bolhuis and Lerk (1986) using different types of crystalline lactose. The tablet strength was shown to be dependant on the extent of fragmentation and limiting factors such as addition of magnesium stearate lubricant.

Higuchi et al (1953) were among the first to report experimental data to support the compaction mechanisms for pharmaceutical materials. The specific surface area of a sulphathiazole starch granulation was measured during compression using a gas adsorption technique. A gradual increase in the surface area was observed and attributed to fragmentation of particles. This was followed by a fall in surface area at higher pressures which was thought to be due to interparticulate bonding of surfaces as they became pressed together. This sequence of events was confirmed by Khan and Rhodes (1975) by particle size analysis of disintegrated compacts prepared under increasing pressures. Mean particle diameter depended on the balance between fragmentation which dominated initially and bonding which become more significant at higher pressures. Armstrong and Griffiths (1970) described similar specific area curves to those of Higuchi but observed an additional rise in surface area at high pressures. This increase was associated with lamination and was attributed to elastic recovery of the particles.

The investigation of deformation mechanisms by surface area measurement has been continued using the alternative permeametry method by Alderborn, Nyström et al (1982-86). These workers proposed a fragmentation propensity coefficient based on the linear relationship found between the increase in surface area with pressure and the surface area of the starting material to the power 2/3. This was

subsequently used to quantify the effect of particle size and shape on the extent of fragmentation. More brittle materials were found to produce compacts independent of initial particle size and shape. Some doubt has been cast on the validity of results produced by permeametry by Selkirk (1985), however the results although not absolute did produce useful comparative data.

The adsorption method was employed by Stanley-Wood and Johansson (1986) to demonstrate modification of the brittle nature of dicalcium phosphate by mixture with microcrystalline cellulose and magnesium stearate. Calculation of the adsorption energy potential per unit area of such mixtures during compression showed that no fragmentation occurred within the mixture. This indicates that although the behaviour of materials may be readily classified according to their mechanism of deformation, when incorporated into a mixture consolidation may be far from a simple additive relationship.

Again the direct method of monitoring compaction mechanisms, electron microscopy has been used to investigate fragmentation. Krycer, Pope and Hersey (1982) observed the initial fragmentation stage experienced by single lactose monohydrate crystals. A modification of this technique was introduced by Down (1983), Actual compacts were viewed at advancing stages of compression and electron micrographs taken. Sodium chloride a "classical" plastic material was found to undergo some localized particle fracture during the early stages of rearrangement and consolidation. This would tend to confirm that most materials possess some elastic, plastic and brittle character. Although one mechanism usually dominates it is important to bear in mind that the other mechanisms contribute to the overall compaction process. This fact becomes all the more relevant when the contribution of each mechanism changes with the tableting conditions. Dramatic changes in deformation character have been reported for

materials compressed at different rates Roberts and Rowe (1986), Bateman, Rubinstein and Wright (1987).

#### 1.1.8 Bonding

Several theories of bonding during compaction have been proposed, but they have proved difficult to substantiate experimentally. The mechanical theory suggested, that under pressure the particles experienced deformation and or brittle fracture. The edges of the particles then interlock forming a mechanical bond. It is probable that little of a compacts strength is attributable to mechanical interlocking. The intermolecular forces theory proposes that during compression particles are brought into contact and the close proximity of freshly generated surfaces enables van der Waals' forces to interact

The liquid surface film theory attributes bonding to the presence of a thin liquid film at particle interfaces. In the case of absorbed moisture, the high pressures at points of contact will affect the solubility of the material. Some of the contact area may dissolve and recrystallize forming a bridge between particles.

Interparticulate friction has been suggested as an important mechanism for increasing compact strength. Pressure applied to the bed must be transmitted through the points of contact and any particle movement may generate substantial frictional heat. If this heat is not dissipated the local rise in temperature could be sufficient to cause melting of the contact area, which would relieve the stress in that region. On cooling the melt solidifies causing fusion bonding. This mechanism could be important in increasing the strength of compacts prepared from materials with low specific heat and poor thermal conductivity. Rankell and Higuchi (1968) quantified this type of behaviour using heat transfer kinetics to estimate that

temperatures high enough to fuse organic materials occurred during compression. Krycer and Pope (1982) identified fusion bonding as being an important mechanism for increasing the strength of compacts with increasing intra-granular porosity. A more porous and friable material will undergo relatively more movement in order to produce a compact. This will generate more hot spots that cause localized melting and subsequent fusion bonding. It was also proposed that the increased interparticulate friction results in increased surface energy, stored as lattice defects. As a result the surface becomes amorphous, acquires a high reactivity and releases excessive energy by the formation of interparticulate bonds.

Under pressure the surfaces of a powder approach each other closely enough (within about 50nm) that their free surface energies result in strong attractive forces. The bonds formed are similar to the internal bonds of the particle; the process is termed cold welding. This hypothesis is the major reason for the increasing strength of a powder bed under compression. Hence the internal bonding of materials must be understood before we can determine what type of bonding is occurring between particles.

Ionic Crystals: An ion in such a crystal is equally bound to all the ions to which it is co-ordinated, thus there are no discrete molecules. The whole crystal may be regarded as a macromolecule. Such materials are often transparent and moderately hard such as sodium chloride.

Covalent Crystals: 1) Discrete molecules are held together by weak van der Waals forces which may easily be overcome. Consequently they are soft, have low melting points and high coefficients of expansion. The second type of covalent crystal is very different. ii) In homopolar crystals the atoms are strongly bound in three

dimensions and form a giant molecule. Such crystals are very hard, have very high melting points and low coefficients of expansion.

Neutral molecules may be held together by two principal kinds of intermolecular forces dipole-dipole interactions and van der Waals forces. A dipole-dipole interaction is the attraction of a positive end of one polar molecule for the negative end of another polar molecule. An especially strong kind of dipole-dipole attraction is hydrogen bonding in which a hydrogen atom serves as a bridge between two electronegative atoms, holding one by a covalent bond and the other by electrostatic forces. When hydrogen is attached to a highly electronegative atom, the electron cloud is greatly distorted toward the electronegative atom, exposing the hydrogen nucleus. The positive charge of the thinly shielded hydrogen nucleus is attracted by the electro negative atom of a second molecule

Van der Waals forces act between non polar molecules and their existence may be accounted for by quantum mechanics. The average distribution of charge about such a molecule is symmetrical, so that there is no dipole moment. However the electrons are dynamic and at any one moment in time their distribution could be distorted, generating a small dipole. This transient dipole will induce an oppositely oriented dipole in the neighbouring molecule. Although these momentary dipoles are constantly changing the net result is attraction between the two molecules.

Pilpel et al (1981-84) investigated bonding mechanisms by coating powders. The tensile strength of tablets compressed from such powders were seen to relate to the thickness and viscosity of the coating layer. As more coating was added, it increasingly coats the surface asperities of the powder, reducing the number of solid-solid bonds by masking the London and van der Waals' forces.

A bonding index (BI) was proposed by Hiestand and Smith (1984), it was claimed to give a measure of the survival during decompression of bonded areas established at maximum compressive stress:

$$BI = \sigma_T / P$$

Where  $\sigma_T$  is the observed tensile strength and P is the indentation hardness. This index compares the tensile strength which is the strength after elastic recovery, with a measure of the shear strength when under compressive load. This was thought to present a realistic measure of the behaviour of the bonded areas after release of the stress. An equation to predict this index was developed by Hiestand (1985) :-

$$\sigma_T/P = \gamma^d / \epsilon_1 r [n\theta / (2 - \rho_r) P^0]^{1/2}$$

Where  $\gamma^d$  is the surface energy (from dispersion interactions),  $\epsilon_1$  is the strain index, r is the radius of particles,  $n\theta$  are the number of contacts per unit area,  $\rho_r$  is the solid fraction, and  $P^0$  is the hardness of the solid particle. The equation assumes that i) only dispersion forces are acting, ii) plastic deformation takes place during compression, and iii) only elastic deformation takes place during unloading. Consequently the widespread use of this equation would appear to be limited. Experimental data was provided to show reasonable agreement between the equation and poorly bonded materials. For Avicel, a strongly bonded material, the predicted strength was only six percent of the experimental value. This was thought to be due to extensive plastic deformation during unloading, which increases the actual contact areas and consequently increases the compact strength; a process called isthmus formation. The contribution of non-dispersion forces such as hydrogen bonding and mechanical properties were considered to have a minor effect.

The area over which bonding takes place was investigated by Nyström and Karehill (1986) using gas adsorption and permeametry. The

actual bonding area could not be isolated. It was therefore concluded that bonding takes place over a minute fraction of external geometrical surface area. An alternative explanation could be that bonding was taking place by long range forces such as van der Waals' forces which would not be detected by these techniques.

It would appear that the bonding process is complex and the extent of each type of bond will vary from material to material. Although the main source of compact strength has been attributed to cold welding, the importance of the lesser bonding mechanisms should not be underestimated. The bonding characteristics of a material may be totally changed by a second substance or a change in the compression environment. It is thus critical that each system being compacted should be considered individually.

#### 1.1.9 Recovery

When the compression pressure is at its maximum, a bonded solid structure of a certain overall strength will have been formed. This structure must be strong enough to withstand the new series of stresses induced during release of the compressive pressure and those experienced during ejection from the die. On removal of the upper punch the compact will be able to recover in an axial direction, it will also be subject to the residual die wall pressure from the die wall created during compression. Following the ejection of the tablet from the die the tablet will be able to recover in a radial direction in addition to axially.

If the material was brittle and consolidated only by fragmentation, the removal of the compressive force would have no effect as the fragments cannot recombine. Similarly a purely plastic material would not be expected to disrupt the interparticulate bonds as the compressed form of the particles would be retained during

decompression. If a material possess any elastic character it will tend to revert to its original shape, this will reduce the contact area and disrupt bonds previously formed. As previously mentioned most pharmaceutical materials possess elastic, plastic and brittle nature and would thus be expected to experience a degree of bond disruption and may be some rebonding during decompression.

When a particulate system is compacted and held under load, stress relaxation occurs in the compressing device if the volume of the compact can reduce. The mechanism by which this takes place may be by plastic flow of the material into the void spaces of the compact. With ionic crystalline substances such as sodium chloride, plastic flow is able to proceed by repeated dislocations of the simple cubic lattice. The occurrence of plastic flow in some pharmaceutical materials has been determined by comparing their stress relaxation under constant strain. Shlanta and Milosovich (1964) reported that the compression stresses were relieved with time. It was concluded that materials possessing satisfactory compaction properties exhibited intermediate stress relaxation and when the stress relaxation was either high or low, a suitable compact was not formed. Plastic flow was believed to be an important factor in counteracting the disruptive effects of elastic recovery.

Cole , Rees, and Hersey (1975) proposed that internal stress relaxation mechanisms may be responsible for the increase in strength of sodium chloride compacts after ejection. Frictional contact with the die during compaction may result in case hardening, the production of an outer skin. If this skin is sufficiently rigid to maintain a confining stress on the particles within the compact, stress relaxation will continue even after the compact has been ejected.

Hiestand et al (1977) showed that shear stresses developed during decompression which caused fracture in some materials but not in

others. Failure of a compact to fracture was attributed to the ability to relieve stress by plastic deformation. A factor to predict this property was proposed called Brittle Fracture Propensity (BFP). The test consisted of measuring the tensile strength of a large square compact with and without a small central hole which acted as a stress concentrator.

$$BFP = \frac{1}{2} [ (\sigma_T / \sigma_{T0}) - 1 ]$$

Where  $\sigma_T$  is the tensile strength without a hole and  $\sigma_{T0}$  is the apparent tensile strength with a hole present. The BFP is the quantitation of the stress relief by plastic deformation of the compact at the edge of the hole. If no stress relief occurs, the tensile strength should be approximately one third of the tensile strength of a compact without a hole. If the stresses at the edge of the hole are relieved by plastic flow then no differences in tensile strength should be observed. Therefore a high value of BFP indicates a tendency of the material to laminate. This investigation was carried out using slow compression-decompression speeds and very large compacts which are not transferable to the production situation. The BFP test was modified by Roberts and Rowe (1986) such that it could be measured at strain rates and conditions similar to those normally used in tableting.

The percentage elastic recovery of a compact (ER) was defined by Armstrong and Haines-Nutt (1972):

$$ER = [ (H_0 - H_p) / H_p ] \times 100\%$$

Where  $H_p$  and  $H_0$  are the heights of the compact under pressure and after ejection respectively. E will give a measure of the disruptive effects of elastic deformation. The stress relaxation (SR) was defined by Bangudu and Pilpel (1985):

$$SR = [ (H_p - H_t) / H_t ] \times 100\%$$

Where  $H_c$  is the thickness of the tablet having been held at maximum load for thirty seconds. The tensile strength of tablets prepared from paracetamol- avicel mixtures were found to be inversely proportional to ratio ER/SR. The ratio was used to predict capping and lamination. Although both materials had similar ER values, the greater plasticity and increased bond strength of avicel enabled it to withstand elastic recovery. This ratio is in fact measuring the same parameters as the BFP mentioned earlier. This was confirmed by Esezobo and Pilpel (1986).

Rippie and Danielson (1981) applied three dimensional linear viscoelastic theory to the generation and decay of axial and radial stresses within compacts. The mechanical components of a material were represented by models. Elastic character was represented by a massless spring and plastic flow by a dashpot. Different types of solid were represented by the use of springs and dashpots in series or parallel. This concept was then expanded to represent the effect of stresses and strains in three dimensions. With subsequent experimental work material behaviour was separated into dilation and distortion components. Dilation was found to be elastic while distortion could be represented by a Kelvin solid model. The Kelvin solid model consists of a spring and dashpot in parallel hence it exhibits elastic and plastic characteristics. In an extension of this investigation Danielson, Morehead and Rippie (1983) used the extent of the elastic and plastic components to predict the incidence of tableting faults such as capping and lamination.

Thus the decompression event and subsequent ejection have a significant effect on the tablet properties.

The interpretation of compaction data has received considerable attention in the pharmaceutical literature. With the advent of widespread instrumentation of tableting machines and testing equipment it became possible to monitor axial upper and lower punch pressures and displacements, radial die wall pressures, temperature generated, and acoustic emissions during the compaction event. The most popular methods for interpreting compaction data include the use of terms to quantitate the energy required for elastic and plastic deformation, pressure volume relationships, stress relaxation and elastic recovery measurements, and pressure cycle plots of radial versus axial pressure.

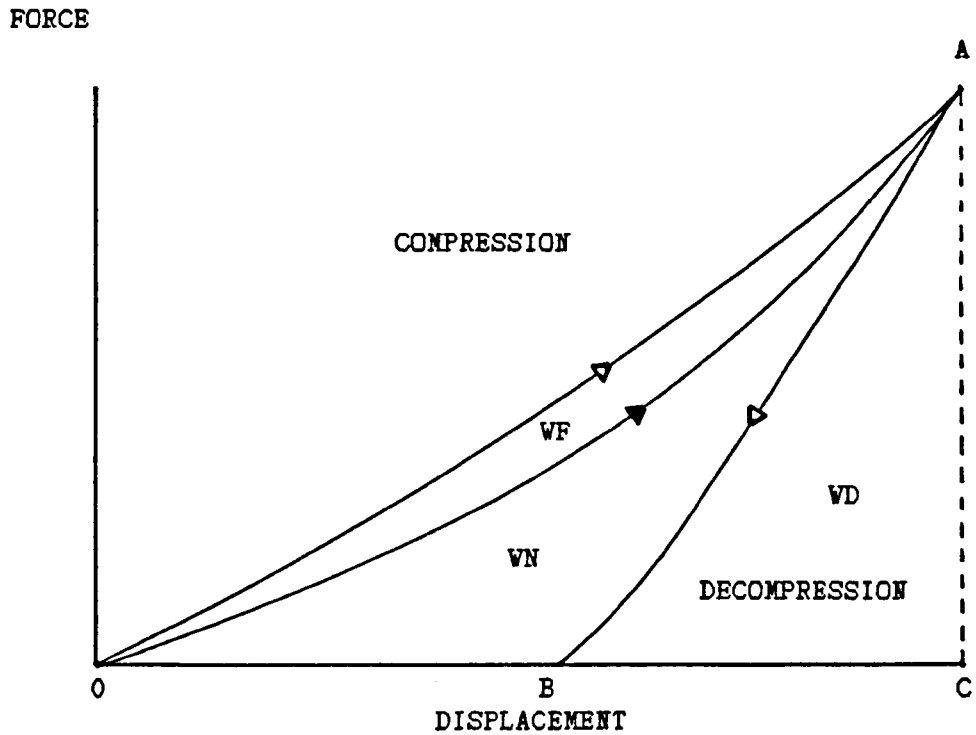
The work involved in the stages of compaction detailed previously includes, that necessary to overcome friction between the particles, that necessary to overcome friction between the particles and the machine parts, that required to induce elastic and or plastic deformation of the material, and that required to cause brittle fracture within the material. In the tableting operation, energy will also be lost as heat which provides a means of monitoring the energy balance of the system Nelson *et al* (1955), Hanus and King (1968). Similarly loss of energy in the form of acoustic emissions has also been employed in investigating the compaction event Waring *et al* (1987a,b).

De Blaey *et al* (1970,71a,b,c) used energy to quantitate the stages of compaction. Force displacement data may be plotted as seen in FIG 1.1a. It can be seen that the area under the curve OAC represents the gross work done by the upper and lower punches. The force experienced by the upper punch will incorporate a contribution

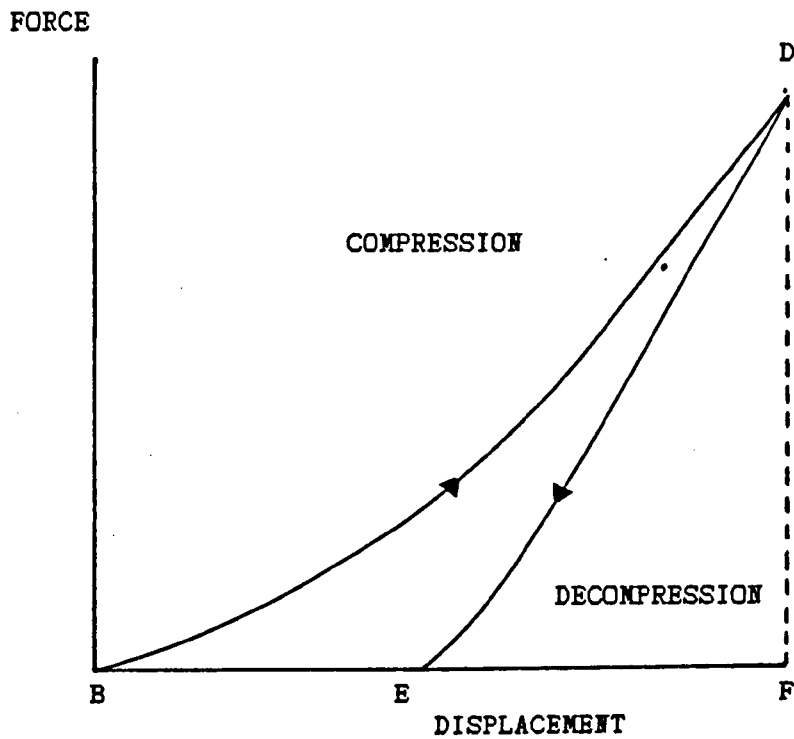
FIG 1.1 Typical Force Displacement Curves

△ Upper Punch Force, ▲ Lower Punch Force. WF represents the work of friction, WD is the Elastic Deformation Energy and WN is the Net Mechanical Energy used to Form The Tablet. (Not Drawn to Scale)

a) First Compression



b) Recompression



due to overcoming friction with the die wall, while the force transmitted to the lower punch will be independent of friction. Consequently the difference between the area under the upper and the lower punch force displacement curves  $W_f$  represents the the work done in overcoming friction and may be calculated by:

$$W_f = \int_{00}^{DC} (UPF - LPF) dD$$

Where UPF and LPF are the upper and lower punch forces respectively and D is the displacement of the upper punch measured relative to the lower punch. An alternative formula for the work of friction was suggested by Järvinen and Juslin (1974). They included a point of action for the frictional forces. During compression only the particles in the upper layer of the compact will move the same distance as the upper punch while particles at the lower punch remain stationary. They derived the following equation:

$$W_f = \int_{00}^{DC} UPF - (UPF - LPF) / \ln (UPF / LPF) dD$$

This was shown to give a better indication of the work of friction by Ragnarsson and Sjögren (1983), while the equation of de Blaey and Polderman (1971) appeared to give an over estimation.

A small component of the work done by the upper punch is recoverable as work done by the compact on the receding top punch, area ABC. However the total elastic energy stored in the tablet during compression will not be represented by ABC if the punch loses contact with the compact before elastic recovery is complete. Area OAB for the lower punch is termed the apparent net energy as it contains this element of elastic energy. Early investigators overcame this problem by compressing the tablet a second time before ejecting it from the die. The net energy required to recompress the compact shown in FIG 1.1b was proposed to be equivalent to the amount of elastic energy

in the elastic recovery of the compact. However Patel, Staniforth, and Hart (1985) maintained that in order to obtain the true work of compaction upto nineteen multiple compressions were required. It must be assumed that values for elastic energy obtained in this way contain no contribution from further plastic deformation. This may not be the case for materials which undergo stress relaxation, as the extended time at maximum force due to recompression will permit some degree of plastic flow. An alternative to using recompression to indicate elasticity is the percentage elastic recovery (ER) employed by Armstrong and Haines-Nutt (1972), mentioned earlier.

In a review of interpretation of compaction data Krycer, Pope and Hersey (1982) suggested that work done by the lower punch OAC was the most useful means of assessing energy utilization in compaction. The lower punch work LPW may be calculated as follows.

$$LPW = \int_{00}^{DC} LPF \, dx$$

Energy analysis will be employed in the investigation reported in this thesis. As compression will be achieved by movement of both punches, mean punch force and punch separation will be used to calculate the work done during compression.

### 1.2.2 Stress Relaxation

Although stress relaxation will not be employed for the present investigation it will briefly be discussed due to its importance in the elucidation of time dependent mechanisms.

Compression is carried out in the usual manner until the maximum pressure has been attained, after which the upper punch is held static and the force monitored. The force decreases with time, eventually leveling off when the stress relaxation is complete. This phenomenon is known as stress relaxation or creep and it results from plastic

deformation of the compressed material into remaining voids. David and Augsburger (1977) treated this plastic flow concept mathematically as a Maxwell model under constant strain. That is one viscous and one elastic parameter in series. They derived the following equation to quantitate the degree of plastic flow:

$$\ln \Delta F = \ln \Delta F_0 - kt$$

Where  $\Delta F$  is the amount of force left in the compression stage where plastic flow takes place at time  $t$ .  $\Delta F_0$  is the total magnitude of force at  $t = 0$  and  $k$  is the viscoelastic slope. The viscoelastic slope was used to quantify the extent of plastic flow of direct compression tablet fillers under compression.

Hiestand *et al* (1977) extended the stress relaxation times up to one thousand seconds. It was found that the rate of stress relaxation changed after a short period (two to six seconds) and materials susceptible to capping had slower stress relaxation. An equation was developed to indicate the brittle fracture propensity (BFP) of a material mentioned earlier. The BFP is a useful indicator of capping due the properties of the material. However it should be remembered that capping may also result from the stresses imposed on the compact during compression and ejection.

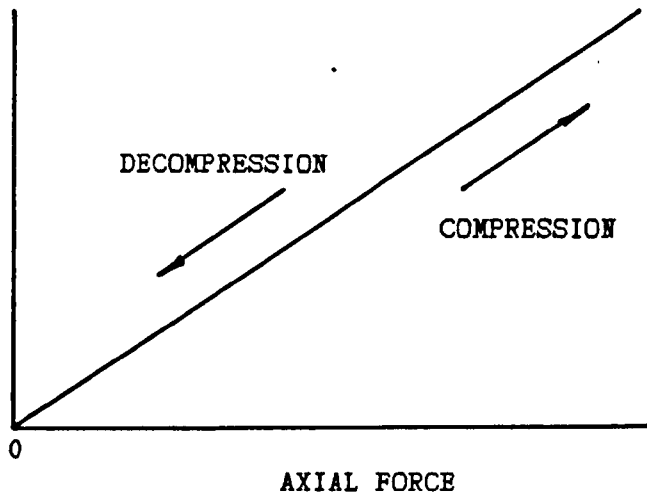
### 1.2.3 Radial Versus Axial Compaction Cycles

A radial die wall force arises as a result of the tableting mass attempting to expand in the horizontal plane in response to the axial compression. The proportion of the force transferred to the die wall when plotted against the axial pressure produces characteristic hysteresis curves. Long (1960) elucidated the usefulness of pressure cycle plots. Since then materials have been classified as perfectly elastic, exhibiting a constant yield stress in shear ie plastic flow or as a Mohr body which consolidates by brittle fracture as shown in

FIG 1.2 Theoretical Pressure Cycles

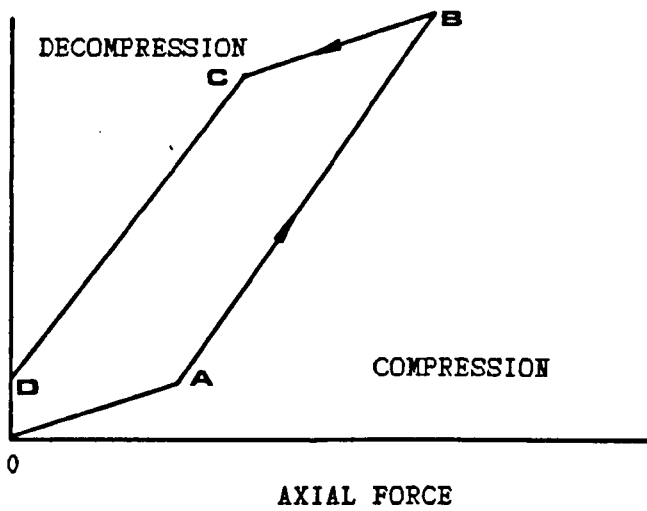
a) Perfect Elastic Body

RADIAL FORCE



b) Body with Constant Yield Stress in Shear

RADIAL FORCE



c) Mohr's Body

RADIAL FORCE

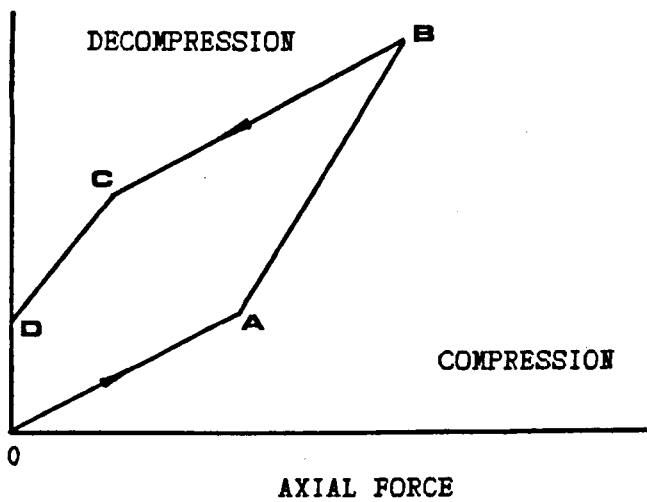


FIG 1.2a,b,c respectively. The hysteresis areas have also been used to indicate compaction mechanisms by Carstensen and Touré (1980). Another parameter that has been derived from compaction cycles is the Poisson ratio, defined as the transverse expansion per unit dimension of a solid of uniform cross section to its contraction per unit length when subjected to uniaxial compression stress. This has been used to measure the ability of a material to deform elastically, but its use is open to debate as tableting involves porous materials and not uniform solids as mentioned in the definition. The type of deformation indicated using such cycles has not been consistent for pharmaceutical materials, but they have proved useful in indicating the extent of plastic flow during compaction. The radial die wall pressure will not be measured during this investigation.

#### 1.2.4 Force Volume Relationships

Many equations have been proposed to represent the compaction event, but only the most widely accepted will be discussed here. Kawakita and Ludde (1970) reviewed a large number of equations and concluded that Kawakita's equation (1956) had wide applicability in the field of powder compaction:

$$C = \frac{V_0 - V}{V_0} = \frac{abP}{1 + bP}$$

Where C is the degree of volume reduction,  $V_0$  is the initial apparent volume, V the powder volume under applied pressure P and both a and b are constants characteristic of the powder. The constant a was shown to be initial porosity of the powder and b was related to the cohesive forces between the powder particles during rearrangement.

Probably the most informative equations used to date are based on the equation:

$$\ln [ 1 / ( 1 - D ) ] = KP + A$$

Where  $D$  is the relative density at pressure  $P$ , and both  $K$  and  $A$  are constants. The equation was first developed by Athy (1930) but is more commonly referred to as the Heckel equation (1961a,b). The Heckel equation is based upon analogous behaviour to a first order reaction, where the pores in the mass are the reactant. A schematic representation of the Heckel equation is shown in FIG 1.2d. The constant  $A$  is a function of the original compact volume, the constant  $K$  may be calculated from the slope of a plot of  $\ln [ 1 / ( 1 - D ) ]$  versus  $P$ . Hersey and Rees (1970) showed that:

$$K = \frac{1}{P_y}$$

Where  $P_y$  is the mean yield pressure of the material. This has since been used extensively to indicate the nature of a materials deformation. Hersey and Rees (1971) defined type A and type B compaction behaviour using Heckel analysis as shown in FIG 1.2e,f. Type A behaviour is characteristic of a material that has an initial particle size dependent on bulk density. Consolidation is due initially to particle slippage or repacking, and then plastic deformation. The compacts retain different degrees of porosity depending on the initial packing in the die. Such materials are usually softer and have a lower mean yield pressure. Materials exhibiting type B behaviour show coincident behaviour above a certain pressure irrespective of initial bed porosity or particle size. This was thought due to the progressive destruction of particles by fragmentation and then plastic deformation. A further behaviour type C was introduced by York and Pilpel (1973) working with lactose coated with fatty acids. This behaviour was attributed to the absence of a rearrangement stage combined with plastic deformation and the possible melting of asperities as shown in FIG 1.2g. An indication of the extent of particle rearrangement and slippage may be taken from the

FIG1.2d Schematic Representation of the Heckel Equation

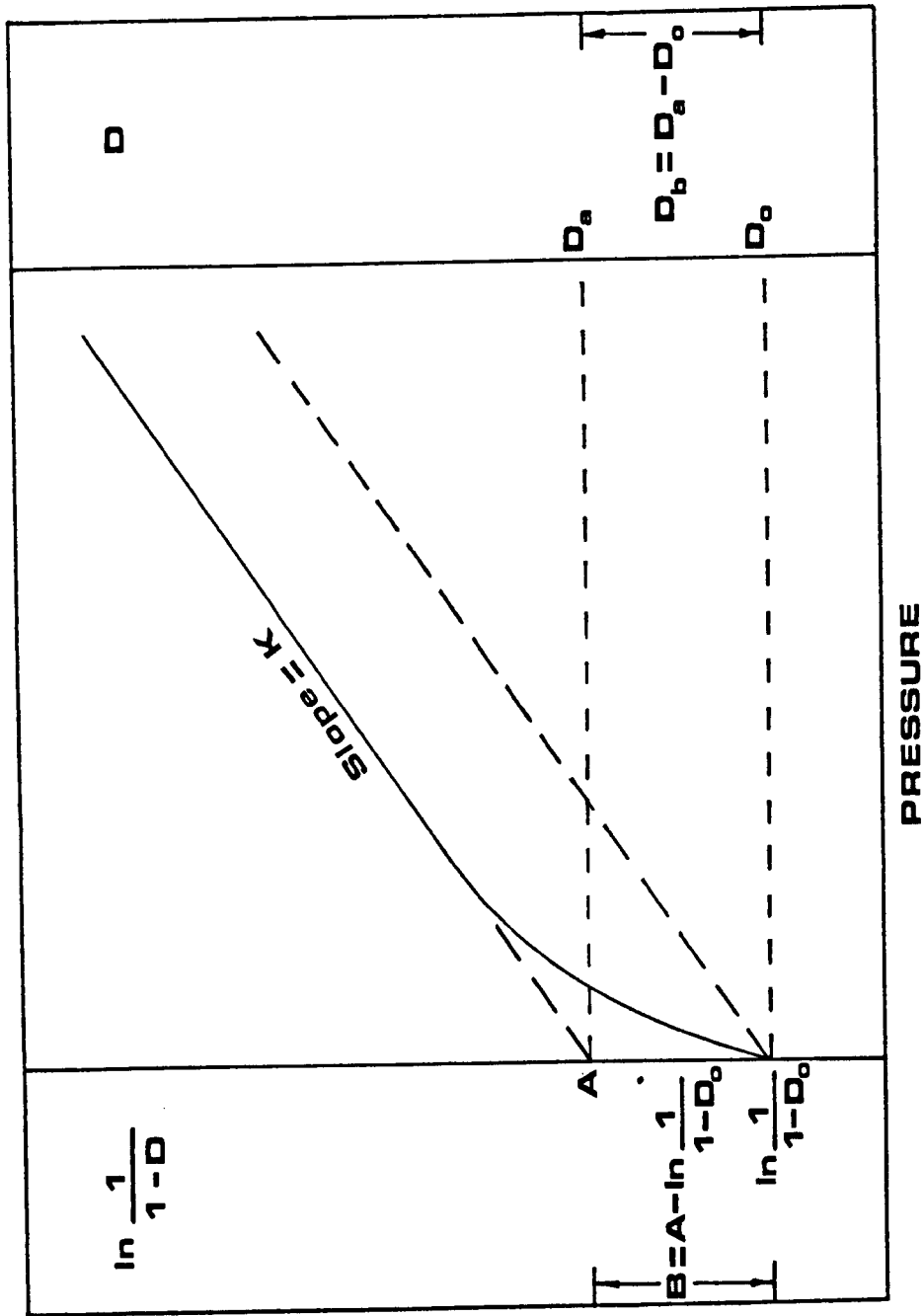
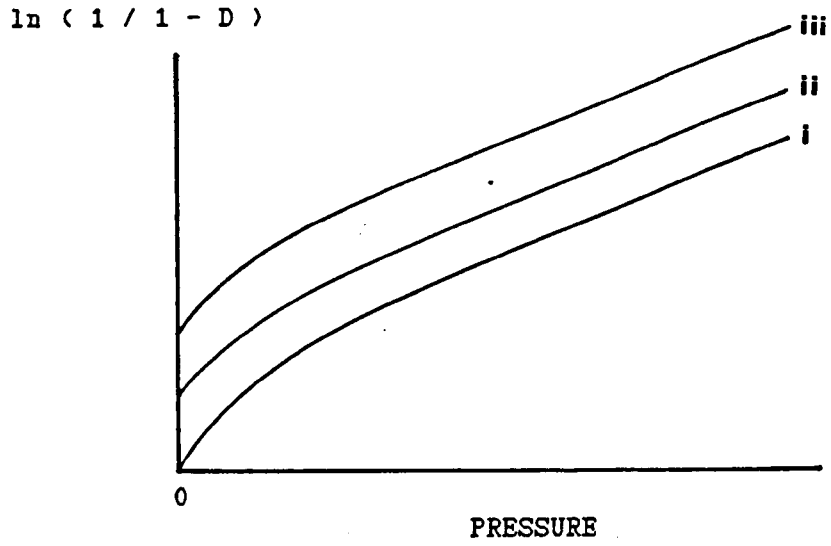
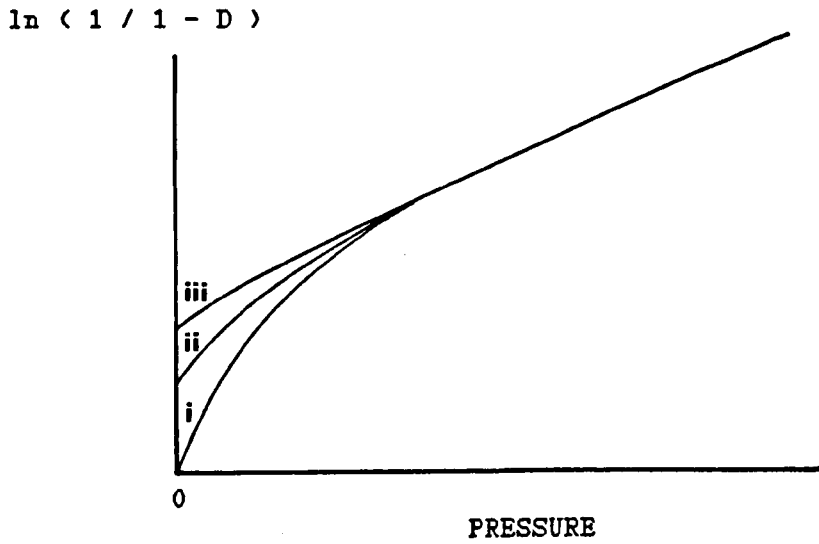


FIG 1.2 Heckel plots for Types of Compaction Behaviour

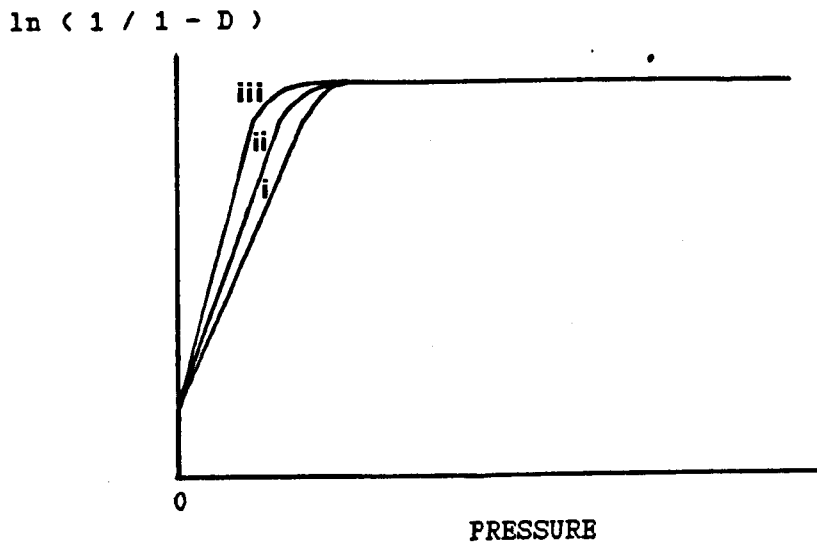
e) Type A Behaviour



f) Type B Behaviour



g) Type C Behaviour



initial curved portion of the curve. This may be analysed quantitatively using the Heckel parameter  $D_b$ , which may be obtained from the equation:

$$D_b = D_a - D_0$$

Where  $D_a$  and  $D_0$  are the relative density of the compact at the intercept of the regression line of the linear portion of the curve and at the first measureable force respectively.  $D_a$  may be calculated from regression data using the equation:

$$D_a = 1 - e^{-k}$$

A comparison of the Kawakita and Heckel equations by Hersey Rees and Cole (1973) concluded that both offered assistance in understanding consolidation processes under compression, however neither treatment was considered ideal. The Heckel equation is strictly only applicable to plastically deforming systems, thus there is non linearity at low pressures for brittle materials. The Kawakita equation could not identify the different deformation mechanisms of materials which placed it at a disadvantage to the Heckel equation. The Heckel equation was thus selected for use in the investigation reported in this thesis.

Heckel used density measurements taken in the die at zero pressure, with current technology however it is possible to measure density at pressure during compression. Fell and Newton (1971) have shown that measurements of density taken at pressure will contain an elastic component which results in falsely low yield pressure values. Krycer, Pope and Hersey recommended that density measurements should be taken at zero pressure after ejection to avoid the elastic contribution. However in order to investigate the effects of compression speed for this investigation it was necessary to measure density at pressure during compression.

### 1.3 Post Compression Assessments

The properties of compacts formed by compaction are of great importance, and have been measured using many different methods including tablet strength, hardness, friability, disintegration and dissolution. The mechanical strength of tablets has been measured in a variety of ways as described below.

#### 1.3.1 Tablet Strength

Crushing strength of a tablet may be defined as the compressional force which, when applied diametrically to a tablet, just fractures it. Most tests used to measure this parameter involve placing the tablet on or against a fixed anvil and transmitting force to it via a moving platen, until the tablet just fractures. Since tablets are often anisotropic (having different physical properties in all directions) and test conditions rarely provide well defined uniform stresses, exact interpretation of results can be difficult. However if the test is tensile where the tablet splits open across the diameter the tensile strength ( $\sigma_x$ ) may be as described by Fell and Newton (1970):

$$\sigma_x = \frac{2P}{\pi Dt}$$

Where P is the applied load, D and t are the tablet diameter and thickness respectively. This useful equation enables comparison of the tensile strength of tablets with different dimensions (Newton et al (1971)). The tensile strength of compacts calculated using this equation may still vary depending on test conditions. Variables such as the use of padding (Fell and Newton (1970)) and the rate of loading (Rees, Hersey and Cole (1970)) have been shown to effect the tensile strength. Padding inserted between the tablet and the platen may increase or decrease the tensile strength depending on how soft it is,

while an increase in the rate of loading was shown to produce a significant increase in the tensile strength. Due to the lack of uniform density within a compact, tensile strength values are only an estimate of the correct value.

The deformation undergone by the tablet during diametral testing has been measured by Rees and Rue (1978) and used to calculate the work of failure (Wf):

$$Wf = \frac{2}{\pi Dt} \int_0^x F dx$$

Where F is the applied force and x is the tablet deformation. It was claimed that this was a more sensitive parameter. However Wf does not take into account the rate of crack propagation through the tablet prior to failure which is influenced by the physicomachanical properties of the material. Patel and Staniforth (1987) proposed three possible parameters for tablet strength. The power of failure, where the work required to cause tensile failure (Wf) was divided by the time of load application. The normalized work of failure (NWF) given by:

$$NWF = \frac{2\pi}{Dt} \int_0^x F dx$$

A further parameter was suggested where the material was treated as a non Newtonian solid. The apparent failure viscosity (AFV) was calculated by dividing the tensile strength by the strain rate of deformation. The AFV and NWF determinations gave a good indication of the plasticity of excipients, while the power of failure was insensitive to changes in plasticity. However power of failure was considered a useful method of comparing tablet strengths using different rates of load application.

Flexure testing of compacted rectangular beams has been used to compare the mechanical properties of pharmaceutical materials (Church

and Kennerley (1982,83,84)). The advantage of the flexure test is that a uniform tensile stress is produced in the specimen. Moschos and Rees (1985) compared flexure testing with diametral testing. It was found that the failure deformation and deformation mechanism were the same for both tests. The flexure test however produced a greater coefficient of variance.

Micro-indentation tests as described by Ridgway, Aulton and Rosser (1970) have been used to indicate the surface hardness of tablets. The strength varies over the surface of a tablet due to varying densities caused by the stress distribution during compression. These tests are less reliable when employed on tablets due to their heterogenous nature, and have thus found limited acceptance with the pharmaceutical industry. However useful data has been obtained and used to derive further parameters such as Brinell hardness used by Leuvenberger (1982), to develop his equation to predict deformation hardness, and the strain index, bonding index and brittle fracture index of Hiestand and Smith (1984) used to quantify tableting performance.

Although the  $W_f$  probably represents the best measure of a compacts strength, it requires the ability to measure force and displacement from the compression device. An instron testing machine which was not equipped with a displacement transducer at the beginning of this investigation will be used to measure compact strength for this investigation. Consequently the tensile strength given by Fell and Newton (1970) will be employed through out this investigation. There is no such value as the true tensile strength, but values obtained under any conditions are true values for those conditions. Consequently for the comparison of tablet tensile strengths the conditions of the test will remain constant.

### 1.3.2 Friability

The crushing strength type test may not be the best test to indicate the behaviour of a tablet during the tumbling motions experienced with coating, packaging, handling and transportation. The most popular method for testing friability is the Roche Friabilator. The resistance of a tablet to surface abrasion or friability may be measured by subjecting the tablets to controlled tumbling, then quantifying the weight loss from the tablets. The friability (f) is given by:

$$f = 100 \times [ 1 - ( W_o / W ) ]$$

Where  $W_o$  is the initial tablet weight (6g), and  $W$  is the weight after one hundred free falls in a rotating drum. Values of 0.8 to 1.0 % are regarded as the upper limit of acceptability. The resistance of compacts to surface abrasion will not be utilized in this investigation.

### 1.3.3 Disintegration and Dissolution

These test are used to confirm that the tablet will break up into its constituent particles, and an accurate dose of the drug is released and passed into solution after ingestion by the patient. The disintegration test provides a uniform means of agitating the tablet in an aqueous medium at body temperature with a reasonably non-subjective end point. Disintegration is dependant on penetration of water into the tablet, swelling of the disintegrating agent and sometimes the heat of interaction between the disintegrant and the dissolution fluid which causes bonds to break. In general as the applied pressure used to form the tablet increases so the void space is reduced, which reduces the rate of water penetration and consequently increases the disintegration. However if the void space becomes too large then the disintegration time can increase as the

disruptive swelling action of the disintegrant cannot be exerted across the large voids.

The disintegration process has been described in terms of the number of particles released (N) by Kitamori and Shimamoto (1976):

$$N = \frac{T_0}{(t / t_d)^m}$$

where  $T_0$  is the number of particles in the tablet,  $t$  is the time,  $t_d$  is the disintegration time and  $m$  is a constant. As bioavailability of the drug is not of specific importance to this investigation the theory of dissolution will not be discussed.

The time taken for disintegration is related to the compression force. As such it will be employed in this investigation to study the effects of compression to a constant force and compression to a constant thickness.

#### 1.4 Factors Effecting Compaction

Many parameters have been shown to exert an effect on the compaction process. They may be classified according to material properties, machine variables or environmental factors. The identification and quantification of such parameters with an effect on compaction is of great importance during manufacture where the production of a uniform product is essential.

##### 1.4.1 Material Properties

The process of chemical synthesis or isolation of a drug substance, although designed to produce materials of reproducible high chemical purity, may not result in batches of product with equivalent properties. This is of importance when considering drugs or excipients to be used in a tablet formulation. Jones (1981) advised that the physico-technical properties of any tablet formulation starting

material should be evaluated from several batches in order to assess its grade variability. This variability is one of the most common problems experienced by the pharmaceutical industry, and has necessitated the implementation of strict quality assurance procedures. Some of the most important variables investigated to date are discussed below.

#### 1.4.2 Crystal Form

The type and degree of crystallinity in a particular material influences its consolidation. Jaffe and Foss (1959) investigated the role of crystal properties on the ability of materials to form tablets. They found that materials with a cubic crystal lattice could be more readily compressed than materials with a rhombohedral lattice. This could be because the cubic lattice is isotropic (has the same physical properties in all directions) and consequently requires no special orientation of the three equal lattice planes at right angles to each other for stress relief to occur. Substances such as ferrous sulphate, magnesium sulphate and sodium phosphate having water of crystallization could be compressed directly but did not form a tablet if the water of crystallization was removed.

The influence of crystal form was investigated by Summers, Enever and Carless (1977) for aspirin, barbital and sulphathiazole. Different crystal forms of each material produced tablets of varying strengths. Two factors were thought to influence the strength of compacts. The less stable polymeric form has higher potential energy and weaker bonding, the strength of its particle-particle bonds should be less than that of the stable form. However the extent of plastic flow and hence area of inter-particle contact would be expected to be greater for the unstable polymeric form. It was shown that the latter

mechanism; the extent of plastic flow, was the major influence on compact strength.

The compression event itself has been shown to induce polymorphic change of phenylbutazone by Ibrahim, Pisano and Bruno (1977). Polymorphs may vary in solubility, surface tension, density, crystal shape and hardness. It was found that one of the phenylbutazone polymorphs had an effectively reduced surface area resulting in slow dissolution. Polymorphism of phenylbutazone was also investigated by Tuladhar, Carless and Summers (1983). Two forms were found to have different bonding capacities and extents of plasticity.

Unfortunately no general relationship, which would allow the prediction of compressibility of a formulation based on the chemical nature and crystalline structure of its constituents, has been proposed.

#### 1.4.3 Particle Size

Particle size has an extensive influence on the behaviour of elastic, plastic, and brittle materials during compaction. It may even determine the deformation mechanism of a material Gregory (1962).

The Heckel equation (1961a) has been used to determine the effect of particle size on compaction (Hersey and Rees (1971)). Plastic materials, for example sodium chloride, have been shown to exhibit type A behaviour, where the different degrees of porosity dependent on the initial packing in the die are retained during compaction. The packing density is influenced by the size distribution, and shape of the original particles. For type B materials such as lactose where consolidation is mainly by fragmentation, the initial structure is progressively destroyed, followed by coincident behaviour of all original particle size fractions. The yield pressures obtained using the Heckel equation have been shown to increase with a reduction in

particle size for materials deforming by fragmentation but be independent of particle size for plastic materials (Hersey , Cole and Rees (1973)). The explanation for this phenomena for a brittle material such as lactose was, as the particle size decreases, the stress required to fracture the particles along cracks increases as predicted from crack theory (Griffiths (1920)).

McKenna and McCafferty (1982), investigated the effect of particle size on the compaction of lactose, starch and Avicel. It was shown that the tensile strength of lactose and starch compacts increased with decreasing particle size due to increased cohesive and frictional forces. For smaller particles there was a reduction in fragmentation with lactose and an increase in plastic flow with starch. For Avicel the cohesion and interparticular frictional forces remained independent of particle size resulting in little change in tensile strength or mechanism of deformation.

Kendall (1978) proposed that it was impossible to comminute very small particles by compression since, when the deformation zone was small enough even the most brittle material will flow. He developed an equation to predict the critical particle size below which flow would occur:

$$d_{crit} = 32ER / 3Py^2$$

Where E is the Youngs' modulus, Py is the yield pressure and R is the fracture toughness of the material. The fracture toughness may be considered to be a measure of the ease of crack propagation and thus brittleness. This parameter was used by Roberts and Rowe (1987) to evaluate pharmaceutical materials. Lactose and Avicel were found to have brittle / ductile transition points of 27.4µm and 1172µm respectively. A similar transition was noted by Alderborn and Nyström (1985) using surface area measurements. Alderborn et al (1988) have been able to summarise the effects of particle size with respect to

the compaction mechanism involved. For high fragmenting materials the original particle size of the material is of less importance and the tablet strength is fairly independent of particle size. For intermediate fragmenting materials, the tablet strength is increased with reducing particle size, probably due to the increased number of points of contact in the tablet. For low fragmenting materials the situation is more complex. A reduction in particle size can give an increase in tablet strength, probably due to the increased points of contact. The tablet strength may also be independent of particle size or, as with sodium chloride the tablet strength can increase with an increase in particle size, due to increasing stress at each particle-particle contact which could facilitate plastic flow or solid bridge formation. Hence the classical Heckel type A and B behaviours appear to be an over simplification of the effects of particle size. Once again each system must be considered individually, with its contributions of plastic and brittle character.

Particle size must also be considered in processing prior to compaction. Here the time taken for a number of powders to form an ordered mix increases with decreasing particle size van der Watt (1987). The larger the particles in the mixer, the greater are the shear forces in the mixer. This will lead to a faster rate of film formation with powders such as magnesium stearate. Formation of such a film may reduce the tablet strength and increase the disintegration time.

The effects of particle size on the tableting of a primidone granulation were investigated by Hunter (1974). The capping pressure and tablet strength were found to increase with specific surface area. Consequently quality control of particle size is of the utmost importance in ensuring the compaction of a formulation proceeds as originally intended.

#### 1.4.4 Particle Shape

The effects due to particle shape have been demonstrated to occur prior to compression. Particle shape has an influence on filling the die Ridgway and Scotten (1970). Irregular particles flow less freely from the feed shoe, and are less readily rearranged into a closer packed random arrangement when they fall into the die. Irregular particles also cause random variations in fill weight to increase. Similar effects due to poor particle flow have been noted during the initial stages of compression Heckel (1961b). Spherical powders were found to form dense initial packings which underwent very little rearrangement as pressure was applied.

The effects of particle shape during compression have been difficult to isolate from other parameters such as size, surface energy, crystal form and the deformation mechanism. Alderborn and Nyström (1982) and Alderborn et al (1988) produced different particle shapes by using milled and untreated samples of pharmaceutical materials. Different size fractions of material were shape classified and compacted. Particle shape had a significant influence on compact strength for sodium chloride and sodium bicarbonate, which are known to deform mainly by plastic deformation. Explanations for this effect were proposed. An increase in surface irregularities increased the number of contact points between particles, increasing the total bonding surface area. Alternatively the increased irregularity may have enhanced the interparticulate friction and induced plastic flow at contact points producing stronger tablets. Another explanation was that the milling process modified the surface properties of the material according to Hüttenrauch (1978), the activated surfaces resulting in stronger tablets. Brittle materials such as saccharose and sodium citrate showed no difference in tablet strength for the varying original particle shape. This was explained by the majority of

the tablet strength arising from the large number of small particles with freshly generated surfaces.

Although particle size and shape have been presented as important factors in the compaction behaviour of materials, it should be remembered that there may be exceptions to the rule. Particle size and shape were reported to have no definite influence on the tableting performances of celluloses (Doelker et al (1987)).

#### 1.4.5 Effect of Moisture

Moisture is present in virtually all tablet formulations to some extent, and at concentrations well below the 1% level, can dramatically affect the behaviour of the material and the finished product.

The effect of moisture on the transmission of the applied punch force to the lower punch was investigated by Shotton and Rees (1966). With no moisture present the transmission of force through the bed decreased with increasing applied pressure, and as little as 0.02% moisture produced a significant increase in the transmission of force. Further increasing the moisture content to between 0.55% and 2.4% resulted in reversal of the previous trend, and transmission of force through the bed increased with applied force. It was observed that compacts prepared in the presence of moisture and subsequently dried showed an increase in strength due to interparticulate recrystallization. Following apparently conflicting reports indicated that moisture could produce a decrease in mechanical strength. The dominating effect is a function of the physical and chemical form of the powder and the level of moisture.

Water can be present in powders in different forms; as adsorbed monolayers or multilayers on the surface of particles, as an actual water layer on the surface capable of forming pendular bonds between

particles (Eaves and Jones (1971)), as physically absorbed water within the particles or as strongly bound chemisorbed water.

Khan and Pilpel (1986) showed the effect of moisture concentration on the compression of Avicel. The first three percent of moisture were found to be internally chemisorbed by the particles. The water was strongly bound by hydrogen bonds to the hydroxyl groups in the cellulose structure. Consequently this water was not available on the particle surfaces, which prevented it from contributing to the bonding forces between them and hence to the strength of the bed. Higher moisture concentrations resulted in the formation of pendular bonds on the particle surfaces which would be expected to contribute to the compact strength. The addition of moisture increases the surface energy of the particles and the binding forces between them. Similar results had been presented earlier by Bangudu and Pilpel (1985). In this case compacts formed from mixtures of paracetamol and avicel were found to increase in strength between two and four percent moisture. But further increases in moisture content reduced compact strength due to the formation of multilayers of water which were said to reduce friction effects and rupture hydrogen bonds between the cellulose particles.

If the amount of water present is just sufficient to fill the remaining voids in the powder bed, any increase in the applied force will squeeze water out to the surface of the tablet Chowhan and Palagyi (1978). The expelled water may then form a continuous film at the die wall which acts as a lubricant. A slight reduction from this amount of water removes the lubricant effect and increases the die wall friction which may contribute to the strength of the compact.

The other extreme is dehydration of powders studied by Lerk, Zuurman and Kussendragger (1984). The strength of particulate hydrate compacts were seen to increase with the temperature of dehydration.

Scanning electron microscopy confirmed that dehydration had been accompanied by a change in texture of the crystals which led to a more porous mass.

The evidence provided to date would tend to indicate that optimum moisture levels exist for particular formulations, this will be particularly significant for moist granulation formulations. Accurate moisture levels should therefore be determined routinely during formulation research, development and production.

## 1.5 Environmental Factors

The room temperature and humidity can cause problems during tablet manufacture if not controlled. The main contributions made by humidity are during the storage of the materials for compression which could result in the effects detailed above or during storage of the compacted materials.

### 1.5.1 Humidity

The changes in compact strength with storage in different environmental conditions have been well documented. Chowhan and Palagyi (1978) concluded that the increase in tablet strength with storage time was due to partial moisture loss, which was dependent on the humidity during storage. The moisture loss from the tablets was due to the recrystallization of water-soluble excipients or drug which are expelled into the void spaces during compression. The extent of strength increase is dependent on the aqueous solubility and crystalline properties of the drug and excipients. Bhatia and Lordi (1979) came to similar conclusions by measurement of conductance of compacts during storage. The conductance is related to the number of interparticulate points of contact and the effective internal surface area within a compact. As compacts harden the conductance decreases

reflecting an increase in contact area. The principal hardening mechanism was considered to be due to loss of trace water. In a later study Lordi and Shiromani (1984) attributed similar strength changes to the "healing" effect of moisture on fractures or flaws within the compact, which brought the points of contact closer together. The hardening effect due to moisture loss and recrystallization has been confirmed by Chowhan (1980) with respect to binders and by Nyqvist and Nicklasson (1981) using sorption isotherms.

Friction during compaction results in surface energy being stored as lattice defects. As a result the surface becomes amorphous and highly reactive. The available atmospheric moisture was proposed to act as a medium for structural rearrangement at these sites by Down and McMullen (1985).

#### 1.5.2 Temperature

Temperature changes will affect the cohesion, deformation and flowability of certain powders. Ambient temperatures should only vary by a small amount in a production tableting facility even between different latitudes due to effective air conditioning. However during the tableting of pharmaceutical powders, temperatures of 5-30°C above ambient occur due to the generation of frictional heat at points of contact between particles Nelson et al (1955), Hanus and King (1968), Travers and Merriman (1970).

Powder particles are only in contact at the tips of their asperities, the application of pressure to the bed will result in very high pressures at these points. Melting of the asperities may then follow. The melting of asperities that occurs under pressure will be dependent on ambient temperature York and Pilpel (1972). As a result of melting, the contact area between the particles will increase causing pressure relief. Solidification will then take place

increasing the strength of the bed. If the temperature is raised as the pressure is applied then complete melting of the asperities may occur and a liquid film form around the particles. This will reduce the friction and adhesion between the particles.

Densification and compression of materials are facilitated as they are cooled from homologous temperatures of 0.7 to 0.5. This was attributed to a reduction of cohesive forces between particles by Onyekweli and Pilpel (1981). Esezobo and Pilpel (1986) used four directly compressible fillers and a paracetamol formulation to investigate the effect of temperatures between -10 and +65°C on the ER/SR parameter. It was found that as temperature increases the extent of plasticity and stress relaxation increase while the elasticity of a material decreases.

#### 1.6 Machine Variables

There are two types of press in common use: i) The single punch or eccentric press, which uses a single pair of punches and a die to output between 150-200 tablets per minute. Compression is applied by the upper punch which is connected to an eccentric cam against the stationary lower punch. ii) The multi-station rotary press, which has a number of sets of punches mounted in a rotating turret and dies in a central table. As the turret rotates the punches are guided up and down fixed cam tracks which govern the filling and ejection. Compression is achieved by passing the punches between sets of rollers. The output of such machines can exceed 10,000 tablets per minute. Single punch machines are mainly used for formulation research and development while the higher output rates of the rotary machines are utilized in tablet manufacture. The specifications of each tablet machine manufacturer and indeed each model differ widely with respect to the number and magnitude of compressions, the compression profile,

tooling specification, and the compression speed. These factors will exert an effect on the properties of the tablets produced, consequently knowledge of these factors are of importance to the formulator.

#### 1.6.1 Compression Force

This parameter is a major influence on many tablet properties including strength, hardness, friability, specific surface, porosity, density, dissolution and disintegration time. As the applied force is increased the density of the bed is increased according to the sequence of events described earlier in section 1.1. The apparent density of a tablet is exponentially related to the compressional force, until the limiting density of the material is approached (Higuchi *et al* (1954)).

Train and Lewis (1957) showed that the distribution of forces within a powder bed during one sided compression were not distributed evenly. In fact a complex force pattern was formed by the force being transmitted to and reflected from the die wall. The deformation during compaction will be proportional to the applied force. Consequently the zones of high and low force produce similar zones of high and low density through out the bed. High density wedges developed in the top corners of the compact, while the centre top face was less consolidated. At the base of the compact the density was highest in the centre although the values were lower than the upper surface. Thus the strength will vary within the tablet. Aulton (1981) demonstrated that the density distributions outlined by Train were subject to the material and the pressure attained during compression. The density distributions of Train were confirmed at 70% relative density, but increasing consolidation towards 100% modified the density distribution to the reverse of that previously described.

Avicel compacts were found to assume the 'reverse' density configuration over the whole compression range studied.

The increasing density associated with increasing compression force would be expected to increase the time taken for disintegration. Often there is an exponential relationship between compression force and disintegration time as seen for aspirin and lactose by Higuchi, Elowe and Busse (1954). In other formulations there is an optimum compression force / disintegration time ratio, such as aspirin lactose and starch. Some disintegrating agents act by imbibing water, swelling and exerting disruptive forces on adjacent particles. Under low compression forces the distance between adjacent particles will be relatively great. Consequently such systems would experience a lag time in disintegration due to the time taken to make contact across the large voids between particles. For tablets prepared at higher forces the contact between disintegrant particles may be continuous, hence swelling immediately initiates disintegration, causing the most rapid disintegration. For tablets compressed at greater forces the porosity is reduced increasing the time for water penetration, increasing the disintegration time.

The effect of compressional force on the dissolution of disintegrating tablets is difficult to predict. For a conventional tablet dissolution will be dependent to some extent on the pressure range, the dissolution medium, and the properties of the drug and excipients. However dissolution may vary with compression force in four general ways, it may increase, decrease, increase to a maximum then decrease or decrease to a minimum then increase. If fragmentation of the granules occurs during compression, dissolution is faster as the compression force is increased. If bonding of the particles is predominant the increase in compressional force causes a decrease in dissolution.

The complex nature of the effects of compression force were illustrated by Khan and Rhodes (1976). The properties of six direct compression tablet formulations were investigated with respect to compression force. Tablet hardness and apparent density increased with the applied force as expected while the disintegration times were found to increase, decrease or be independent of the applied force over the range studied.

#### 1.6.2 Precompression

Precompression is the smaller preliminary compression force which may be applied immediately prior to the main compression on some rotary tableting machines. Precompression is usually applied by a pair of small diameter rollers between which the upper and lower punches pass. The pre and main compression pressure may be altered independently in order to optimise compression conditions. It has long been recognised that the use of precompression can reduce the incidence of capping and lamination.

Two mechanisms are thought to be responsible for this precompression effect. Gungel and Kanig (1976) proposed that the tamping action of the precompression removed some or all of the air from the powder bed, the de-aerated compact was then subjected to the main compression to form a robust tablet. If the air is not removed by precompression then during decompression the entrapped air expands within the tablet developing internal faults which result in lamination and capping. Hiestand et al (1977) explained the capping event as failure of the tablet to withstand the internal stresses of strain recovery and proposed that precompression effectively extended the dwell time of the compression. As the compact is held under load for an increased period the extent of stress relaxation is increased resulting in more particle-particle bonds and a stronger tablet.

Mann *et al* (1982,84) confirmed that the effects of precompression were in fact a combination of these two mechanisms. The extent of each depending on the powder bed porosity, speed and magnitude of the pre and main compression pressure. Vezin *et al* (1983) stated that the increase in dwell time was not sufficient to account for the improvements in tablet quality seen with precompression, and that the separation of the two compression events was of greater importance. This indicates the involvement of a relatively slow time dependant phenomena.

### 1.6.3 Tooling

The stress distribution within tablets discussed to date have been based on cylinders; if other than flat faced punches are used then the stress distribution will change. Aulton and Tebby (1975), Aulton (1981) produced compacts using punches with increasing concavity and measured the indentation hardness across the compact surfaces. As the curvature of the punch tip increased from flat to shallow concave to normal concave the indentation hardness reduced and became more uniform. This indicated that the stress distribution within the compact was also becoming more uniform. It was proposed that the curved surface of the punch tip was directing the stress towards the centre of the compact. A further increase in punch curvature from normal concave to deep concave to ball shaped resulted in a more dramatic reduction in indentation hardness especially towards the centre of the compact surface.

The forces required to achieve zero porosity for a range of different punch tip shapes were calculated by Sixsmith (1980). As the punch curvature increased a higher force would be required to achieve zero porosity. This phenomenon was explained by considering the powder adjacent to the moving punch face being 'protected'. Hence for a

curved punch the powder within its arc is relatively protected until the main body of the tablet is compacted. As compression proceeds the compacted main body acts as a secondary punch face against which the 'protected' region is compressed. The movement of powder under similar compression conditions were monitored by Sixsmith and McCluskey (1981). The presence of the 'protected' region adjacent to the moving punch was confirmed, and the greater compression of the bottom half of the tablet demonstrated. The resolution of the compressive forces acting on particles using curved punches was towards the centre of the compact; the greater the curvature the nearer to the punch face was the action of the resultant forces. Hence the high density regions would be situated closer to the moving punch. These regions then support the load forming the protective regions. Lateral powder movement also increased with punch curvature forming a high density region within the main body of the compact. Between this dense region and the soft 'protected' region stress boundaries will form. Capping will tend to occur along these stress boundaries; the stress difference and hence capping tendency become more pronounced with an increase in punch curvature.

In a single punch tablet machine the compressional force on the upper punch is greater than that on the lower punch. The difference between the two forces is the force required to overcome die wall friction. The die-wall friction will be dependant on the surface smoothness and the diameter of the die. Lammens et al (1980,81) investigated the effects of punch and die diameter on compaction. It was demonstrated that the upper punch pressure required to effect a certain compact density decreased with increasing diameter, whereas the lower punch pressure proved to be independent of diameter. This was shown to be due to the influence of die-wall friction.

The precision of the fit between the punches and die was shown to have an effect on the capping pressure of pharmaceutical materials by Mann et al (1981). As the punch tolerance was reduced the capping pressure was also reduced, this phenomenon was exacerbated by increased compression speeds and increased initial bed porosity. Thus the precision of tooling may control the escape of air from a compact during compression which is a contributory factor in the capping of tablets.

#### 1.6.4 Time-Displacement Profiles

The time-displacement profile of a particular tableting machine will be peculiar to that machine under the setting conditions defined. The most obvious differences will be between a single punch and rotary tableting machines. The physical differences observed between tablets produced on the two types of machines have been largely attributed to differences in the punch dwell time (time at peak force Jones 1981) during the compaction process. Charlton and Newton (1984) calculated and compared some cycle parameters for these two types of machine. Although the initial punch speeds of the two machines were similar the compression times were 0.1 seconds on a single punch machine and 0.052 seconds on a rotary machine. While the compression times for a single punch machine are equal to the contact time between the powder and the punches, the rotary machine has extra dwell time due to the flat portion of the punch head giving a contact time of 0.083 seconds. The rotary machine takes a shorter time to reach maximum displacement inducing greater elastic strains in the material being compressed which will be more likely to cause capping or lamination. This explains why scale up problems are often encountered when formulations are developed on single punch machines used in the laboratory and then transferred to the high speed rotary machines used in production.

More subtle differences in the physical properties of compacts will be noticed between rotary machines made by different manufacturers and between different models. Hoblitzell and Rhodes (1986) investigated these effects using three different rotary tableting machines. No significant differences between compacts produced by each machine could be isolated. This was perhaps due to the similarity between the displacement-time profiles for the machines tested. However significant differences would be predicted for machines with different displacement-time profiles due to the diameter of the compression roll and gradients of the punch guides, especially when the presence of a precompression roller comes into play. To investigate the effect of changing displacement time profiles using traditional instrumented tableting machines would not be easy, a more versatile machine was required.

The influence of the individual segments of the tableting cycle were investigated by Mann (1984,87) using a compression simulator. The cycle was divided into compression, decompression, residence and ejection, and the contribution of the rate of each segment to the capping and lamination of two formulations were assessed. The compression segment was found to have the greatest influence, with decompression having a minimal effect. This indicated that the mechanism of capping for these formulations involved air entrapment which occurs only during compression.

#### 1.6.5 Speed of Compression

As relatively high rates of compression are used in the pharmaceutical industry the effects of strain rate and dwell time will be important. Tablet machine design features such as precompression rolls, cam profiles, main pressure roll diameter, punch head profile and the rate of operation of the press will determine the time

available for bonding processes to occur. A common example of the effect of compression speed is the deterioration in tablet quality, including reduction of tablet strength, development of lamination and capping that sometimes occurs after transferring a formulation from a single punch to a rotary tableting machine.

The importance of time dependent deformation has been known for some time. Stress relaxation investigations have been used to quantify plastic flow of pharmaceutical materials under constant strain Shlanta and Milosovich (1964). As plastic deformation is a time dependent phenomena, the compression rate will effect the extent to which it occurs. David and Augsburg (1977) examined the effects of the overall duration of the compression cycle and dwell time on the tablet strength of various direct compression fillers. No increase in tablet strength for brittle materials such as lactose and compressible sugar were observed when the duration of the compression cycle was increased from 0.1 seconds to 10 seconds. Under the same conditions compacts prepared from plastic materials, microcrystalline cellulose and compressible starch showed an increase in compact strength with increased cycle time. This confirmed the importance of plastic deformation in creating strong bonds within a compact. However for a perfectly elastic brittle material the compact strength does not depend significantly on the rate at which the compression force is applied, or the time for which the force is maintained (Rees (1980)).

The Heckel equation (1961a,b) was employed by Rees and Rue (1978) to examine the effects of changes of the relative density with contact time. Tablet density increased with contact time for plastic materials such as Avicel and Sta-Rx, due to the increased time available for plastic deformation. Brittle materials such as Emcompress showed no change in density with contact time. The strength of Emcompress compacts were shown to be independent of compression speed by

Armstrong and Blundell (1985). For lactose the effects of speed were shown to depend on the substance rather than its physical form.

The effect of compression rate on the dissolution of phenylbutazone polymorphs was reported by Tuladhar, Carless and Summers (1983). When the contact time during compression was decreased from 29 seconds to 0.26 seconds the dissolution time of the 6 $\mu$ m particles of drug decreased indicating less bonding had occurred. This effect however was not observed for larger particles of +137 $\mu$ m. Although an explanation of this phenomenon was not offered at the time the work by Kendall (1978) may provide one solution. If the critical particle size below which flow will occur is between 6 and 137 $\mu$ m then greater plastic nature would be expected from the 6 $\mu$ m size fraction. Consequently the time dependant deformation of the 6 $\mu$ m size fraction would be greater.

The recovery of ibuprofen was shown to be dependent on the compression speed by Marshall, York and Richardson (1986). The reduction in the extent of recovery at a given pressure with increasing duration of compression was attributed to a shift of energy from elastic to plastic deformation.

The strain rate sensitivity of pharmaceutical materials has been investigated by several workers over a wide range strain rate, using various combinations of compressing devices. Barton (1978) investigated the effect of strain rate on the degree of volume reduction of sodium chloride, potassium bromide and Dipac sugar and found that larger volume reductions occurred at lower rates. Compression rates beyond those experienced in tableting, 2m/s to 5m/s were investigated using a drop hammer but results were inconclusive due to the inaccuracies of the method. Al-Hassani and Es-Saheb (1984) utilised a compression simulator, a drop hammer and a air gun apparatus to produce strain rates from 10<sup>-3</sup>/s to 10<sup>5</sup>/s. Most materials

were found to produce an increase in axial pressure with strain rate. This increase was considered to be a consequence of a change in deformation mechanism from plastic to brittle. Paracetamol D.C showed behaviour to the contrary and actually softened up to a strain rate of  $10^2/s$ . No explanation was offered for this peculiar behaviour.

Morimoto, Hayashi and Nakanishi (1984) used an Instron type testing machine and a gas gun to attain strain rates of  $2 \times 10^{-3}/s$  and  $2.7 \times 10^3/s$  respectively in aluminium powders. It was proposed that plastic deformation occurred first in the larger particles at lower relative density and smaller particles began to deform plastically as the relative density increased at both strain rates. However the smaller particles started to deform earlier at the higher strain rate. At such compression speeds deformation occurs in a very short time during the passage of a shock wave front through the particle. There is also insufficient time for particle rearrangement. The extrapolation of data obtained from such investigations must be questioned due to the different loading profile produced by such as a drop hammer or a gas gun compared to a tableting machine, additionally these strain rates are well in excess of those of current tableting machines.

The effect of compression speeds between 0.033mm/s and 400mm/s were investigated by Roberts and Rowe (1985) using a Compression Simulator. This range of speeds encompasses the velocities of research testing machines (0.05-5cm/min) through single punch machines (50-150mm/s) to rotary machines (100-1000mm/s). Data were analysed using the Heckel equation (1961a,b) and a proposed strain rate sensitivity index (SRS):

$$SRS = [ ( P_{v2} - P_{v1} ) / P_{v2} ] \times 100$$

Where  $P_{v1}$  is the yield pressure at a 0.033mm/s and  $P_{v2}$  is the yield pressure at 300mm/s. Materials expected to consolidate by plastic

deformation produced higher strain rate sensitivities. The mechanisms suggested that for an increase in yield pressure there was a reduction in the amount of plastic deformation and thus bond formation and or an increase in brittle behaviour. The former mechanism was favoured for plastic materials such as Avicel, maize starch and Corvic. Other materials were thought to undergo changes from ductile to brittle behaviour. For materials known to consolidate by fragmentation such as magnesium and calcium carbonate there was no change in yield pressure with compression speed. The extent of particle slippage and rearrangement was noted to decrease with all materials as compression speed increased. This was explained by an increase in the frictional and adhesive forces between particles opposing the rearrangement, and a secondary contribution at higher compression speeds of air escaping from the powder bed. The same workers extended this study in 1986 to include the effect of particle size. For brittle materials such as lactose the SRS index decreased as the particle size was reduced indicating a reduction in the extent of fragmentation. For microcrystalline cellulose a material that deforms mainly by plastic deformation the SRS index was independent of particle size. However as the aggregate size of this material increased the SRS decreased, indicating an additional initial fragmentation of particles was tending to restrict the main deformation mechanism of plastic flow. The mechanical pretreatment of materials was shown to have an effect on the deformation mechanism of a phthalazine derivative. As the particle size decreased the SRS decreased suggesting a change in deformation mechanism from plastic to brittle, which was contrary to that expected. This was thought due to the method of size reduction employed, the smallest size fraction was prepared by fluid energy milling. Size reduction by fluid energy milling was proposed to

generate work hardened material which would behave as a brittle material.

Armstrong and Palfrey (1987) proposed three methods of calculating power expenditure during compression. It was found that as the compression speed was increased the power expenditure increased due to the decrease in the time over which the work was done. Discrepancies were found between the three methods due to differences between the predicted and actual punch velocities.

The effects of speed of compression can be seen to be of fundamental importance in the compaction of powdered materials. Until recently the technology to investigate this parameter has not been available, which accounts for the limited amount of research carried out into this critical parameter. With the advent of the Compression Simulator an ideal versatile machine has been made available for this purpose. Such a machine will be utilised during the investigation into the effects of compression speed reported in this thesis.

## 1.7 Investigative Equipment

### 1.7.1 Instrumented Single Punch Machine

Initial research into the tableting process was hindered by an inability to measure force and displacement during the compression event. In 1954 Higuchi *et al* attached strain gauges to various parts of a tablet press, facilitating the accurate measurement of force. This enabled the physics of tablet compression to be studied. Since this time instrumentation of single punch presses has developed. Piezoelectric transducers and linear variable differential transformers (LVDTs) have been used to monitor the forces and displacement experienced by the punches during a compression. Although some useful data may be obtained by such methods it cannot always be

correlated to the production situation where high speed rotary machines are used.

### 1.7.2 Instrumented Rotary Machines

One of the major differences in the instrumentation of a rotary machine as opposed to a single punch machine is the inherent difficulty in retrieving electrical signals from the revolving turret. This was overcome using radio telemetry to transmit the signals from strain gauges and LVDTs on the upper and lower punches as described by Ho, Greer and Clare (1978). Alternative indirect methods have been proposed where load transducers have been attached to remote stationary sites on the machine, mainly compression roll carrier systems, tie rods, compression columns and ejection cams. Such machines relate directly to the production situation and yield useful compression, lubrication and powder flow data. However large quantities of a formulation are required which may not be available for a new chemical entity formulation. Diversity of tablet machine design may prohibit the transfer of results to a different model of machine due to variation of the time, magnitude and rate of application of the pre and main compression force.

### 1.7.3 Physical Testing Machines

Mechanical testing machines have been used for fundamental investigations. Such machines rely on a screw feed drive to compress materials in a single punch and die set often supported in a specially constructed jig. As with the single punch machines, conditions differ from those of a rotary machine with respect to the stress distribution produced in the tablet and the friction effects at the die wall. In an attempt to overcome these factors a simulation device was developed by Rees, Hersey and Cole (1972) which produced the double acting

compression effect of a rotary tableting machine. The device was designed for use with mechanical testing machines and as such was limited by its relatively slow compression speed.

#### 1.7.4 Compression Simulators

In 1972 details of the first high speed compression Simulator were presented by Hunter *et al*. The details of this type of machine will be detailed later. Since the development of the first simulator by ICI Pharmaceuticals five further Simulators have been developed world wide and are located at The Boots Company Nottingham, The Wellcome Foundation Dartford, Glaxo Group Research Ware, SK&F Philadelphia USA, and Liverpool School of Pharmacy.

Although it may be expected that compression Simulators in the industry would be used mainly for formulation development and production trouble shooting, a great deal of valuable research has been produced. In the early 1980s research based around the Simulators began to appear in the literature.

Mann *et al* (1981,82,83,84,87) investigated the phenomena of tablet capping with respect to punch tolerance, air entrappment and precompression. More recently Roberts and Rowe (1985,86a,b,87a,b,c) have used the same machine to investigate fundamental material properties including brittle fracture propensity, strain rate sensitivity, ductile brittle transitions and Young's modulus of pharmaceutical materials.

Marshall York and Richardson (1986) using the Boots Simulator determined the nature of and quantified recovery by Ibuprofen following compression. Using the same machine Pitt, Newton and Richardson (1987) investigated the effect of punch velocity on aspirin. The Wellcome Simulator was used by Ho (1986) to investigate the fundamental properties of tableting excipients.

The trend towards the use of Simulators by the Pharmaceutical industry appears to be increasing and should yield an increased knowledge of the causes of compression problems and improved development of formulations.

#### 1.8 Conclusions

The compaction of powders has been investigated in some depth, and has produced detailed knowledge of the mechanisms which occur during compaction and the factors that influence them. One of these factors namely the speed of compaction has received little attention to date over the range of speeds used by current production tableting machines. This is probably due to the lack of equipment available capable of operating at such rates of strain and with sufficiently rapid data collection . However with the advent of the Compression Simulator it will now be possible to further investigate the effects of speed of compaction with respect to the properties of compacts.

In order to investigate the effects of speed of compaction a high speed hydraulic press will be commissioned, validated and developed into a Compression Simulator with a suitable control system, instrumentation, data acquisition and data analysis.

Much of the work to date in the field of compaction has been concerned with model systems, such as sodium chloride and paracetamol. Although data from such systems has provided the basis for todays compaction theory, it is often difficult to extrapolate such data to real formulations. For this reason a material that has proved difficult to compress, and has received little attention previously, namely ibuprofen will be investigated. The pure drug will be characterised in terms of its mechanism of compaction and its strain rate dependance. This system will be brought closer to the production situation by incorporation of various excipients. 'Real' formulations

will then be utilized to evaluate other machine variables such as compression force and precompression.

The most appropriate evaluation of the effects of speed were considered by Heckel and energy analysis combined with tensile strength determinations. The other machine parameters will be investigated using disintegration and tensile strength tests. It would be expected that the studies described above will contribute to a better understanding of the effects of machine variables on the properties of compacts already established by previous investigators.

## 2.1 The High Speed Hydraulic Press

The high speed hydraulic press was supplied by ESH Testing LTD of Leys Road, Brockmoor, Brierley Hill, West Midlands. It consisted of three main sections; the load frame, the hydraulic power supply, and the electronic console. These sections are related as shown in FIG 2.1a

### 2.1.1 The Load Frame

The load frame shown in FIG 2.1b has four columns which provide rigidity and stability. These columns support a hydraulically adjustable upper crosshead, a fixed lower crosshead, and the centre crosshead which houses the die holder. Identical hydraulic servo actuators are mounted centrally on the upper and lower crossheads. The actuators are cylindrical pistons under the control of two Moog three stage five port servo valves. Hydro-pneumatic accumulators are fitted to the pressure and return hydraulic lines to provide power for single shot compressions and clamping of the upper crosshead.

One  $\pm 25\text{mm}$  Linear variable differential transformer (LVDT) is mounted concentrically within the rear ram of each actuator to provide stroke control data. At the other end of the actuator is a  $\pm 50\text{KN}$  low profile strain gauge load cell, which can accept 'F' machine punch holders.

### 2.1.2 The Hydraulic Power Supply

The Actuators are driven by the hydraulic power supply see FIG 2.1c. This consists of a 22kW (30hp) electric motor and fixed capacity hydraulic pump mounted on a 250l hydraulic fluid reservoir. This unit is capable of delivering the Hydraulic fluid (Shell Tellus 68) at a rate of 45l/min at a pressure of 28MPa. This can drive the actuators up to a theoretical maximum speed of 3m/s and apply a force

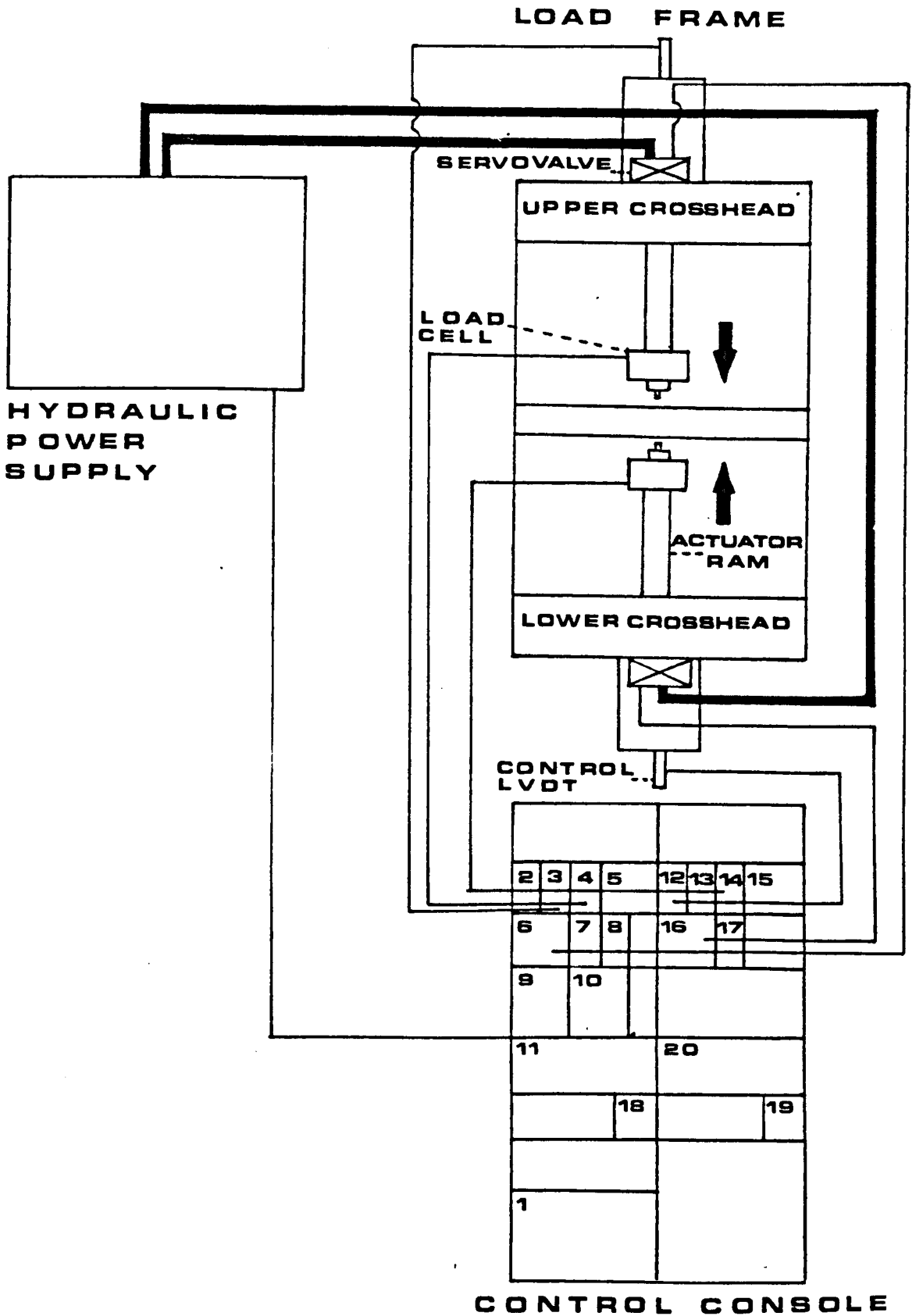


FIG 2.1a Diagramatic Representation of The High Speed Hydraulic Press. For an Explanation of the Modules 1 - 20 see the Text.



FIG 2.1b The Load Frame



FIG 2.1c The Hydraulic Power Supply

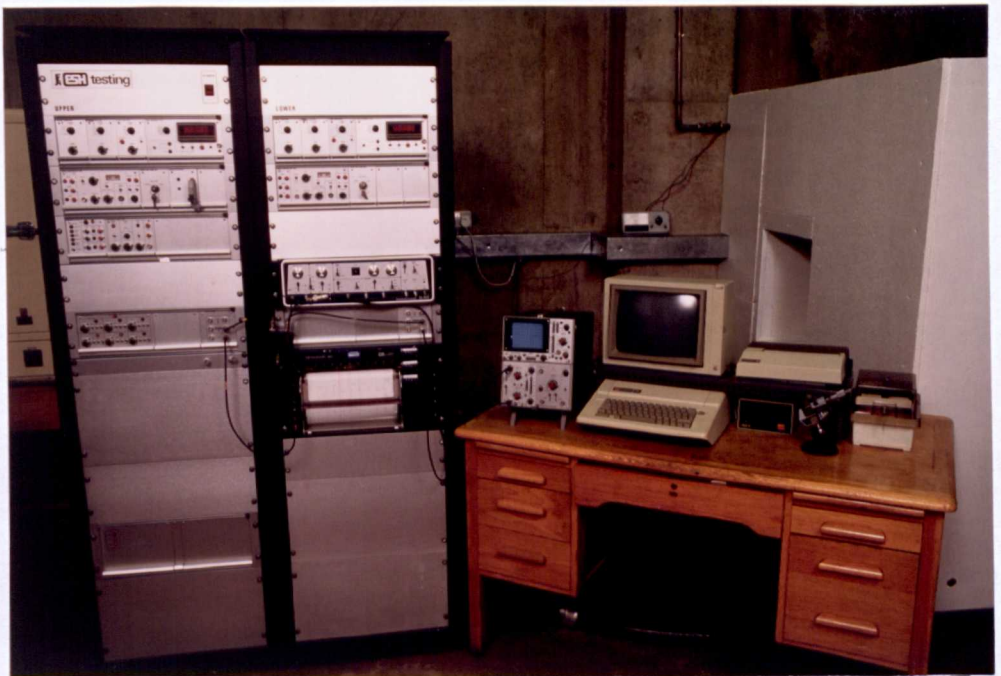


FIG 2.1d The Electronic Control Console and Microcomputer

of up to 50kN. The hydraulic fluid is maintained at 55°C during operation by cooling water supplied at a rate of 30l/min.

This unit generated in excess of 80db at 1m and was consequently housed in an acoustic box. This box was constructed using composite walls with layers of pegboard, polythene sheet, fibreglass and high density chipboard. The box was ventilated to prevent the electric motor over-heating using a Hatton 204mm diameter high speed fan.

### 2.1.3 The Electronic Control Console

This consists of a number of different modules as shown in Fig 2.1a.

1) The control and measurement system depends for its performance on a number of amplifiers in the various units. These amplifiers in turn require high quality DC supplies to ensure correct operation. The power supply module generates these supplies to the required standard from the AC mains input, and in addition an auxiliary DC supply for operating relays, indicators and logic circuits. Interruption of the mains supply to the electro-hydraulic system may cause the actuator to make uncontrolled movements. This danger is averted by the use of back-up batteries which maintain the DC power supplies.

2,3,12,13,) These modules are AC conditioning amplifiers for the displacement transducers. They contain an adjustable stable AC excitation source and a AC amplifier.

4,14) DC conditioning amplifiers for use with the upper and lower load cells. A four position switch selects the load range. Zero adjustment is obtained by a ten turn calibrated potentiometer, and overall calibration may be checked using the push button electrical calibration.

5,15) The digital meter provides a readout of the output signal of any of the transducer conditioning amplifiers in the system. The meter has an analogue memory circuit which may be set to store a maximum or minimum peak value. The readout may be displayed in volts or converted to engineering units.

6,16) The servo controllers. These are the basis of any closed loop control system. They continuously compare the actual value (feedback) of the controlled parameter with the desired value (command value), and derive the difference, or error signal. This is used to drive the system towards the desired value and thus the error signal towards zero. The selection of the mode of control either load or displacement is implemented using this unit.

7,17) These modules were designed to enable or disable operation of the press at high speed. In practise this interlock has limited effect and is not used.

8) The control console/computer interface. This provides the facility to connect a computer to the system. Control and or data acquisition may then be achieved with suitable hardware and software.

9) The hydraulics control module, provides remote control of the hydraulic power supply. It also contains the system interlocks, relays and indicators which act as the systems fault detector.

10) The high speed ramp generator. This module provides a linear voltage ramp input signal at a preset rate. If used in displacement mode such a linear ramp may be used to effect a compression, however

the decompression requires a second button press. The variability this causes limits the use of this module for tableting.

11) The limit detector. The function of this module is to warn the operator or shut down the hydraulic system if a pre-set parameter is exceeded. However as this machine operates at high speeds this module is of little use, as the time taken to respond is often greater than the time over which the compression takes place.

18,19) Output panels. These modules provide output to external devices of the signals from the transducer conditioner amplifiers in the system.

20) Datalab DL902 two channel transient recorder. This instrument is capable of recording two independent waveforms simultaneously at variable sample rates up to 1MHz with 8bit amplitude resolution.

#### 2.1.4 Displacement Closed Loop Feed-Back Method of Actuator Control

The flow of hydraulic fluid to and from the actuator is controlled by a Moog servo valve . This is a pilot operated closed centre, four way sliding spool valve in which the output flow to a constant load is proportional to electric input current. In the simulator they are used in the closed loop position to give a precise fast response control at high power levels.

See FIG 2.3e

When the system is under displacement control and the actuator is at the command position, the servo controller monitors the difference between the command signal and the feed-back signal. As no output is being sent to the servo controller the system remains in dynamic balance and the actuator remains stationary at this 'null position'.

FIG 2.1e Servo valve in the closed loop configuration

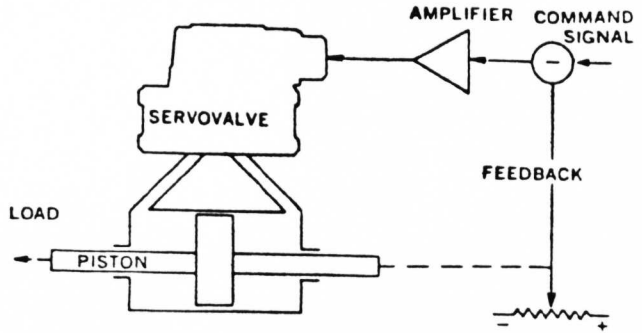
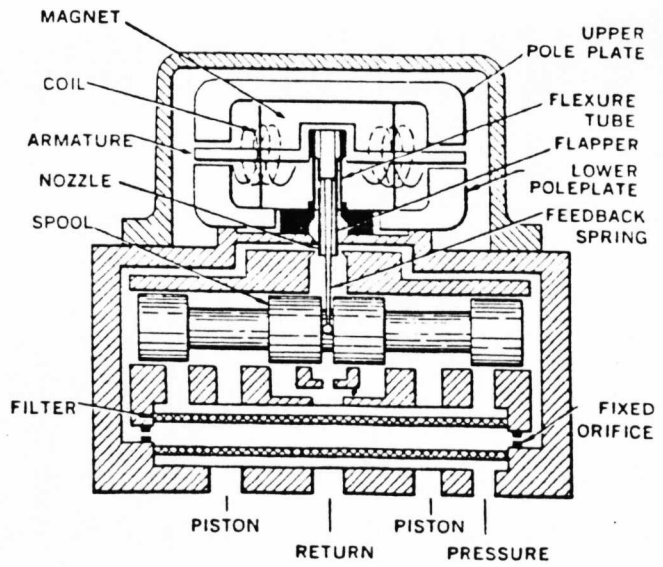


FIG 2.1f Cross section through a servo valve



The 'null position' can be set at any point within the  $\pm 25$ mm stroke range of the system. The stroke range can be shifted by adjusting the zeroing potentiometer on the control displacement LVDT amplifier (3). This generates a command signal which is transferred to the servo controller, where it will be compared with the present feed-back signal. The voltage difference will then be converted to a current called the error signal, which will then be amplified and sent to the servo valve mounted on the load frame.

The servo valve consists of a polarized electrical torque motor as shown in FIG 2.1f and three stages of hydraulic power amplification. The input signal induces a magnetic change in the armature and causes a deflection of the armature and the flapper. This assembly pivots about the flexure tube and increases the size of one nozzle orifice and decreases the size of the other. This creates a differential pressure from one end of the spool to the other, displacing the spool and causing torque in the feed back wire which opposes the original signal torque. Spool movement continues until the feedback wire torque equals the input signal torque. The oil flow through the valve is proportional to the spool position. The flow through the valve into the actuator housing causes the actuator ram to move.

The control LVDT attached to the end of the actuator ram will detect the resulting displacement and send a corresponding feed-back signal to the servo controller. This feed-back signal will cause a reduction in the difference between the command signal and the feed-back signal, which in turn reduces the error signal. This process continues until the actuator has moved to a point where the output of the controlling LVDT is equal to the command signal. The voltage difference is then zero and the valve is at the 'null position' with no flow of oil.

The hydraulic press could perform single unidirectional high speed compression ramps. Displacement and force could be monitored during compression using the control LVDT's, and the load cells respectively. The transient recorder could be used to store the data. In order to convert the high speed press into a Compression Simulator capable of reproducing the time displacement profiles seen on tableting machines, considerable modifications to the control and data acquisition systems would be required. These modifications were made during the commissioning and validation of the machine.

## 2.2 Commissioning

The commissioning of a piece of equipment may be defined as the procedures carried out to bring the machine into operation. In the case of the high speed press this could be divided into hardware and software projects. The mechanical and electronic engineering consisted of; securing the hydraulic system against leaks, refitting and sealing the pneumatic shock absorbent feet of the load frame, response optimisation and alignment of the actuators, design and fabrication of a die holder and measurement LVDTs mountings. Software and hardware had to be developed to permit microcomputer control of the system and enable data transfer from the transient recorder to a computer for analysis.

The securing of hydraulic leaks and sealing of the pneumatic absorbers are not peculiar to this system and will not be discussed further.

### 2.2.1 Design and Installation of the Die Holder and Measurement LVDTs

The simulator was supplied with 'F' machine compatible punch and die holders. The die holder supplied was designed such that the die itself was recessed into the centre crosshead which reduced visibility and accessibility. It required potentially dangerous procedures to lubricate or fill the die and to remove the tablet. Consequently a new die holder was designed in which the die was flush with the top of the centre crosshead as shown in FIG 2.2a. A lower punch adjustment ring was also required to effectively raise the punch, compensating for the increased level of the die which can be seen in FIG 2.2b.

The simulator was supplied fitted with two  $\pm 25\text{mm}$  control LVDTs. These LVDTs are only used when controlling the motion of the actuator and not for measuring dimensional changes in the compact as they are located too far away from the punch tips for accurate measurements.

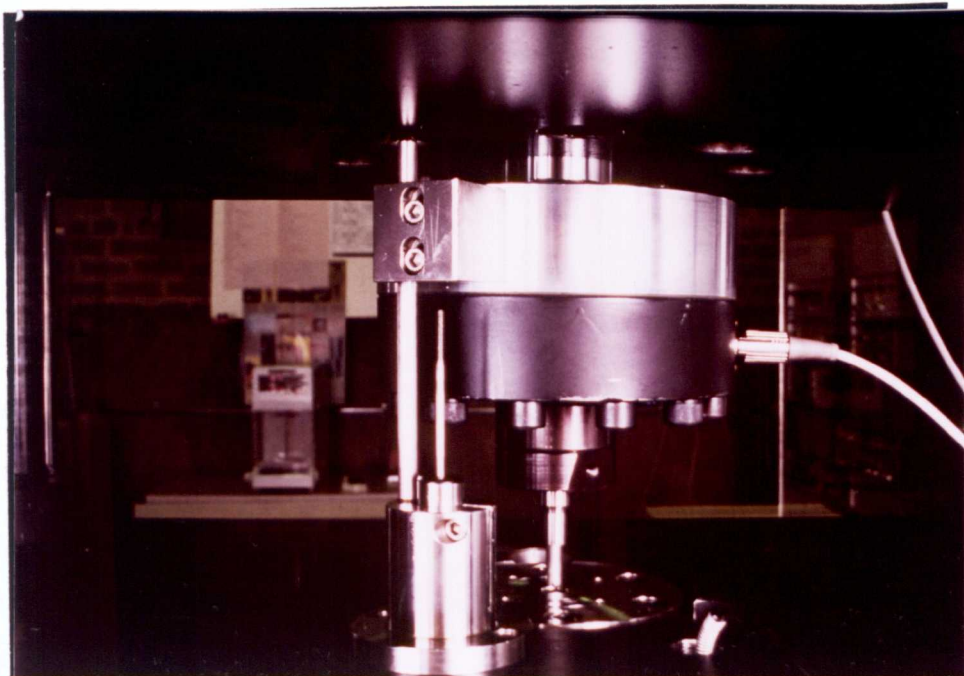


FIG 2.2a Upper Load Cell, Die and LVDT Support with Guide Rail

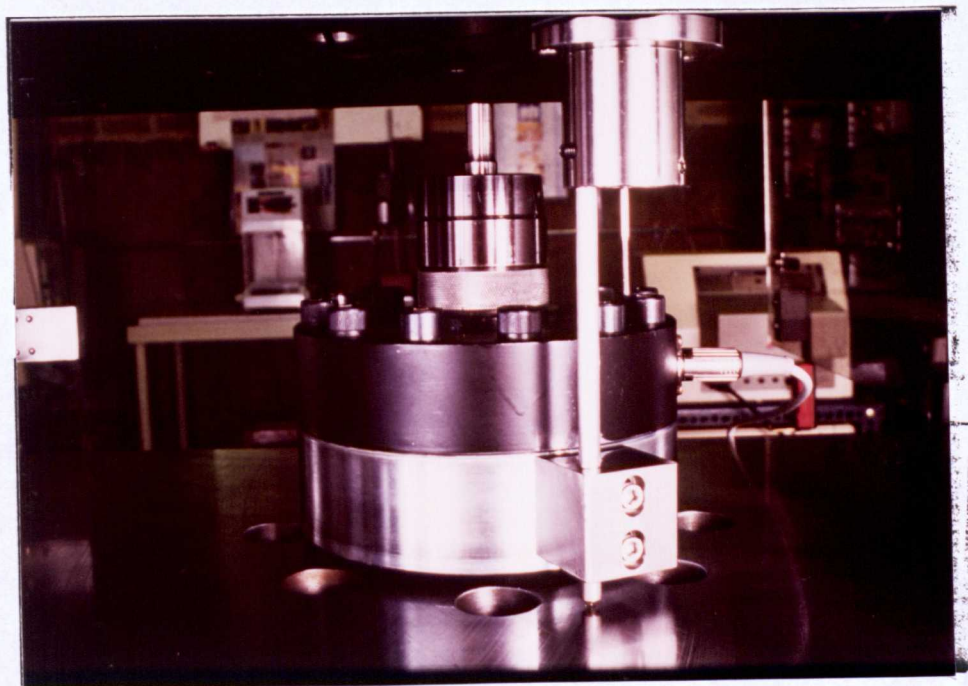


FIG 2.2b Lower Load Cell, Spacer Ring and LVDT Support

For measurement of punch displacement within and close to the die two  $\pm 10$ mm LVDTs (model ACR/15/S, Sangamo Schlumberger) were selected. The  $\pm 10$ mm LVDTs required the design of a system to accommodate them.

It was decided to install the transducers within the centre crosshead supported by stainless steel clamping devices. The LVDT armature would make contact with a stop or striker block associated with the punch. The striker blocks were located as close to the punch tips as physically possible which in practice was against the load cell backing plate.

This system was found to have poor reproducibility due to rotation of the actuators. Modifications were made to rectify this. A guide rod was installed preventing rotation as seen in FIGS 2.2a,b which produced excellent reproducibility as demonstrated during the validation.

### 2.2.2 Alignment of the Actuators

The actuator rams were housed independently on the upper and lower crossheads. In order to ensure normal transmission of axial force the alignment of the actuators must coincide.

To assess the actuator alignment 12.5 mm flat faced Manesty 'F' machine punches were fitted in the punch holders. The punches were then allowed to make contact by bringing the actuators together. It was seen that the upper and lower punches overlapped. The actuator rams were then rotated to ensure the fault was not due to non parallelism of the rams. The misalignment remained.

Alignment was corrected by unbolting the eight bolts securing the actuator housing to the upper crosshead and adjusting the three alignment bolts on the upper crosshead until the actuator housing was in the correct position. The eight securing bolts were then tightened.

It was seen that tightening of the securing bolts shifted the alignment of the upper actuator. This was found to be due to a protruding threaded plug in the upper actuator housing acting as a lever against the crosshead. The housing was removed from the crosshead using the actuator as a jack. The plug was unscrewed, cut to an appropriate length and refitted. The alignment was readjusted and the housing secured.

### 2.2.3 Static Control and Response Optimisation

In order to attain the hydraulic fluid flow rates required to move the actuators at speeds of up to 3m/s, large servo valve orifices are required. A consequence of this is that very small fluctuations in the error signal cause relatively large movements of the spool as described earlier. With three further stages of hydraulic amplification the increased or decreased flow of oil through the valve will cause the actuator to move. This sequence of effects becomes important when there is no error signal and the actuator is at its 'null position'. Even a small amount of electrical noise on the error signal will result in movement of the actuator resulting in an apparent 'wobble'. The magnitude of this 'wobble' will be a function of the response of the system.

The response of the system is dependent on several adjustable parameters; dither, overall displacement system gain and the inner loop displacement gain. Dither is a low level high frequency (500Hz) signal which is fed to the servo valve to reduce the static friction. It reduces the maximum increment of input current required to produce a change in valve output flow. The gain of the displacement control system is the degree of amplification or attenuation of the error signal. If the gain is too low then control will be sluggish, conversely if the gain is too high, a command signal step-change may

cause the actuator to overshoot excessively and the system may go into violent oscillation.

The static displacement control was measured via the  $\pm 10\text{mm}$  LVDTs and the transient recorder. It was found to be unacceptably high at  $\pm 60\mu\text{m}$  for both actuators. The above parameters were optimised reducing this value to  $\pm 8\mu$ . Typical actuator static displacement control traces are shown in FIG 2.2c

Further improvement of static stability was investigated but could only be achieved by installing a second smaller master control servo valve to fill the dead space of the existing larger servo valve. This option could not be followed due to financial restraints. It was shown that the instability was confined to static control and did not effect dynamic displacement profiles. However stress relaxation work where static control would be required could not be carried out on this machine.

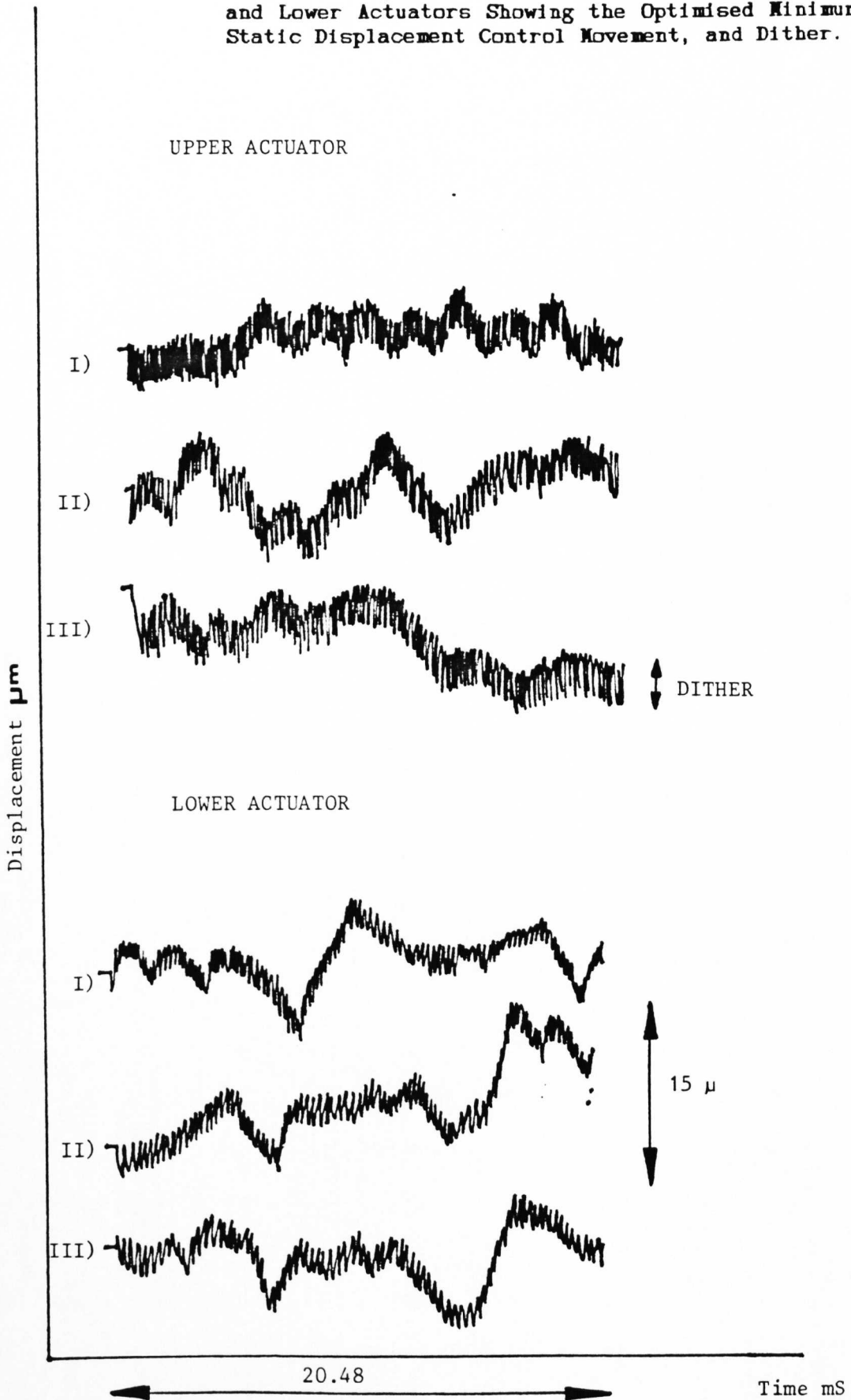
#### 2.2.4 Microcomputer Control of The Press

The simulator was supplied with an Apple IIe microcomputer fitted with an ESH digital to analogue converter board (D/A), and an analogue to digital converter board (A/D). In order to use the computer to control the simulator, software was required, which would fulfil the following criteria :-

- i) Create, store and edit displacement time profiles.
- ii) Drive the actuators according to these profiles.
- iii) Vary the speed of execution of these profiles.

A program was developed using Applesoft basic. It was capable of creating upper and lower punch displacement profiles, each defined using one hundred data points in millimeters entered via the keyboard. Alternatively sawtooth or haversine shaped profiles could be generated automatically by the software. These data points could be saved onto

FIG 2.2c Displacement / Time traces For The Upper and Lower Actuators Showing the Optimised Minimum Static Displacement Control Movement, and Dither.



floppy disk for permanent storage, recalled from disk, edited point by point and output via the interface at variable rates. Initially a basic subroutine was used to output the data points. The subroutine converted the data points to three four bit nibbles which were written to consecutive addresses on the D/A board starting at the channel base address. They were subsequently transferred to the twelve bit output buffer with a write operation to the fourth address. The output was handled as a percentage of the stroke range ( $\pm 25\text{mm}$ ). The following routine was used to output a percentage V1 to the channel whose base address was OC.

```
10 VO = V1 / 12.8 + 8 : POKE OC + 2 , VO
20 VO = ( VO - INT ( VO ) ) X 16 : POKE OC + 1 , VO
30 POKE OC , VO X 16
40 POKE OC + 3 , 0
```

This routine was found to be of limited use due to the slow rate of data output. The minimum displacement profile output time was four seconds. In practice profile output times would be required in the order of milliseconds. The program was improved by developing a machine code data output routine (see appendix for the subroutine listing). The resolution of the one hundred data points was found to be insufficient and so a further hundred were added (see appendix for the program listing).

The D/A card had four potential control output channels which were transmitted down a 25 way ribbon with Cannon D connectors to the control unit interface. This cable also supplied data output power and reference voltages to the card from the control unit. The displacement profile to be used for commissioning was a simple 'F' machine profile obtained from published data. The integrity of the control signal produced by the software and its effect on the actuators required confirmation.

The actuators were deactivated to reduce the risk of damage to the load frame. The Cannon D connector housing was removed exposing wire/connector soldered junctions, and a probe from a storage oscilloscope was connected to the upper and lower D/A output signal wires. The 'F' machine displacement profile was executed and the upper and lower signal outputs monitored.

The upper and lower control profiles were seen to be superimposed on an offset voltage. This offset was found to be due to a programming error. See line 10 of the routine listed on the previous page, the +8 was deleted, but this only reduced the offset. A second contributing offset was found to be due to a faulty circuit on the D/A card. An alternative output channel was used avoiding the faulty circuit. A parasitic interference and erratic spikes developed on the upper control signal. The parasitic interference on the upper control signal was due to a faulty integrated circuit on the D/A card; the faulty operational amplifier was replaced removing the interference. The erratic spikes on the control profile were traced to a poor connection between the D/A card and its edge connector. The connection was remade removing the offending spikes.

The actuators were then enabled, the profile executed and the control signals and actuator displacements monitored. The lower actuator displacement profile was seen to follow the control signal as expected. The upper actuator displacement was superimposed on a second offset displacement. This displacement offset was found to be due to an incorrect joining of wires in the servo control module. The incorrect wire junction was desoldered, removed and insulated, which removed the displacement offset. The command output signals from the computer were now seen to match the displacement profiles produced by the actuators.

Data from the transducer amplifiers may be plotted on a servogor 461 XY chart recorder, displayed on a storage oscilloscope or captured using the transient recorder (Datalabs model DL902). If data capture is required at tableting speeds only the latter two options are viable. Due to the inherent inaccuracy of taking measurements from the oscilloscope screen the transient recorder was used for quantitative results.

The transient recorder has two independent channels each with a memory capacity of 2048 data points and eight bit amplitude resolution, capable of sample rates upto 1MHz. Analogue outputs from the transient recorder may be displayed on an oscilloscope or directed to a plotter, however analysis from such traces would be labour intensive and tedious which could give rise to unacceptable errors.

Several options were considered to obtain data from the transducer amplifiers including direct acquisition by a microcomputer or the polytechnic mainframe computer. The most versatile and cost effective method was to use the digital downloading capacity of the transient recorder to the existing Apple IIe microcomputer. The software to operate this system was written under contract. The accuracy and reproducibility of this system would be determined during validation .

In order to analyse compression data using Heckel plots or force displacement plots, both the upper and lower punch displacements are required. Ideally upper and lower forces and displacements would be recorded and undergo individual calibration and analysis, however only two channels are available on the transient recorder; one for force the other for displacement. To overcome this limitation the punch separation and mean punch force would be derived electronically. A potential divider was constructed from precision resistors and

installed between the  $\pm 10\text{mm}$  LVDT  $\pm 1\text{V}$  outputs in the control unit output modules as shown in FIG 2.2d. The output of this system should be half the difference between the two LVDT outputs. This would be calibrated during validation.

The mean punch force was derived using the simple circuit shown in FIG 2.2e, in this case:

$$V_3 = \frac{V_1 + V_2}{2} \quad \text{or} \quad \text{MPF} = \frac{\text{UPF} + \text{LPF}}{2}$$

Where UPF and LPF are the upper and lower punch force respectively and MPF is the mean punch force.

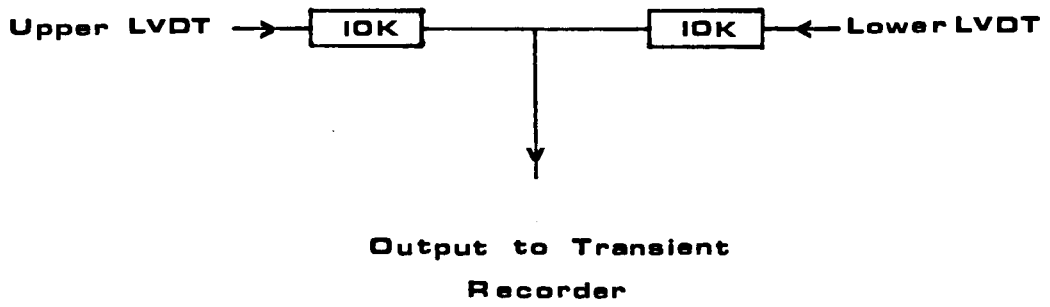


**FIG 2.2d Differential Displacement Potential Divider**

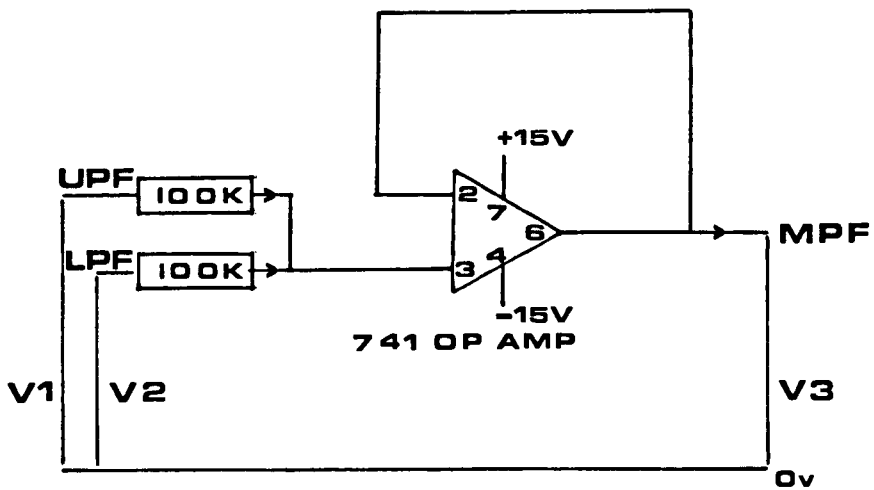


**FIG 2.2e Mean Punch Force Circuit**

## 2.3 Validation

The validation of a piece of equipment may be defined as the procedures carried out to prove the system operates as it purports to do, with the establishment of accuracy, precision and reproducibility. Validation of the high speed press was concentrated on the displacement and force measuring systems and the computer software. It is essential to fully validate any system prior to its inclusion in a research program in order to establish confidence in the results produced.

### 2.3.1 Measurement of Displacement

#### Remote Calibration of the $\pm 10\text{mm}$ Measurement LVDTs

Prior to installation of the  $\pm 10\text{mm}$  measurement LVDTs the correct operation of system had to be confirmed. A bench test was developed using a barrel micrometer (Russel Gauges Romford Essex) to optimise the system.

#### Experimental

The barrel micrometer body was drilled to accept the LVDT casing. The upper LVDT was connected to its amplifier in the control console via the load frame socket. The LVDT was secured in the barrel micrometer such that the armature was central against the measuring stop. The amplifier was adjusted to mid range when the LVDT output was zero volts as indicated by the digital meter in the control console. The micrometer was adjusted such that LVDT output incremented by 0.5V between +10V and -10V. The corresponding LVDT output and micrometer readings were recorded. The procedure was repeated for the lower LVDT.

The LVDT readings were found to be 2.5 times the actual displacement given by the micrometer. Investigation revealed the LVDT amplifier had been fitted with the incorrect range card during manufacture. The diode configuration on the range card was then corrected to match the range of the LVDT and the procedure repeated.

The LVDTs were shown to have an unacceptable response error of up to  $\pm 130$  microns as shown in FIG 2.3a. The error was reduced by fine tuning the amplifier circuit such that the minimum displacement error range was produced for each LVDT as shown in FIGS 2.3b. The second lower LVDT was a replacement transducer installed after the destruction of the original transducer during a later investigation. A summary of the non linearity of the transducers is shown below in table 2.3a.

Table 2.3a Displacement Error for the  $\pm 10$ mm Measurement LVDTs

LVDT	POSITIVE ERROR/microns	NEGATIVE ERROR/microns
UPPER SN' 45868	26	6
LOWER SN' 45876	11	18
LOWER SN' 76566	2	22

The response of each LVDT has been optimised under remote laboratory conditions.

### 2.3.2 Insitu Calibration of the $\pm 10$ mm LVDTs

Transducer response may be modified insitu by clamping, vibration and electrical interference. Physical limitations prevented the use of the barrel micrometer insitu so a direct calibration method was developed using grade A slip gauges (Coventry Gauge LTD Matrix Pinter M112/BS4311 SN' 8379c). Due to actuator 'wobble' the calibration was carried out using manual actuator movement. Displacement data was collected via the transient recorder and output via the chart recorder and microcomputer. It was necessary therefore to quantify and calibrate the output from each piece of equipment. The resolution of each piece of equipment will determine the accuracy of the system.

#### Experimental

The  $\pm 10$ mm LVDTs were installed in the centre crosshead and the zeroing potentiometers adjusted to give the displacement ranges shown in FIG 2.3c. The  $\pm 10$ mm LVDTs were connected to the punch separation

**FIG2.3a** NON LINEARITY OF THE UPPER AND LOWER 10mm LVDTs BEFORE OPTIMISATION.

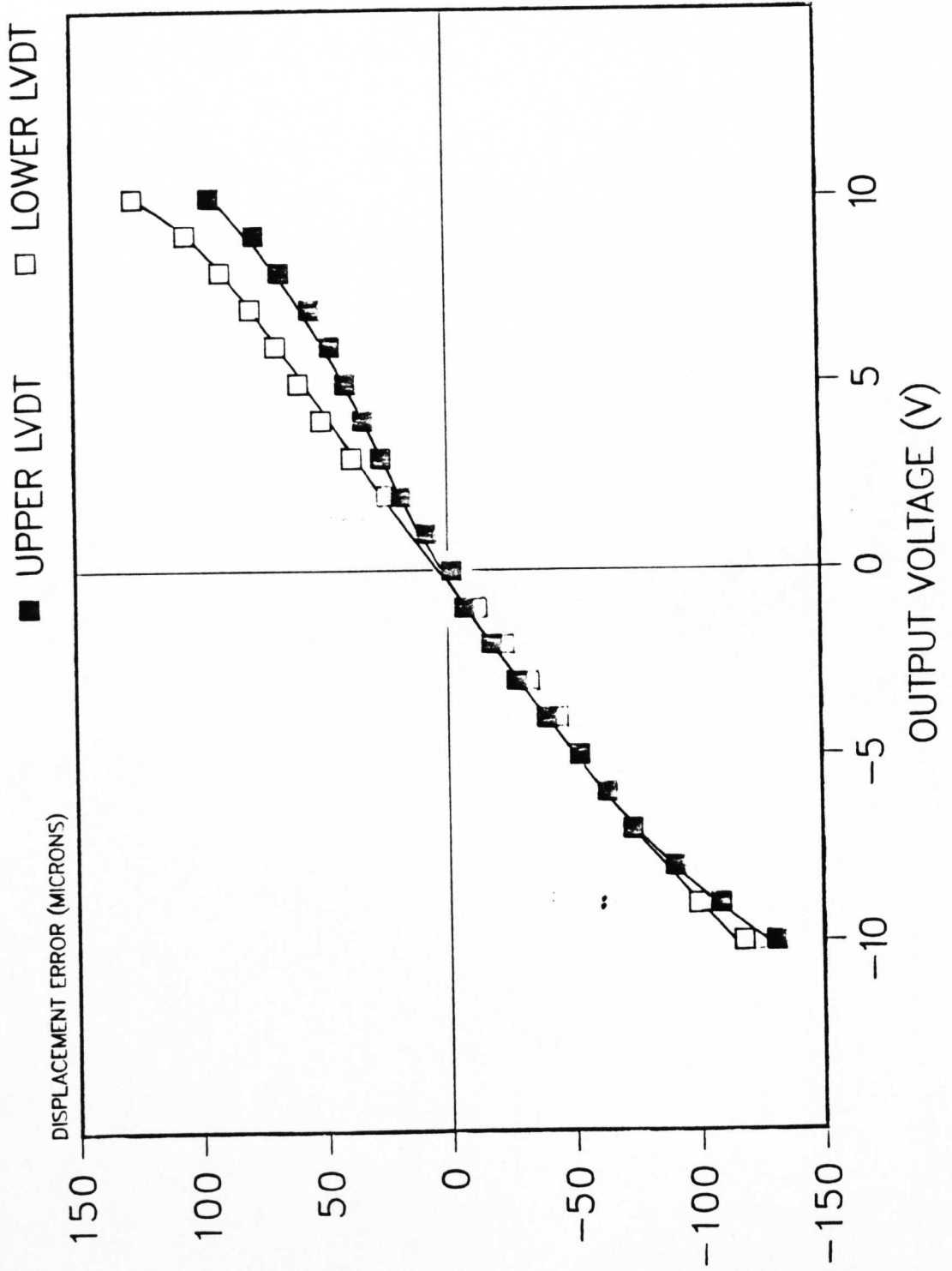


**FIG2.3b** NON LINEARITY OF THE UPPER AND LOWER LYDTs AFTER OPTIMISATION

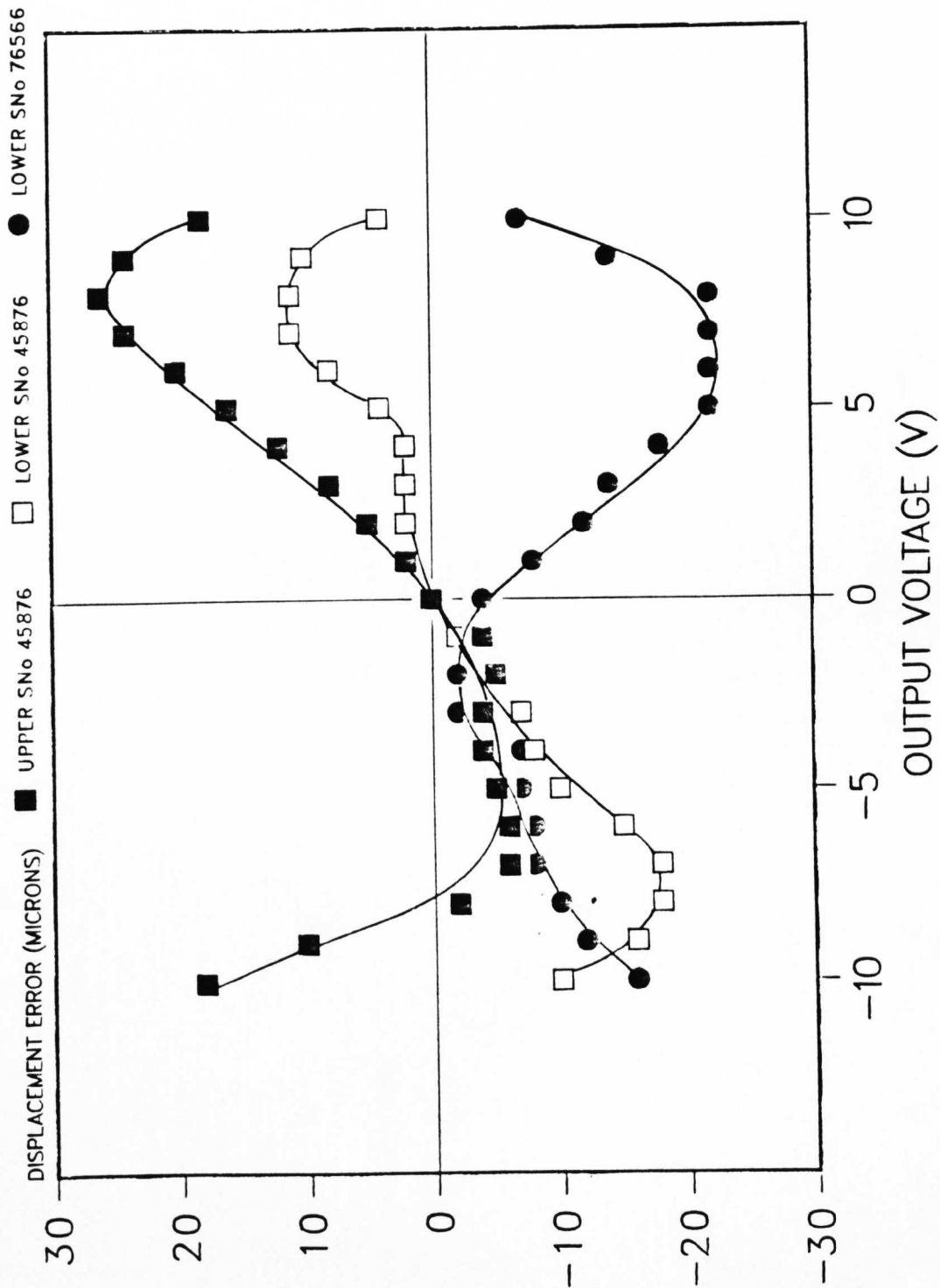
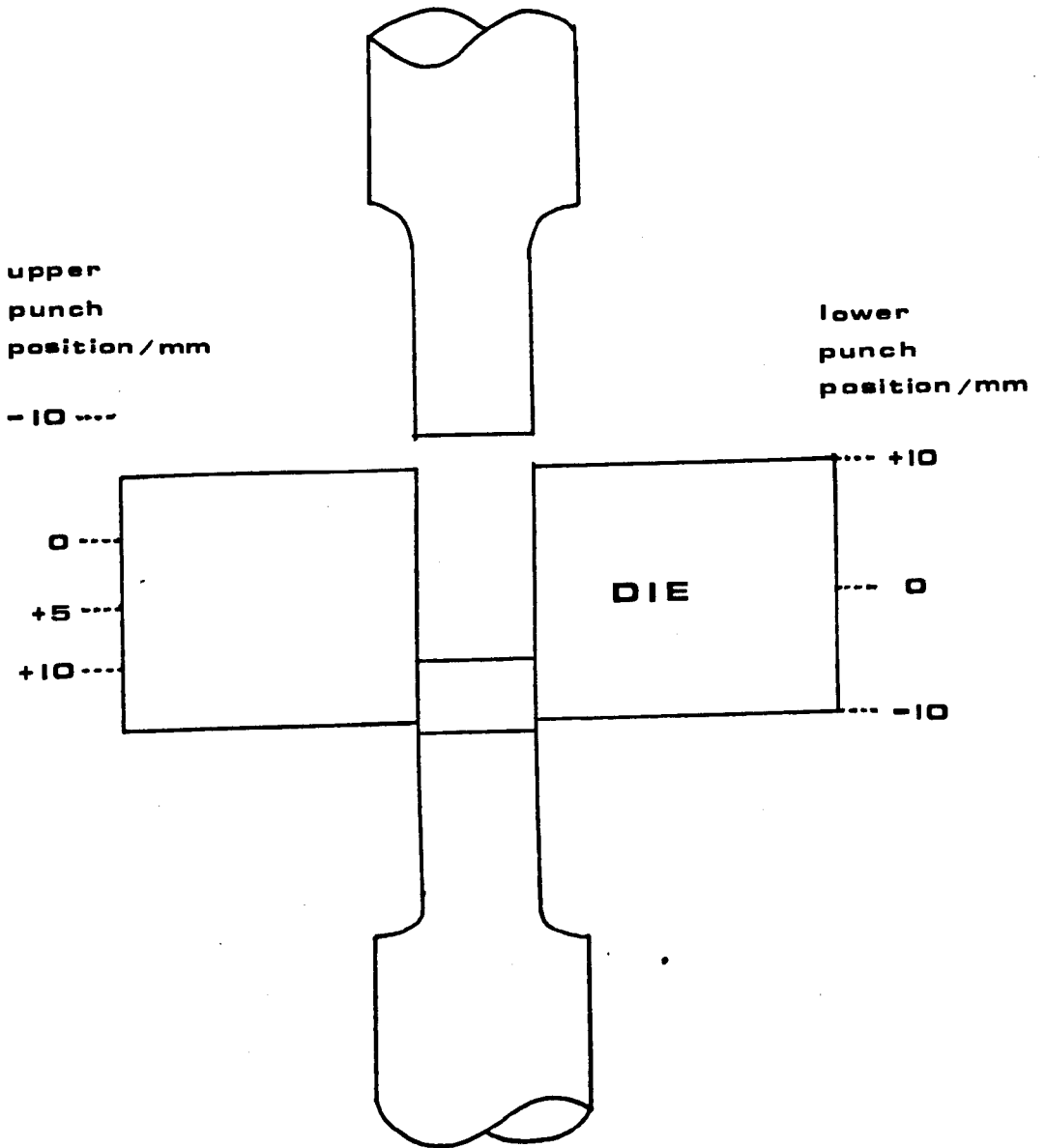


**FIG 2.3c**

**Upper & Lower  $\pm 10$ mm LVDT Displacement Ranges**



potential divider and the output commoned between the transient recorder channel one and a digital voltmeter. Data captured via the transient recorder was displayed using the chart recorder and the microcomputer.

A range of slip gauges were inserted between the upper and lower punches in increasing order of magnitude. The voltage output of the potential divider, digital displacement readings and transient recorder output were recorded. The procedure was repeated with decreasing then increasing slip gauge size. The load during the test was monitored from the upper load cell to ensure the slip gauges were not being compressed. Three replicates were taken for each measurement.

Displacement measurements lacked reproducibility due to rotation of the actuators and consequent travel of the LVDT armature across the striker block during the test. For this reason the actuator rotation was prevented by the installation of guide rails as mentioned during the commissioning. Reproducibility was thereby greatly improved. This calibration was repeated at each sensitivity range of the transient recorder to be used and the data output calibrations calculated.

The non linearity of the punch separation measurement system was found to be  $+12\mu$  to  $-2\mu$  over the operational displacement range as shown in FIG 2.3d. It can be seen that these errors due to non linearity of the LVDTs are not regular and as such would be difficult to correct, however they are of an acceptable level to give good accuracy.

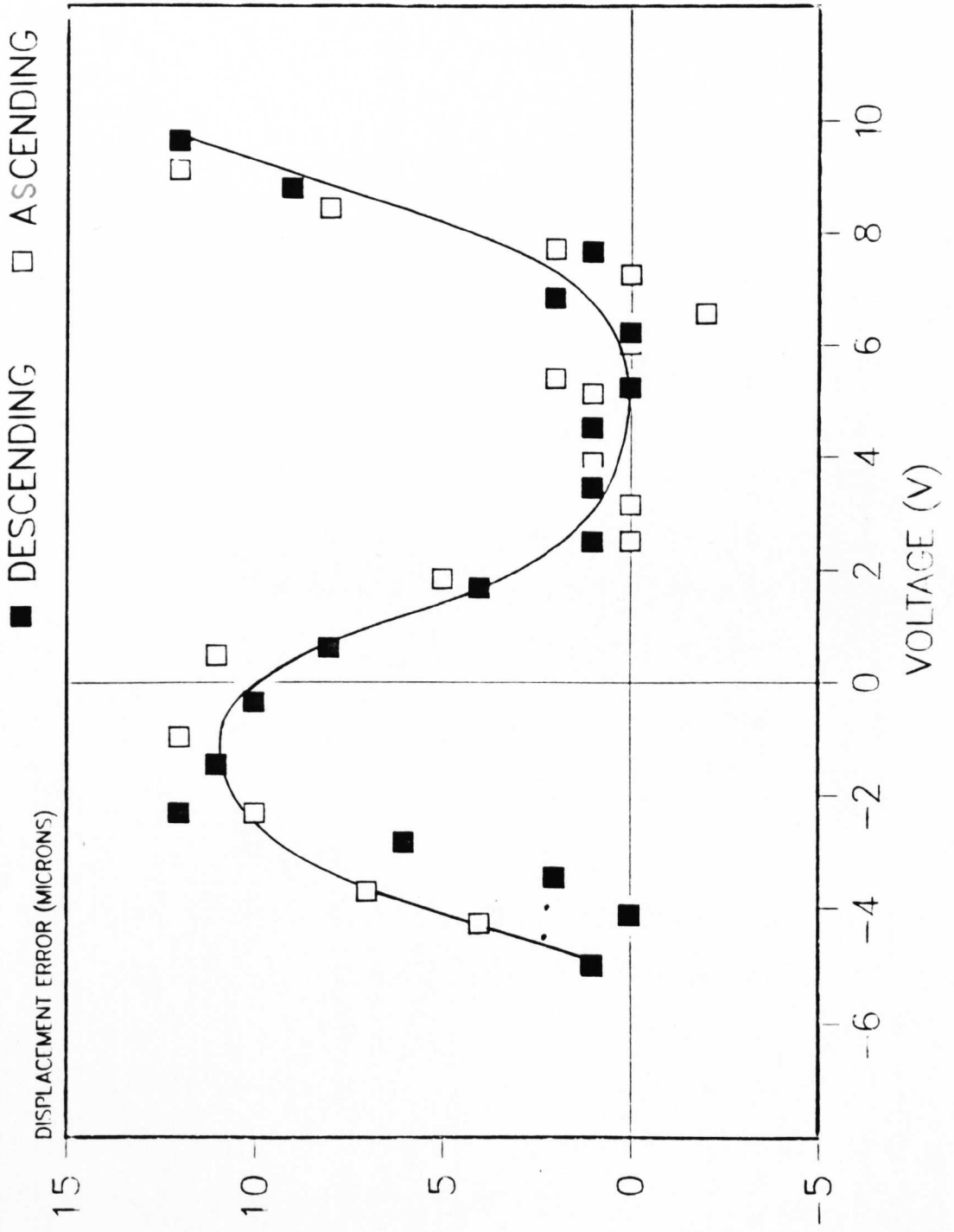
#### Calibration Values

Potential divider punch separation output =  $0.0475 \pm 0.00087$  V/mm

Table 2.3b Transient Recorder Displacement Data Output Calibrations.

<u>Sensitivity</u>	<u>mm Chart Trace/mm Actual</u>	<u>Logger Units/mm Actual</u>
0.2 V(FS)	58.680 $\pm 0.25$	63.364 $\pm 0.0098$
0.5 V(FS)	24.333 $\pm 0.25$	25.146 $\pm 0.0062$

**FIG 2.3d** NON LINEARITY OF THE 10mm LVDT PUNCH SEPARATION SYSTEM



The punch separation displacement system shows excellent reproducibility. The accuracy of this system is now limited by the resolution of the transient recorder which is dependant on the selected sensitivity which in turn will be dictated by the maximum punch separation required. The transient recorder has a theoretical resolution of eight bits which is equivalent to 1 in 255. In practise the resolution of the displacement measurement system is  $15.78\mu$  and  $39.77\mu$  for the 0.2V and 0.5V transient recorder sensitivity settings respectively (taken from the above figures).

### 2.3.3 Calibration of the $\pm 25\text{mm}$ Control LVDTs

The  $\pm 25$  mm stroke control transducers are located at the tip of the actuator housing with the armature connected to the end of the actuator ram. It is the output from these transducers, that determines the feedback in the closed loop for comparison with the desired position generating the error signal to control the valve.

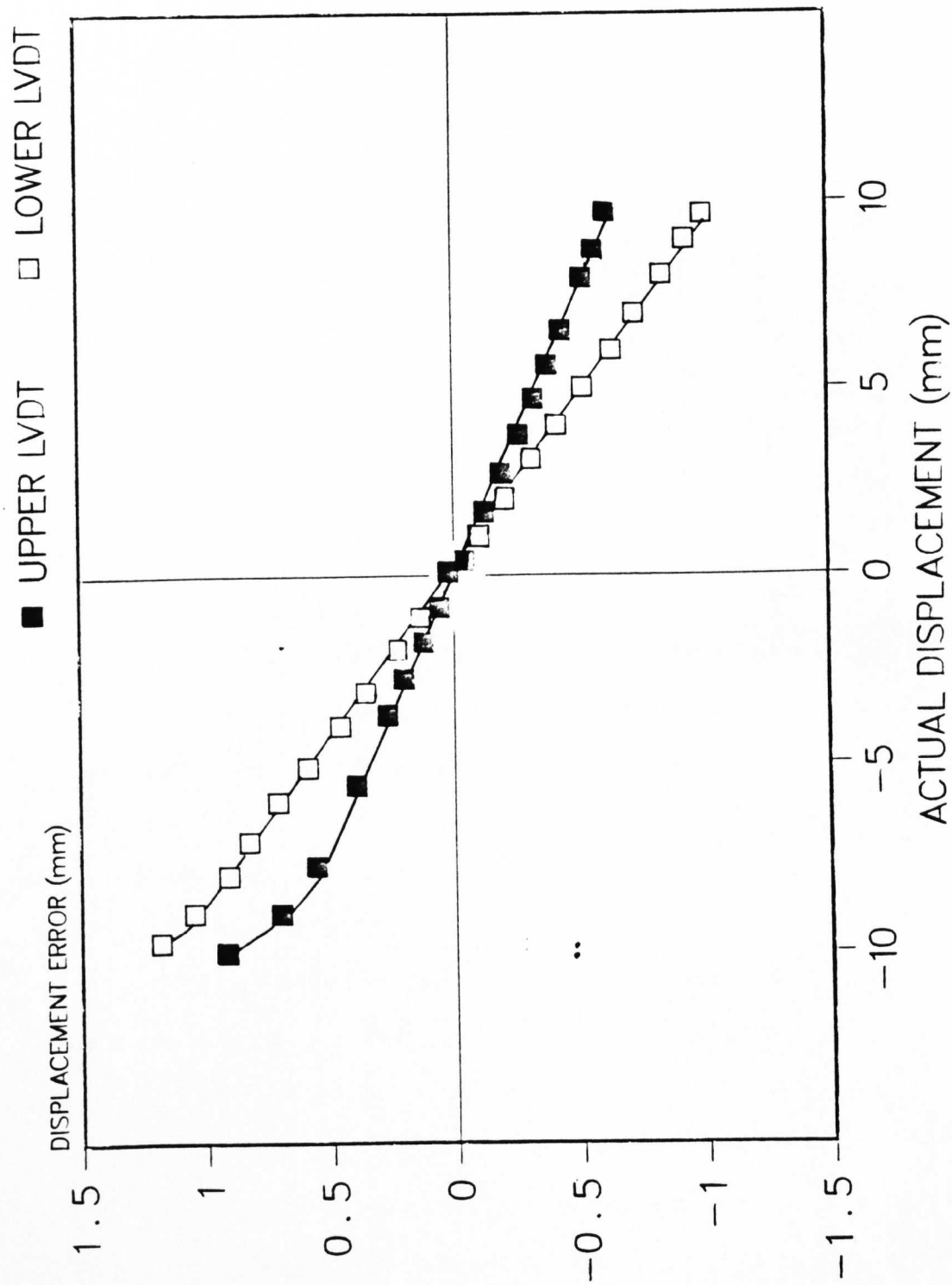
The control LVDTs cannot be detached from the simulator and are remote from the punch tips. Calibration was carried out against the pre-calibrated  $\pm 10\text{mm}$  LVDTs in situ.

#### Experimental

The upper actuator was allowed to fall until the striker block made contact with the  $\pm 10\text{mm}$  LVDT armature. It was then supported by an adjustable screw jack. The upper actuator was lowered over the  $\pm 10\text{mm}$  LVDT stroke range by adjustment of the jack in about 1mm intervals. Corresponding  $\pm 25$  mm and  $\pm 10\text{mm}$  LVDT positions were monitored via the digital display in the control unit and readings recorded. The actuator was then raised in a similar manner and a similar procedure was repeated for the lower  $\pm 25\text{mm}$  LVDT

Over the 20mm measuring range of the centre crosshead transducers the control transducers were found to be accurate to  $+0.9\text{mm}$  to  $-0.6\text{mm}$ .

**FIG2.3e** NON LINEARITY OF THE UPPER AND LOWER 25mm DISPLACEMENT CONTROL LVDTs



The error was not linear as shown in FIG 2.3e. The increased stroke range and the remote location of these transducers has resulted in very poor accuracy which prevents use of these LVDTs for quantitative measurement. Accuracy may have been improved by amplifier optimisation as for the  $\pm 10$ mm LVDTs. This was not considered necessary as control output could be modified using the computer as will be described later.

#### 2.3.4 Measurement of Applied Load

The simulator was supplied with two load cells ESH 1715a and 1715b. These were calibrated in situ by ESH Testing LTD using a proving ring ESH PR10T. A calibration certificate for each load cell at each load range was supplied to better than BS1610 Grade A1 specification. That is up to 20% of the range in use has a reading accurate to within 0.1% of range, and above 20% of the range in use has a reading accurate to within 0.5% of that indicated.

A calibration check button on the load cell amplifier connects a precision resistor across one arm of the load cells strain gauge bridge, electrically simulating application of a fixed compressive load. The magnitude of the resulting electrical output may be compared to the calibrated values provided by ESH Testing LTD. Any drift may be corrected for by adjustment of the span potentiometer. Compensation for weight of punches and their holders is made using the zeroing load potentiometer. The calibration check button is used daily to ensure the electrical system remained constant, however it would not detect physical failure of the system ie detachment of a strain gauge bridge. In order to confirm the integrity of the loadcells and produce confidence in the original calibration, validation would be required. As a  $\pm 50$  KN calibrated loadcell or proving ring was not available a simplified test was developed.

## Experimental

The simulator was fitted with 12.5 mm 'F' machine flat faced punches. The  $\pm 10\text{KN}$  load range was selected. Upper and lower load outputs were zeroed on the loadcell amplifiers and the electrical calibration checked. Upper and lower load outputs were connected to channels one and two of the transient recorder with a sample rate of 2ms. Data capture was set to start at the first registered load. A signal generator was connected to the external inputs of the upper and lower servo control modules and 0.2 cycles/s at +1V. A piece of rubber was placed on the centre crosshead between the punches to reduce impact shock. The actuators were brought towards each other by adjusting the zeroing potentiometers on the stroke amplifier. The digital load meters were set to peak and a load of about 6KN applied. Captured data was XY plotted using the Servogor 461 and the peak loads recorded. The procedure was repeated three times and the trace calibrations calculated as shown in table 2.3c.

Table 2.3c Calibration of the Upper and Lower Load Cell Outputs via the Servogor Plotter

UPPER LOAD CELL			LOWER LOAD CELL		
PEAK LOAD KN	PEAK TRACE mm	mm/KN	PEAK LOAD KN	PEAK TRACE mm	mm/KN
6.18	75	12.13	6.14	75	12.21
6.89	84.5	12.26	6.86	84.5	12.31
4.65	56	12.04	4.63	57	12.31
x		12.14			12.28
rn-1		0.111			0.058

The upper and lower load cells show good correlation in loading and unloading. As the upper and lower load cells produce similar loading profiles it may be assumed the strain gauge bridges were still bonded correctly unless the same defects are present in each. This could be tested over the lower load ranges at least using a precalibrated test load cell. The calibrated test load cell was connected to a Bruel and Kjaer excitation / strain indicator and the appropriate supply and measuring range selected. The load cell was

positioned over the die on the centre crosshead, and a load distribution plate was placed on top of the load cell. A 15mm diameter nut and bolt were fitted into the upper punch holder such that the head made contact with the load distribution plate. The calibrated load cell was zeroed. Load was applied by unscrewing the bolt against the upper load cell and distribution plate. Corresponding test load cell output and digital upper load reading from the control unit were recorded. The system was loaded and unloaded between 0 KN and 10 KN in 1 KN intervals.

Table 2.3d Loading and Unloading Calibrations For the Upper Load Cell Using a Pre-calibrated Test Load Cell

TEST LOAD CELL $\mu$ STRAIN	KN	UPPER LOADCELL								
		LOADING ERROR		UNLOADING ERROR		LOADING ERROR		UNLOADING ERROR		
		KN	N	KN	N	KN	N	KN	N	
ZERO OFFSET	0	-0.298				-0.146				
61 *	1	1.253	- 43	1.331	+ 33	1.178	+ 32	1.179	+ 33	
122 *	2	2.286	- 12	2.376	+ 78	2.159	+ 13	2.180	+ 34	
183 *	3	3.321	+ 23	3.422	+124	3.137	- 9	3.188	+ 42	
244	4	4.345	+ 47	4.411	+113	4.130	- 16	4.166	+ 20	
305	5	5.360	+ 62	5.425	+127	5.115	- 31	5.155	+ 9	
366	6	6.377	+ 79	6.422	+124	6.094	- 52	6.139	- 7	
427	7	7.371	+ 73	7.390	+ 92	7.072	- 74	7.100	- 46	
488	8	8.370	+ 72	8.364	+ 66	8.049	- 97	8.065	- 81	
549	9	9.350	+ 52	9.377	+ 79	9.015	-131	9.037	-109	
610	10	10.330	+ 32	10.329	+ 31	10.003	-143	10.014	-132	

\* Test load cell sensitivity range 0-200  $\mu$  strain all other readings taken at 0-2000  $\mu$  strain

Results lacked reproducibility and showed large variation between loading and unloading combined with rate of change of load. The hysteresis of the loading and unloading was thought to be due to recovery of the system, and to confirm this the test load cell was recalibrated using a similar system to that above on a hydraulic Instron press. The difference between loading and unloading during the recalibration was seen to be 98.4N, hence the poor reproducibility was due to the recovery of the test load cell.

This calibration of the load cells confirms the correct functioning of the simulator load measuring system up to 10 KN, although only  $\pm 143\text{N}$  may be claimed. For an absolute calibration a  $\pm 50\text{KN}$  grade A1 load cell would be required. This could not be obtained so the ESH Testing LTD calibration was accepted.

### 2.3.5 Load Calibration of The Transient Recorder

The development of the digital data transfer from the transient recorder to the Apple IIe necessitated insitu calibration.

#### Experimental

The desired load range was selected and the zeroing potentiometer on the load cell amplifier adjusted to give zero load with the punch holders and 12.5 mm flat faced punches fitted. The output from the load cell amplifier was connected to the second channel of the transient recorder. A steel plate was placed over the die on the centre crosshead, a 15 mm diameter nut and bolt were centred on the plate under the upper load cell. The nut was unscrewed to apply a load to the punch, which was recorded from the digital load meter in the control console. The transient recorder was triggered manually and the data plotted and transferred to the computer where the 2048 values were averaged. This procedure was repeated three times with increasing load and zero load. The plotter chart trace and data logger load calibrations were then calculated and recorded in Table 2.3e

Table 2.3e Transient Recorder Load Data Output Calibrations

<u>FULLSCALE LOAD kN</u>	<u>mm CHART TRACE/kN</u>	<u>LOGGER UNITS/kN</u>
$\pm 10$	24.571 $\pm 0.1710$	25.260 $\pm 0.0564$
$\pm 50$	4.929 $\pm 0.0976$	5.048 $\pm 0.0211$

The calibration method shows good reproducibility.

### 2.3.6 Determination of the Punch and Load Frame Distortion

During tablet manufacture using the simulator, the load applied by the actuators will be transmitted through the punches and load cells which will deform elastically. The reaction to the punch loading will be experienced by the load frame which will also deform.

Deformation of the system becomes significant when measuring displacement. The punch shortening during compression results in an under estimation of punch separation. Distortion required investigation and quantification for incorporation into displacement calibrations.

A remote method was developed where the load cell fitted with punch was loaded between the platens of an Instron. This showed very poor reproducibility thought to be due to bedding in effects and irregular loading by the Instron. An insitu method was developed to include load frame distortion. A blank die was installed into the centre crosshead, the punches then applied an increasing load against the die; the change in displacement was noted. It was difficult to assess the displacement due to compression of the die. However with development of the differential displacement potential divider, an absolute calibration could be used.

#### Experimental

The 10mm flat faced 'F' machine punches were fitted into the punch holders and secured under manual loading. The upper and lower  $\pm 10$ mm LVDT  $\pm 1$ V outputs were connected from the control unit to the differential displacement potential divider. The transient recorder was used to capture the load experienced by the upper punch and the change in relative displacement between the punches.

The maximum upper punch force experienced by the upper punch during the test was recorded using the digital load meter in the control console. The upper and lower stroke amplifier zeroing

potentiometers were adjusted to bring the punches together, and adjustment was continued until the load exceeded 50KN. The punches were separated in a similar manner. The data was plotted using the servogor 461 and the peak load recorded.

The procedure was repeated three times. The punches were then replaced by 12.5 mm 'F' machine flat faced Manesty punches and the procedure repeated.

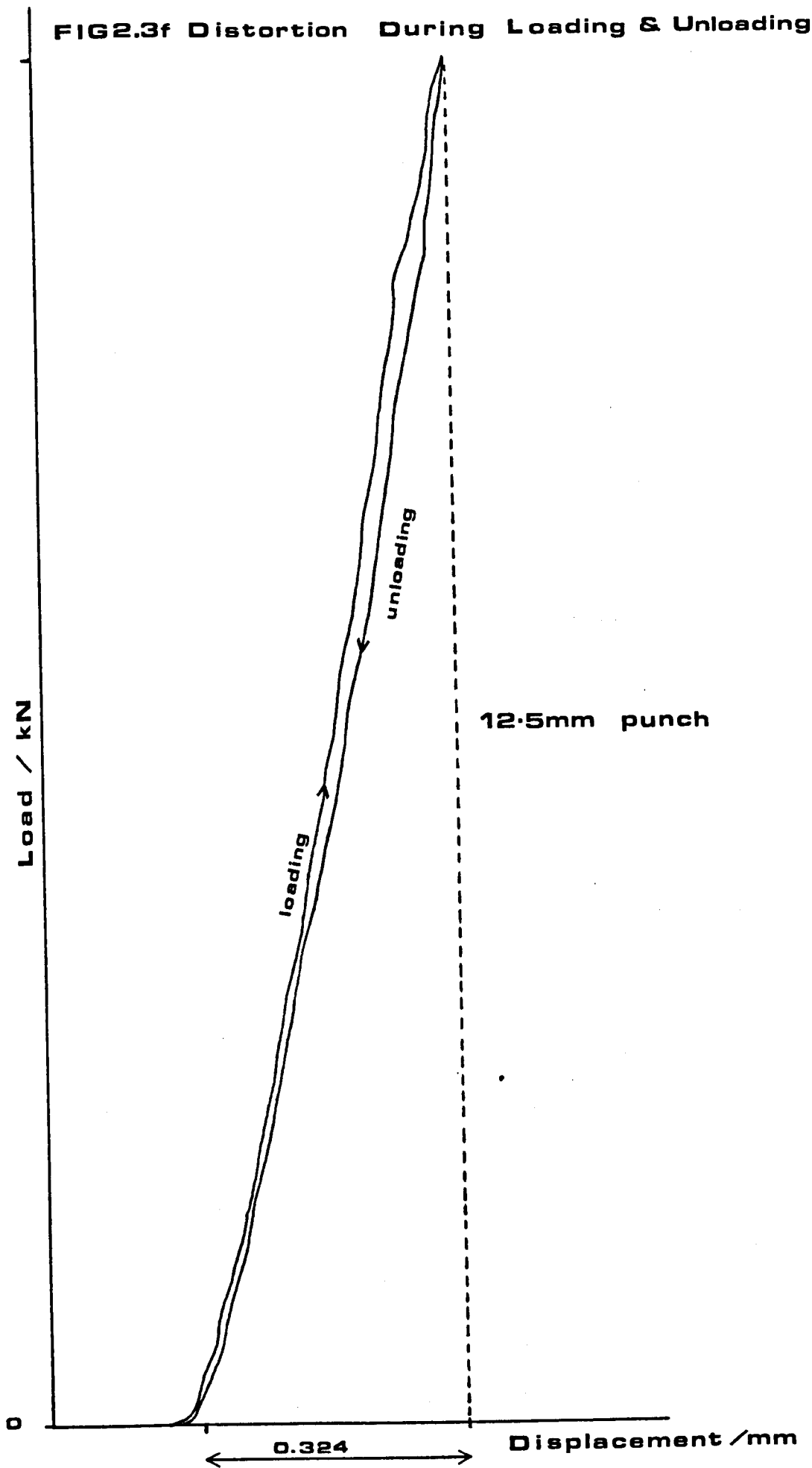
Table 2.3f Distortion of the Hydraulic Press Under Load

	d PUNCH SEPARATION $\mu$	PEAK LOAD kN	DISTORTION $\mu$ kN <sup>-1</sup>
<b>10.0 mm PUNCHES</b>			
i	472	45.16	10.45
ii	536	48.89	10.96
iii	539	49.30	10.93
MEAN			10.78 $\pm$ 0.286
<b>12.5 mm PUNCHES</b>			
i	326	41.59	7.83
ii	377	50.05	7.53
iii	394	52.44	7.51
iv	358	46.80	7.65
MEAN			7.63 $\pm$ 0.147

Deformation of the system is mainly elastic shown by a small difference between the loading and unloading force displacement curves FIG 2.3f. The plot was linear permitting incorporation of a correction factor for displacement calibrations. It should be remembered that this correction factor is only an approximate correction. In order to make an absolute correction, the distortion should be measured at the same loading rates as those to be used in the investigation. This is because the deformation of the punches and load frame will be partially time dependant. Unfortunately repeating the distortion test at high loading rates could be dangerous and was therefore not attempted.

FIG2.3f Distortion During Loading & Unloading

52.44



## 2.4 Computers and Software

Computers with appropriate software were used to control the tableting process and transfer and analyse the data. Consequently validation of each of these systems was required prior to commencing the research program.

### 2.4.1 Microcomputer Control of the High Speed Press

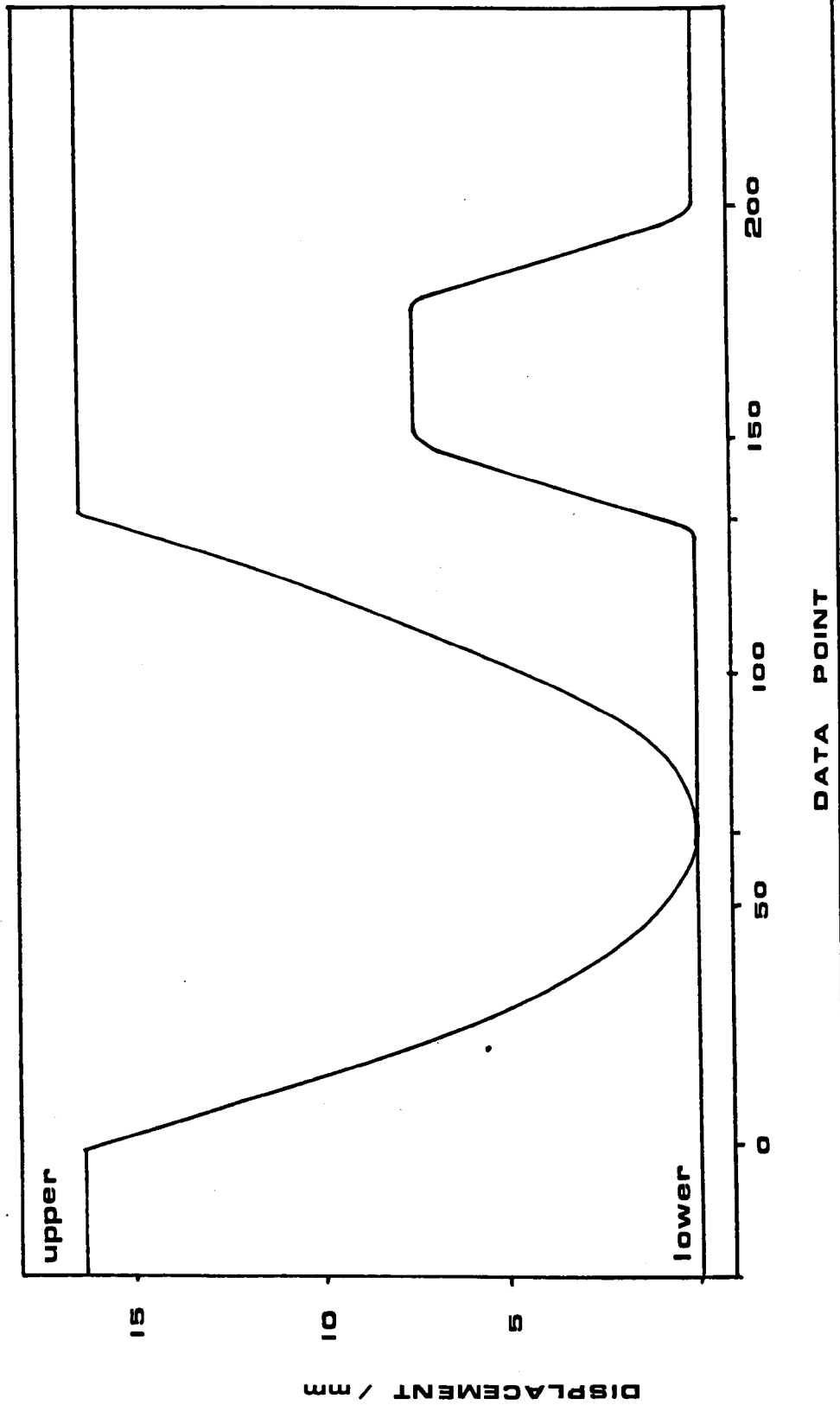
Once the software described during the commissioning had been developed, the integrity of the displacement profiles during storage and retrieval from floppy disk and output as the control profile, had to be established. The integrity of the displacement profile transferred between the microcomputer and the floppy disk was readily checked by repeatedly storing, retrieving and checking a known profile. As expected the integrity of the profile was maintained. The ability of the actuators to follow a displacement profile at various speeds had to be established.

### Experimental

A stylised 'F' machine profile shown in FIG 2.4a was entered into the microcomputer manually via the keyboard. The output rate of the profile was set by entering a delay factor between 1 and 255. This determined the number of times the microcomputer would execute a delay loop before outputting the next data point. The  $\pm 10$  mm LVDTs  $\pm 1V$  outputs were connected to channels one and two of the transient recorder and the appropriate sensitivity selected.

The profile was then executed and the actuator displacement captured and plotted using the Servogor 461. The trace was analysed to give the actual displacement produced at the compression and ejection peaks by the upper and lower actuators respectively. The total cycle time and compression rate were calculated. The procedure was repeated using decreasing delay factors to increase output rate. Two testing

**FIG2.4a Manesty "F" Machine Displacement Profile**



probes were then connected to the transient recorder and linked to the upper and lower displacement control outputs from the computer at the interface junction. The profile was executed with delays between 250 and 1. Data was captured plotted and the compression rates calculated as shown in Table 2.4a

Table 2.4a Cycle Times and Displacements For the Actual and Control 'F' Machine Profiles Executed at Variable Output Rates

PROFILE DELAY	CYCLE TIME		COMPRESSION RATE $\text{mm s}^{-1}$	DISPLACEMENT $\text{mm}$		CONTROL SIGNAL	
	ACTUAL $\text{ms}$	CONTROL $\text{ms}$		COMP	EJECT	COMP $\text{mmT}$	EJECT
250	27371.3	26144.6	2.0	15.2	5.72	80.0	37
200	17762.2	17570.9	3.2	15.2	5.8	80.0	37
150	10094.4	10123.6	5.5	15.2	5.8	80.0	37
100	4385.2	4363.3	13.4	14.7	5.5	80.0	37
90	2892.2	3630.5	19.3	15.2	6.1	80.0	37
80	2608.1	2825.3	23.0	15.2	6.1	80.0	37
70	2030.5	2210.9	29.0	15.2	6.1	80.0	37
60	1549.1	1605.8	38.7	15.2	6.1	80.0	37
50	1102.7	1117.1	52.6	15.2	6.1	80.0	37
40	783.3	721.4	74.0	15.1	5.9	80.0	37
30	483.5	440.5	103.4	13.7	4.9	80.0	37
20	281.8	163.2	151.6	11.0	3.3	80.0	37
10	161.5	58.1	383.9	5.1	1.6	80.5	37
1	0.0	11.1	0.0	0.0	0.0	80.5	37

The control profile followed the displacement data points and was not output rate dependent.

The actuator displacement time profile was output rate dependent. The profile distorted and reduced displacement at profile delays of less than forty. Even at long cycle times the response was less than defined. Upper displacement should have been 16.3 mm and lower 7.3 mm.

This reduced response at low rates indicates the control signal requires calibration. Poor simulator performance at high rates could be due to a hardware fault within the electronics or hydraulics, or the design fails the original specification. The ability of the actuators to respond at high rates was confirmed using the High Speed Ramp Generator module in the control console. The upper and lower actuators produced ramp rates of 1.87  $\text{ms}^{-1}$  and 1.62  $\text{ms}^{-1}$  respectively.

The difference in velocity between the two actuators was probably due to the variation of system gain between the upper and lower servo control modules. Although these values are lower than the 3 mS<sup>-1</sup> specification they are acceptable as the specification is for a dynamic test using a continuous sine wave.

This test demonstrated the simulator capable of ramp rates well in excess of the 0.38 mS<sup>-1</sup> seen during the computer controlled trial. This indicated the problem to be between the Apple IIe computer and the servo control module ie cables, computer interface module, and servo controller junction. The control signal did not change with output rate at the computer interface input connector, but significant signal distortion was seen at the servo controller module junction. This indicated distortion occurred within the interface .

Removal of filter capacitors from the control console interface removed the output rate distortion from the signal and produced constant displacement by the actuators. The interface had been designed to filter out electrical spikes caused by current fluctuations from the computer. The filter capacitors were treating the high rate control signal as a spike, effectively reducing the control signal. Removal of the filter capacitors solved the problem.

#### 2.4.2 Calibration of the Digital to Analogue Card Output

Actuator movement was less than the theoretical control signal even at slow output rates. This indicated that calibration of the D/A board was required. An output adjustment potentiometer was available to vary the level of control output from the D/A board for each channel. The usual calibration procedure would involve adjustment of the D/A board output to give +10V at fullscale (25mm) from the computer program. Considering the control console irregularities reported previously it was considered better to calibrate through the

entire system by measuring actual displacement produced by the actuators.

### Experimental

A displacement calibration profile was developed, generated and saved using the Apple IIe computer. It consisted of increasing displacement in 5mm increments up to 25mm then similarly decreasing to the baseline 0mm. The upper and lower displacement was monitored using the  $\pm 10$ mm LVDTs via the transient recorder. The output rate delay was set to 100 and the profile executed. The captured data was plotted using the Servogor 461. Actual displacement produced by the actuators was compared to the data point profile values and the potentiometers adjusted as required until actual displacement matched theoretical.

The profile was executed three times and the displacement time trace analysed. A 25mm control input via the Apple IIe computer produced a 10V output from the D/A board producing 25mm displacement by the actuators. The Apple IIe computer control system has been validated and calibrated.

#### 2.4.3 Validation of the Transfer of Data From the Transient Recorder to the Apple IIe and to the Dec 20 Mainframe

The data transfer software (See appendix) consisted of a basic user interactive operating program with a machine code subroutine to download the data from the transient recorder memory to the Apple IIe computer. Data in the transient recorder was stored as 2048 integers between 0 and 255 in each of two channels. A MKII TTL binary digital interface was supplied to output the data from the transient recorder to the Apple IIe microcomputer. Data was input to the Apple IIe via an eight bit parallel 6522 interface which was constructed as shown in FIG 2.4b. Data transfer was initiated by a key press. Data could then

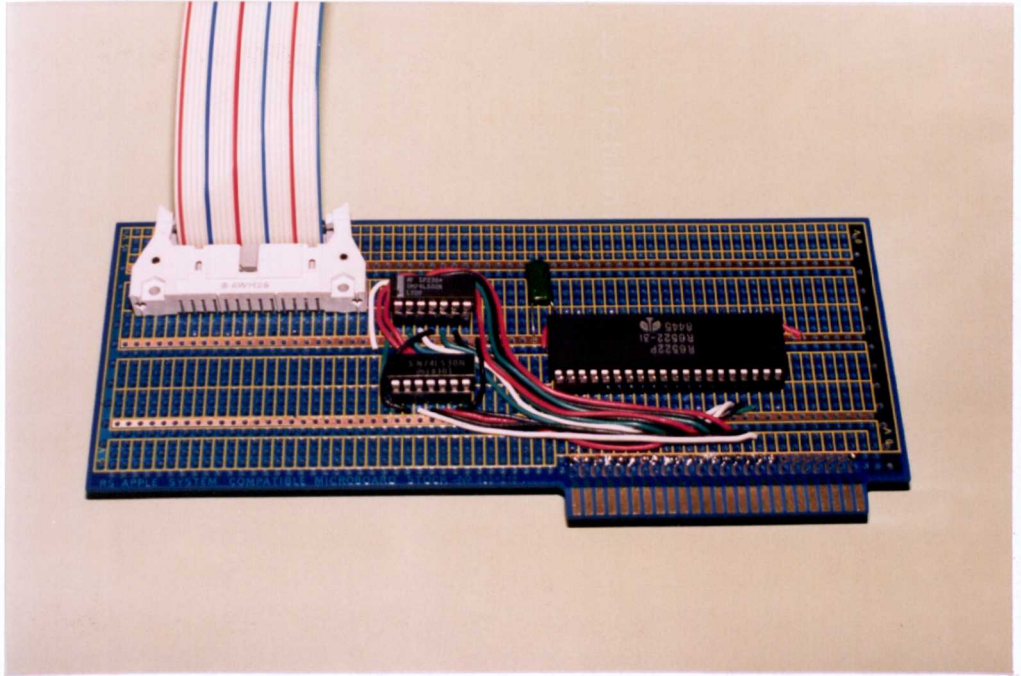


FIG 2.4b The 6522 Parallel Interface Used to Down Load Data From the Transient Recorder to the Apple IIe Microcomputer.

be viewed or saved on to floppy disk in the form of a text file for storage. The data text file could be transferred to the polytechnic mainframe computer via a second Apple IIe computer interfaced with it. The software to do this was a standard package called KERMIT. The data could then be analysed using any of the mainframe packages or purpose written software. The integrity of the data through out each of the transfer stages is of importance and as such must be validated.

### Experimental

The simulator Apple IIe computer parallel 6522 interface was connected to the transient recorder using Cannon D 25 way connectors and cable. The internal channel offset controls of the transient recorder were adjusted to minimum for both channels. The recorder was then triggered manually, theoretically filling both channels with 2048 zeros. Data was then transferred to the Apple IIe computer where it was viewed and saved to disk. The process was repeated with the offset control at maximum, theoretically filling both channels with 255's. The process was repeated to a total of three times for each setting.

Irregular data was entered into the transient recorder by manual adjustment of both offset controls during data capture. Channel one was plotted against channel two using the Servogor 461. The data was then transferred and saved to floppy disk. The floppy disk was installed in a second Apple IIe microcomputer which was interfaced with the Dec 20 mainframe computer. The data text files were then transferred using the KERMIT program.

The data was transferred without problem from the transient recorder to the Apple IIe computer. Transfer took a fraction of a second. The integrity of the data was maintained except for the first data pair which was often presented as a random value. Saving the data to disk took about two minutes, and the text file occupied about 66 sectors of the floppy disk. Data transfer from the Apple IIe

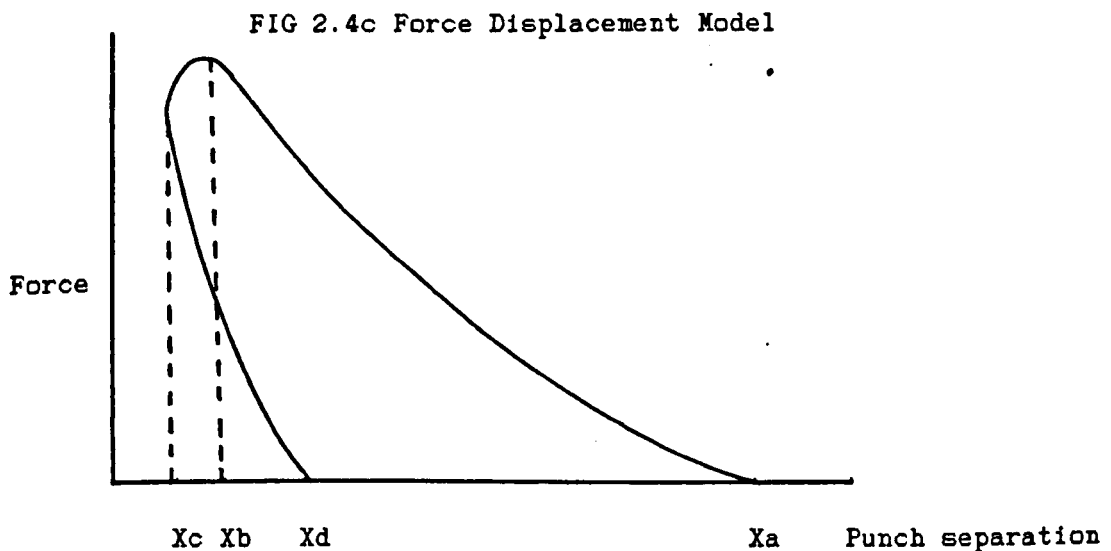
computer to the mainframe was initially impaired by incorrect CASE settings and connections. The data was transferred without corruption. This procedure took about four minutes due to the internal checking system of the KERMIT program. The irregular data produced the same plot from the Servogor 461 as from the mainframe computer.

The data transfer hardware and software operates satisfactorily. The occurrence of a rogue first data pair could not be prevented and is thought to be an artefact of the MKII TTL interface. The rogue values will be edited out during analysis

#### 2.4.4 Software to be used for Analysis of Compaction Data

Powders with different packing characteristics, elastic and plastic deformation properties absorb varying amounts of energy during compaction for equally applied pressures. Energy of compaction may thus be a useful parameter to study the effect of compression rate in terms of plastic and elastic deformation.

For a system where both punches are mobile, the punch separation may be plotted against upper, lower or mean punch force. The area under this curve will be the work done or energy. In order to develop a computer program to calculate energy from the transient recorder data, a model specification had to be produced as shown in FIG 2.4c.



Where  $X_a$  = Punch separation at the first measurable force

$X_b$  = First occurrence of the peak force

$X_c$  = Minimum punch separation

$X_d$  = Decompression force equal to zero or less

AUC  $X_a X_b$  = Compression energy

AUC  $X_c X_d$  = Decompression energy

#### Specification for Area Under the Curve Software

- 1) Named data file consists of 4096 integers between 0 and 255, read first 2048 as displacement, second 2048 as force.
- 2) Sort into data pairs.
- 3) Disregard first four data points.
- 4) Calibrate data using programmable conversion factors and set machine constants.
- 5) Order data according to X values.
- 6) Remove duplicated values.
- 7) Find  $X_a$ ,  $X_b$ ,  $X_c$ ,  $X_d$ .
- 8) Calculate the area under the compression curve  $X_a-X_b$ , and decompression curve  $X_c-X_d$ .
- 9) Calculate the time taken for  $X_a-X_b$  and  $X_c-X_d$ .
- 10) Output a data file of calibrated and sorted punch separation and force data for Heckel analysis.

#### Experimental

Dr D. Clegg Liverpool Polytechnic Mathematics department developed software to this specification to operate on the given model. To confirm the correct functioning of the Fortran program, simple triangular models were created as shown in FIGS 2.4d,e,f. The data points of these profiles were entered as pairs into the Energy program which computed the corresponding areas under the compression and decompression curves. The areas under the curves were also derived manually by dividing the profiles into triangles, calculating the

**FIG 2-4d** TRIANGULAR FORCE DISPLACEMENT MODEL ATEST1

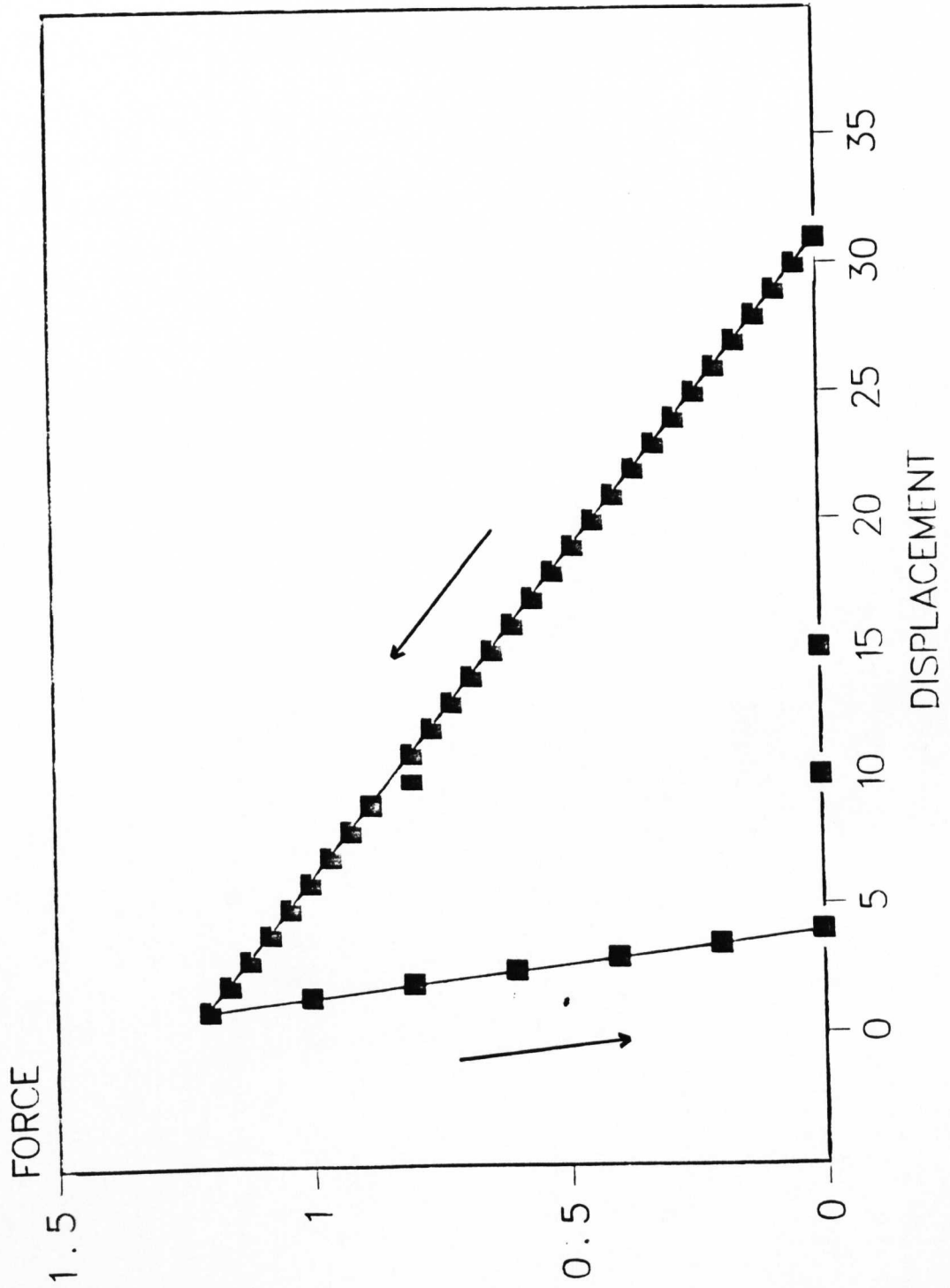


**FIG 2.4e** TRIANGULAR FORCE DISPLACEMENT MODEL ATEST2

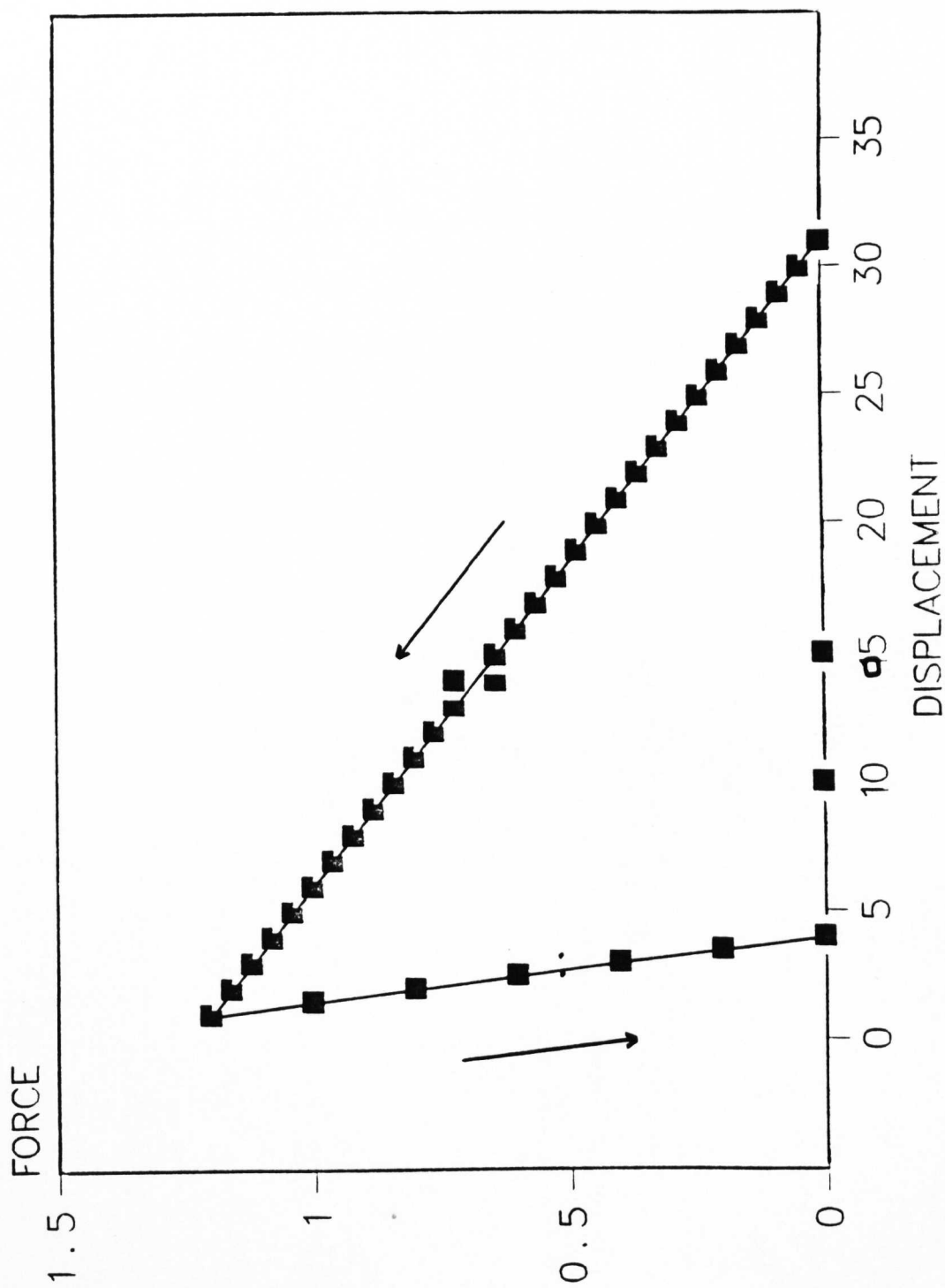
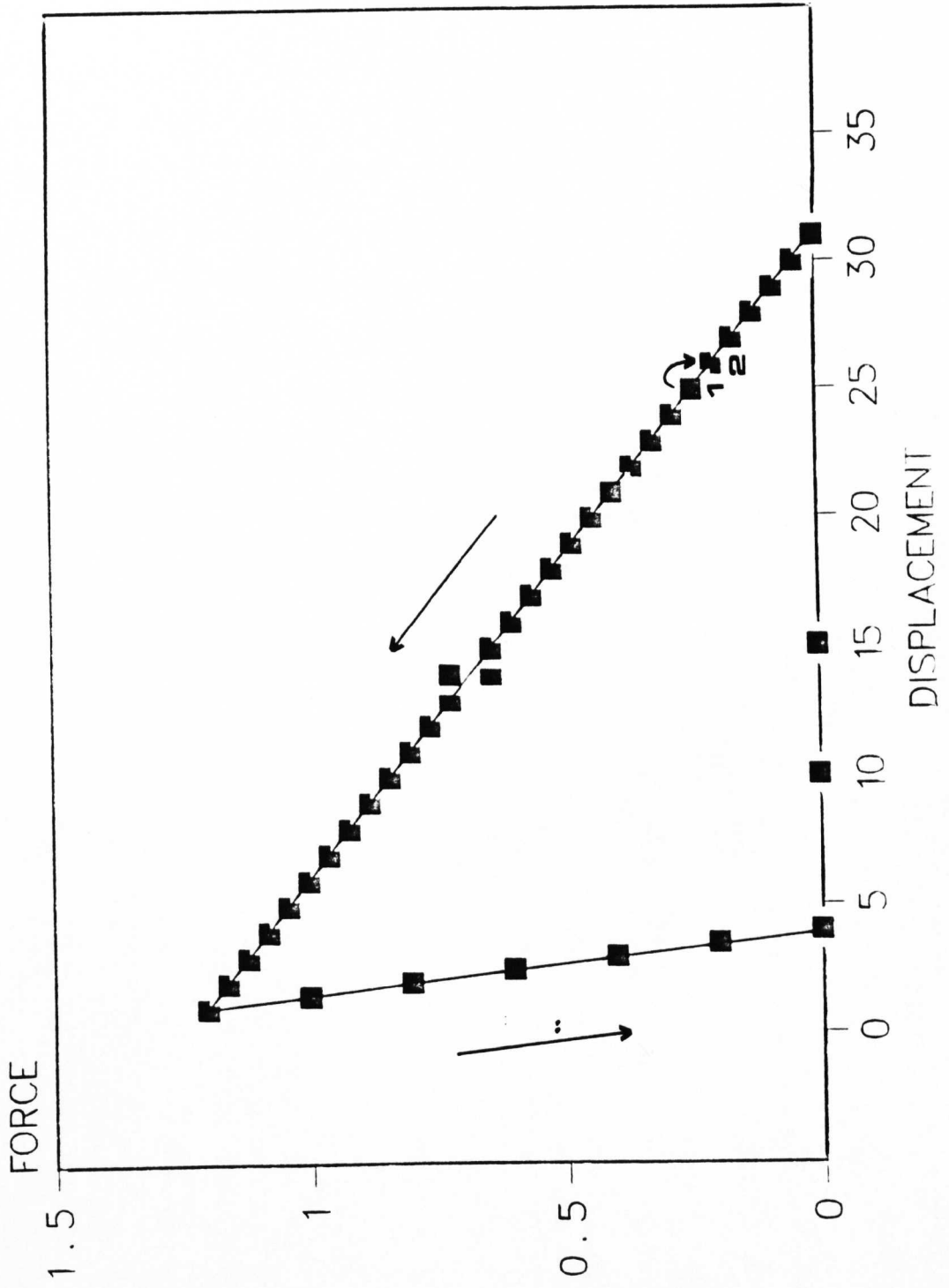


**FIG 2-4f** TRIANGULAR FORCE DISPLACEMENT MODEL ATEST3



respective areas and summing them. The areas under the curves derived manually and using the Energy program are shown in table 2.4b

Table 2.4b Area Under the Compression and Decompression Curves for profiles ATEST1-3 Derived by Manual Calculation and Using the Energy Program

ANALYSIS METHOD	AUC ATEST1		AUC ATEST2		AUC ATEST3	
	COMP'	DECOMP'	COMP'	DECOMP'	COMP'	DECOMP'
MANUAL	18	1.8	18	1.8	18	1.8
PROGRAM	18	1.8	18	1.8	18	1.8

Further profiles were then created as shown in FIGS 2.4g,h,i and drawn on small square graph paper. The area under the compression and decompression curves were derived by counting the number of squares enclosed by the profile. The data were compiled into single column data sets with four rogue data values at the beginning of each set mimicking the format of the transient recorder data files. This data was subjected to analysis by a modified Energy program capable of sorting the data into XY pairs and deleting the first four rogue values. An indication of error of the curve fitting routine was programmed to be displayed.

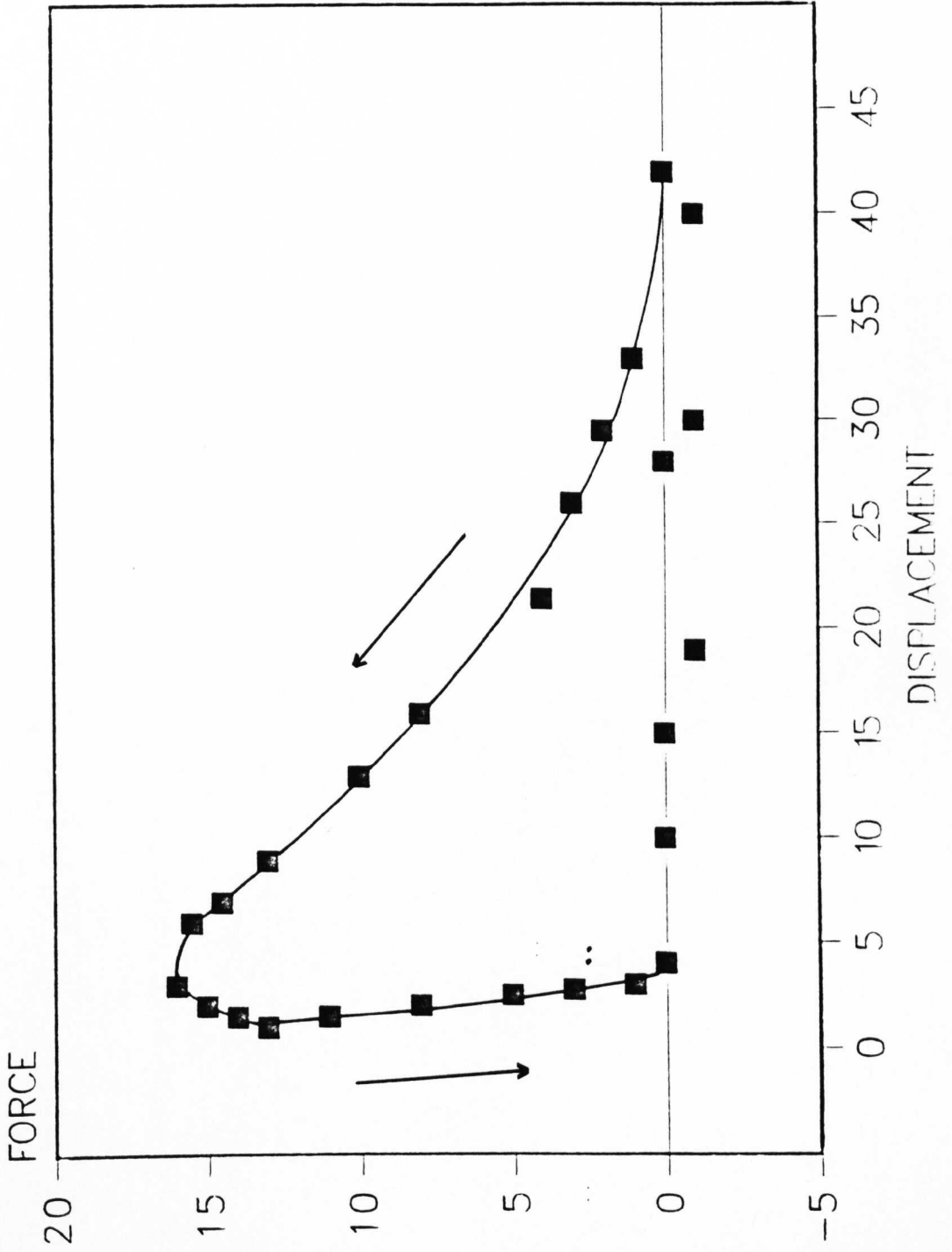
Table 2.4c Area Under the Compression and Decompression Curves for profiles ATEST4-6 Derived by Manual Calculation and Using the Energy Program

PROFILE	ANALYSIS	COMPRESSION	ERROR	DECOMPRESSION	ERROR
ATEST4	MANUAL	228.1	-	15.8	-
	PROGRAM	225.76	0.203	14.67	-0.048
ATEST5	MANUAL	225.3	-	18.5	-
	PROGRAM	225.6	0.217	14.8	-2.435
ATEST6	MANUAL	218.7	-	27	-
	PROGRAM	219.2	0.297	25.9	0.183

The values of Xa, Xb, Xc, Xd were found to be correct in each case. The software split the single column, paired the data and deleted the first four data pairs according to the specification.

Good correlation was seen between the compression energies calculated theoretically and those computed by the software for profiles ATEST4-6. The curves fitted to the data were all good fits

**FIG 2.49** FORCE DISPLACEMENT MODEL ATEST4



# FORCE DISPLACEMENT MODEL ATEST5

FIG 2-4h

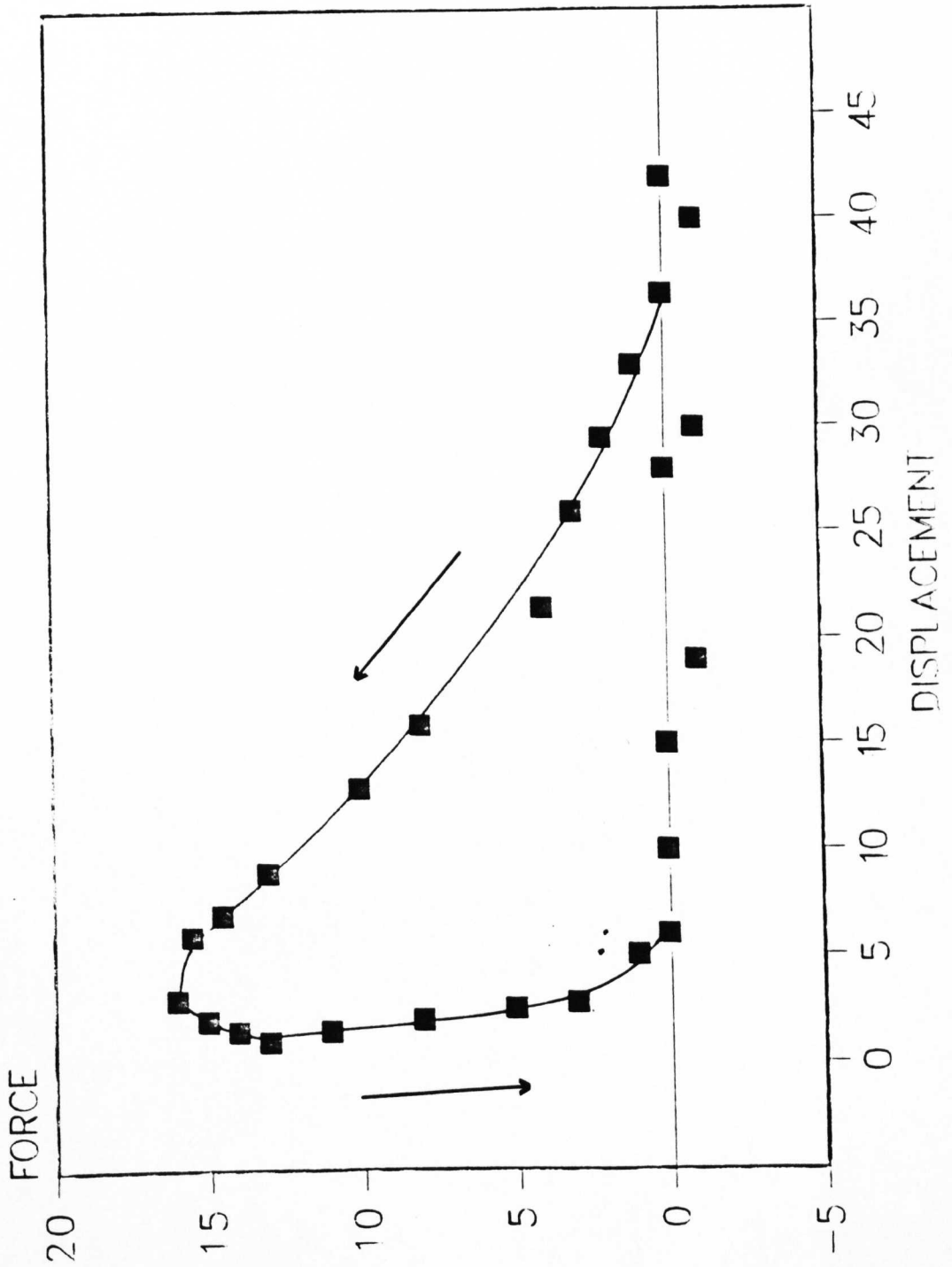
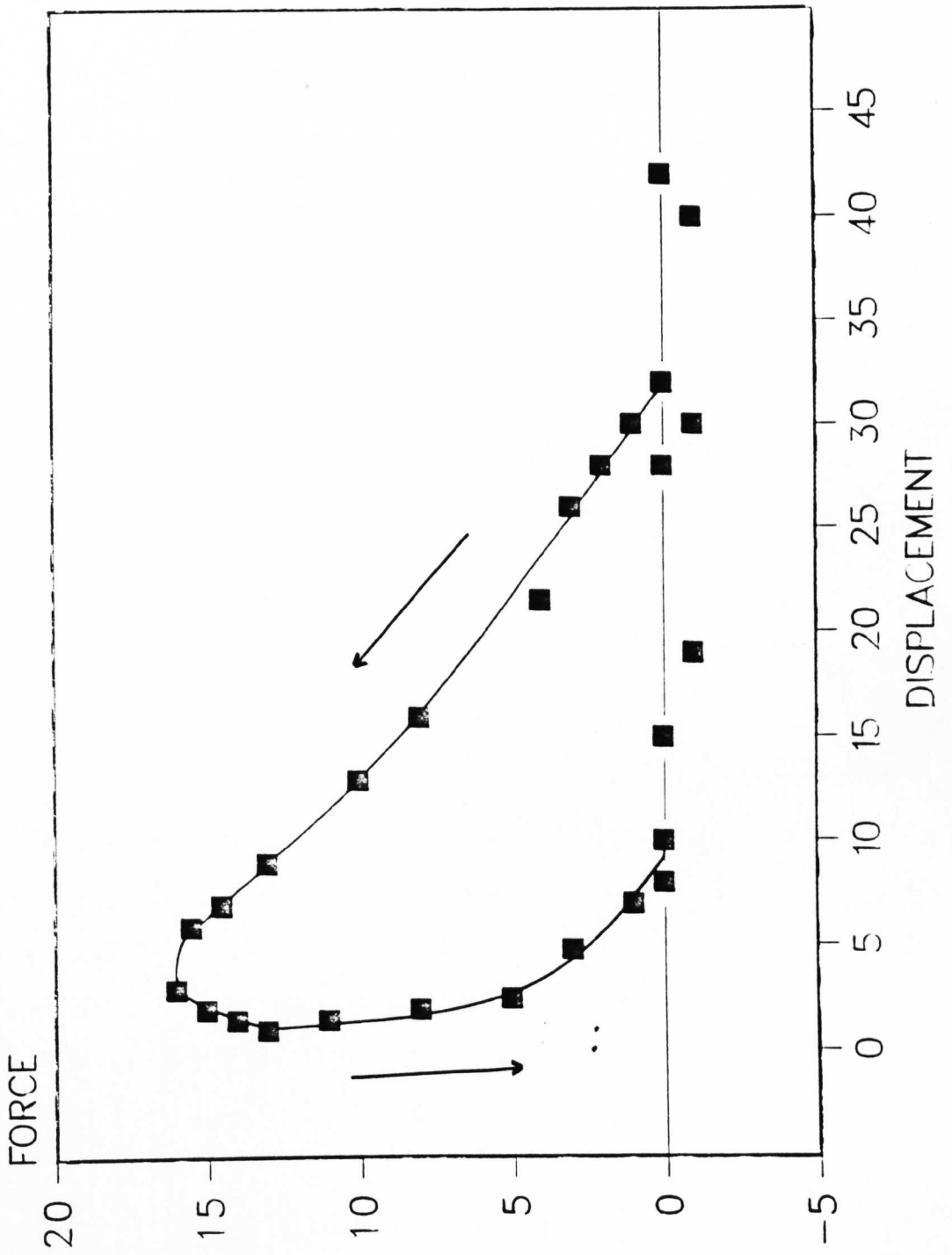


**FIG 2-4i** FORCE DISPLACEMENT MODEL ATEST6



as indicated by the low error values. The ATEST5 decompression curve could not be fitted sufficiently well to the data to give an accurate result as indicated by the high error value. This was thought due to the unrealistic excessive curvature between two data points which could not be compensated for by the software. This degree of curvature would be unlikely to occur in a real data set but care will be taken to monitor the curve fitting error value.

When this software was used to analyse a real data set, the compression and decompression curves, after sorting and correction for distortion were seen to be of a sawtooth nature rather than a smooth curve. The irregular curves were accompanied by a high curve fitting error value. This effect was due to the limited resolution of the transient recorder which resulted in a range of force values for a given displacement. When the adjustment for distortion was made this range would tend to skew the data towards the higher forces. To eliminate this effect the mean of the force range was calculated prior to the distortion adjustment.

The sorted and calibrated force displacement data may be saved from the Energy program as a named file for analysis by another program if required. A spreadsheet package called Minitab®, will be used to analyse these files using such as the Heckel equation (1961a,b). Heckel plots may be plotted and linear regression carried out on any part of the curve using a control program an example of which may be seen listed in the appendix.

#### 2.4.5 The High Speed Compression Simulator

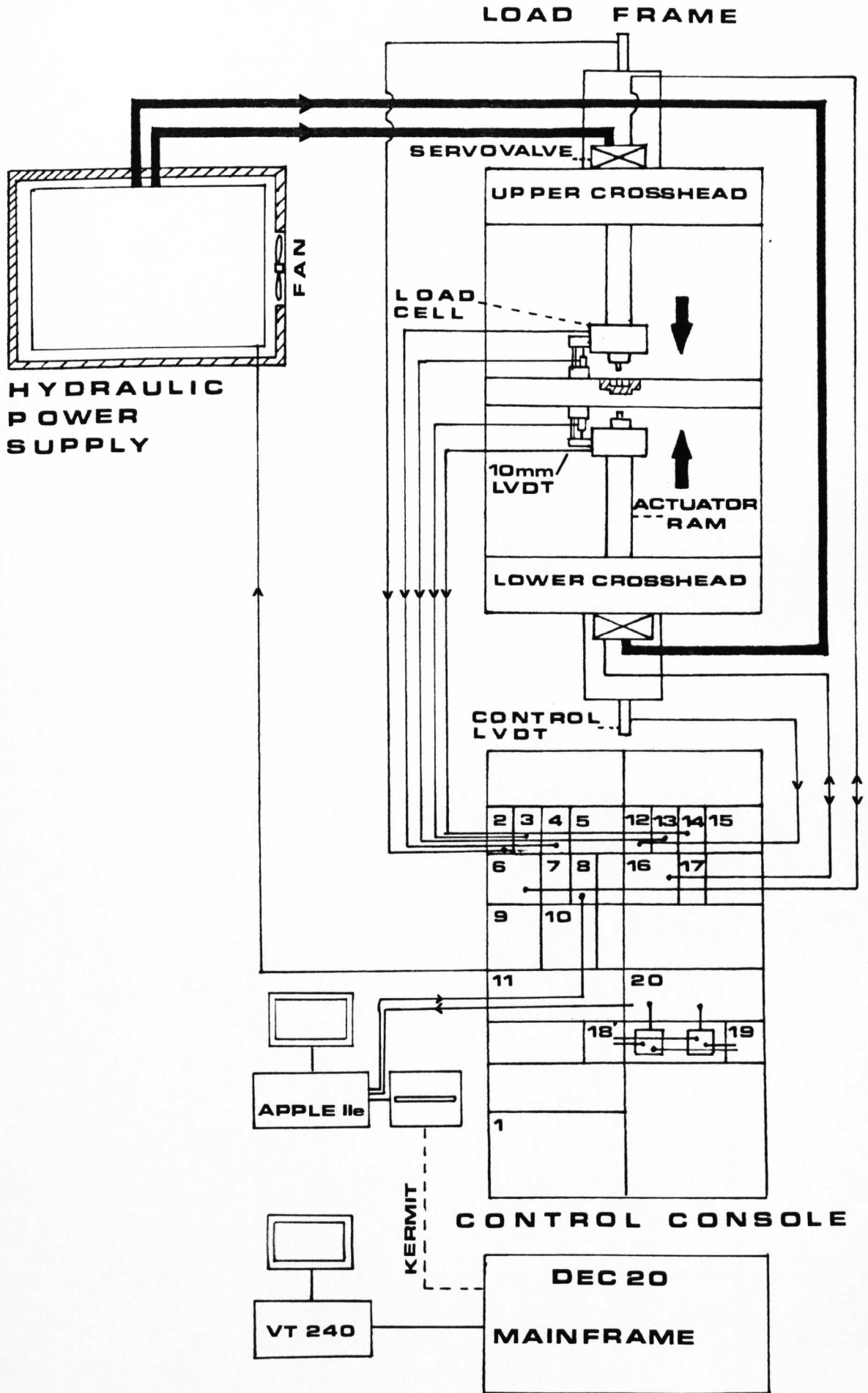
A commissioned and validated system is available to compress materials within a die at variable compression rates in excess of 1.8m/s. The punch separation and load may be monitored to  $\pm 12 \mu\text{m}$  and  $\pm 0.05\text{kN}$  (at 10kN range) respectively. Punch displacement time profiles

defined by two hundred data points may be generated, edited, stored and used to control punch movement using the Apple IIe computer and simulator software.

Data may be captured using the transient recorder and subsequently plotted on the Servogor 461 or transferred digitally via the Apple IIe computer to the Dec 20 mainframe computer for analysis. Analytical validated packages available to treat the data include force displacement plotting with energy calculation and Heckel plots. A diagrammatic representation of this system may be seen in FIG 2.4j. This system may now be considered to fulfil the requirements of a High Speed Compression Simulator.

Although 'Simulator' is the accepted terminology for such a machine it should be remembered that such a system only partially simulates the events which take place on a tableting machine. It is only the compression event which can be simulated, consequently the effects centripetal force, machine vibration and the flow of a material are not represented. However a versatile machine is now available to give comparative compression data under similar conditions to those experienced on tableting machines.

FIG 2.4j Diagrammatic Representation of the Simulator



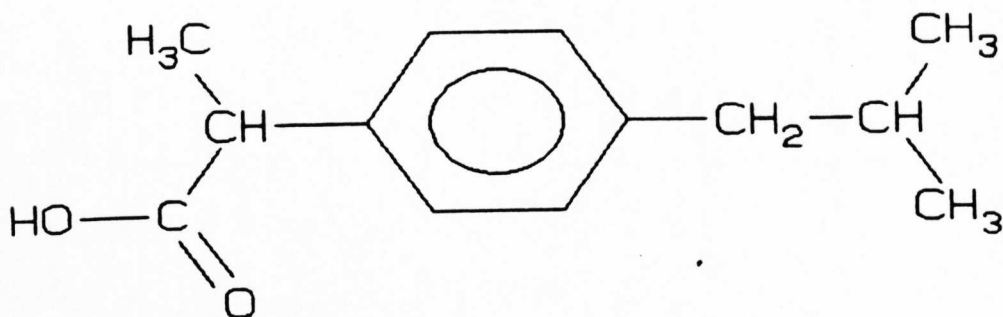
Three materials were selected to investigate the effects of compression speed. They were a material which consolidates mainly by plastic deformation; microcrystalline cellulose; a material which consolidates mainly by brittle fracture; lactose and a solid drug substance. A poorly compressible drug which was known to present tableting problems at high compression speeds was selected namely ibuprofen. The literature to date contains little information about the physical or compaction properties of ibuprofen. The use of this drug has increased dramatically in recent years due to its change in status to a 'pharmacy medicine'. As this drug has recently exhausted its patent life it is now readily available for research purposes.

Ibuprofen

Chemical Name :  $\alpha$ -p-Isobutylphenylprop ionic acid

Empirical Formula :  $C_{13}H_{16}O_2$

Structural Formula:



Molecular Weight : 206.3

Description : White crystals with characteristic odour and taste

Melting Point : 76°C

Supplier : Fisons Pharmaceuticals BN 77700004

Uses : Indicated for its analgesic and anti-inflammatory

effect in the treatment of rheumatoid arthritis, ankylosing spondylitis, and osteoarthritis. It is used in the treatment of periarticular conditions such as frozen shoulder, bursitis, tendinitis, tenosynovitis and low-back pain and in soft tissue injuries such as sprains and strains. It is also indicated for its analgesic effect in the relief of mild to moderate pain and for the relief of migraine.

#### Ibuprofen Granulation

This granulation was supplied by The Boots Co Ltd from a production batch. It will be used in the investigation comparing compact properties made to constant thickness with those made to a constant force. Unfortunately only limited details of this commercial product are available. It contains 64.9% ibuprofen.

Supplier : The Boots Co Ltd BN 68724

#### Paracetamol Granulation

This granulation was supplied by The Boots Co Ltd from a production batch. It will be used in the investigation comparing compact properties prepared using varying pre and main compression forces. Unfortunately only limited details of this commercial product are available. It contains 83.3% of paracetamol.

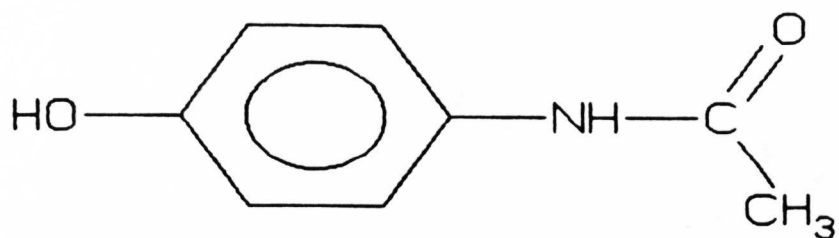
Supplier : The Boots Co Ltd BN 61714

#### Paracetamol

Chemical Name : N-p-Hydroxyphenylacetamide

Empirical Formula :  $C_8H_9NO_2$

Structural Formula:



Molecular Weight : 151.2

Description : White odourless crystals or crystalline powder with a bitter taste

Melting Point : 169°C to 172°C

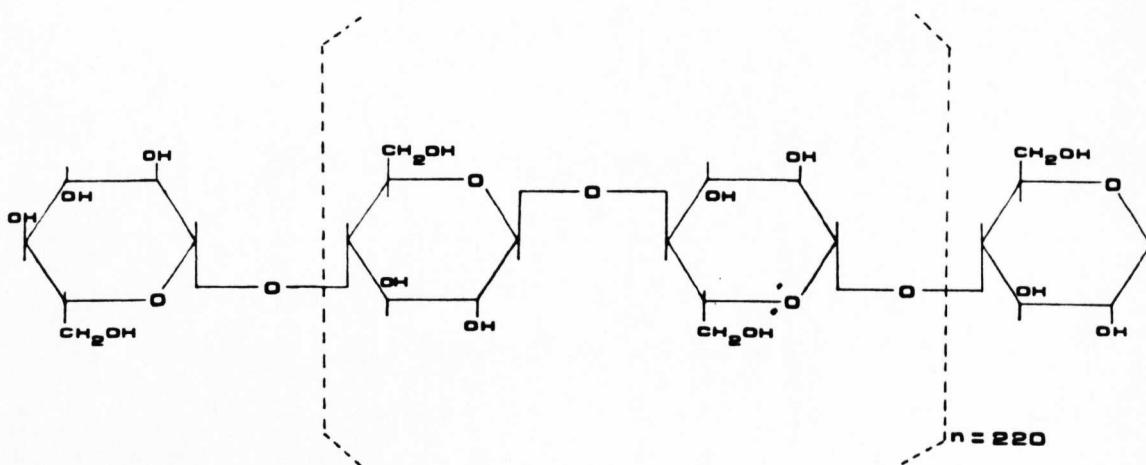
Uses : Paracetamol is a mild analgesic and antipyretic. It is recommended for the treatment of most painful and febrile conditions, for example; headache, toothache, colds, influenza and rheumatic pain.

#### Microcrystalline Cellulose

Chemical Name : Cellulose

Empirical Formula :  $(C_6H_{10}O_5)_n$  where  $n = 220$

Structural Formula:



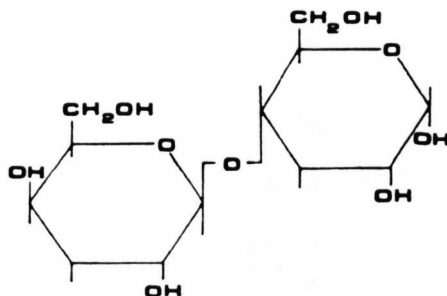
Molecular Weight : 36,000 (approximate)

Description : Purified partially depolymerized cellulose occurs as a white odourless, tasteless, crystalline powder composed of porous particles.

Melting Point : 260°C to 270°C  
Supplier : FMC Corporation Avicel® PH-101 BN 62866  
Uses : Tablet diluent and disintegrant

α-Anhydrous Lactose

Chemical Name : 4-O-β-D-galactopyranosyl-α-D-glucopyranose  
Empirical Formula : C<sub>12</sub>H<sub>22</sub>O<sub>11</sub>  
Structural Formula:



Molecular Weight : 342.3  
Description : Creamy white crystalline particles with no odour and a sweet taste.  
Melting Point : 223°C  
Supplier : De Melkindustrie Veghel bv DCL-30 BN 001438  
Uses : Tablet diluent

α-Monohydrate Spraydried Lactose

Chemical Name : 4-(β-galactosido)-D-glucose  
Empirical Formula : C<sub>12</sub>H<sub>22</sub>O<sub>11</sub>·H<sub>2</sub>O  
Structural Formula: As for α-anhydrous lactose  
Molecular Weight : 360.31  
Description : Creamy white crystalline particles with no odour and a sweet taste.  
Melting Point : 202°C  
Supplier : Meggle Milchindustrie GMBH Tablettose  
Uses : Tablet diluent

## Magnesium Stearate

Chemical Name : Magnesium Stearate

Empirical Formula :  $(C_{17}H_{35}CO_2)_2Mg$

Description : It is a very fine, white, bulky, impalpable, unctuous powder, tasteless and odourless.

Supplier : BDH General purpose reagent grade BN 4500860F

Uses : Tableting lubricant and glidant

### 3.2 Characterisation of Materials

#### 3.2.1 True Density Determinations

The ratio of the mass to volume is known as the density of a material. If the true volume of the solid particles, that is the volume of a sample enclosed by its outer surface and excluding its open pores is measured then the theoretical or true density may be calculated. Several practical techniques are available for measuring the volume of powder samples. The nearest approach to true volume is probably provided by a pycnometer. This instrument compares the differential pressure generated by moving two pistons within two similar cylindrical chambers. The introduction of a sample effectively into one of the chambers reduces the volume of that chamber increasing the differential pressure. The volume of the sample may be read directly in cubic centimetres once the differential pressure has been balanced.

#### Experimental

Determinations were carried out using the Beckman air pycnometer model 930. The pycnometer and all samples were allowed to equilibrate to room temperature before measuring commenced. The measuring piston was positioned at the predetermined starting number as indicated by the differential pressure indicator. The empty sample cup was connected to the measuring chamber and sixty seconds equilibration

time allowed to pass. The coupling valve was then closed. Both pistons were adjusted such that the differential pressure indicator remained on the scale until the reference piston made contact with its end stop. Thirty seconds were allowed to pass enabling equilibration of the system. The differential pressure indicator was then adjusted to the null position by moving the measuring piston. The coupling valve was opened and the corresponding 'zero' volume recorded.

This basic procedure was used to measure volume of the small and large standard volume stainless steel spheres provided. The null indicator offset, counter offset and span offset were adjusted until the instrument produced results within the calibration tolerance of  $\pm 0.015\text{cm}^3$ . A typical set of calibration results are shown in table 3.2a.

The powder was weighed into the tarred sample cup and the volume measured as previously described. The true density was calculated by dividing the mass of powder by its true volume. At least three determinations were made for each material. The true densities are detailed for each material in table 3.2b. The true density value for  $\alpha$ -monohydrate spraydried lactose (Tablettose®) was provided by ICI pharmaceuticals. This material will only be used for the Simulator comparison investigation. Consequently this value will be used by all participants in this investigation to avoid introducing variable results due to differences in measuring the true density of the powder.

Table 3.2a Typical Calibration Values for the Small and Large Stainless Steel Spheres

Calibration	Zero	Small Volume $\text{cm}^3$		Large Volume $\text{cm}^3$	
		(Actual: $8.58 \pm 0.015\text{cm}^3$ )		(Actual: $28.96 \pm 0.015\text{cm}^3$ )	
		Reading	Corrected	Reading	Corrected
i	0.05	8.63	8.58	29.015	28.955
ii	0.05	8.64	8.59	29.015	28.955
iii	0.00	8.58	8.58	28.975	28.975
iv	0.00	8.59	8.59	28.975	28.975
Within Specification			YES	YES	

Table 3.2b True Densities of Powders as Determined Using the Beckman 930 Air Comparison Pycnometer

IBUPROFEN "as supplied"	WEIGHT g	VOLUME cm <sup>3</sup>	TRUE DENSITY gcm <sup>-3</sup>
i	11.7598	10.500	1.1199
ii	12.8438	11.470	1.1198
iii	10.5358	9.390	1.1220
MEAN $\sigma_{n-1}$			1.1206 0.00124
IBUPROFEN <40 $\mu$ m			
i	15.42	13.815	1.1162
ii	19.01	17.040	1.1156
iii	19.48	17.380	1.1208
iv	19.93	17.800	1.1197
MEAN $\sigma_{n-1}$			1.1181 0.00256
IBUPROFEN 40-105 $\mu$ m			
i	19.33	17.240	1.1212
ii	20.81	18.480	1.1261
iii	16.90	14.995	1.1270
iv	17.58	15.605	1.1266
MEAN $\sigma_{n-1}$			1.1252 0.00271
AVICEL "as supplied"			
i	11.133	7.213	1.5435
ii	13.295	8.602	1.5456
iii	13.372	8.642	1.5473
MEAN $\sigma_{n-1}$			1.5455 0.00190
AVICEL 40-105 $\mu$ m			
i	13.10	8.465	1.5475
ii	15.44	10.015	1.5417
iii	15.94	10.375	1.5364
iv	15.54	10.120	1.5355
MEAN $\sigma_{n-1}$			1.5403 0.00554
$\alpha$ -ANHYDROUS LACTOSE 40-105 $\mu$ m			
i	24.382	16.330	1.4931
ii	31.4654	21.060	1.4941
iii	27.3236	18.330	1.4906
iv	30.2957	20.290	1.4931
MEAN $\sigma_{n-1}$			1.4927 0.00149
$\alpha$ -MONOHYDRATE SPRAYDRIED LACTOSE "as supplied"			
Data supplied by ICI			1.53

## 3.2.2

Moisture Content DeterminationExperimental

Three samples of each powder were poured into individual evaporating basins and accurately weighed. A fourth evaporating basin was partially filled with phosphorous pentoxide. A vacuum oven was set to a predetermined temperature and allowed to equilibrate. Due to the low melting point of ibuprofen (78°C) a lower drying temperature had to be used, 50°C was found to be satisfactory.

The basins were placed in the oven. An Edwards vacuum pump was connected to the oven and the oven chamber evacuated to -0.85bar or better. The system was allowed to stand, the samples were removed at regular intervals and reweighed. When consistent weights were maintained the weight loss was calculated. the moisture content of the materials are shown in table 3.2c.

Table 3.2c Percentage Moisture Contents of Materials

	INITIAL WEIGHTg	FINAL WEIGHTg	%MOISTURE
<u>IBUPROFEN 50°C</u>			
i	16.749	16.737	0.067
ii	18.789	18.774	0.081
iii	16.019	16.007	0.075
MEAN $\sigma_{n-1}$			0.074 0.007
<u>AVICEL 100°C</u>			
i	5.952	5.669	4.765
ii	8.375	8.031	4.659
iii	5.236	5.029	4.700
MEAN $\sigma_{n-1}$			4.708 0.053
<u>ANHYDROUS <math>\alpha</math>-LACTOSE 100°C</u>			
i	10.002	9.952	0.500
ii	10.001	9.931	0.700
iii	10.000	9.930	0.700
MEAN $\sigma_{n-1}$			0.633 0.115
<u>IBUPROFEN GRANULATION 50°C</u>			
i	10.000	9.780	2.200
ii	10.001	9.791	2.100
iii	10.001	9.771	2.300
MEAN $\sigma_{n-1}$			2.200 0.100
<u>PARACETAMOL GRANULATION 100°C</u>			
i	10.002	9.822	1.799
ii	10.000	9.830	1.700
iii	10.000	9.820	1.800
MEAN $\sigma_{n-1}$			1.767 0.058

It was observed that the Avicel samples gained weight during weighing. The hygroscopic nature of the microcrystalline cellulose presented difficulties in obtaining the true moisture content. The first recorded weight was used, consequently this should be regarded as an approximate value. This value however does correspond well with the percent equilibrium moisture content of Avicel PH101 at 25°C and 50% relative humidity, The Handbook of Pharmaceutical Excipients (1986). Avicel samples will require controlled storage. A constant temperature and humidity cabinet was used to store all powder samples prior to testing. A thermostatically controlled water jacket regulated the temperature of the cabinet while a saturated solution of potassium carbonate maintained the relative humidity at 44%. All powder samples were stored in well-closed glass containers. Ideally the controlled environmental conditions should have been extended to the testing area, however this was not practical. The environmental conditions of the storage area were monitored using a relative humidity and temperature monitor and probe (Vaisala HMI14). The relative humidity was maintained between 40 and 46% while the temperature was regulated between 23 and 25°C during a standard working day including the removal of samples from the cabinet.

### 3.2.3 Particle Size Analysis

The particle size of a material influences the compression properties of that material as discussed in the introduction. Consequently if more than one material is being compressed the effect of particle size should be reduced by selecting the same size fraction of each material. The investigation into the effect of compression speed on the properties of mixtures of ibuprofen, microcrystalline cellulose and lactose required control over particle size. Different particle size ranges of microcrystalline cellulose and lactose are

readily available, The particle size distribution of the ibuprofen will be determined in order to select the excipients with a similar particle size range.

The method of choice depends on the approximate size and physical nature of the material under investigation. Microscopy was used to give an indication of the ibuprofen particle size range and shape. Using a light microscope fitted with a calibrated graticule, crystals were shown to be needle shaped between 3 $\mu$ m and 170 $\mu$ m. The smaller crystals tended to form agglomerates. Although microscopy provides an absolute method of size analysis, there is a dependence on operator skill and problems sizing irregular, needle shaped and agglomerated crystals. For these reasons a method based on particle volume was selected, the Coulter counter.

The Coulter counter is an electronic method of counting and sizing particles. A constant voltage is applied between two electrodes, providing a current across an orifice of known size. The major resistance to the current is concentrated on the volume of electrolyte within the orifice. The particles to be measured are passed through the orifice, this momentarily increases the orifice resistance by an amount proportional to the volume of electrolyte displaced by the particle. The change in resistance is converted to a voltage pulse which is amplified and passed through a pulse height analyser with attenuable threshold control. Those pulses which exceed the threshold level are counted. The instrument measures particle volume which is expressed as the diameter of a sphere with the same volume. The system is calibrated by measuring the pulse heights produced by spheres of known size. The instrument to be used in this investigation had previously been calibrated. Obviously the material should not be soluble in the electrolyte. As ibuprofen was sparingly

soluble in water a pre-saturated solution was prepared to act as electrolyte.

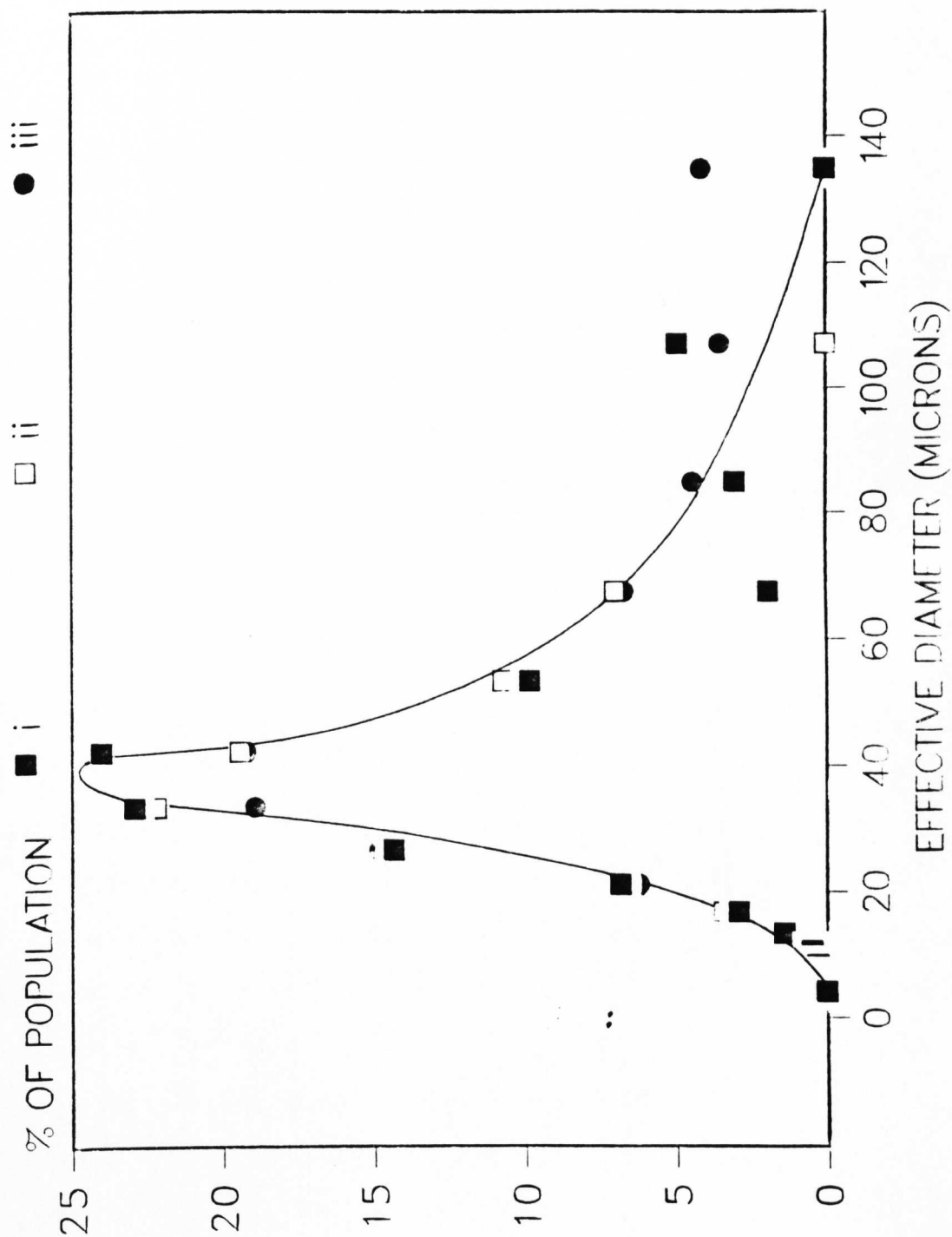
### Experimental

Excess ibuprofen was added to a 1 % sodium chloride solution and mixed for twenty four hours using a mechanical roller. The mixture was clarified by passing it through a Buchner filter. Undissolved solid was removed by passing the mixture through a 1.2  $\mu\text{m}$  pre-filter and a 0.22  $\mu\text{m}$  Sartorius membrane filter. The solution was passed through the 0.22  $\mu\text{m}$  filter a second time into the final container, which had been rinsed with a little of the previous filtrate. Two drops of surfactant were added to 250 ml of the solution and mixed. About 5mg of Ibuprofen was dispersed in the solution, which was placed in a water filled ultrasonic bath for fifteen minutes to break up agglomerates.

The precalibrated Coulter counter TaII was fitted with a 280 $\mu\text{m}$  orifice sampling tube and set to 0.5ml manometer volume and a sampling time of twenty seconds. The choice of orifice diameter is dictated by the particle size range. Generally the particles should be between 2-40% of the orifice diameter. The sampling time was set to give in excess of 40,000 particles for each sample. The background level was determined by measuring the number of counts in each size range using the filtered saturated electrolyte. The ibuprofen sample was then analysed. The number of particles in a number of size ranges between 3.75 $\mu\text{m}$  and 170 $\mu\text{m}$  were determined. The procedure was repeated to a total of three times. Readings were corrected for background levels, and the effective diameter of the ibuprofen was plotted against the percentage of the population as shown in FIG 3.2a.

The ability of the Coulter counter to sample such large numbers of particle provided a statistically precise method of size analysis for ibuprofen. The size fractions selected for the investigation were

**FIG 3.2a** PARTICLE SIZE RANGE DISTRIBUTION FOR IBUPROFEN AS DETERMINED USING THE COULTER COUNTER



split about the mode, 45 $\mu$ m-105 $\mu$ m representing the upper cut and <45 $\mu$ m representing the lower cut. The 45 $\mu$ m-105 $\mu$ m cut may be obtained from Avicel PH101 which has an average particle size of 50 $\mu$ m and from anhydrous  $\alpha$ -lactose DCL30. The traditional sieving of such particle size ranges would be time consuming and expose the materials to considerable physical stress, which could fracture some of the brittle lactose particles. The air jet type of sieve may provide an alternative method.

#### 3.2.4 Alpine Air Jet Sieving to Obtain Size Fractions Of Powders

This piece of equipment is limited to using one sieve at a time. The sieve is placed over a rotating slit equal in length to the radius of the sieve. Air is forced up through the slit and sieve mesh clearing any blocked apertures and mobilising the powder on the mesh. Continuous suction is applied over the area of the mesh, effectively drawing through any particles smaller than the mesh aperture. This system is especially useful for materials which agglomerate or blind conventional equipment.

#### Experimental

A 105 $\mu$ m aperture sieve was fitted to the Air jet sieve and a clean filter inserted into the undersize collector. 100g of powder was weighed into a jar and about 20g of this was placed onto the sieve. The sieve was then sealed and the air jet activated. After fifteen minutes a further 20g of powder was placed onto the sieve and so on until all of the powder had been used. The filter was removed and the undersize fraction collected and weighed. The oversize powder remaining on the sieve was brushed onto a collecting paper and weighed. The 105 $\mu$ m sieve was replaced by a 45 $\mu$ m sieve and the 105 $\mu$ m undersize fraction treated as before.

This process was repeated using ibuprofen, Avicel PH101 and anhydrous  $\alpha$ -lactose DCL30. The percentage size range distribution for each powder is shown in table 3.2d.

Table 3.2d Powder Size Fraction Distributions Determined Using the Alpine Air Jet Sieve.

POWDER SIZE FRACTION $\mu\text{m}$	AVICEL PH101		IBUPROFEN		ANHYDROUS $\alpha$ -LACTOSE	
	WEIGHT/g	%TOTAL	WEIGHT/g	%TOTAL	WEIGHT/g	%TOTAL
>105	5.36	5.51	0.24	0.26	81.82	83.3
45-105	57.42	59.08	66.25	72.93	16.33	16.63
<45	34.41	35.41	24.35	26.81	0.05	0.05
TOTAL	97.19		90.84		98.2	

From the Coulter counter data it would have been expected that the percentage of particles <45 $\mu\text{m}$  be approximately equivalent to the percentage of particles >45 $\mu\text{m}$ . This was not the case probably due to the fact that the Coulter Counter data was based on spheres of equivalent diameter. As the ibuprofen crystals were needle shaped many particles of apparently <45 $\mu\text{m}$  would only be able to pass through the sieve in one orientation or not at all. This would have the effect of reducing the passage of particles through the mesh. The large variation of the percentage of particles in each size fraction between materials confirms the need to extract these limited size fractions in this way.

### 3.2.5 Electron Microscopy of Materials,

Samples of the ibuprofen crystals, anhydrous  $\alpha$ -lactose crystals, Avicel PH101 particles, ibuprofen granules, paracetamol granules and magnesium stearate were examined by Scanning Electron Microscopy (SEM). The samples were first mounted on aluminium studs using M-glue(g3664). The studs were then placed in the coating chamber of a Polaron E5000 diode sputter coating unit. The chamber was evacuated, refilled with argon and the samples coated with gold emitted at 1.2kV.

During this process the materials were subjected to elevated temperatures and greatly reduced pressures. This combination of conditions melted the ibuprofen crystals, this became evident, due to the inability of the coating unit to hold the reduced pressures and the formation of a shiny film over the sample. An alternative coating method was required for the ibuprofen crystals. The Hexland cryosystem CT1000 maintains the stage on which the studs are mounted during the coating process at  $-196^{\circ}\text{C}$  using liquid nitrogen. Using this system enabled coating to be achieved within strict control of the coating conditions. More reproducible results were obtained using a AEI evaporation coating unit.

The coated samples were individually placed on the specimen holder of a Jeol T200 Scanning Electron Microscope which was inserted into the vacuum chamber. The chamber was evacuated and the voltage required to accelerate the electrons from the electron gun selected. A low voltage was selected (5kV) to reduce the effect of temperature rise during viewing. The electron beam was focused by the electromagnetic lens system onto the specimen, the resulting secondary electrons emitted from its surface were collected by an electron detector. The image formed could be viewed directly via a screen or recorded photographically using a Jeol T20CSI mounting connected to a Mamiya 6x7 roll film adaptor unit loaded with 120 Ilford FP4 iso 125/22 film.

The photomicrographs of the materials to be used in this investigation are shown in FIGS 3.2b-1.

### 3.2.6 Measurement and Pretreatment of Tooling

In order to calculate the pressure and volume of a compact during a compression the measurements of the punch faces and internal die diameter were required. These dimensions were obtained using a three

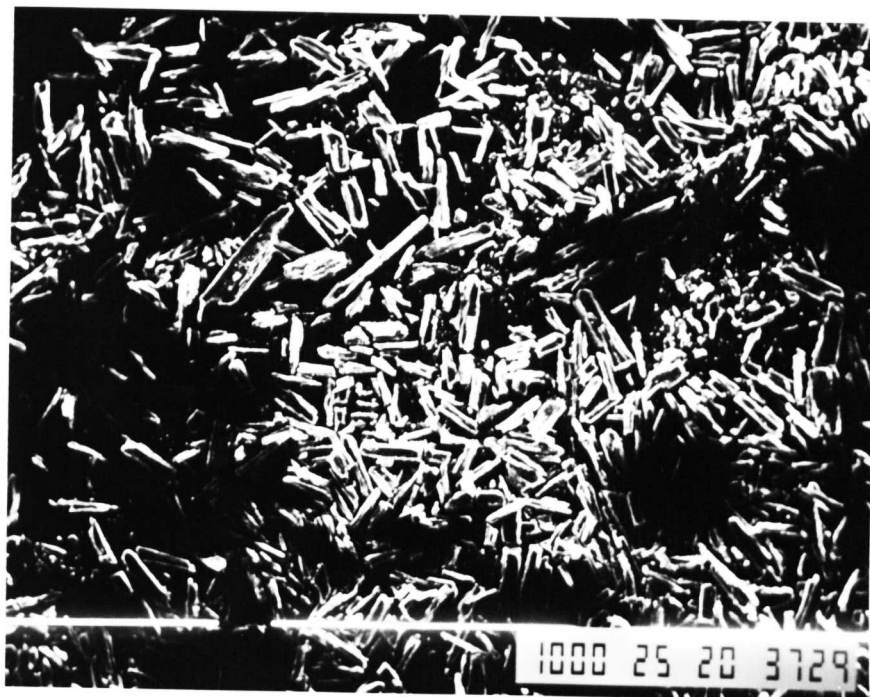


FIG 3.2b Scanning Electron Micrograph at Magnification X35  
Ibuprofen Crystals

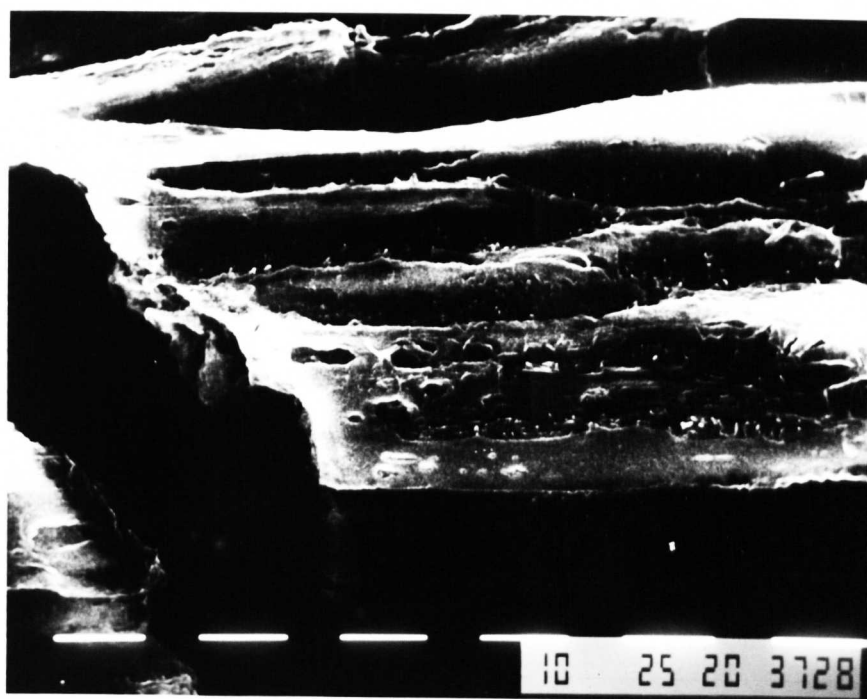


FIG 3.2c Scanning Electron Micrograph at Magnification X1000  
Ibuprofen Crystals

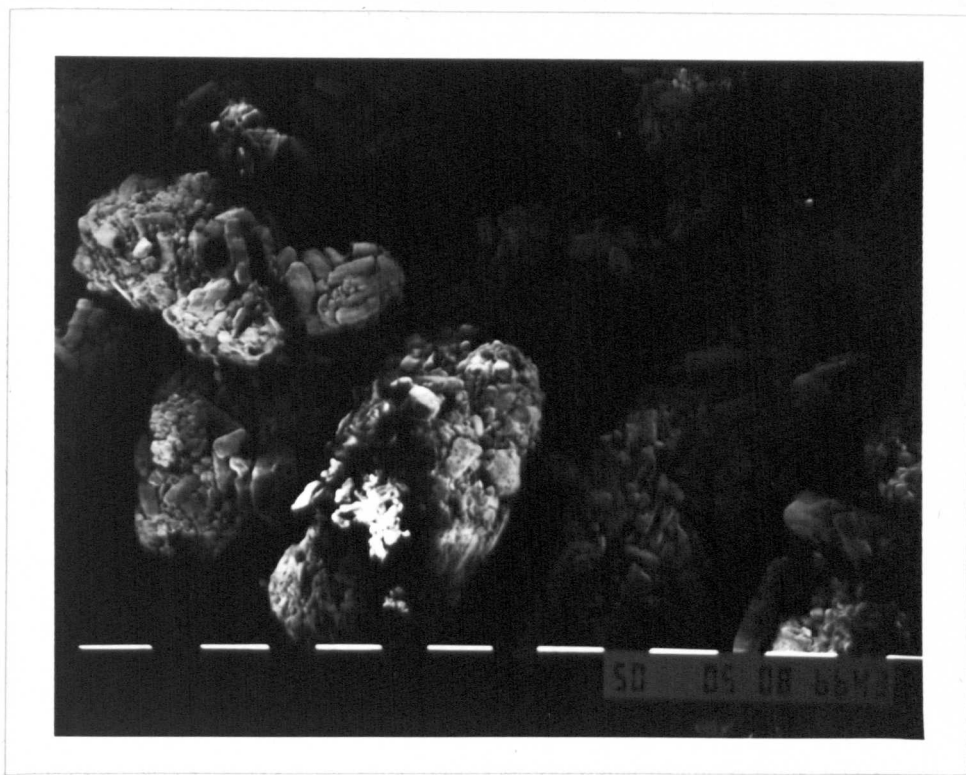


FIG 3.2d Scanning Electron Micrograph at Magnification X100  
Ibuprofen Granulation.

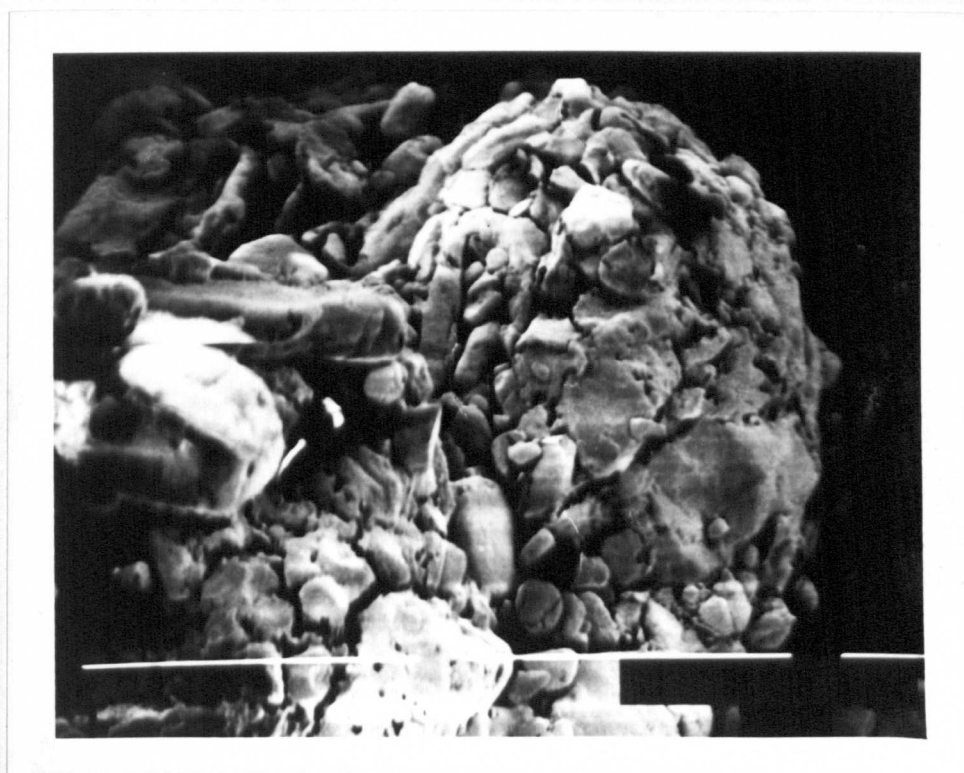


FIG 3.2e Scanning Electron Micrograph at Magnification X500  
Ibuprofen Granulation.

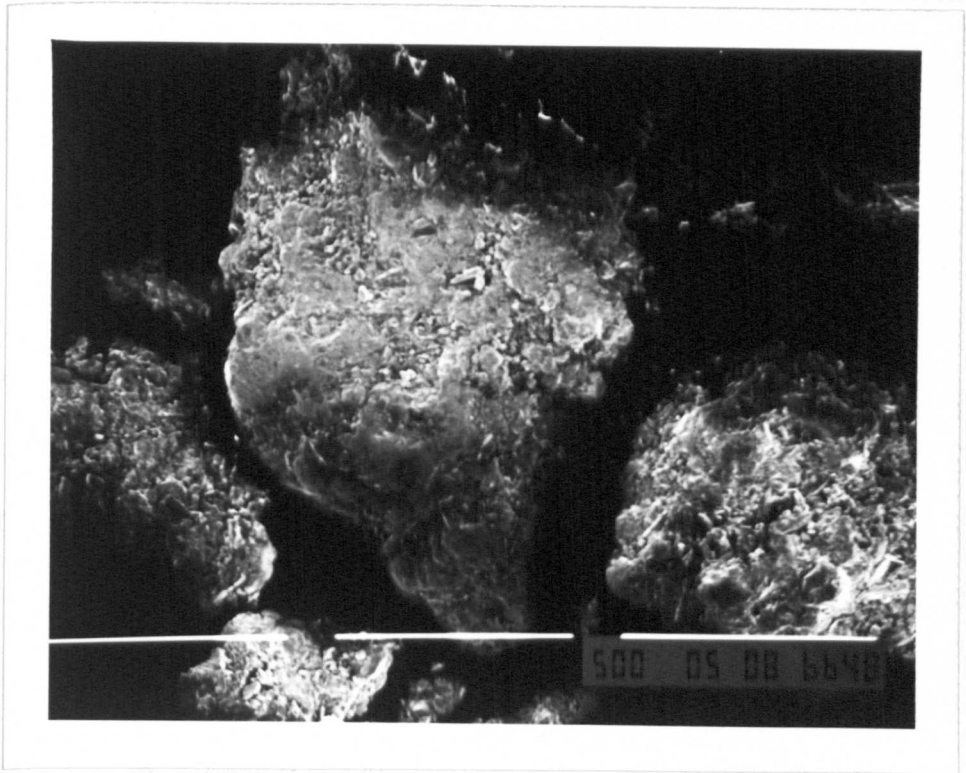


FIG 3.2f Scanning Electron Micrograph at Magnification X35  
Paracetamol Granulation.

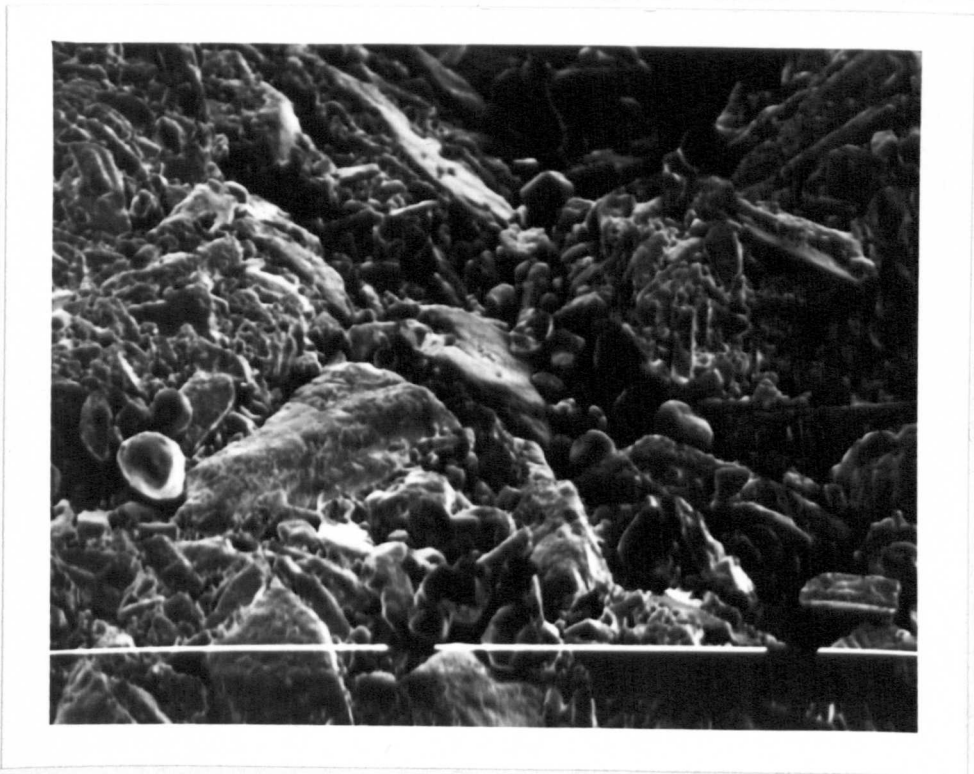


FIG 3.2g Scanning Electron Micrograph at Magnification X500  
Paracetamol Granulation.



FIG 3.2h Scanning Electron Micrograph at Magnification X100  
Microcrystalline cellulose.

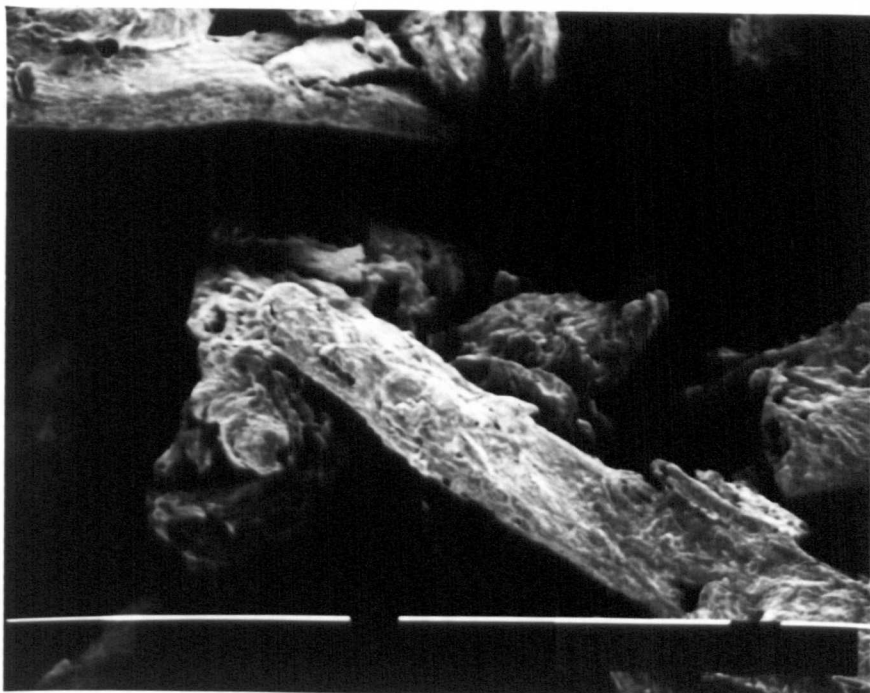


FIG 3.2i Scanning Electron Micrograph at Magnification X500  
Microcrystalline cellulose.

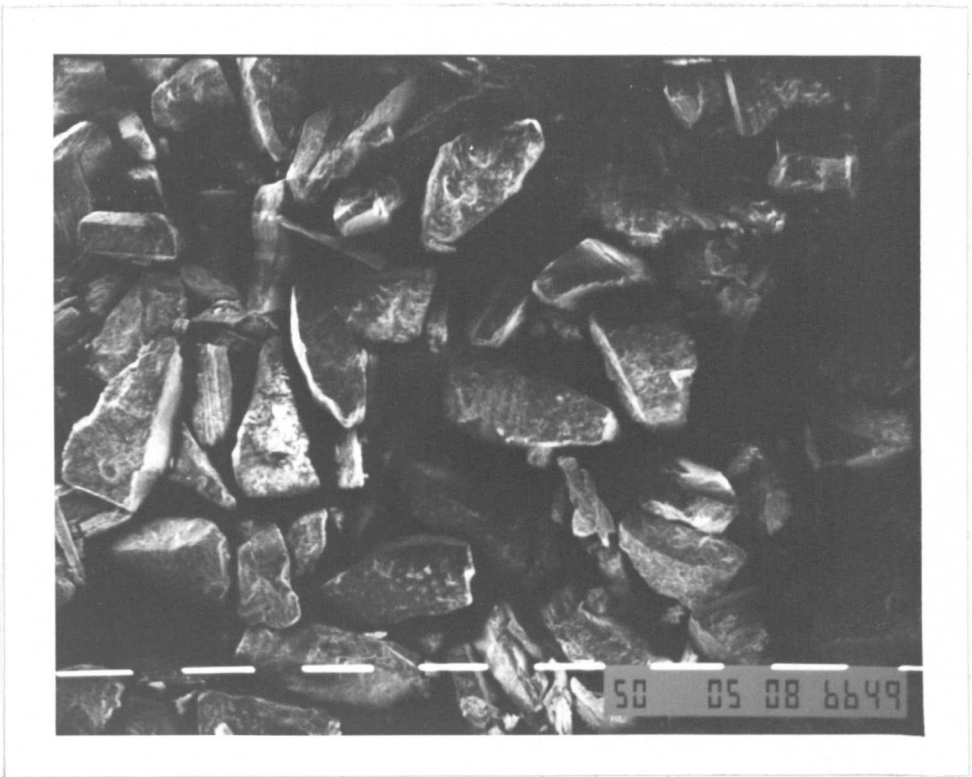


FIG 3.2j Scanning Electron Micrograph at Magnification X100  
 $\alpha$ -Anhydrous Lactose DCL-30.

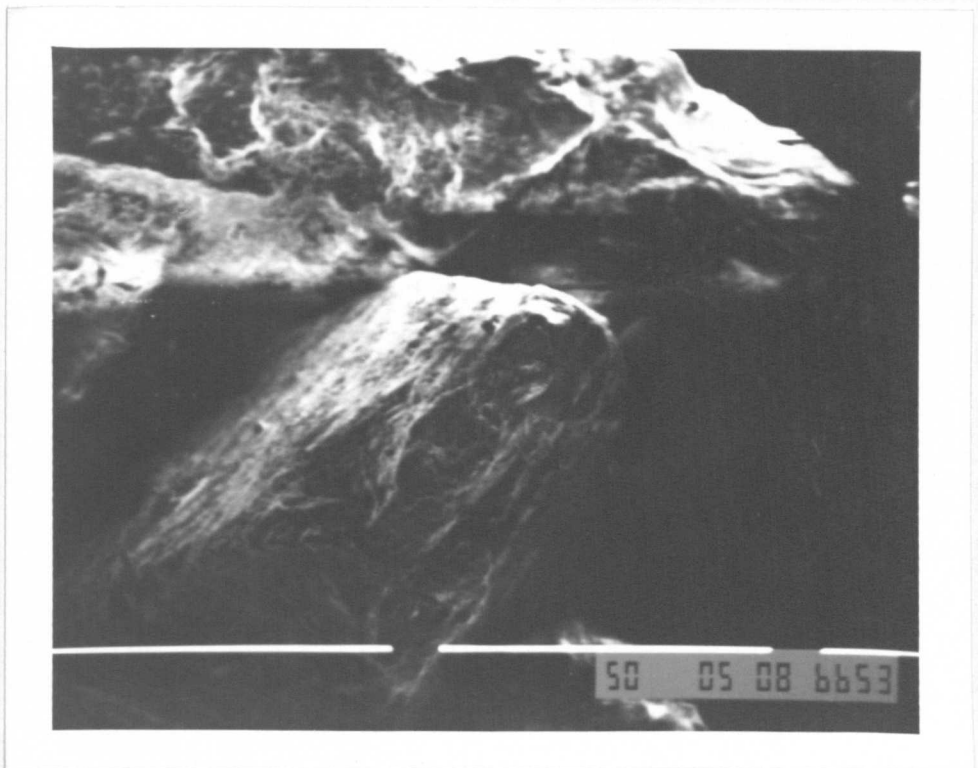


FIG 3.2k Scanning Electron Micrograph at Magnification X500  
 $\alpha$ -Anhydrous Lactose DCL-30.

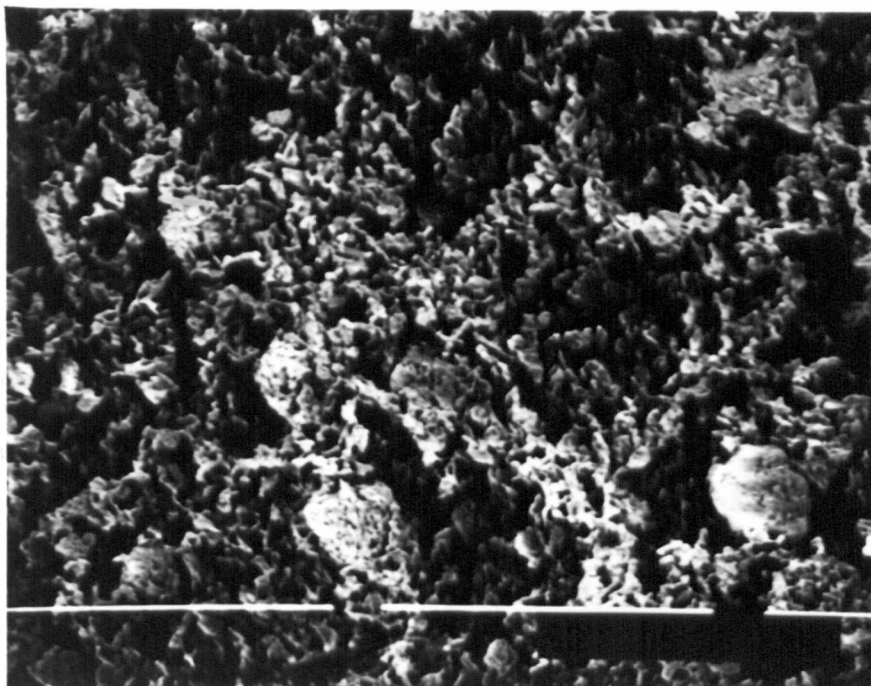


FIG 3.21 Scanning Electron Micrograph at Magnification X500  
Magnesium Stearate.

axis measuring machine SIP 414M (Societe Genevoise Switzerland). The die was placed on the measuring table and the microscope focused on the upper surface of the die. The intercept of the eye-piece cross-wires were aligned tangentially with the inner diameter of the die and the instrument zeroed. The stage was then moved until the eye-piece cross-wires were aligned tangentially with the opposite inner diameter of the die and the distance moved recorded from the digital read-out.

A similar procedure was repeated for the upper punch tip face. The measurements taken for the 12.5mm diameter flat faced tooling are shown in table 3.2e.

Table 3.2e Dimensions of the 12.5mm Flat Faced Tooling

ITEM	i	ii	iii	iv	NEAN	$\sigma_{n-1}$
Upper Punch Diameter	12.626	12.628	12.628	12.627	12.627	0.00094
Die Internal Diameter	12.716	12.716	12.714	12.711	12.714	0.00236
Die Internal Diameter (Replacement)	12.728	12.728	12.722	12.729	12.727	0.00320

Prior to compression the powder contact faces of the tooling were cleaned and lubricated to minimise the effects of friction. The addition of lubricant to the material being compressed could have modified the compaction behaviour. Consequently it was decided to coat the contact surfaces with lubricant by hand. Before each compression the internal surface of the die, upper and lower punch tips were cleaned with acetone using a cotton wool swab. The same areas were then lubricated with a suspension of magnesium stearate in carbon tetra chloride applied by means of a cotton wool swab. The solvent was then allowed to evaporate leaving a thin layer of lubricant. The time allowed for evaporation of the solvent was a minimum of five minutes; this time was taken to weigh the next sample, plot and store the current data. Initially a 2% suspension was used but ibuprofen was found to stick to the punch faces after compression. Increasing the

concentration of magnesium stearate to 4% was found to prevent this phenomenon.

### 3.3 Preparation of Compacts

The required tooling were fitted into the punch and die holders and cleaned with acetone. The punch retaining grub-screws were tightened under load to reduce bedding in effects. The Simulator and its control system were activated and allowed to equilibrate to its running temperature. The Simulator was then depressurized and the tooling lubricated after which the system was repressurized. The actuators were adjusted to their fill positions. The required weight of test sample was weighed by difference into the die cavity via a glass weighing boat to an accuracy of  $\pm 0.1\text{mg}$ . The desired time displacement control profile was loaded into the memory of the Apple IIe from floppy disk and its output rate programmed.

The sample was then compressed and ejected. The force and displacement data was captured via the transient recorder and transferred to the Dec 20 mainframe computer via the Apple IIe microcomputer. Prior to analysis the data were calibrated and corrected for distortion of the Simulator. The analysis carried out on each data set varied depending on the investigation. Analysis programs available included the Energy program described earlier and a pre-programmed spreadsheet (Minitab) for Heckel analysis. A hard copy of the transient recorder data was obtained via the Servogor 461 plotter. The maximum peak upper and lower punch forces were recorded from the digital peak meters in the control console and identified from the transient recorder data using a peak searching subroutine on the Apple IIe.

The tablet was retrieved, it was then weighed ( $\pm 0.1\text{mg}$ ), and its thickness and diameter measured using a Mitutoyo (293-601, 0-25mm)

digital micrometer ( $\pm 0.001\text{mm}$ ). The tablet was then allowed to recover for two hours after which its diameter and thickness were remeasured. At this stage the compacts were characterised according to the investigation. These included the radial tensile strength determined using the Instron 1121, disintegration time or examination by Scanning Electron Microscopy.

### 3.4 Characterisation of Compacts

#### 3.4.1 Radial Tensile Strength

Radial tensile strength was selected to show compact strength as it enables comparison between tablets of different thicknesses. An Instron 1121 was used to perform this test as shown in FIG 3.4a. The output of an instrumented upper punch was captured using a Kemo transient recorder (AM104, AM201). A hard copy of the captured data was obtained by plotting the data on the Instron chart recorder.

To measure the tensile strength of the compact, the tablet was placed edgewise between the faces of the punches. The crosshead of the Instron was lowered at a speed of  $0.83\text{mm/s}$  until fracture of the tablet was observed. Particular attention was paid to the mode of failure. If the fracture did not occur cleanly across the vertical diameter then the results from this test were ignored and the tendency to crumble, laminate or fracture irregularly recorded.

For each successful diametral compression test in which the compact broke cleanly across the vertical diameter, the force required for fracture was obtained by measuring the height of the peak force on the Instron trace and multiplying it by the calibration factor. This was then converted to the radial tensile strength using the formula described by Fell and Newton (1970):

$$\sigma_r = \frac{2P}{\pi Dt}$$

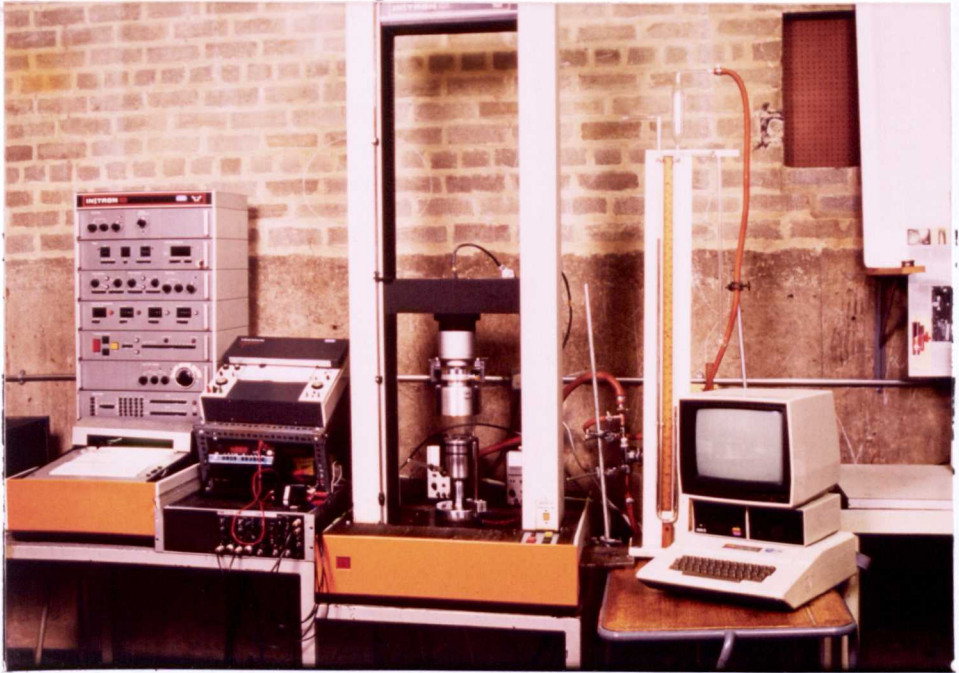


FIG 3.4a Instron Testing Machine Fitted with the Instrumented Upper Punch Connected to the Transient Recorder

Where P is the applied load, D and t are the tablet diameter and thickness respectively. Four good results were obtained for each condition within an investigation and used to calculate the mean and standard deviation of radial tensile strength.

#### 3.4.2 Disintegration Test

The disintegration test B.P was performed on four tablets from each batch of tablets under test. One tablet was placed in one of the glass vials in each of the four carousels. The total time taken for disintegration for each tablet was recorded, the mean and standard deviation for each batch was calculated.

#### 3.4.3 Electron Microscopy of Compacts

A similar process to that described for examination of materials by electron microscopy was used to examine tablets. These specimens were attached to the aluminium studs using silver-deg adhesive. The specimens were positioned such that a punch contact surface, die contact surface or a fractured edge could be viewed. The specimens were coated using the AEI evaporation coating unit. Electron photomicrographs were taken of features of interest or surface detail as described previously.

## 4.1

A Comparative Investigation of Compression Simulators

In 1976 Hunter *et al* presented details of the first High Speed Compression Simulator. This was a computer controlled hydraulic press capable of compressing materials according to a programmable displacement/time profile at rates up to 400mm/s to loads of 40kN. Five further High Speed Compression Simulators have been developed, each with slightly different specifications as shown in table 4.1a. Due to the diversity of each system, a comparative investigation was undertaken to confirm that results obtained from each machine could be interchanged and that each system produced equivalent quantitative data.

Table 4.1a High Speed Compression Simulator Specifications

INSTITUTION	NUMBER OF COLUMNS	MAXIMUM LOAD kN	MAXIMUM RATE mm/s	DISPLACEMENT STROKE RANGE		CONTROLLING COMPUTER	MANUFACTURER
				UPPER	LOWER		
ICI	4	50	400	±50mm	±25mm	PET	KEELAVITE
BOOTS	4	50	1000	±50	±50	H.P mini	MAND
WELLCOME	2	22.5	400	±12.5	-	PET	MAND
SK&F	4	50	1000	±5	±5	APPLE IIe	MAND
GLAXO	4	50	3000	±10	±10	OLIVETTI	ESH
LSP	4	50	3000	±10	±10	APPLE IIe	ESH

## Experimental

The High Speed Compression Simulator was fitted with a common set of 10mm diameter flat faced punches. The elastic deformation of the punches and other parts of the simulator were determined to allow true displacements to be calculated. The punches and die were cleaned and lubricated by painting a suspension of 2% magnesium stearate in carbon tetrachloride, on the inner die surface. The amount of material to give a 3.5mm thick compact at zero porosity was calculated from the true density. 421mg of Tabletose was accurately weighed out and poured into the die cavity. A simple sawtooth displacement/time profile was used to control the compression by the upper punch while the lower punch remained stationary. The material was compressed at a

speed of 100mm/s to a maximum pressure of 500MPa. Throughout the compression, upper and lower punch displacement and compression force were monitored and stored for subsequent processing. A total of six compressions were carried out by each group.

The force/displacement data were calibrated and corrected for elastic deformation using the procedures validated by each group. The data were then analysed using the Heckel equation (1961a,b):

$$\ln [ 1 / ( 1 - D ) ] = KP + A$$

Regression analyses were carried out on the Heckel plots over the ranges 50-200MPa, 50-300MPa, 50-350MPa and 50-400MPa. The relative density  $D_A$  was calculated using the following equation:

$$D_A = 1 - e^{-A}$$

The relative density of the powder bed at the point when a measurable force is applied, was determined and recorded as  $D_0$ . The mean and standard deviations of the mean yield pressure,  $A$  and  $D_A$  from the six compressions were then determined.

The Liverpool School of Pharmacy Simulator produced two data sets one year apart in order to act as a control for the material. A different set of tooling had to be used for this control data set.

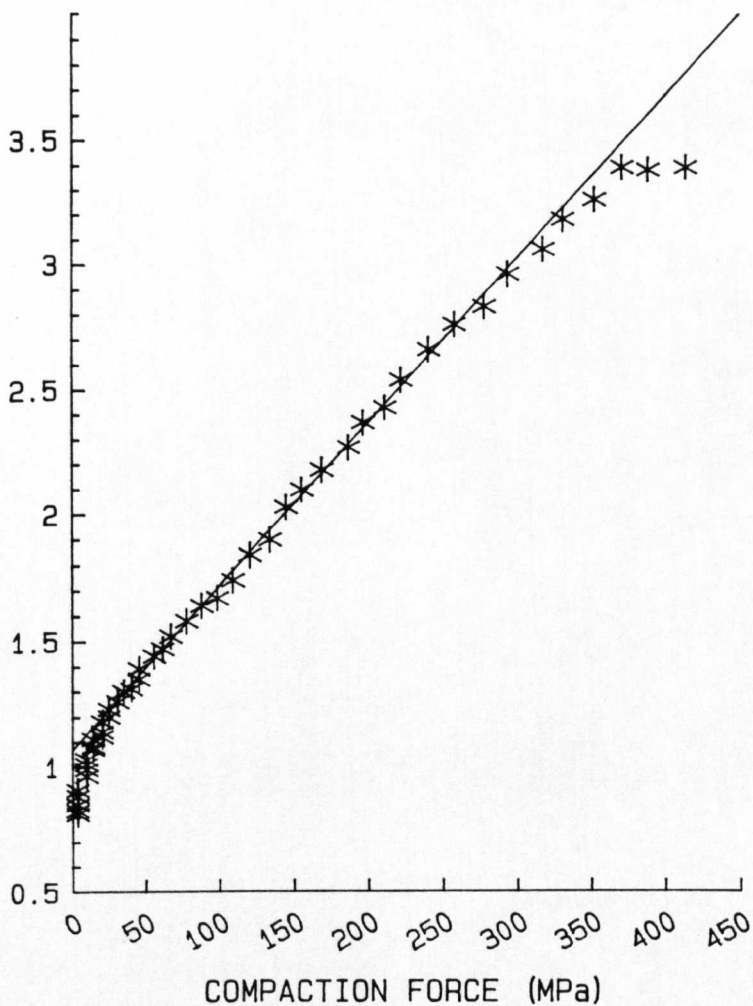
### Results and Discussion

FIG 4.1a shows a typical Heckel plot obtained using the Liverpool School of Pharmacy High Speed Compression Simulator. Table 4.1b depicts a summary of the results obtained from all of the operational Simulators to date.

The mechanism of compaction of lactose under these conditions have been reported previously by Roberts and Rowe (1985). Densification was predominantly by fragmentation but some strain rate sensitivity indicated that a certain amount of plastic deformation could be taking place.

**FIG 4.1a**                      **HECKEL PLOT**  
**TABLETTOSE**  
**LIVERPOOL POLYTECHNIC COMPACTION SIMULATOR**

LOG N (1/1-D)



50-400 MPa REGRESSION



The Liverpool School of Pharmacy data sets confirm that only a minimal change in the material could have occurred over the time period of the investigation. The slight increase in the mean yield pressures between the first and second data sets are more probably due to the change in the tooling, rather than a change in the material. 12.5mm flat faced tooling were used for the second data set. This increase in die diameter would be expected to decrease the applied pressure required to achieve a given density according to Lammens *et al* (1980). This would tend to shift the Heckel plot and could account for the slight differences between the data sets. The reduction in the standard deviation between the first and second data sets reflects the improvements made to displacement measuring system and the introduction of digital data transfer during the commissioning and validation of the Simulator.

For the rest of the results the same lactose sample and tooling were used by each group in turn. Hence any differences in the results must be due to the Simulators, data acquisition, or analysis techniques. The values for mean yield pressure in the range 50-200MPa shown in table 4.1b with the exception of SK&F are all within 10% of the mean. This is an acceptable level of experimental variation between different laboratories.

The SK&F data in all pressure ranges was seen to be considerably higher than that of any other group. The most likely explanation for this difference is the correction made for distortion of the punches and load frame. The SK&F data before and after correction for distortion is shown in table 4.1c.

Table 4.1c SK&F Mean Yield Pressure Analysis Before and After Correction for Distortion.

PRESSURE RANGE/MPa	BEFORE x. Py /MPa	AFTER x. Py /MPa
50 - 200	190.50	234.75
50 - 300	181.00	257.41
50 - 350	169.17	266.96
50 - 400	153.29	275.14

The measured distortion was  $3.2\mu\text{m/kN}$  for the upper punch and  $2.9\mu\text{m/kN}$  for the lower punch. The correction of data using these values of distortion would not be expected to cause changes of Mean yield pressure of the magnitudes proposed. It is possible that these differences are due to a mathematical error. It is likely therefore that the true SK&F values are nearer to the uncorrected values. In which case all pressure range values for mean yield pressure for all machines would be within 16.54%.

These differences in the mean yield pressure values are most probably due to the actual methods employed by the different groups to determine distortion. The general methods used were similar to that described for the Liverpool School of Pharmacy High Speed Compression Simulator described previously. The Boots Co.Ltd derived independent upper and lower punch distortion values using an additional LVDT installed in close proximity to the punch tip. ICI quantified the distortion of the individual parts of the simulator using a number of dial gauges positioned about the load frame. The method used by The Wellcome Foundation was as described by Ho 1986. It is difficult to state that any one method gives a more accurate measure of the actual distortion than another. Differences in the measured distortion would also be expected due to non parallelism of the punch faces and 'bedding in effects' which would differ between machines. It should be remembered that all of the methods used were at best approximate corrections, as the distortion was not measured under the same

conditions as those used during the comparison investigation in terms of rate of loading and compliance of the system.

Each of the machines has a different hydraulic system characterised by an individual valve configuration which is driven by different control systems. This could have an influence on the rate of compression once the punch tip has made contact with the powder. As Tablettose does exhibit some strain rate sensitivity Roberts and Rowe (1985) this too could influence the mean yield pressure results.

The accuracy of the displacement and load measuring systems are also important factors. Different displacement accuracies are claimed for each machine which are dependant on the stroke range of the LVDTs used. Claimed accuracies range from  $\pm 10\mu$  by ICI to  $\pm 50\mu$  for Wellcome and Boots. However all machines exhibited excellent reproducibility shown by the low values for standard deviation of mean yield pressure results. The  $D_0$  values reflect the sensitivity of the load measuring system, the lower this value the more sensitive the system.

### Conclusions

Most of the Simulators in this investigation may be considered to produce comparable data namely L.S.P, ICI, Wellcome and Boots. The true Heckel parameters under these conditions cannot be isolated, nor can the results from one machine be said to be more correct than those from another. However considerable confidence in the validation procedures detailed previously has been established by producing comparable data to the named machines above.

This investigation emphasises the importance of proper measurements of distortion during displacement measurements under load and indicates that a degree of caution should be exercised when comparing data produced by different research groups.

## 5.1 The Effect of Compression Speed on the Properties of Ibuprofen Tablets

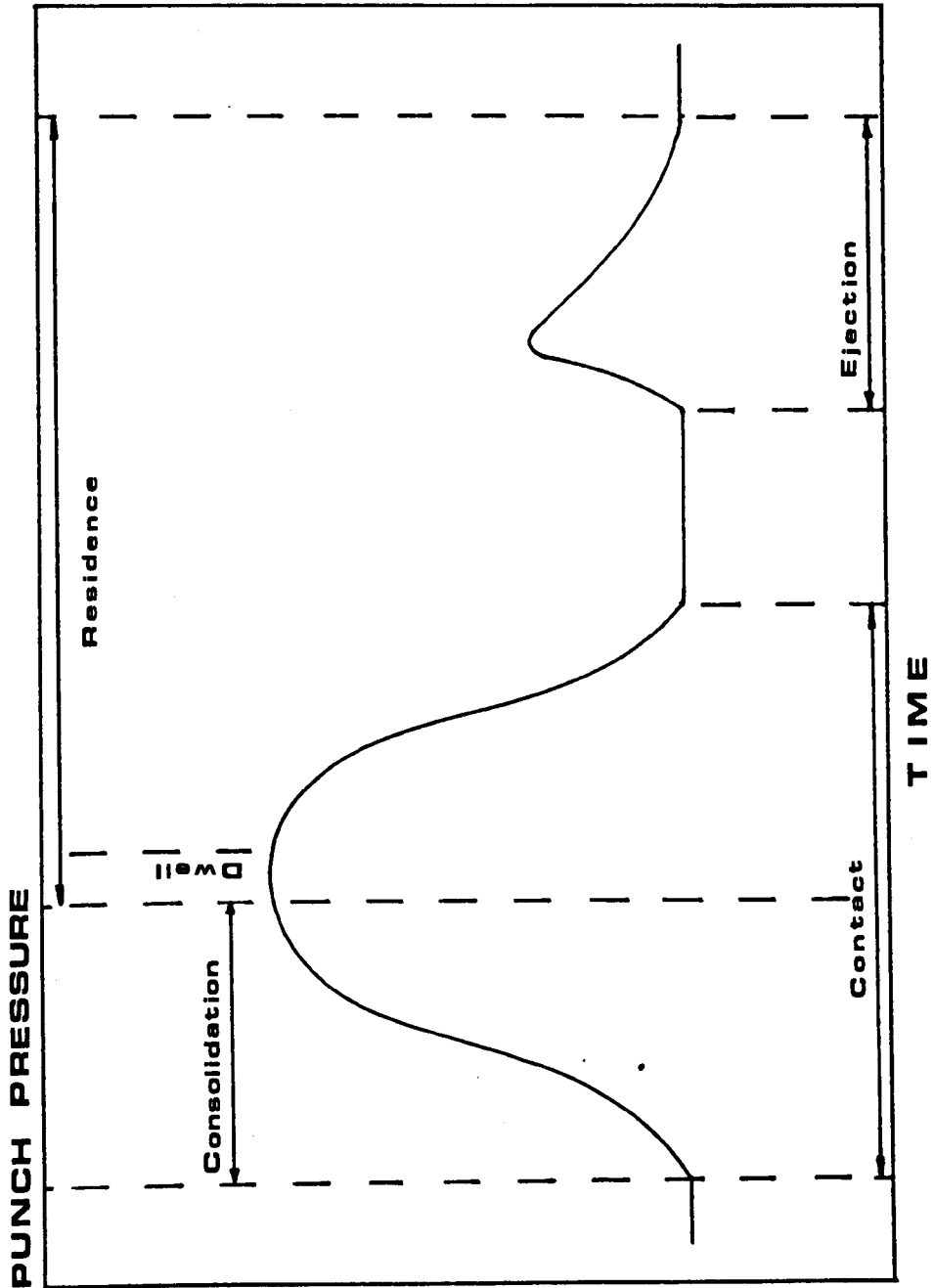
The aim of this initial investigation was to determine if ibuprofen was sensitive to the speed at which it is compressed, and if it is, then to identify suitable parameters to quantify any changes that occur.

### Introduction

Some of the earliest observations regarding the effects of compression speed were in relation to the capping phenomenon. Burlinson (1954) noted that if the compression was too rapid, the incidence of capping increased. This was explained by consolidation being induced by a 'stamp' rather than a 'squeeze', which was more likely to prevent the expulsion of air, resulting in capping.

The tableting event was divided into a number of punch pressure time relationships by Jones (1977). These included; consolidation; contact; dwell; residence and ejection times as shown in FIG 5.1a. It was recognised that each of these events would be altered when transferring a formulation from slow rotary or single punch reciprocating machines to the high speed rotary machines used during full scale manufacture. The rate and duration of each part of the tableting cycle will depend on the machine model and to a lesser extent the tooling used. Tableting machines have been developed to provide increasingly greater production rates. This has been achieved by increasing the number of tooling stations and compression rollers, combined with higher die table circumferential velocities. Consequently the time available for the tableting cycle has been reduced. In an attempt to overcome the resulting speed related problems, tablet machine manufacturers have introduced larger diameter compression rollers and modified cam profiles.

FIG5:1a PRESSURE-TIME PROFILE FOR A ROTARY MACHINE



A number of workers have investigated the effect of varying different parts of the tableting cycle. Ritter and Sucker (1980) used a mechanical press to show that the rate of decompression had more influence than the rate of compression on capping. Prolonging the decompression phase was shown to reduce the capping tendency by Sagawa et al (1977). A compression Simulator was used by Mann (1984), to quantify the contribution of each part of a Manesty Rotapress time displacement cycle, to the capping tendency strength and porosity of two tablet formulations. At compression rates in the order of 2,500 tablets/min, it was shown that the overriding factor which influenced capping pressure was the compression rate. Decompression and residence had a limited effect and the rate of ejection produced almost no effect. This tended to confirm air entrapment as a contributory factor to capping, as it could only take place during the compression phase. Tablet strength was seen to increase as the overall cycle time was reduced. The decompression rate was found to be the predominant factor influencing tablet strength and porosity for one formulation, while decompression rate was the most important factor for the other formulation. For this investigation the compression rate will be maintained equivalent to the decompression rate. The ejection rate will also be kept constant between different compression rates.

The effects of compression speed have been investigated in a number of ways. Earlier investigators such as Shlanta and Milosovich (1964) employed stress relaxation to elucidate time dependant mechanisms in tablet formation. David and Augsburg (1977) varied the overall compression cycle duration and the duration of the maximum compressive force to demonstrate the time dependant nature of plastic flow. Marshall et al (1986) monitored the percentage total recovery of compacts for cycle times of between 1s and 10s. These results indicated that the consolidation of ibuprofen was a balance between

elastic and time dependent plastic deformation. Rees and Rue (1978a,b) suggested an alternative technique for the evaluation of time dependent plastic flow during compaction, based on the effect of dwell time on Heckel plots. Contact times were varied between 0.17s and 10s on a Wilkinson STD1 reciprocating tableting machine. An adjunct to this was the quantification of the effect of strain rate on the deformation of preformed tablets. The non-recoverable deformation (NRD) for the tablets of plastically deforming materials was influenced by strain rate, whereas the NRD for tablets of brittle materials was not. It was proposed, that these techniques would be useful in predicting possible changes in tablet properties, when transferring a formulation from reciprocating to rotary machines. A similar scale up factor strain rate sensitivity index was proposed by Roberts and Rowe (1985), based on mean yield pressures obtained from Heckel plots over a range of punch velocities from 0.033mm/s to 300mm/s. A further parameter called rise time was proposed by Ho (1986) working at compression rates of up to 15mm/s. Higher strain rates have been investigated by Sanyo (1977), who used projectile impact velocities of 35m/s with copper powder; Barton (1978) using a drop hammer and by Al-Hassani and Es-Saheb (1984) using a drop hammer (10<sup>-3</sup>s) and an air gun apparatus (10<sup>-6</sup>s). However the high compression rate effects described by these authors are probably not applicable to pharmaceutical tableting where the compression rates are orders of magnitudes lower.

Several workers have calculated or measured the punch speeds experienced during tableting with both single punch and rotary machines. Charlton and Newton (1984) calculated initial punch speeds of 103.6mm/s for a Manesty 'F' single punch machine at a tableting rate of 60/min, and 102.4mm/s for a Manesty 'D3B' rotary tablet machine at a tableting rate of 480/min. Depraetère et al (1978) used

the Doppler effect of a laser beam to gauge the speed of tablet punches, but unfortunately did not publish the data. Mueller and Caspar (1984) measured the compression rate of the upper punch of an eccentric Hanseaten Exacta press as a function of its displacement. Rates were shown to decrease from 20mm/s at a tableting rate of 37/min to zero. The theoretical and actual punch velocities were compared by Armstrong and Palferey (1987) using a modified Apex eccentric press. Up to the point of maximum punch penetration, actual speeds were shown to be less than the predicted speeds due to loading of the system which tended to slow the driving motor. After the maximum punch penetration was reached, the actual speed may exceed the predicted speed due to elastic expansion of the tablet assisting the punch ejection. Roberts and Rowe (1985) defined the range of punch velocities experienced on tableting machines; single punch machine speeds from 50mm/s up to 150mm/s and rotary machines from 100mm/s to 400mm/s. No mention was made of the actual machines involved or the methods used to derive this data. It is probable that today's high speed rotary machines operate in excess of these ranges.

Compression rates in this investigation will cover the range from the lower end of the single punch machines 20mm/s and beyond that attainable by today's production machines 1800mm/s.

### Experimental

The methods used were as described earlier in the 'Preparation of Compacts'. Any supplementary details have been detailed below.

The simulator was fitted with 12.5mm flat faced 'F' machine tooling. 500mg of ibuprofen used 'as supplied' was compressed and then ejected from the die by raising the lower punch by adjustment of the lower displacement zeroing potentiometer. Uniaxial compression was provided by using a simple sawtooth time displacement profile for the top punch while the lower punch remained stationary. The punch speed

measured as impact velocity from the Servogor trace was varied between 22mm/s and 1750mm/s. Four compacts were made at each speed. Initial compressions were performed up to a maximum of 400MPa, a second series of compacts were formed at compressive pressures up to 60MPa. During compression the upper punch force and punch separation were monitored. The force displacement data were subjected to Heckel analysis using the Minitab spread-sheet package with the pre-programmed control routine listed in the appendix. The linear region of the Heckel plot was identified by eye. Regression analysis using the method of least squares was performed between 13MPa and 40MPa. The slope, intercept and the compact density at the first measurable force were recorded and used to calculate the mean yield pressure,  $D_a$ ,  $D_o$  and  $D_b$ . The tensile strength of the compacts were determined using the Instron testing machine. The fractured compacts were examined by electron microscopy.

#### 5.1.1 The Effect of Pressure

Compacts prepared using maximum pressures of 400MPa were of poor quality even at the slowest compression speed. Compacts showed signs of lamination and sticking. Comparison of the weight of powder placed in the die and the weight of the compact revealed that 1.89% of the ibuprofen had been lost during compression. A white flaky film was observed around the upper and lower punch tips after compression. This indicated that a small amount of the ibuprofen was escaping from the die during compression. The examination of the compact by electron microscopy revealed some amorphous regions on the punch contact surfaces as seen in FIG 5.1b. This combination of observations indicated that during the compression of the ibuprofen, melting on a relatively large scale was occurring followed by extrusion of the melt out of the die cavity.

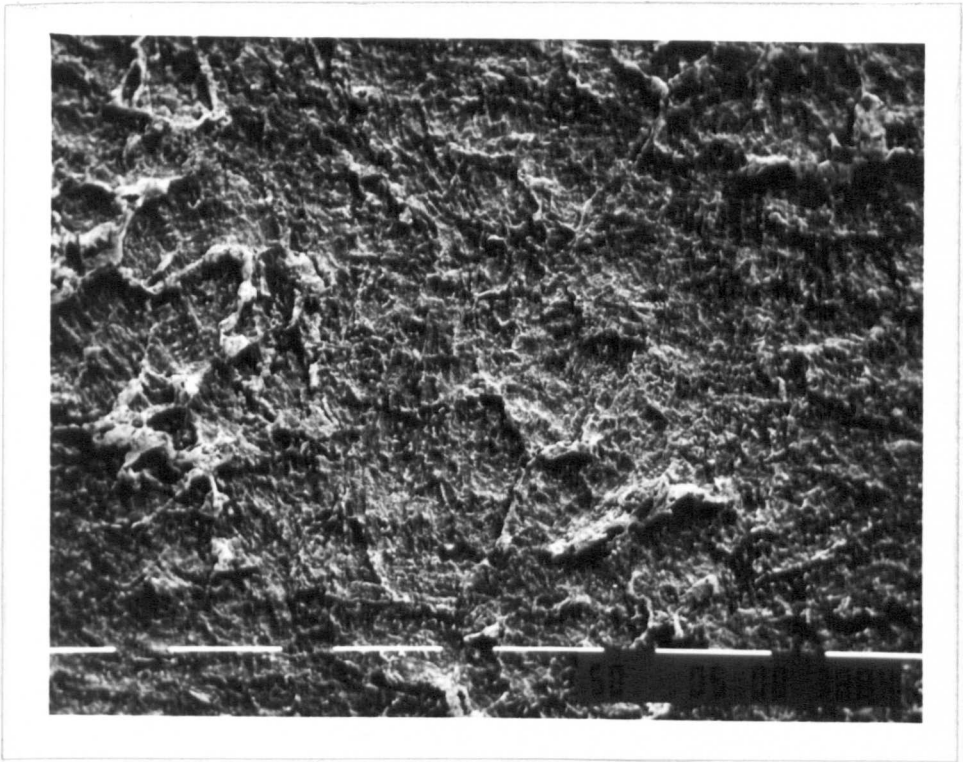


FIG 5.1b Scanning Electron Micrograph at Magnification 150X  
Ibuprofen Compact Upper Punch Contact Surface  
Compressed at 22mm/s to 400MPa

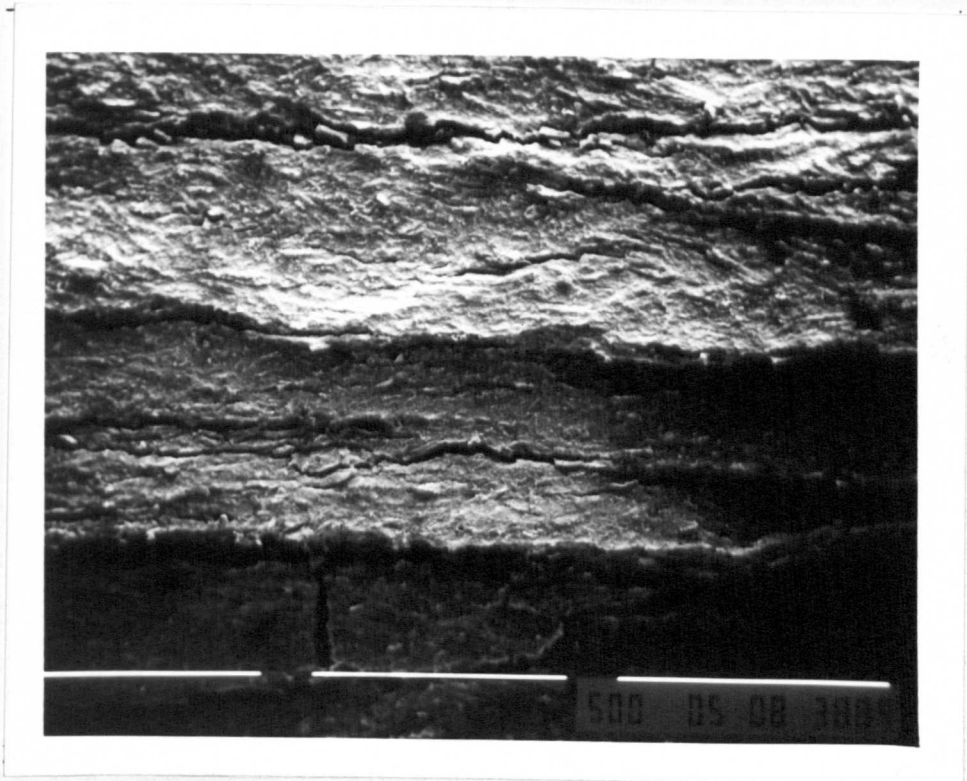


FIG 5.1d Scanning Electron Micrograph at Magnification 35X  
Ibuprofen Fractured Compact Edge Compressed at  
22mm/s to 400MPa

Nelson *et al* (1955) stated that during compression, the first law of thermodynamics requires that the energy expended manifest itself as heat or change the internal energy of the compressed material. The bulk of this energy was probably used to raise the temperature of the compact. Under the conditions of high pressure experienced during the tableting of pharmaceutical materials, temperature rises have been reported to occur between 5°C and 30°C by Hanus and King (1968) and Travers and Merriman (1970). These temperatures represent the the average temperature rises for the whole tablet. It would be expected that the temperatures at points of contact were higher as the frictional heat within the powder bed develops at these points.

Skotnicky (1953) has shown that under conditions where any liquid formed is not subjected to the same pressure as the neighbouring solid phase, the melting point of the latter could be lowered by an amount  $dT$  given by:

$$\frac{dT}{dP} = -\frac{VT}{\Delta L}$$

Where  $dT/dP$  is the change in melting point with pressure,  $T$  is the absolute temperature,  $V$  is the volume per mole of solid and  $\Delta L$  is the molar latent heat of fusion. This equation is relevant in the formation of a compact. Under the very high localized pressures occurring at the asperities, the melting point of ibuprofen would be expected to decrease during compression according to this equation. As a result of melting asperities the average distance between adjacent particles would decrease. This in turn would increase the contribution of Van der Waals forces, increasing the strength of the compact. The melting of asperities phenomenon has been previously reported as being a contributory factor in the consolidation of some materials by Jayashinghe *et al* (1969) and York and Pilpel (1972). Due to the

melting asperities the particles move closer together and the molten material may form a meniscus between them. Upon removal of the pressure, solidification occurs with the formation of fusion bonds between particles.

A similar process where raised temperatures and pressures act together to form a coherent body, has been reported in metallurgy and the briquetting of coal called sintering. Sintering has been defined by The Society for Metals, as the heating of metal powders or compacts to convert them into coalesced, alloyed, brazed or welded masses under controlled conditions of time temperature and pressure. Alternatively it has been defined by J. Wulff as the bonding of solid bodies by atomic forces and also as the bonding of solid bodies by the application of pressure and heat. Sintering always occurs below the melting point of the material. It is suggested that this process increases the bonding between particles by widening the amplitude of atomic motion. This increases the radius of action of the surface forces, effectively narrowing the the gap between the two adjacent surfaces.

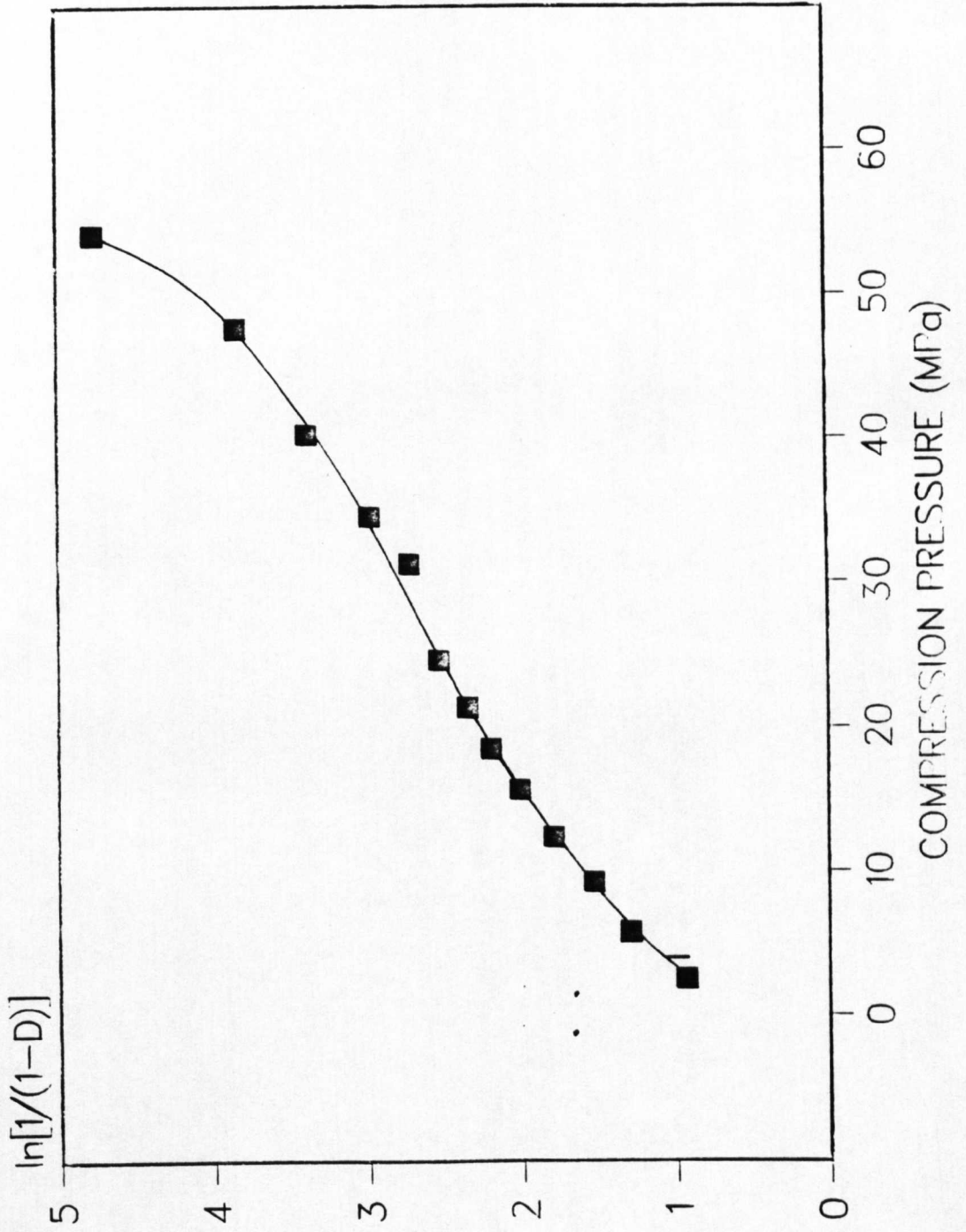
The melting of asperities concept may be extended in the case of ibuprofen due to its relatively low melting point of 76°C. The regions experiencing the greatest localized temperature rises will be the material in contact with the die wall and punch faces. At these locations the melting may well progress beyond the asperities. If the pressure further increases the molten material may be forced to the surface of the tablet and subsequently out of the die cavity. The molten material forced through the punch-die space, then solidifies on contact with the vertical surface of the punch tip and the punch shank forming the white film which was observed after compression. On removal of the punches the remaining molten material will solidify forming the amorphous regions seen in FIG 5.1b. This extensive melting

could also account for the tendency of this material to stick to metallic surfaces during compression.

A typical Heckel plot for ibuprofen compressed up to 400MPa is shown in FIG 5.1c. The relative density function exceeded unity at 60MPa which tends to confirm the loss of material during compression. This gives an approximate indication of when the effects of melting became significant. The Heckel analysis of this data would not be valid due to loss of material from the die. It should be mentioned that it is possible for the relative density to exceed unity due to other factors. These include; radial expansion of the die during compression, which effectively gives a greater actual compact volume or the use of a low true density value, possibly due to the contribution of totally enclosed pores in the material not detected during true density measurements.

The examination of the fractured edge of the compact by electron microscopy shown in FIG5.1d confirmed the lamination first detected by the unaided eye. These almost parallel horizontal fractures are a direct result of the high pressures used during compression. They probably formed as a result of the inability of ibuprofen-ibuprofen bonds to accommodate the stresses induced by elastic recovery during decompression and ejection. The parallel laminations are similar to those produced during ejection seen by Hiestand *et al* (1977) using erythromycin. A similar mechanism of lamination could occur with ibuprofen. During ejection the edge of the die concentrates relatively large stresses at the edge of the compact, a crack initiated at the edge may then propagate across the compact.

**FIG 51C** HECKEL PLOT OF IBUPROFEN COMPRESSED TO HIGH PRESSURE AT SLOW SPEED (22mm/s)



### 5.1.2 The Effect of Speed

Compacts prepared under lower pressures with increasing compression speeds developed defects as shown in the series of photographs FIGS 5.1e-h. The ibuprofen compressed at the slowest compression speed and low pressure formed the stronger coherent compacts of good quality. The scanning electron micrographs of such a compact seen in FIGS 5.1i,j show clearly defined crystals with few fractures or other defects. The amorphous regions and lamination seen at higher pressures could not be identified, indicating that the extent of melting had been dramatically reduced by decreasing the compression pressure. As the compression speed was increased signs of lamination became apparent. Examination of compacts by scanning electron microscopy, revealed that the lamination developed first at the centre of the upper punch contact surface and propagated outwards and down as the compression speed was increased. At compression speeds in excess of 240mm/s capping occurred within the die. The cap developed into the shape of an inverted cone which penetrated deeper into the body of the compact as the compression speed increased. At compression speeds in excess of 1100mm/s, the tip of the cone actually penetrated the lower punch contact surface forming a hole through the compact as shown in FIG 5.1h. Details of the associated lamination found at these speeds are shown in FIG 5.1k. The shape of the cap and the laminated regions could indicate the irregular density distribution within the compact.

These compression speed related effects are probably due to a combination of factors. Firstly the reduction of the time available for escape of air from the powder bed, may have caused increasing quantities of air to be entrapped within the compact as the compression speed increased. During decompression the air expands rupturing the compact. The increased compression and decompression

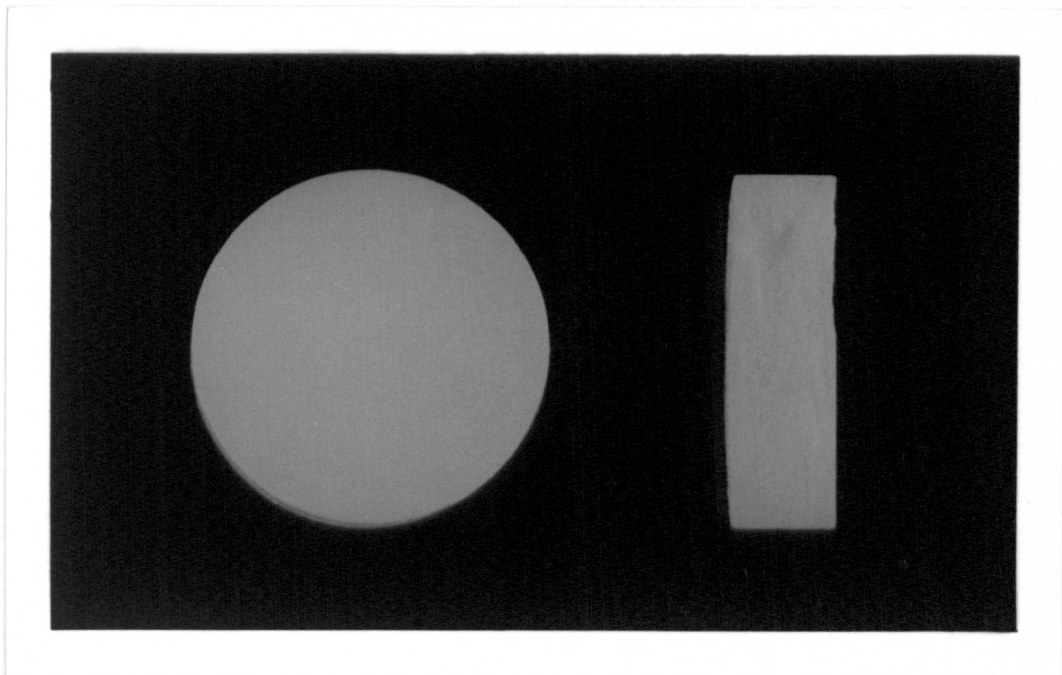


FIG 5.1e Ibuprofen Compact Compressed at 22mm/s up to 60MPa

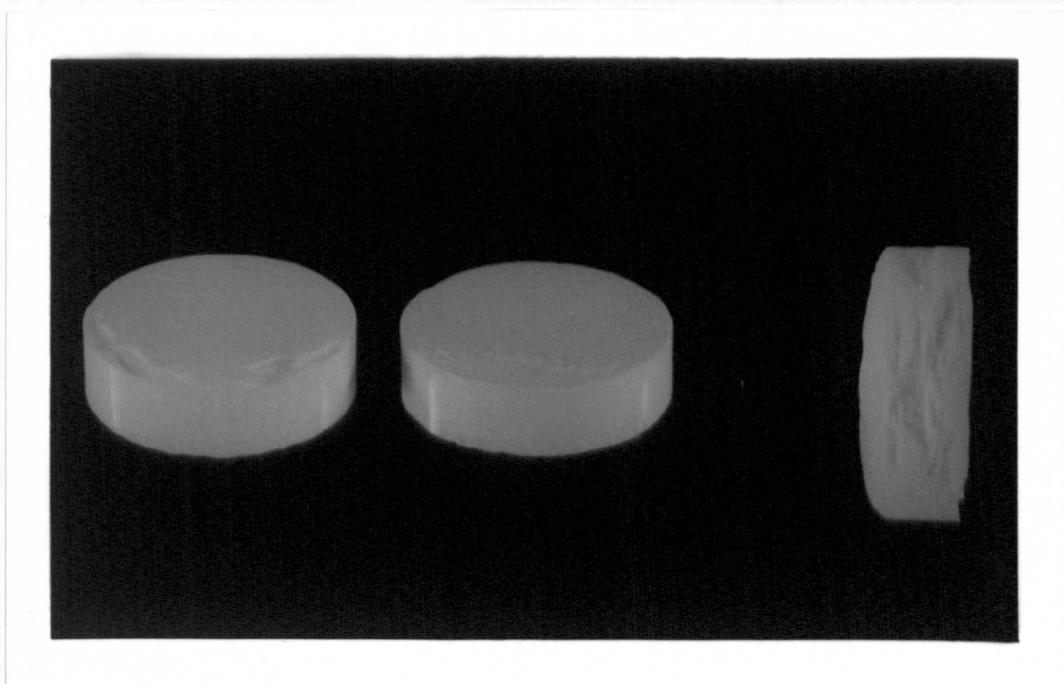


FIG 5.1f Ibuprofen Compact Compressed at 144mm/s up to 60MPa

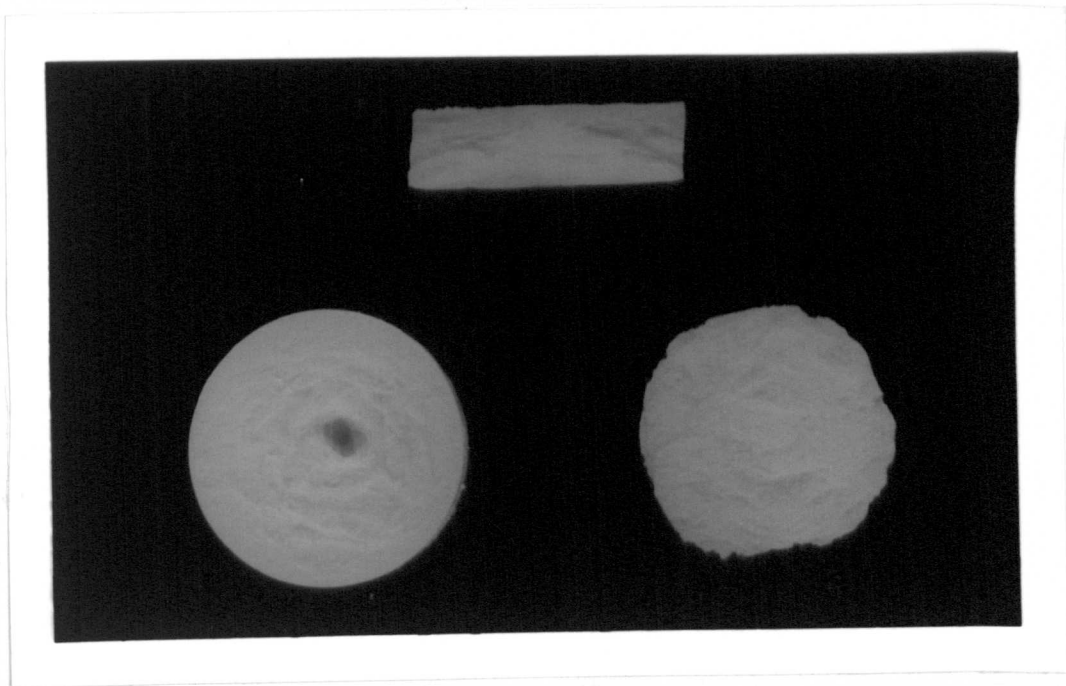


FIG 5.1g Ibuprofen Compact Compressed at 647mm/s up to 60MPa

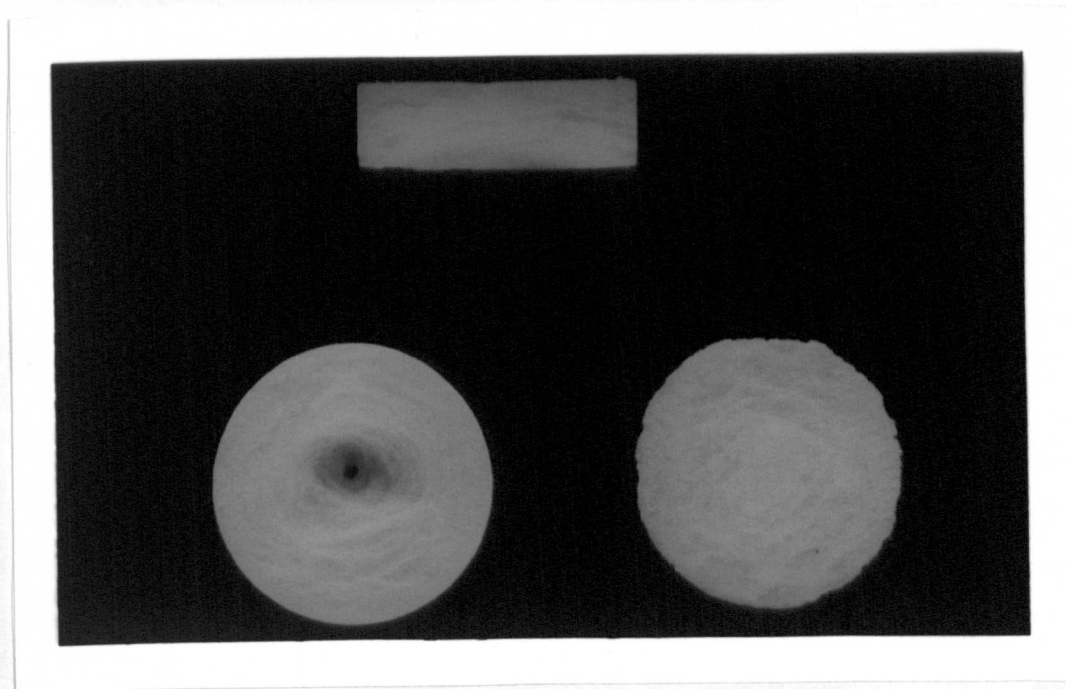


FIG 5.1h Ibuprofen Compact Compressed at 1123mm/s up to 60MPa

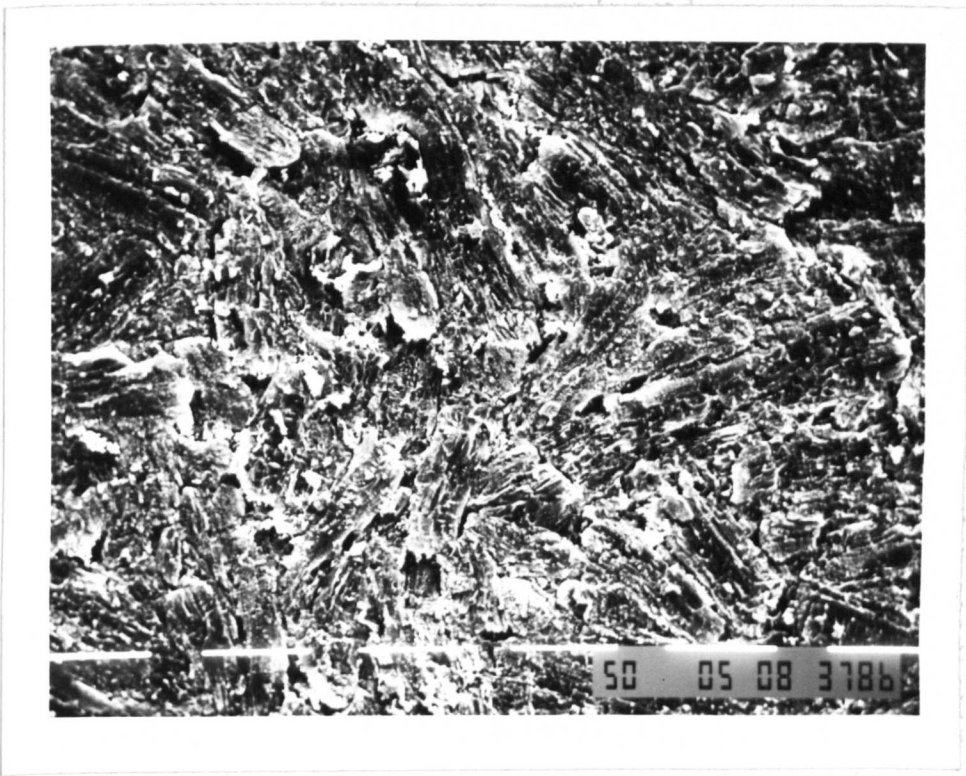


FIG 5.1i Scanning Electron Micrograph at Magnification 150X  
Ibuprofen Compact Upper Punch Contact Surface  
Compressed at 22mm/s up to 60MPa

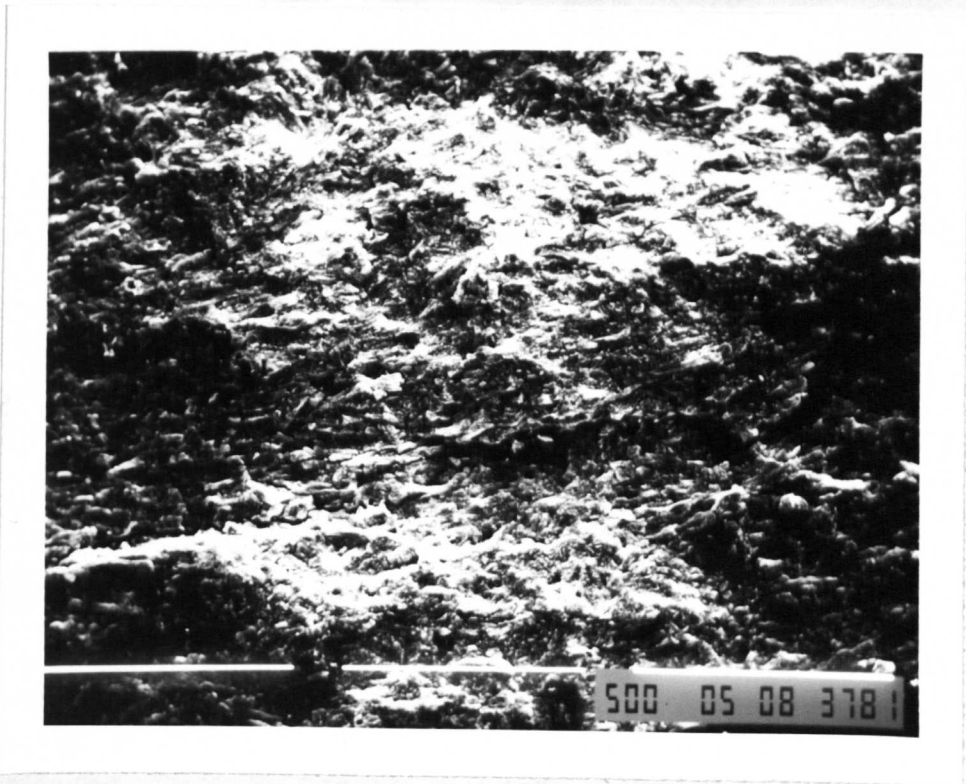


FIG 5.1j Scanning Electron Micrograph at Magnification 35X  
Ibuprofen Fractured Compact Edge Compressed at  
22mm/s up to 60MPa



rate would effect the stress relaxation and strain recovery of the compact. As the dwell times become shorter the stress relaxation will be reduced, less particle-particle bonds will be formed and consequently, the compact will be less able to withstand the stresses imposed during strain recovery. In addition the recovery event will occur more rapidly. This means that less time would be available for the ibuprofen to accommodate the stresses due to strain recovery. During the decompression there is insufficient time for the ibuprofen to deform and some interparticulate bonds will be broken weakening the compact. The faster the decompression, the greater the proportion of bonds broken and the weaker the compact.

The compact strength was found to decrease with increasing compression speed as shown in FIG 5.11. This tends to indicate that time dependant bonding mechanisms contribute to the consolidation of ibuprofen. All of the compacts formed were relatively weak confirming the poor compactability of ibuprofen. Such low compact strengths indicate that relatively few areas of true contact survive the decompression and ejection events. Although the strengths of compacts prepared at higher compression speeds could not be measured due to capping, it is probable, that the intact parts of the compacts would have been poorly bonded due to the reduced time available for plastic flow. The fracture planes induced by compression speed occur when insufficient areas of true contact form during compression which cannot withstand the stresses of elastic recovery. It is interesting to note that the compacts prepared under high pressures which experienced particle fusion due to melting, were in fact weaker than compacts prepared under lower pressures. An indication as to why this was the case may be seen from the large variation between the strengths of compacts prepared under high pressure. This large variation is probably a result of the internal fractures seen in

**FIG 5-1L** TENSILE STRENGTH OF IBUPROFEN COMPACTS COMPRESSED AT INCREASING SPEEDS

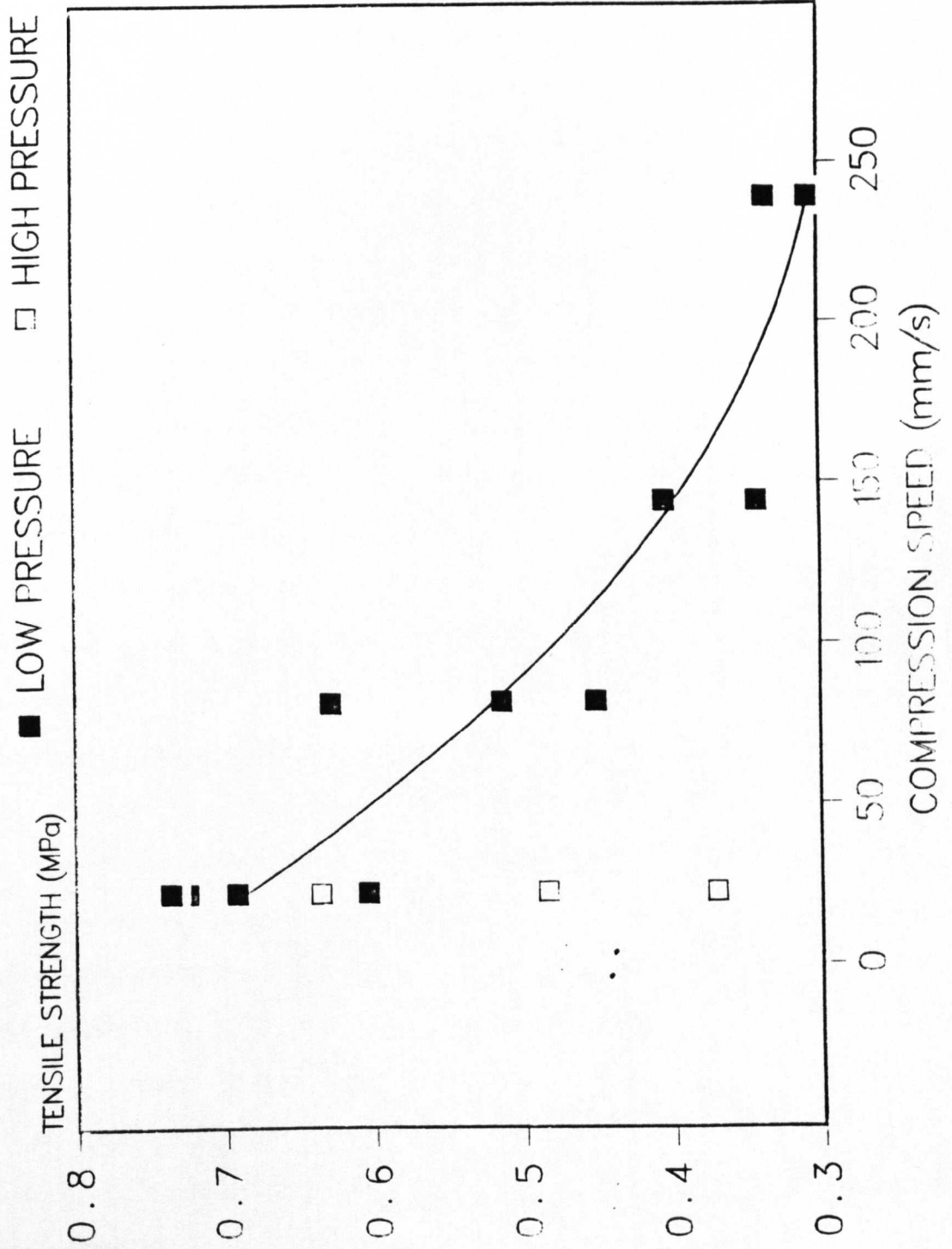


FIG 5.1d. The compacts prepared under higher pressures consist of dense strongly bonded regions separated by fracture planes which weaken the compacts in an irregular manner.

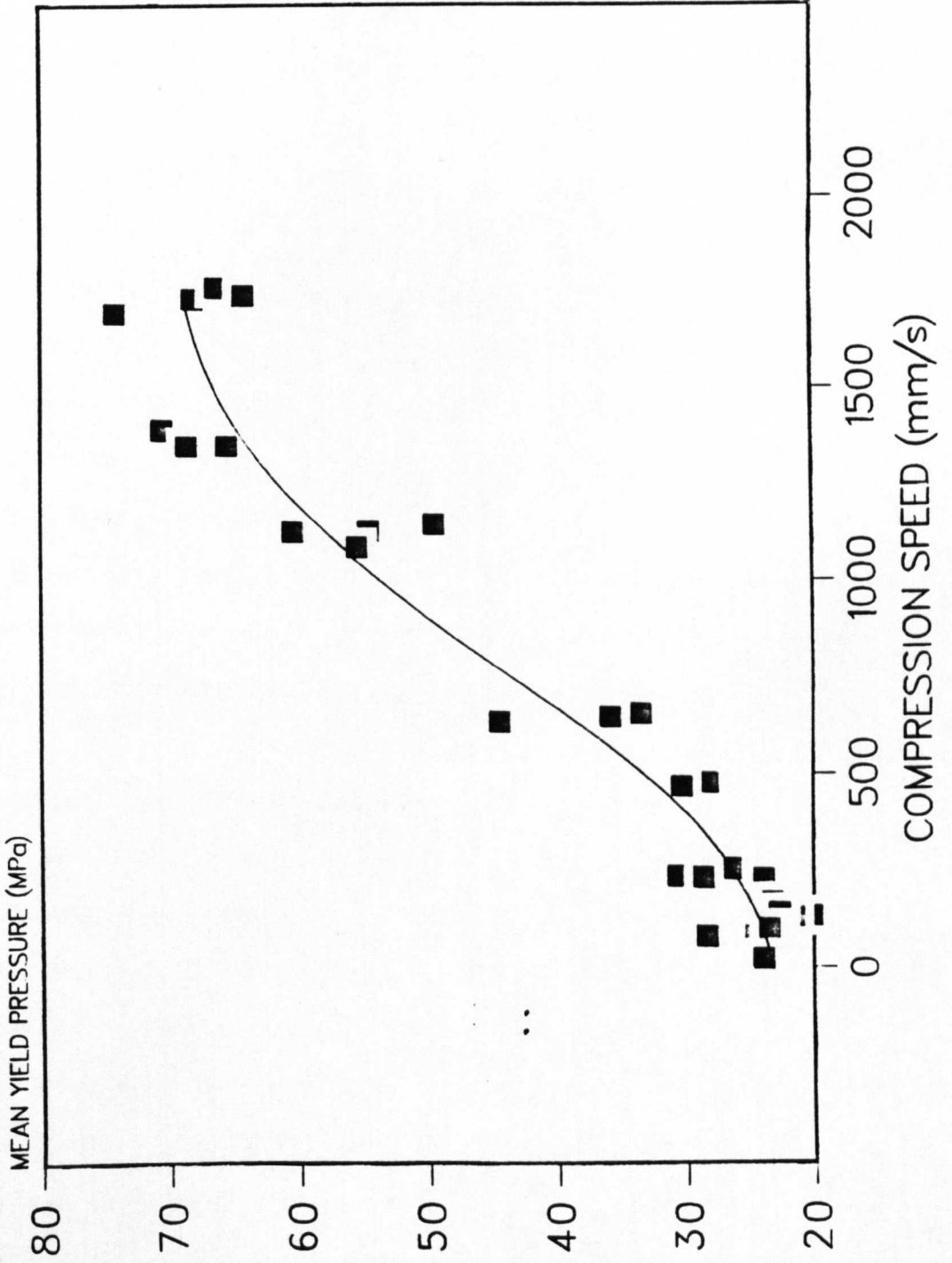
The Heckel analysis of the compaction data has been summarised in Table 5.1a. The  $R^2$  value for the regression analysis was better than 99.1% for all samples indicating that the linear portion of the curve had in fact been selected. As the compression speed increases, the slope of the Heckel plots decreases and the curve moves down the y axis, indicating a decrease in densification. These effects tend to increase the mean yield pressure and decrease the value of  $D_a$  (the relative density of the compact at the intercept of the regression line, as detailed earlier in the introduction). The low values for mean yield pressure indicate that ibuprofen crystals are soft and yield readily at relatively low pressures, indicative of densification by plastic flow. It should be remembered that such density determinations taken under pressure, will contain an elastic component which can give a false low value of mean yield pressure. The elasticity of this material will be determined during subsequent experiments. The elasticity of this material would not be expected to alter the conclusions drawn from this investigation.

The strain rate sensitivity of ibuprofen can be quantified from the mean yield pressure values which have been plotted against compression speed in FIG 5.1m. This increase in mean yield pressure with compression speed may be accounted for by a reduction in the amount of plastic deformation, which will occur due to the reduction in the time available for plastic flow. An alternative explanation could be an increase in the brittle behaviour of the material or a combination of the two. Even at the highest compression speed the mean yield pressure is relatively low indicating that the ibuprofen probably still deforms mainly by plastic flow. At compression speeds

Table 5.1a Heckel Analysis For Ibuprofen Compressed Between 22mm/s and 1700mm/s

Compression Speed mm/s	Mean Yield Pressure MPa	Intercept A	DA	Do	Db
23.07	23.92	1.447	0.764	0.483	0.281
23.19	24.33	1.440	0.763	0.483	0.280
22.95	23.98	1.402	0.753	0.483	0.270
21.19	23.98	1.422	0.759	0.483	0.276
x 22.60	24.05	1.428	0.760	0.483	0.277
σn-1 0.94	0.19	0.020	0.005		0.005
81.99	23.47	1.131	0.677	0.465	0.212
81.99	24.57	1.154	0.684	0.465	0.219
81.61	28.34	1.268	0.718	0.465	0.253
81.99	23.47	1.133	0.671	0.465	0.206
x 81.91	24.96	1.171	0.687	0.465	0.222
σn-1 0.16	2.31	0.065	0.021		0.021
141.02	22.67	1.101	0.667	0.464	0.204
131.55	21.55	1.041	0.647	0.464	0.184
169.50	23.20	1.126	0.675	0.464	0.212
133.54	20.16	1.014	0.637	0.464	0.210
x 143.90	21.89	1.085	0.656	0.464	0.202
σn-1 17.54	1.34	0.049	0.017		0.013
234.41	28.57	0.934	0.607	0.458	0.149
229.53	23.87	0.916	0.600	0.458	0.142
256.22	26.45	0.921	0.601	0.458	0.143
236.93	30.58	1.016	0.638	0.458	0.180
x 239.27	27.33	0.947	0.612	0.458	0.153
σn-1 11.71	2.83	0.047	0.018		0.179
468.82	30.21	0.887	0.588	0.458	0.130
479.10	28.80	0.857	0.576	0.458	0.118
479.01	28.17	0.857	0.575	0.458	0.117
489.66	28.09	0.830	0.564	0.458	0.106
x 479.15	28.82	0.858	0.576	0.458	0.118
σn-1 8.51	0.98	0.023	0.010		0.010
648.08	35.71	0.884	0.587	0.454	0.133
648.08	36.36	0.911	0.598	0.463	0.135
634.09	44.24	0.934	0.607	0.463	0.144
657.75	33.33	0.874	0.583	0.460	0.123
x 647.00	37.41	0.901	0.582	0.460	0.134
σn-1 9.74	4.73	0.027	0.031	0.004	0.009
1144.66	49.26	0.885	0.587	0.462	0.125
1088.13	55.25	0.875	0.583	0.462	0.121
1129.98	60.24	0.884	0.587	0.469	0.118
1129.98	54.35	0.882	0.586	0.467	0.119
x 1123.19	54.77	0.881	0.586	0.465	0.121
σn-1 24.37	4.50	0.005	0.002	0.004	0.003
1355.98	68.49	0.869	0.581	0.482	0.099
1355.98	65.36	0.878	0.584	0.486	0.098
1399.03	70.42	0.882	0.586	0.486	0.100
1377.17	66.22	0.889	0.589	0.488	0.101
x 1372.04	67.62	0.879	0.585	0.485	0.099
σn-1 20.58	2.28	0.008	0.003	0.003	0.001
1748.78	64.10	0.867	0.579	0.468	0.111
1769.85	66.22	0.862	0.577	0.468	0.109
1701.52	74.07	0.827	0.563	0.469	0.094
1739.00	68.01	0.834	0.569	0.469	0.100
x 1739.77	68.10	0.847	0.572	0.468	0.103
σn-1 28.57	4.28	0.020	0.007	0.001	0.008

FIG 5-1M THE EFFECT OF COMPRESSION SPEED ON THE MEAN YIELD PRESSURE OF IBUPROFEN



below 479mm/s little change of the mean yield pressure occurs, at higher compression speeds the increase in mean yield pressure is more dramatic. This coincides with the point at which capping and lamination become significant. At this compression speed the time available for plastic flow is reduced below that required to form sufficient particle-particle contact to withstand the stresses of decompression.

The reduction of Db with compression speed is shown in FIG 5.1a. This Heckel parameter gives an indication of the extent of particle rearrangement and slippage (as described earlier in the introduction). The reduction of Db could be due to an increase in the frictional and adhesive forces between the particles opposing the rearrangement. The escape of air from the powder bed would be expected to disrupt these packing processes, especially at high compression speeds. Additionally, as this process involves movement of particles it will be time dependent, consequently, at higher compression speeds less time is available for rearrangement, so Db is reduced.

It can be seen that the compression speed has a profound effect on the amount of particle rearrangement and slippage over the range 22mm/s to 479mm/s. This range of speeds are of particular importance, as it encompasses the compression speeds of single punch machines through to high speed rotary machines. This reduction in particle rearrangement and slippage may be expected to cause an increase in the quantity of entrapped air within the compact prior to application of higher pressures. The increase in the entrapped air may be expected to contribute to the capping phenomena.

Long and Alderton (1960) noted that the amount of entrapped gas varied from 12-83% of the initial quantity of gas present when compressing wax compacts. The amount of gas entrapped was shown to increase with compression rate, die size, and decreasing particle



size. They also demonstrated that very little entrapped gas escaped during the latter stages of compaction. Once the quantity of entrapped gas had exceeded a critical volume, the final compacts became laminated. These observations may be applicable to the compression of ibuprofen. At a compression speed of 479mm/s the extent of particle rearrangement and slippage has been dramatically reduced. This means that the powder bed porosity just prior to the onset of plastic deformation is much higher. At this increased porosity the powder bed contains the critical volume of air for ibuprofen. Consequently, during decompression the air expands within the compact developing internal faults which result in lamination and capping. Beyond compression speeds of 479mm/s the extent of particle rearrangement and slippage reduces only slightly. At such compression speeds little particle rearrangement and slippage occurs before the onset of plastic deformation.

### Conclusions

This investigation has shown ibuprofen to be sensitive to the magnitude and rate of application of the compression pressure. The extent of plastic flow exhibited by ibuprofen during compression was found to decrease as the compression speed increased.

Ibuprofen was found to consolidate mainly by plastic deformation with a lesser contribution from the melting of asperities. A significant amount of pressure induced melting and subsequent fusion bonding occurred at higher pressures. The elastic component of ibuprofen contributed to the lamination and capping processes.

The cause of lamination and capping was thought to be a combination of air entrapment and the inability of the compact to withstand the stresses of decompression.

The aim of this investigation was to determine how the addition of a second material altered the compression behaviour of ibuprofen with respect to compression speed. Further compression parameters will be employed to elucidate the mechanisms by which the mixtures consolidate at the different compression speeds.

### Introduction

Although the results of the previous section revealed some dramatic compression speed effects with respect to ibuprofen alone, the behaviour of this material in a real formulation remains unknown. Due to the large number of interacting variables which must be considered when compressing a formulation, it can often be difficult to interpret the data and determine what is actually occurring during the compression event. However a knowledge of the behaviour of simple mixtures of powders during tableting would be an advantage in formulation.

Ramaswamy et al (1971) used mixtures of non-pharmaceutical materials to show that pressure porosity data of individual materials could be used to predict the porosity of compacts prepared from two components. Fell and Newton (1970) found that the tensile strength of tablets prepared from mixtures of different forms of lactose could be predicted from a knowledge of the tablet tensile strengths of the pure materials. Unfortunately these simple relationships do not hold for all materials as indicated by Newton et al (1977). They found that the strengths of tablets prepared from mixtures of dicalcium phosphate and phenacetin were not a simple function of the tablets individual components. A similar phenomena was observed by Cook and Summers (1985). Emcompress and aspirin mixtures when compressed showed a tablet tensile strength peak at 25%v/v of Emcompress. No relationship with porosity, elastic recovery and lower punch work could be

established to explain the irregular strength relationship. The situation is further complicated by the effect of varying the physical characteristics of each component. The strength of binary mixtures of metallic powders when combined in a fixed ratio were studied by German and Ham (1979). They showed that the compact strength at a given density increased as the particle size of aluminium was decreased, but the compact strength decreased as the particle size of magnetite was decreased. This indicates that the interaction of the components is a critical factor in determining the properties of the compact. In this case the aluminium forms stronger bonds which are weakened by the presence of magnetite. Consequently the smaller the magnetite particles the greater their effective surface area and weakening effect on the compact. For this reason the particle size of all materials in the investigation of mixtures should be controlled. In the following investigation the particle size range of all materials will be maintained between 45 $\mu$ m and 105 $\mu$ m.

The importance of the interaction between materials has also been recognised by Leuenberger (1982,85). He developed the compactibility equation which describes the deformation hardness P of the compact as a function of the applied pressure  $\sigma_c$  and the relative density  $\sigma_r$ :

$$P = P_{max} ( 1 - \exp ( - \gamma_P \sigma_c \sigma_r ) )$$

Where  $P_{max}$  is equal to the maximum possible deformation hardness and  $\gamma_P$  is the compression susceptibility. The  $\gamma_P$  parameter was subsequently shown to be equal to the K proportionality constant in the Heckel equation by Leuenberger and Jetzer (1984). A similar equation may be used to predict the tensile strength of tablets  $\sigma_T$  Leuenberger et al (1981):

$$\sigma_T = \sigma_{Tmax} ( 1 - \exp ( - \gamma_T \sigma_c \sigma_r ) )$$

It was claimed that these equations held for pure substances and mixtures. Bonding forces between the individual particles contribute

significantly to the strength of the tablet. In a binary mixture containing particles of components A and B, he proposed that the interactions contributing to the tablet strength may be: A bonds preferentially with A and B bonds preferentially with B, or A bonds preferentially with B. No interaction occurs in the case that the affinity of A for A is the same as A for B. The interaction term  $P_{ww}$  may be quantified as follows:

$$\ln P_{max}(mixture\ A/B) = x \ln P_{max} + (1 - x) \ln P_{maxB} + x(1 - x) \ln P_{ww}$$

Where  $x(1 - x)$  is the percentage weight in weight of component A with respect to B and adhesive forces A-B dominate over the cohesive forces of A-A and B-B ie a positive interaction is present. It was found that for binary mixtures of brittle and soft materials the cohesive forces dominated which means the interaction was negative. Jetzer (1986a,b) used the compression parameters mentioned and the bonding index to interpret the behaviour of a material during compaction and predict when capping problems occur. It was recognised that more than one parameter was necessary to describe the variety and complexity of compression behaviour.

The addition of small quantities of an elastic component to brittle and plastic systems were investigated by Jackson (1984). It was found that the plastic deformation of sodium chloride was significantly modified with the addition of a small amount of polyethylene by reducing both short and long term interparticulate bonding. In contrast under similar conditions the behaviour of lactose a brittle material remained unaffected. Clearly the mechanism of deformation of the materials constituting a mixture will determine how the mixture behaves relative to the single components.

Bangudu and Pilpel (1984) considered the compressibilities of paracetamol Avicel mixtures in terms of a material constant  $\alpha$  derived using the equations of Cheng (1968) and Chan et al (1983).  $\alpha$  was

thought to be a measure of the strength and range of action of the forces between particles. Materials such as paracetamol have high  $\alpha$  value and are difficult to compress and susceptible to lamination and capping, while soft readily compressible materials such as Avicel have a low  $\alpha$  value. More than 25% of Avicel had to be added to paracetamol to cause a substantial reduction in  $\alpha$  value of the mixture and prevent capping and lamination. Using the same materials Malamataris *et al* (1984) quantified the elasticity and plasticity of mixtures with the ER/PC ratio. These values were derived via the equations derived by Armstrong and Haines-Nutt (1972) discussed earlier in section 1.1.9 ER is the elastic recovery and PC is the plastic compression. When this ratio exceeded nine the mixture laminated or capped. The ER/PC ratio was also shown to be inversely proportional to the tablet tensile strength.

One aspect of the compression of powder mixtures which has received most attention is that of direct compression diluents. Panaggio *et al* (1984) investigated mixtures of dicalcium phosphate dihydrate and a modified pregelatinized starch. They noted that some properties varied linearly with the relative proportions of each constituent but other properties were greater or less than the additive value. The deviations from linearity were attributed to the differences in the particle size distribution of the two powders. No consideration of the interactions between the two components was given. However it was suggested that mixtures of diluents may offer some advantages over the use of individual diluents. One such benefit of the use of mixtures was demonstrated by Armstrong and Lowndes (1984). They showed that increasing the concentration of spray dried lactose relative to microcrystalline cellulose in a binary mixture increased its rework potential. Unfortunately the same change in composition was also found to decrease the tablet strength and weight

uniformity. Abu-Taleb and Aly (1985) found that binary blends of direct compression excipients had advantages when compared with the single components ability to form tablets with oxytetracycline hydrochloride. Duberg and Nyström (1985) investigated binary mixtures with microcrystalline cellulose. They found that the addition of microcrystalline cellulose produced the greatest increase in tablet strength when mixed with a plastic material such as sodium bicarbonate. For all of the fragmenting materials additions of small amounts of microcrystalline cellulose produced limited improvements of tablet strength. The mean yield pressure derived from the heckel plots of the materials were found to be useful in the identification of the deformation mechanisms experienced by the mixtures. The mean yield pressure was found to be directly related to the proportion of microcrystalline cellulose present in the mixture. This indicated that the degree of elastic and plastic deformation was not substantially changed by the addition of a second component.. An isotropy ratio was used to show the degree of bond homogeneity in the tablet. Combined use of both parameters lead to the conclusion that the addition of Avicel reduced the fragmentation tendency of most compounds.

It has been demonstrated that the individual consolidation mechanisms of materials do not often have a simple additive relationship when combined in a binary mixture. This has been attributed to interactions between the materials and to a lesser extent differences in the particle size distributions between the powders. The compression of mixtures of materials with differing consolidation mechanisms has been previously investigated. However it has been shown in the previous section that the mechanism by which a material consolidates may be dependant on the speed of compression. As the speed of compression may be varied considerably during tablet manufacture, the effects of this on the consolidation mechanisms of

mixtures is of particular interest and will be studied during the following investigation.

### Experimental

The methods used were as described earlier in the 'preparation of compacts'. Any supplementary details have been detailed below.

The 45 $\mu$ m-105 $\mu$ m particle size fractions of microcrystalline cellulose and  $\alpha$ -anhydrous lactose were mixed with a similar size fraction of ibuprofen to form 0%w/w, 25%w/w, 50%w/w, 75%w/w and 100%w/w mixtures with respect to ibuprofen. The weight of each mixture required to form a compact of 2.5mm thickness at zero porosity was calculated and compressed at 25mm/s, 380mm/s and 1100mm/s to a maximum applied pressure of 60MPa.

Compression was achieved using a simple sawtooth time displacement profile applied to the upper and lower actuators. The maximum displacement of the upper and lower actuators during compression were 16mm and 3mm respectively. The compact was ejected immediately after compression using a straight ramp time displacement profile, the speed of which remained constant, independent of the speed of compression. Four compacts were prepared for each set of conditions. Within two minutes of compression the compact thickness and diameter were measured using a digital micrometer. The compacts were then allowed to recover for two hours after which they were remeasured and subjected to a tensile strength test.

During the compression the mean punch force and the punch separation were monitored via the transient recorder. The force displacement data were then transferred to the mainframe computer and subjected to analysis. The 'Energy' program (as listed in the appendix) calibrated the data and made corrections for the elastic distortion of the punches and other parts of the Simulator during

compression. The net energy of compression as shown in FIG 1.1a was calculated by subtracting the elastic energy from the total energy input to the system. The elastic recovery of the compact ER was calculated using the equation of Armstrong and Haines-Nutt (1972) detailed in section 1.1.9. The data was then transferred to the Minitab spread-sheet package with the pre-programmed control routine for Heckel analysis. The linear region of the Heckel plot was identified by eye and regression analysis using the method of least squares was performed. The slope, intercept and compact density at the first measurable force were recorded and used to calculate the mean yield pressure,  $D_a$ ,  $D_o$  and  $D_b$ .

### 6.1.1 The Effect of Speed of Compression on Ibuprofen Avicel Mixtures

#### Results

Table 6.1a Ibuprofen Avicel Mixtures Compressed at 25mm/s Showing The Elastic Recovery (ER) Heckel Parameters  $D_a$ ,  $D_o$ ,  $D_b$  and The Mean Yield Pressure ( $P_y$ ), The Tablet Tensile Strength and The Net Energy of Compression.

Codes: IB = Ibuprofen A = Avicel 25 = % Concentration of Ibuprofen

TABLET CODE	ER %	$D_a$	$D_o$	$D_b$	$P_y$ MPa	$\sigma_T$ MPa	Net Energy J
IBA00T1	9.676	0.396	0.181	0.214	53.76	2.796	9.44
IBA00T2	9.676	0.402	0.181	0.221	54.35	2.908	9.60
IBA00T3	8.783	0.389	0.181	0.208	52.36	2.926	9.17
IBA00T4	8.651	0.393	0.181	0.212	53.19	2.770	9.50
x	9.196	-	-	0.214	53.41	2.850	9.43
$\sigma_{n-1}$	0.556	-	-	0.005	0.85	0.078	0.18
IBA25T1	9.917	0.488	0.259	0.229	50.76	1.838	6.84
IBA25T2	9.875	0.497	0.259	0.238	52.08	1.874	7.25
IBA25T3	10.671	0.470	0.259	0.211	47.17	1.832	6.43
IBA25T4	9.393	0.466	0.259	0.207	46.95	1.898	6.91
x	9.964	-	-	0.221	49.24	1.860	6.86
$\sigma_{n-1}$	0.528	-	-	0.015	2.25	0.031	0.34
IBA50T1	7.409	0.578	0.393	0.185	45.04	-	4.67
IBA50T2	7.483	0.573	0.381	0.192	44.64	1.715	4.86
IBA50T3	7.944	0.589	0.381	0.208	46.73	1.697	4.85
IBA50T4	7.052	0.594	0.393	0.201	48.31	1.582	4.75
x	7.222	-	-	0.197	46.18	1.665	4.78
$\sigma_{n-1}$	0.264	-	-	0.010	1.68	0.072	0.09
IBA75T1	5.708	0.677	0.429	0.248	38.91	1.418	3.35
IBA75T2	6.048	0.690	0.429	0.261	40.32	1.273	3.18
IBA75T3	6.468	0.687	0.381	0.305	40.49	1.155	2.98
IBA75T4	5.113	0.690	0.381	0.309	40.98	1.267	3.08
x	5.834	-	-	0.280	40.17	1.278	3.15
$\sigma_{n-1}$	0.572	-	-	0.031	0.89	0.108	0.16
IBA99T1	5.300	0.777	0.451	0.326	25.84	0.751	2.04
IBA99T2	5.033	0.794	0.451	0.343	30.39	0.768	2.05
IBA99T3	5.614	0.800	0.451	0.349	30.12	0.740	2.14
IBA99T4	5.455	0.800	0.451	0.349	29.76	0.680	2.14
x	5.455	-	-	0.342	29.0	0.734	2.09
$\sigma_{n-1}$	0.247	-	-	0.011	2.14	0.382	0.05

Table 6.1b Ibuprofen Avicel Mixtures Compressed at 380mm/s Showing The Elastic Recovery (ER) Heckel Parameters Da, Do, Db and The Mean Yield Pressure (Py), The Tablet Tensile Strength and The Net Energy of Compression.

Codes: IB = Ibuprofen A = Avicel 25 = % Concentration of Ibuprofen

TABLET CODE	ER %	Da	Do	Db	Py MPa	$\sigma T$ MPa	Net Energy J
IBA00T1	9.887	0.370	0.213	0.157	68.96	2.642	11.55
IBA00T2	10.310	0.358	0.213	0.145	65.79	2.814	11.91
IBA00T3	10.699	0.366	0.213	0.153	68.49	2.752	11.71
IBA00T4	10.080	0.355	0.213	0.142	66.67	2.737	11.84
x	10.242	-	-	0.149	67.48	2.736	11.76
$\sigma n-1$	0.350	-	-	0.006	1.49	0.071	0.16
IBA25T1	14.207	0.444	0.274	0.170	61.35	1.347	7.91
IBA25T2	13.964	0.436	0.274	0.162	59.88	1.276	7.73
IBA25T3	13.691	0.454	0.274	0.180	63.69	1.386	7.73
IBA25T4	14.183	0.455	0.274	0.181	65.79	1.309	7.41
x	14.011	-	-	0.173	62.68	1.329	7.69
$\sigma n-1$	0.239	-	-	0.009	2.60	0.047	0.21
IBA50T1	9.532	0.466	0.302	0.164	46.51	1.516	5.22
IBA50T2	9.055	0.475	0.302	0.173	48.54	1.479	7.29
IBA50T3	9.515	0.484	0.302	0.182	49.26	1.645	6.92
IBA50T4	10.388	0.434	0.302	0.132	41.66	1.513	6.92
x	9.623	-	-	0.163	46.49	1.538	6.59
$\sigma n-1$	0.556	-	-	0.022	3.426	0.073	0.93
IBA75T1	14.908	0.599	0.429	0.170	46.95	0.707	4.84
IBA75T2	13.238	0.588	0.429	0.159	42.02	0.745	4.76
IBA75T3	13.383	0.569	0.429	0.140	38.76	0.648	4.82
IBA75T4	13.253	0.585	0.429	0.156	41.67	0.652	4.73
x	13.695	-	-	0.156	42.35	0.688	4.79
$\sigma n-1$	0.811	-	-	0.012	3.40	0.047	0.05
IBA99T1	10.172	0.621	0.451	0.170	29.33	0.551	3.64
IBA99T2	12.495	0.647	0.451	0.196	34.36	C	4.11
IBA99T3	C	0.609	0.451	0.158	30.49	C	4.05
IBA99T4	11.946	0.660	0.451	0.209	36.90	C	4.02
x	11.538	-	-	0.183	32.77	0.551	3.96
$\sigma n-1$	1.214	-	-	0.023	3.49	-	0.215

C = Compact capped.

Table 6.1c Ibuprofen Avicel Mixtures Compressed at 1100mm/s Showing The Elastic Recovery (ER) Heckel Parameters  $D_a$ ,  $D_o$ ,  $D_b$  and The Mean Yield Pressure ( $P_y$ ), The Tablet Tensile Strength and The Net Energy of Compression.

Codes: IB = Ibuprofen A = Avicel 25 = % Concentration of Ibuprofen

TABLET CODE	ER %	$D_a$	$D_o$	$D_b$	$P_y$ MPa	$\sigma_T$ MPa	Net Energy J
IBA00T1	12.175	0.353	0.244	0.109	70.92	2.624	11.76
IBA00T2	12.118	0.343	0.244	0.099	68.02	2.661	11.62
IBA00T3	12.760	0.349	0.244	0.105	68.97	2.537	11.21
IBA00T4	11.982	0.352	0.244	0.108	68.97	2.479	11.05
x	12.259	-	-	0.105	69.22	2.575	11.41
$\sigma_{n-1}$	0.344	-	-	0.005	1.22	0.082	0.34
IBA25T1	14.766	-	-	-	-	1.449	-
IBA25T2	14.820	0.385	0.274	0.111	63.29	1.406	9.49
IBA25T3	15.038	0.370	0.274	0.096	58.14	1.533	9.66
IBA25T4	14.060	0.369	0.274	0.095	58.48	1.520	9.68
x	14.671	-	-	0.101	59.97	1.477	9.61
$\sigma_{n-1}$	0.432	-	-	0.009	2.88	0.059	0.10
IBA50T1	C	0.410	0.302	0.108	51.55	C	9.04
IBA50T2	9.052	0.380	0.302	0.078	46.51	0.914	8.56
IBA50T3	11.333	0.406	0.302	0.104	55.86	0.964	9.69
IBA50T4	C	0.394	0.302	0.092	52.08	C	8.99
x	10.192	-	-	0.095	51.50	0.939	9.07
$\sigma_{n-1}$	1.6	-	-	0.014	3.84	0.035	0.46
IBA75T1	C	0.528	0.451	0.077	53.19	C	5.46
IBA75T2	C	0.528	0.451	0.077	53.47	C	5.06
IBA75T3	C	0.512	0.451	0.061	50.00	C	6.42
IBA75T4	C	0.525	0.451	0.074	57.47	C	4.81
x	C	-	-	0.072	53.53	C	5.44
$\sigma_{n-1}$	C	-	-	0.0007	3.06	C	0.71
IBA99T1	C	0.581	0.451	0.130	55.86	C	3.92
IBA99T2	C	0.590	0.451	0.138	51.81	C	3.73
IBA99T3	C	0.548	0.451	0.096	42.55	C	3.73
IBA99T4	C	0.573	0.451	0.122	51.01	C	3.99
x	C	-	-	0.121	50.30	C	3.84
$\sigma_{n-1}$	C	-	-	0.018	5.59	C	0.13

C = Compact capped.

## Discussion

Before discussing the data with respect to the mixtures, the behaviour of the individual components will be considered.

The consolidation mechanism of microcrystalline cellulose has been investigated by several authors. Reier and Shangraw (1966) visualised microcrystalline cellulose as a special form of cellulose fibril, in which the crystals are compacted close enough so that hydrogen bonding can occur. Lamberson and Raynor (1976) reported that extensive plastic flow occurs during compression due to the numerous slip planes and dislocations present in its structure. David and Augsberger (1977) identified the time dependency of this plastic flow by measurements of stress relaxation of compacts. To-day microcrystalline cellulose is regarded as a model plastic material for use in compression studies

The mean yield pressure obtained for microcrystalline cellulose when compressed at slow speed was 53.41MPa. This is indicative of a soft ductile material which consolidates with little or no brittle fracture. Mean yield pressure values of microcrystalline cellulose found in the literature show considerable variation. This may be explained by the fact that different authors have employed physically different powders with varying moisture levels using different compression conditions. The particle size of this material has been shown to have little effect on the mean yield pressure by McKenna and McCafferty (1982). However the moisture content has been shown to be more significant by Khan *et al* (1981), Khan and Pilpel (1986) and Roberts and Rowe (1987d). The first 3% of moisture is internally chemisorbed and therefore has little effect. As the moisture content is increased it becomes available on the surface of the particles. This has two main effects which improve the compressibility of the

material. Firstly it acts as an internal lubricant which facilitates slippage and flow within the individual microcrystals and secondly it increases the range of interparticle forces. The batch of Avicel PH101 used in this investigation was found to have a moisture content of 4.7%w/w which is high enough to exert the lubricant effect but not sufficient to form pendular bonds with neighbouring particles. Similar material compressed by Roberts and Rowe (1987d) was found to have a mean yield pressure of about 52MPa which corresponds well with the 53.41MPa reported in this investigation.

The extent of plastic flow with compression speed of this material was quantified using the strain rate sensitivity index by Roberts and Rowe (1985). It was proposed that as the compression speed increased, the time available for plastic flow was reduced. In this investigation the mean yield pressure for microcrystalline cellulose was found to increase with increasing compression speed which would tend to confirm that the degree of plastic flow was indeed reduced. This was supported by a similar reduction in tensile strength of the compacts as the compression speed increased.

It has been suggested that microcrystalline cellulose may consolidate beyond its elastic limit predominantly by brittle fracture Sixsmith (1982). However in the light of other overwhelming evidence this is unlikely. For example Roberts and Rowe (1987a) calculated that the critical particle size for microcrystalline cellulose below which flow will occur was 1172 $\mu$ m. As the typical particle size of Avicel PH101 is 50 $\mu$ m (FMC Corporation 1987) very little particle fracture would be expected.

The mechanism of consolidation of the ibuprofen within this range of compression speeds has been discussed in the previous chapter.

The Db values obtained from the Heckel analysis indicate the extent of particle rearrangement during compression. This will be a

function of the surface structure, particle size and shape of the particles. Before the slippage and rearrangement of particles can take place, the applied pressure must overcome the interparticular attractive forces; mainly friction and cohesion. It can be seen from the Db values given in tables 6.1a-c that the ibuprofen undergoes greater particle rearrangement than the microcrystalline cellulose at all compression speeds. This may be accounted for, by the cohesion forces that exist between the microcrystalline cellulose particles (Heng and Staniforth (1988)) which would be expected to offer resistance to the rearrangement process. For both materials the amount of particle rearrangement decreased with increasing compression speed. This could be due to an increase in the frictional and cohesive forces between the particles, combined with a reduction in the time available for this particular process. The disruptive effects of air escape which would be more significant with increased compression speeds would also be expected to hinder the rearrangement processes.

When compressed under relatively low pressures similar to those used in this investigation, microcrystalline cellulose has been shown to have high elastic recovery. Marshall *et al* (1972) proposed that this behaviour was due to its hollow microfibrillar structure. Aulton *et al* (1974) confirmed the high elasticity of microcrystalline cellulose by indentation testing of compacts prepared under 50MPa pressure. The elastic limit for microcrystalline cellulose was proposed to be between 60-80MPa by Sixsmith (1982). In this investigation the elastic recovery (ER) for microcrystalline cellulose was found to be relatively high as expected at 9.196% when compressed at 25mm/s.

The elastic recovery of ibuprofen has previously been reported by Marshall *et al* (1986). The extent of recovery was found to be dependant on the duration of the compression cycle and the maximum

compression pressure applied during compression. A critical pressure was identified above which the change in recovery with increasing pressure became similar for all compression cycle durations. Although no explanation of this critical pressure was offered, it is possible that this represents the point at which melting becomes significant under the conditions used. The elastic recovery reported for ibuprofen compressed using a cycle duration of 1s, was about 8% which is significantly higher than the 5.45% found in this investigation at the slowest speed. This is probably due to the extra two hours allowed for recovery by the other investigators.

The elastic recovery was found to increase with compression speed for microcrystalline cellulose and ibuprofen as shown in the tables 6.1a,b,c. The cause of this increase may be found in the tensile strength data. The reduction in the tensile strength of the compact with increased compression speed indicates that less particle-particle bonds have formed. Consequently during decompression the weaker compacts formed at high speed are less able to resist the recovery of the elastic component of the material. It is probable that as the compression speed is increased there is a shift in the utilization of energy from plastic to elastic. Because ibuprofen forms much weaker compacts this effect was more pronounced, reflected by the 111.5% increase in elastic recovery between compression at 25mm/s and 380mm/s. This may be compared to the 11.4% experienced by the microcrystalline cellulose under similar conditions.

The net energy required to form the ibuprofen compacts were much lower than that required to form the microcrystalline cellulose compacts. If we consider the compacts prepared from the two materials at 380mm/s where the ER values are similar, the energy required to form the microcrystalline cellulose compacts remained significantly higher. It is probable that some of this extra energy has been used to

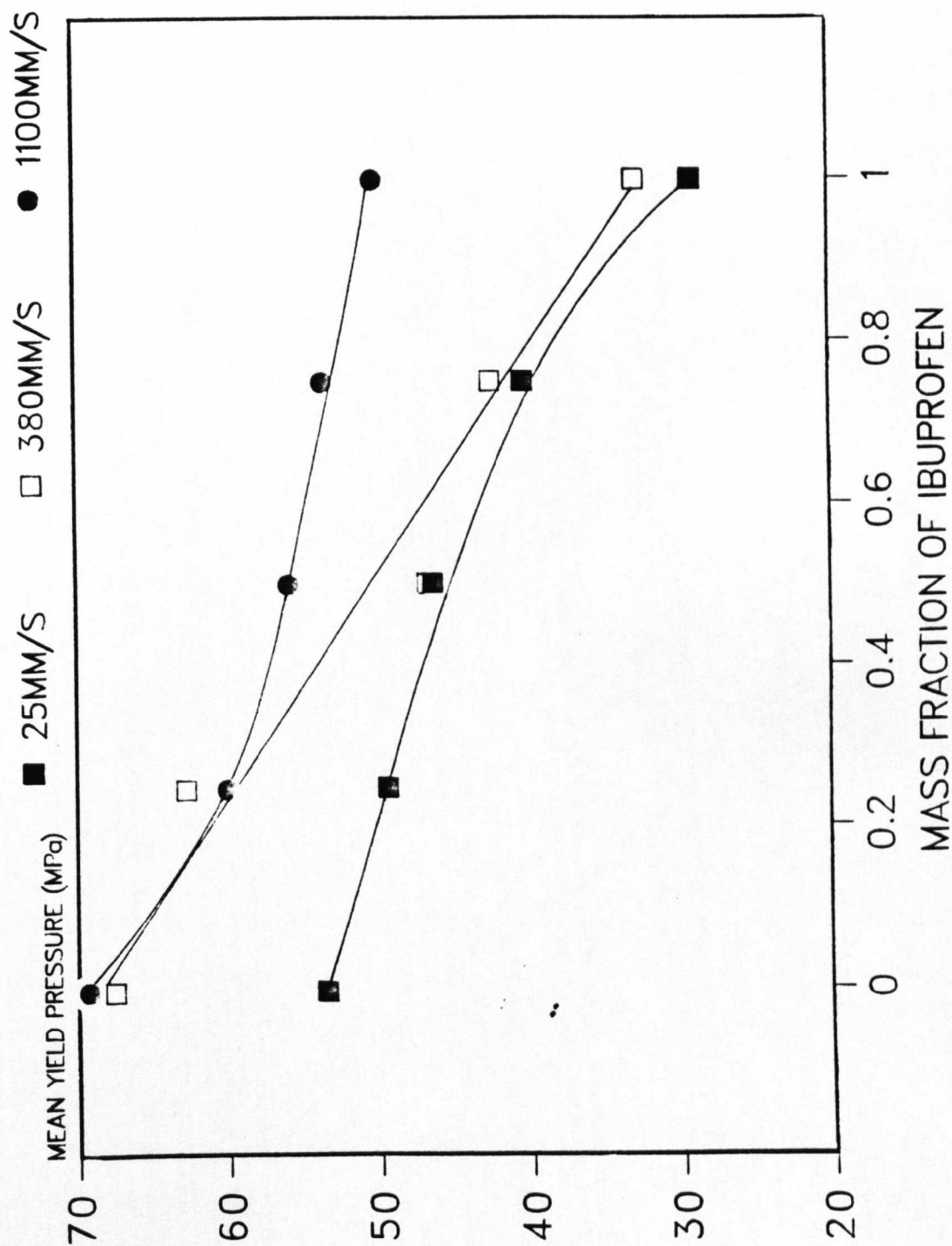
generate more plastic deformation and subsequent bonding. This may be confirmed by the much higher tensile strength of the microcrystalline cellulose compacts. It is appreciated that energy could have been utilized by each material in different proportions as friction, raising the temperature of the compacts, and acoustic emissions but it is difficult to isolate these energies.

If we now consider the effect of compression on mixtures of the ibuprofen and microcrystalline cellulose:-

Both ibuprofen and microcrystalline cellulose consolidate by similar mechanisms, namely plastic deformation. From this information we may expect a simple relationship between the mean yield pressure and the proportion of each component. If we consider the data obtained shown in tables 6.1a,b,c and FIG 6.1a, the relationship appears to be some-what more complex, especially when considering the additional effects of compression speed. Under low compression speed conditions we see a slight positive deviation from linearity which tends towards the mean yield pressure of microcrystalline cellulose. This indicates that to some extent the deformation of the microcrystalline cellulose masks that of the ibuprofen. Under high compression speed conditions there was a slight negative deviation from linearity which tends towards the mean yield pressure of the ibuprofen. The behaviour of the individual materials aids our understanding of these effects.

It can be seen that microcrystalline cellulose was sensitive to the increase in compression speed from 25mm/s to 380mm/s but showed an insignificant increase when the speed was further increased to 1100mm/s. This was thought to be related to the dwell time which limits the extent of plastic flow. Evidently there was a significant reduction in dwell time between 25mm/s and 380mm/s. The change in dwell time between 380mm/s and 1100mm/s is less significant as the extent of plastic flow has already approached a minimum. In contrast

**FIG 6.1a** THE EFFECT OF COMPRESSION SPEED ON THE MEAN YIELD PRESSURE OF IBUPROFEN / AVICEL MIXTURES.



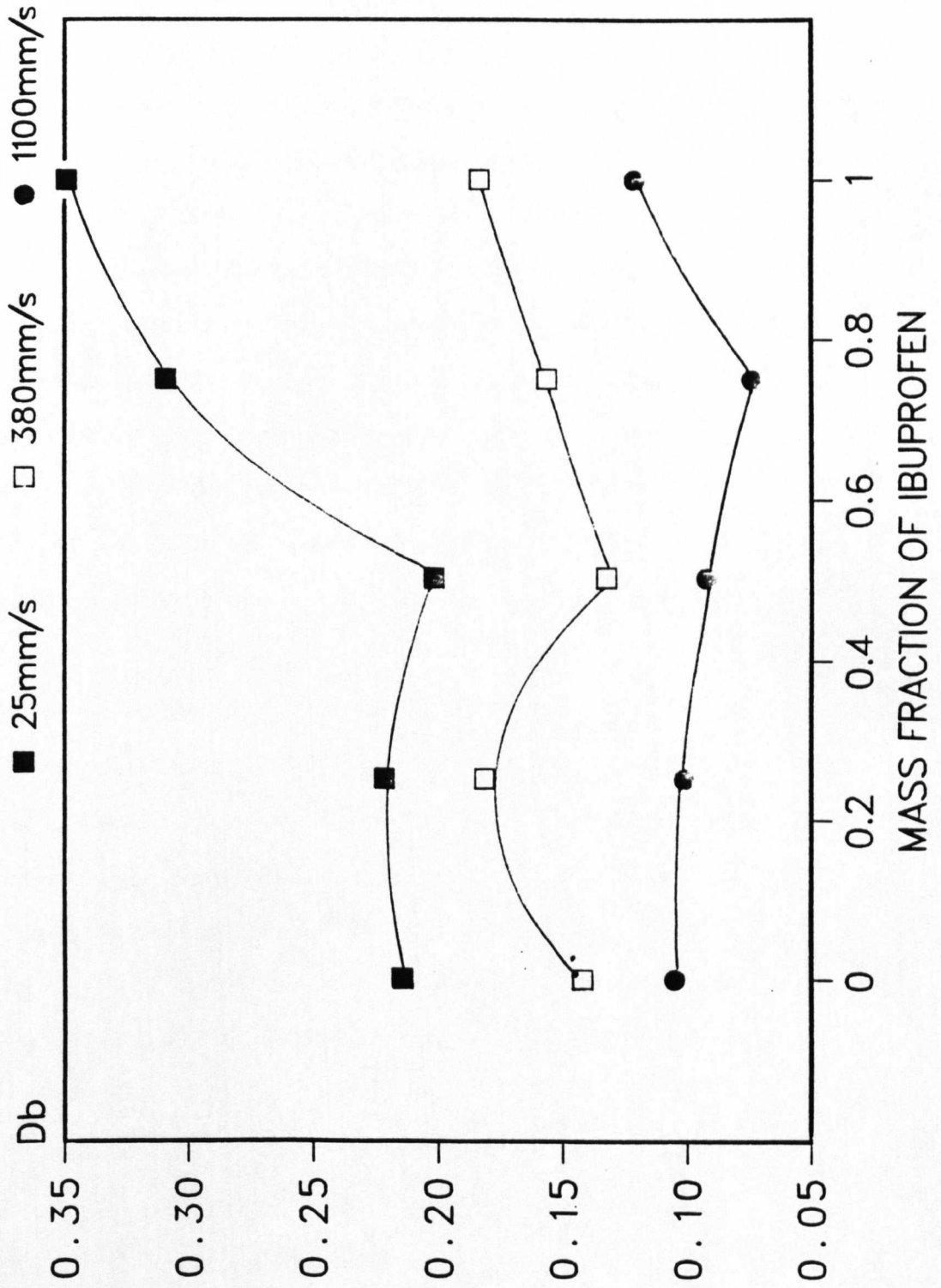
to this, the ibuprofen showed only a little change in mean yield pressure when the compression speed was increased from 25mm/s to 380mm/s. This small change in mean yield pressure indicates that the method of deformation has not been significantly effected in this case. However, a more dramatic change was seen when the compression speed was further increased to 1100mm/s. This change could be as a result of the time dependency of thermal transfer. When a material is compressed some of the mechanical energy may be converted to heat. The temperature reached is a function of the balance between the heat transferred to the surface of the particle and the heat transferred away from the surface of the particle by conduction into the interior of the particle (Rankell and Higuchi 1968). At higher compression speeds, the time available for the transfer of heat is reduced which up sets this balance, effectively increasing the temperature at the surface of the particles. This results in melting of asperities.

Thus at low compression speeds there appears to be a positive interaction which could take the form of bonding between the ibuprofen and the microcrystalline cellulose. While at high compression speeds there is a negative interaction probably due to melting of the ibuprofen. Intermediate behaviour was seen at a compression speed of 380mm/s. With 25% of ibuprofen and less, the mixture behaves in a similar manner to the mixture when compressed at high speed. When the concentration of ibuprofen is greater than 25% the mixture behaves as seen at slow speed.

An interesting phenomenon is shown in FIG 6.1b. The extent of consolidation that occurs due to particle slippage and rearrangement shows a minima for each compression speed. This could be due to adhesion between the ibuprofen and microcrystalline cellulose particles which would be expected to oppose the rearrangement.

FIG 6-1b

EXTENT OF PARTICLE REARRANGEMENT (Db) FOR MIXTURES OF IBUPROFEN AND MICROCRYSTALLINE CELLULOSE COMPRESSED AT VARYING SPEEDS



As expected, the tensile strength of most compacts were reduced as the compression speed increased as shown in FIG 6.1c. This reduction in compact strength may be explained by a decrease in the time available for plastic flow, which is the major mechanism of deformation for both materials. Consequently the area of true contact is effectively reduced resulting in fewer bonds and a weaker compact. It is clear that the microcrystalline cellulose-microcrystalline cellulose bonds were much stronger than the ibuprofen-ibuprofen bonds. The inherent variability of this test made it difficult to make clear distinctions between the behaviour of the mixtures. It is probable that a slight negative deviation from linearity occurred at all speeds of compression indicating that the ibuprofen actively interferes with the microcrystalline cellulose-microcrystalline cellulose bonding. This could be due to bonds forming between the ibuprofen and the microcrystalline cellulose which were weaker than the microcrystalline cellulose-microcrystalline cellulose bonds which may otherwise have formed.

The net energies used to form the compacts are shown in FIG 6.1d. More energy is required to form all of the compacts at higher compression speeds. This may be due to the utilization of more energy to overcome the increased cohesiveness of particles that occur at higher compression speeds. At the low compression speed there is only a slight negative deviation from linearity between the net energy and proportion of ibuprofen. At higher compression speeds the relationship becomes more linear. It is probable that the true relationship between the two components in these mixtures are more complex, involving thermal changes, changes of state and friction effects. Unfortunately it remains difficult to separate the net energy into its lesser components.

**FIG 6.1c** THE EFFECT OF COMPRESSION SPEED ON TABLET RADIAL TENSILE STRENGTH FOR IBUPROFEN / AVICEL MIXTURES.

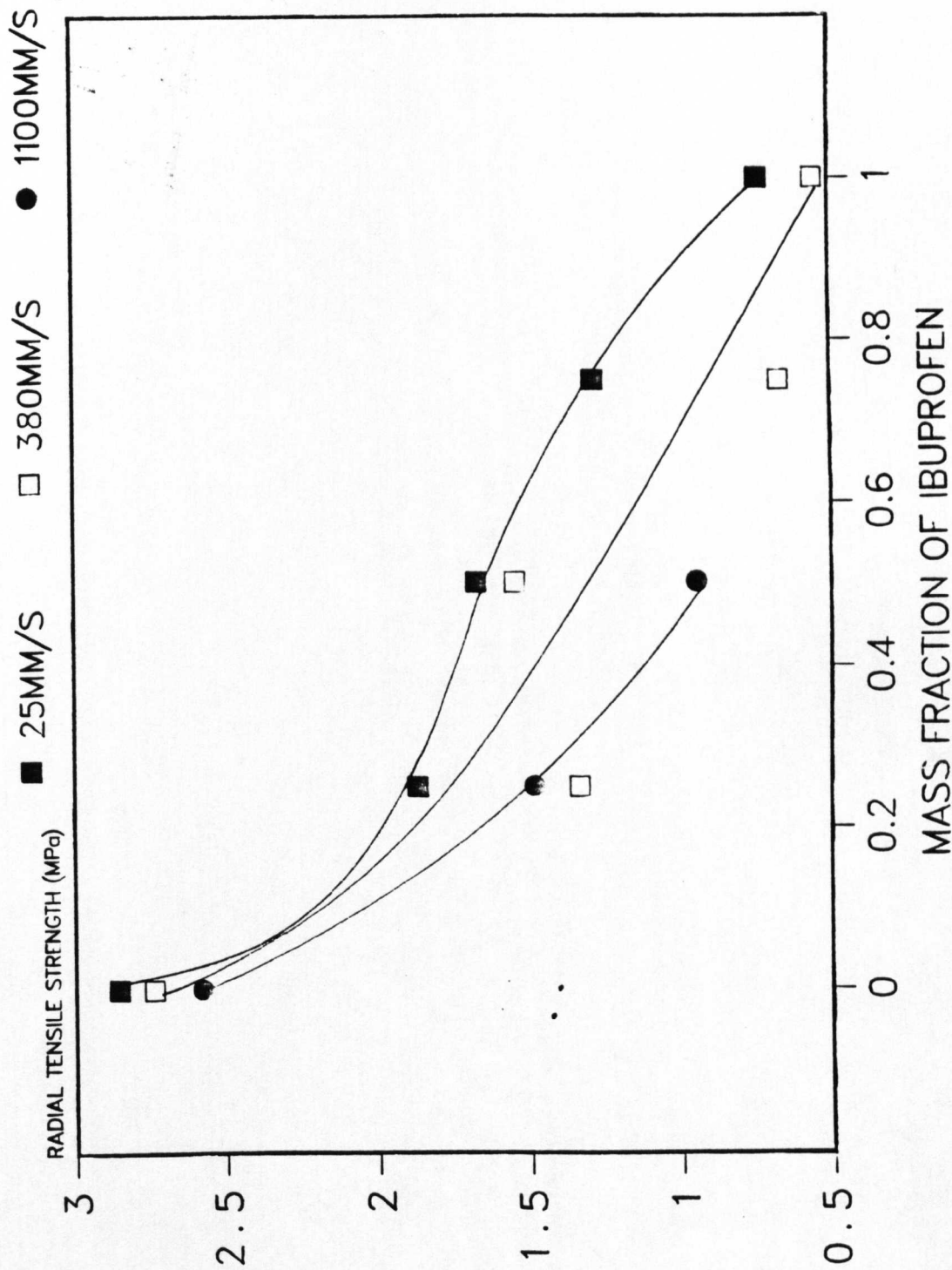
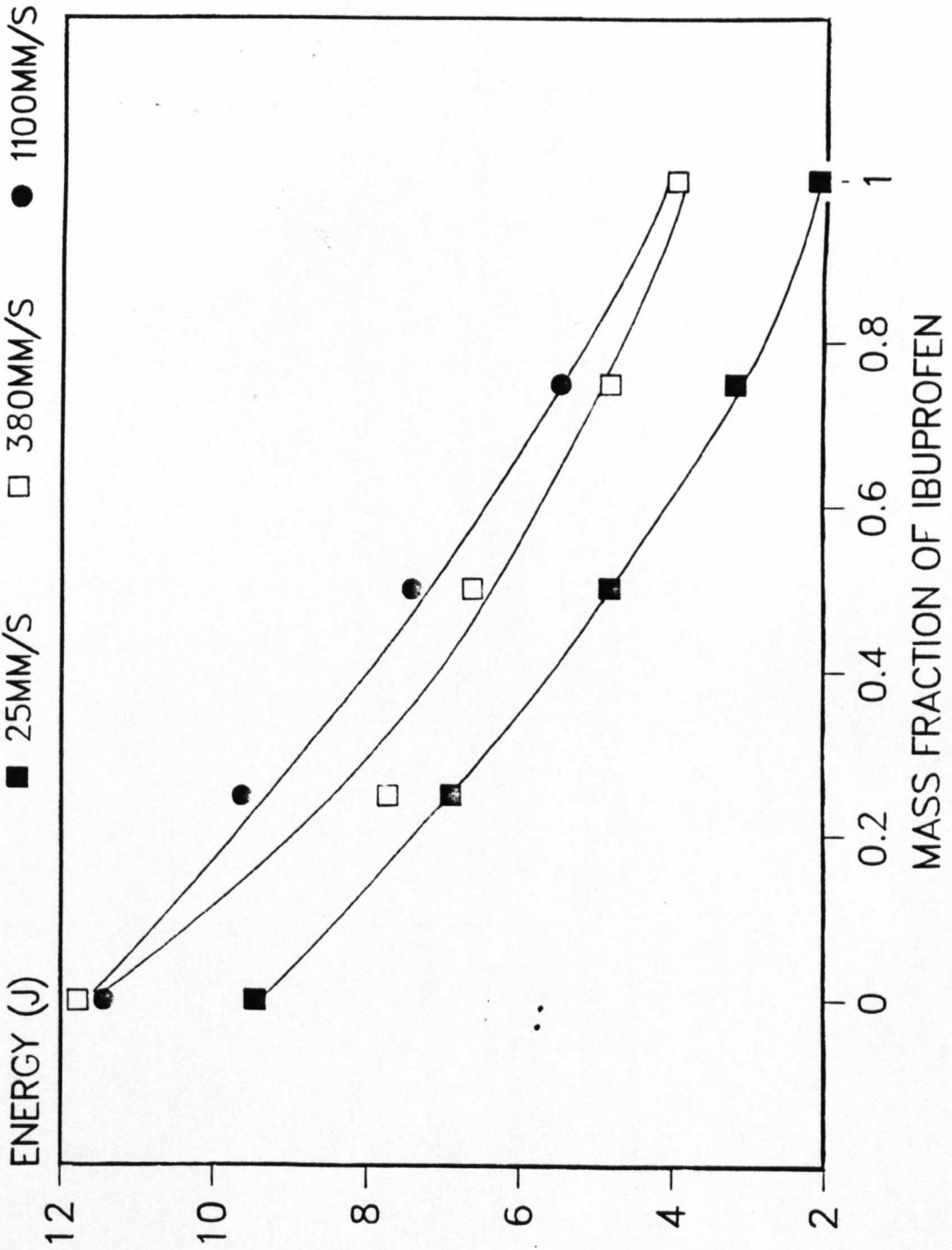


**FIG 6.1d** THE EFFECT OF COMPRESSION SPEED ON THE NET ENERGY OF IBUPROFEN / AVICEL MIXTURES.



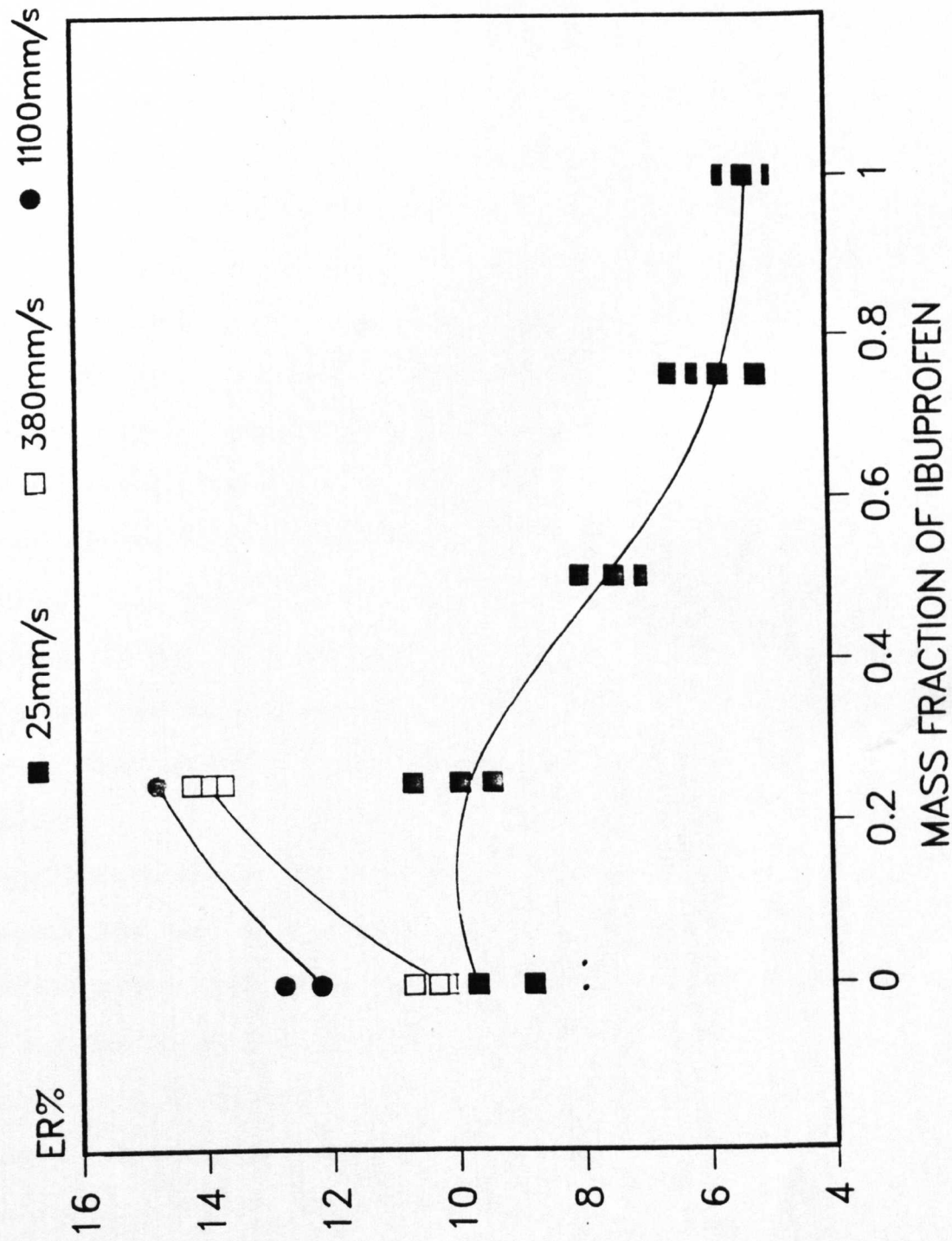
Although the elastic recovery data was incomplete due to capping of the compacts at higher compression speeds, a clear trend was visible at low compression speed as shown in FIG 6.1e. The elastic recovery of compacts prepared from mixtures of these two components is a balance between two factors. Firstly the strength of the bonding between the particles and secondly the elasticity of the particles. Mixtures of 25% ibuprofen show an increase in elastic recovery. Although we may expect addition of a less elastic material to reduce the elastic recovery, this effect is reversed by associated reduction in the strength of the compact. Addition of further ibuprofen has a less dramatic effect on tensile strength and so the lower elasticity of the ibuprofen reduces the elastic recovery of the compact.

### Conclusions

Microcrystalline cellulose was found to consolidate mainly by plastic flow. As the compression speed was increased, the extent of plastic flow was found to reduce, resulting in fewer particle-particle bonds and weaker compacts.

The extent of particle rearrangement during compression was found to be greater with ibuprofen than with microcrystalline cellulose at all compression speeds. This was considered due to the cohesion forces that exist between the microcrystalline cellulose particles which would be expected to offer resistance to the rearrangement process. For both materials the amount of particle rearrangement decreased with increasing compression speed. Several factors were considered responsible for this including an increase in the frictional and cohesive forces between the particles, a reduction in the time available for the movement of particles, and the disruptive effects of air escape.

**FIG 6-1e** THE ELASTIC RECOVERY (ER) OF COMPACTS PREPARED FROM MIXTURES OF IBUPROFEN AND MICROCRYSTALLINE CELLULOSE COMPRESSED AT VARYING COMPRESSION SPEEDS



An increase in the speed of compression was shown to increase the elastic recovery of microcrystalline cellulose and ibuprofen compacts. This was thought due to a reduction in the number of bonds formed which resisted the recovery. The higher net energy required to form the microcrystalline cellulose compacts was accounted for by the increased plastic deformation and subsequent bonding.

The compression of mixtures of ibuprofen and microcrystalline cellulose showed a number of complex interactions, which resulted in positive and negative deviations from simple additive behaviour. With respect to mean yield pressures, at low compression speeds there was a positive interaction which was explained by bonding between the ibuprofen and the microcrystalline cellulose. While at high compression speeds, there was a negative deviation from additive behaviour probably due to melting of the ibuprofen. Intermediate behaviour was seen at a compression speed of 380mm/s.

The affinity between the two components of the mixture resulted in adhesion of the particles which reduced the extent of particle slippage and rearrangement towards a minima between 50% and 75% of ibuprofen. This became less significant as the compression speed increased.

As the bonds between the ibuprofen and microcrystalline cellulose were weaker than the hydrogen bonds that would otherwise have formed between the microcrystalline cellulose particles, the tensile strength of the mixtures showed negative deviation from additive behaviour. The tensile strength of compacts prepared from the mixtures decreased with increasing compression speed due to the reduced time available for plastic flow.

At higher compression speeds more energy was required to form the compacts. This may be due to the utilization of more energy to

overcome the increased cohesiveness of particles that occur at higher compression speeds.

The elastic recovery of compacts prepared from mixtures of these two components was found to be a balance between two factors; the strength of the bonds between the particles and secondly the elasticity of the particles. The elastic recovery increased with compression speed for the same reasons given for the individual components.

6.1.2 The Effect of Speed of Compression on Ibuprofen Lactose Mixtures

Table 6.1d Ibuprofen Lactose Mixtures Compressed at 25mm/s Showing The Elastic Recovery (ER) Heckel Parameters  $D_a$ ,  $D_o$ ,  $D_b$  and The Mean Yield Pressure ( $P_y$ ), The Tablet Tensile Strength and The Net Energy of Compression.

Codes: IB = Ibuprofen L = Lactose 25 = % Concentration of Ibuprofen

TABLET CODE	ER %	$D_a$	$D_o$	$D_b$	$P_y$ MPa	$\sigma_T$ MPa	Net Energy J
IBL00T1	3.246	0.631	0.356	0.275	187.62	0.927	2.50
IBL00T2	4.215	0.632	0.355	0.277	175.75	1.028	2.65
IBL00T3	3.592	0.630	0.358	0.272	176.06	0.894	2.63
IBL00T4	3.947	0.632	0.365	0.267	185.18	0.989	2.55
x	3.750	-	-	0.273	181.15	0.959	2.58
$\sigma_{n-1}$	0.422	-	-	0.004	6.14	0.060	0.07
IBL25T1	4.036	0.660	0.375	0.285	135.68	0.813	2.71
IBL25T2	4.510	0.667	0.382	0.285	142.65	0.720	2.50
IBL25T3	3.922	0.670	0.377	0.293	143.27	0.805	2.62
IBL25T4	3.950	0.674	0.384	0.290	152.20	0.794	2.52
x	4.105	-	-	0.288	143.45	0.784	2.59
$\sigma_{n-1}$	0.275	-	-	0.004	6.77	0.043	0.10
IBL50T1	5.139	0.705	0.409	0.296	102.99	0.885	2.47
IBL50T2	5.433	0.696	0.406	0.290	99.01	0.792	2.58
IBL50T3	4.174	0.713	0.403	0.310	114.41	0.792	2.42
IBL50T4	4.632	0.711	0.410	0.310	104.49	0.854	2.20
x	4.845	-	-	0.301	105.22	0.831	2.42
$\sigma_{n-1}$	0.556	-	-	0.010	6.54	0.046	0.16
IBL75T1	4.790	0.749	0.411	0.383	70.92	0.705	2.33
IBL75T2	3.712	0.781	0.405	0.376	62.89	0.785	2.19
IBL75T3	4.701	0.792	0.406	0.386	70.92	0.857	2.39
IBL75T4	4.188	0.786	0.407	0.379	65.36	0.872	2.37
x	4.348	-	-	0.381	67.52	0.805	2.32
$\sigma_{n-1}$	0.500	-	-	0.004	4.05	0.076	0.09
IBL99T1	5.300	0.777	0.451	0.326	25.84	0.751	2.04
IBL99T2	5.033	0.794	0.451	0.343	30.39	0.768	2.05
IBL99T3	5.614	0.800	0.451	0.349	30.12	0.740	2.14
IBL99T4	5.455	0.800	0.451	0.349	29.76	0.680	2.14
x	5.455	-	-	0.342	29.0	0.734	2.09
$\sigma_{n-1}$	0.247	-	-	0.011	2.14	0.382	0.05

C = Compact capped.

Table 6.1e Ibuprofen Lactose Mixtures Compressed at 380mm/s Showing The Elastic Recovery (ER) Heckel Parameters Da, Do, Db and The Mean Yield Pressure (Py), The Tablet Tensile Strength and The Net Energy of Compression.

Codes: IB = Ibuprofen L = Lactose 25 = % Concentration of Ibuprofen

TABLET CODE	ER %	Da	Do	Db	Py MPa	$\sigma T$ MPa	Net Energy J
IBL00T1	0.196	0.543	0.422	0.121	86.96	0.681	5.55
IBL00T2	0.647	0.566	0.428	0.138	91.74	0.666	4.54
IBL00T3	0.098	0.559	0.437	0.122	90.09	0.743	4.46
IBL00T4	0.326	0.569	0.433	0.136	94.34	0.750	4.15
x	0.317	-	-	0.129	90.78	0.710	4.67
$\sigma n-1$	0.239	-	-	0.009	3.09	0.043	0.61
IBL25T1	8.235	0.569	0.381	0.188	106.49	0.461	4.80
IBL25T2	9.108	0.573	0.381	0.192	107.87	0.439	4.91
IBL25T3	C	0.557	0.382	0.175	97.08	C	4.75
IBL25T4	7.398	0.556	0.381	0.175	97.08	0.367	4.87
x	8.247	-	-	0.183	102.13	0.422	4.83
$\sigma n-1$	0.855	-	-	0.009	5.89	0.049	0.07
IBL50T1	8.543	0.604	0.391	0.213	86.96	0.349	4.64
IBL50T2	C	0.594	0.381	0.213	75.75	C	4.14
IBL50T3	8.377	0.613	0.391	0.222	85.47	0.385	4.45
IBL50T4	9.397	0.600	0.392	0.208	84.03	0.350	4.46
x	8.772	-	-	0.214	83.05	0.361	4.42
$\sigma n-1$	0.547	-	-	0.006	5.01	0.020	0.21
IBL75T1	C	0.597	0.425	0.172	49.50	C	4.23
IBL75T2	3.687	0.602	0.429	0.173	50.50	0.398	3.95
IBL75T3	2.539	0.621	0.406	0.215	68.49	0.444	4.15
IBL75T4	3.218	0.636	0.410	0.226	74.76	0.465	4.76
x	3.148	-	-	0.197	60.77	0.424	4.27
$\sigma n-1$	0.577	-	-	0.028	12.70	0.037	0.34
IBL99T1	10.172	0.621	0.451	0.170	29.33	0.551	3.64
IBL99T2	12.495	0.647	0.451	0.196	34.36	C	4.11
IBL99T3	C	0.609	0.451	0.158	30.49	C	4.05
IBL99T4	11.946	0.660	0.451	0.209	36.90	C	4.02
x	11.538	-	-	0.183	32.77	0.551	3.96
$\sigma n-1$	1.214	-	-	0.023	3.49	-	0.215

C = Compact capped.

Table 6.1f Ibuprofen Lactose Mixtures Compressed at 1100mm/s Showing The Elastic Recovery (ER) Heckel Parameters Da, Do, Db and The Mean Yield Pressure (Py), The Tablet Tensile Strength and The Net Energy of Compression.

Codes: IB = Ibuprofen L = Lactose 25 = % Concentration of Ibuprofen

TABLET CODE	ER %	Da	Do	Db	Py MPa	$\sigma_T$ MPa	Net Energy J
IBL00T1	0.358	0.429	0.430	0.000	51.55	0.621	5.11
IBL00T2	0.488	0.483	0.432	0.051	64.10	0.645	5.36
IBL00T3	0.885	0.446	0.432	0.014	53.19	0.719	5.08
IBL00T4	0.357	0.467	0.429	0.038	62.11	0.697	5.27
x	0.522	-	-	0.034	57.73	0.670	5.20
$\sigma_{n-1}$	0.250	-	-	0.019	6.29	0.045	0.14
IBL25T1	C	0.484	0.390	0.094	74.63	C	5.57
IBL25T2	C	0.482	0.390	0.092	82.64	C	5.35
IBL25T3	C	0.461	0.385	0.076	59.52	C	5.44
IBL25T4	C	0.477	0.388	0.089	67.11	C	5.05
x	C	-	-	0.087	70.97	C	5.35
$\sigma_{n-1}$	C	-	-	0.008	9.93	C	0.27
IBL50T1	C	0.491	0.414	0.076	54.94	C	5.04
IBL50T2	C	0.506	0.413	0.093	61.73	C	4.57
IBL50T3	C	0.511	0.411	0.100	67.57	C	4.50
IBL50T4	C	0.499	0.407	0.092	65.36	C	4.63
x	C	-	-	0.090	62.40	C	4.68
$\sigma_{n-1}$	C	-	-	0.010	5.53	C	0.24
IBL75T1	C	0.584	0.460	0.124	64.10	C	4.17
IBL75T2	C	0.519	0.451	0.068	46.08	C	3.91
IBL75T3	C	0.564	0.460	0.104	50.50	C	4.99
IBL75T4	C	0.561	0.458	0.103	55.86	C	4.35
x	C	-	-	0.099	54.14	C	4.36
$\sigma_{n-1}$	C	-	-	0.023	7.75	C	0.46
IBL99T1	C	0.581	0.451	0.130	55.86	C	3.92
IBL99T2	C	0.590	0.451	0.138	51.81	C	3.73
IBL99T3	C	0.548	0.451	0.096	42.55	C	3.73
IBL99T4	C	0.573	0.451	0.122	51.01	C	3.99
x	C	-	-	0.121	50.30	C	3.84
$\sigma_{n-1}$	C	-	-	0.018	5.59	C	0.13

C = Compact capped.

## Discussion

Lactose, in all of its different physical forms has been widely used in tablet formulations for many years. Consequently extensive work has been carried out to identify its compression characteristics. The main mechanism of consolidation for crystalline lactose has been reported to be by fragmentation (Hersey and Rees (1970,71), Hersey et al (1973), Cole et al (1975)). The consolidation mechanisms of other forms of lactose are less clearly defined. Spray-dried lactose has been reported to consolidate mainly by brittle fracture by McKenna and McCafferty (1982). More recently Vromans et al (1986) reported that the amorphous lactose which accounts for 15% of commercial spray-dried lactose deforms plastically under load, while the remaining 85% of  $\alpha$ -lactose monohydrate was subject to brittle fracture. Both crystalline and spray-dried lactose were shown to exhibit some plastic deformation during compression by Roberts and Rowe (1985).

The material used for this investigation consisted of microfine crystals of  $\alpha$ -anhydrous lactose aggregated to form particles between 45 $\mu$ m and 105 $\mu$ m. The mean yield pressure for this material was found to be 181MPa at the slowest compression speed. This indicates a moderately hard, brittle material. As the speed of compression was increased a somewhat surprising decrease in mean yield pressure was found see tables 6.1d,e,f. This was the opposite trend to that previously reported by Roberts and Rowe (1985) for  $\alpha$ -monohydrate lactose,  $\beta$ -anhydrous lactose, and  $\alpha$ -monohydrate spray-dried lactose. Although this was an unexpected result it was not unprecedented. Other reports of softening of materials with increasing compression speed have been made. Barton (1978) and Al-Hassani and Es-Saheb (1984) noted a softening of paracetamol D.C with increasing compression speed. No mechanism was offered for this effect.

One possible explanation could be based on the plastic deformation and melting of asperities that occur during compression as described by Jayasinghe *et al* (1969/70). These workers showed that due to the very high pressures which occur during compression, the melting point of lactose may be lowered according to the Skottky equation at points where the particles made true contact. Complete melting of lactose asperities was shown to take place at 130°C which is well below its 223°C melting point. If the localized melting continued and the particles became close enough together, then the molten material may form a meniscus between them. The presence of a liquid meniscus would effectively act as an internal lubricant decreasing the resistance to deformation. If this process significantly contributed to the consolidation of a material then we would expect the mean yield pressure to be decreased. As an increase in the speed of compression decreased the extent of particle rearrangement (Db) as shown in tables 6.1d,e,f there would be fewer particle-particle contacts at the start of compression. This in turn would cause greater pressures at the points of contact. The higher pressures would increase the melting effect. This, combined with the decrease in the time available for generated heat to dissipate would increase the plastic flow and melting of asperities. Thus an increase in the speed of compression results in an apparent softening of the material and less brittle fracture.

The extent of particle rearrangement was shown to be less for lactose than ibuprofen at all compression speeds. This is due to the more spherical shape of the lactose particles compared to the needle shaped ibuprofen crystals. Both materials showed similar decreases in the extent of particle rearrangement with increasing compression speed. The explanation for this is the same as described previously, i.e. the time dependency of particle movement.

The tensile strength of the compacts prepared from both materials were relatively weak. The strength of the lactose compacts depends on the extent of fragmentation and the size of the true area contact. The greater the fragmentation of lactose, the greater the number of points of contact between the particles which would be expected to increase the strength of the compacts. However each contact area is relatively small and the cohesion between the particles is low which contributes to a lower bond strength resulting in a relatively weak compact (Cole *et al* (1975)). Tensile strength of the lactose compacts decreased with increasing compression speed. This could be a result of the disruptive effects of air escaping during compression. The disruption would be expected to become more significant as the time available for air escape was reduced, there by reducing the strength of the compact. It was previously suggested that the melting of asperities contributed to the consolidation process. During decompression we would expect the molten material to solidify forming solid bridges between the particles. This fusion bonding would be expected to contribute to the compact strength which is not substantiated by the tensile strength data. The reason for this could be the inability of lactose to relieve the stresses of decompression by plastic flow. Consequently many of the solid bridges could be broken during decompression and ejection.

The elastic recovery of lactose was seen to be relatively low and changed little with increasing compression speed. The net energies used to form the lactose compacts were similar to those required to form the ibuprofen compacts. An increase in the net energy used to form the compacts was seen with increasing compression speed, the reasons for this will be the same as described earlier for microcrystalline cellulose and ibuprofen.

If we consider how the mixtures of ibuprofen and lactose behaved during compression, we can see a contrast with the behaviour already

discussed for microcrystalline cellulose and ibuprofen. The effect of compression speed on the mean yield pressures of ibuprofen lactose mixtures are shown in FIG 6.1F. At the slowest compression speed a simple additive relationship is seen between the brittle fracture of the lactose and the plastic deformation and asperity melting of the ibuprofen. There is no apparent interaction between the materials during compression. However we would expect some interaction due to the dissimilar compaction mechanisms. After the rearrangement process has ceased the fragmentation of the lactose may slow down the plastic deformation of the ibuprofen as its fragments fill pores and its increased contact points bear the applied load. Similarly plastic deformation by the ibuprofen may relieve the applied load preventing the critical force for fracture of the lactose being achieved. The relative effects of these processes will depend on the compression speed and the proportion of each material. These processes may explain the behaviour of the mixtures compressed at the intermediate speed of 380mm/s. The curve shows positive deviation from additive behaviour indicating that the deformation mechanism of the lactose dominates the mixtures. This is probably due to a reduction in the extent of plastic deformation by the ibuprofen. Under high compression speed where both materials exhibit similar mean yield pressures and probably similar deformation mechanisms, again there is no interaction between the materials.

The extent of particle rearrangement and slippage (Db) for the mixtures are shown in FIG 6.1g. Positive deviations from additive behaviour towards ibuprofen were shown at all compression speeds. This is probably a function of the shape of the particles. The lactose particles shown in the scanning electron micrograph FIG 3.2j are more spherical than the needle shaped ibuprofen crystals seen in the scanning electron micrograph FIG 3.2b. When mixed together the lactose

**Fig 1f** THE EFFECT OF COMPRESSION SPEED ON THE MEAN YIELD PRESSURE OF IBUPROFEN / LACTOSE MIXTURES.

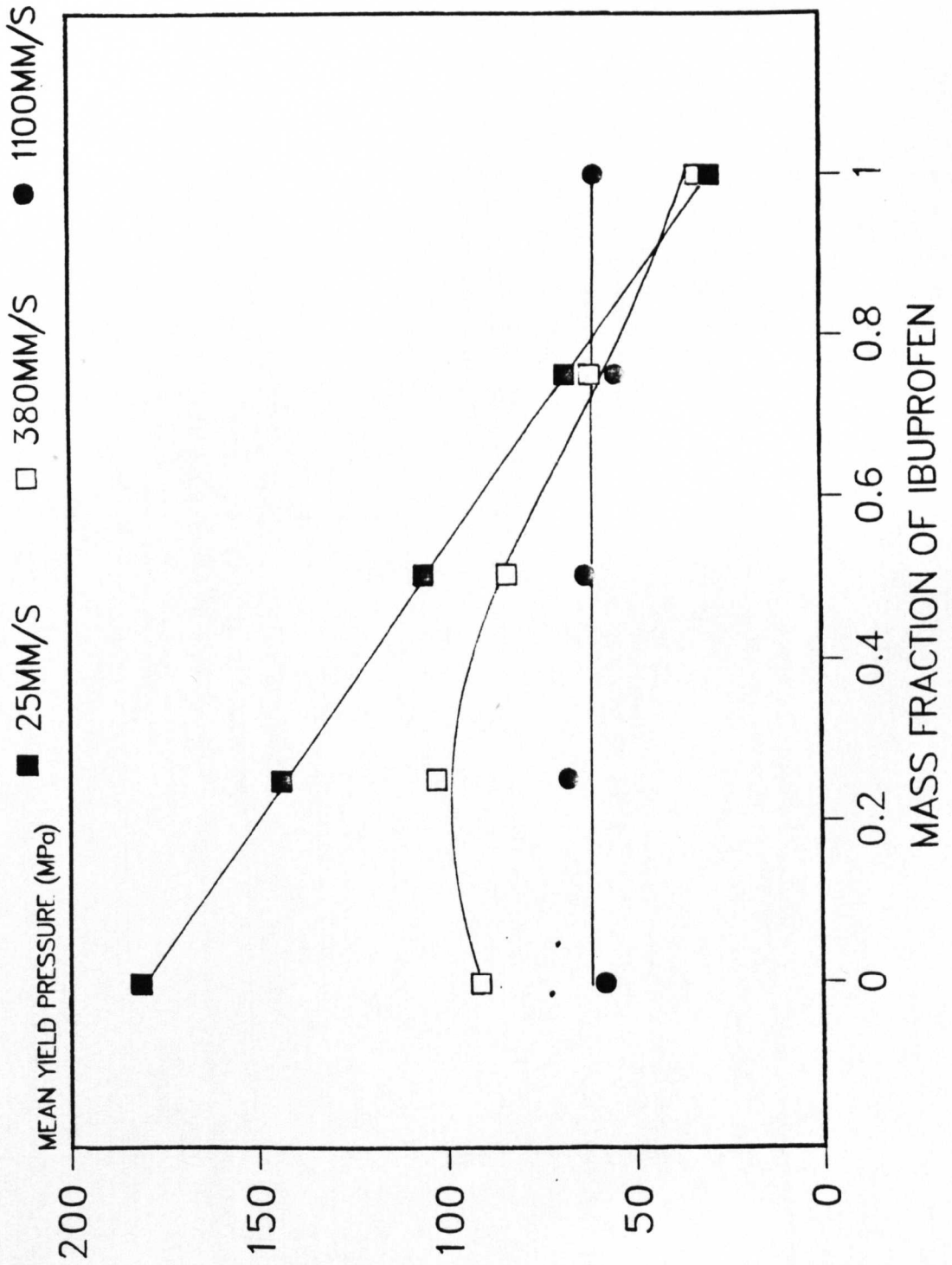
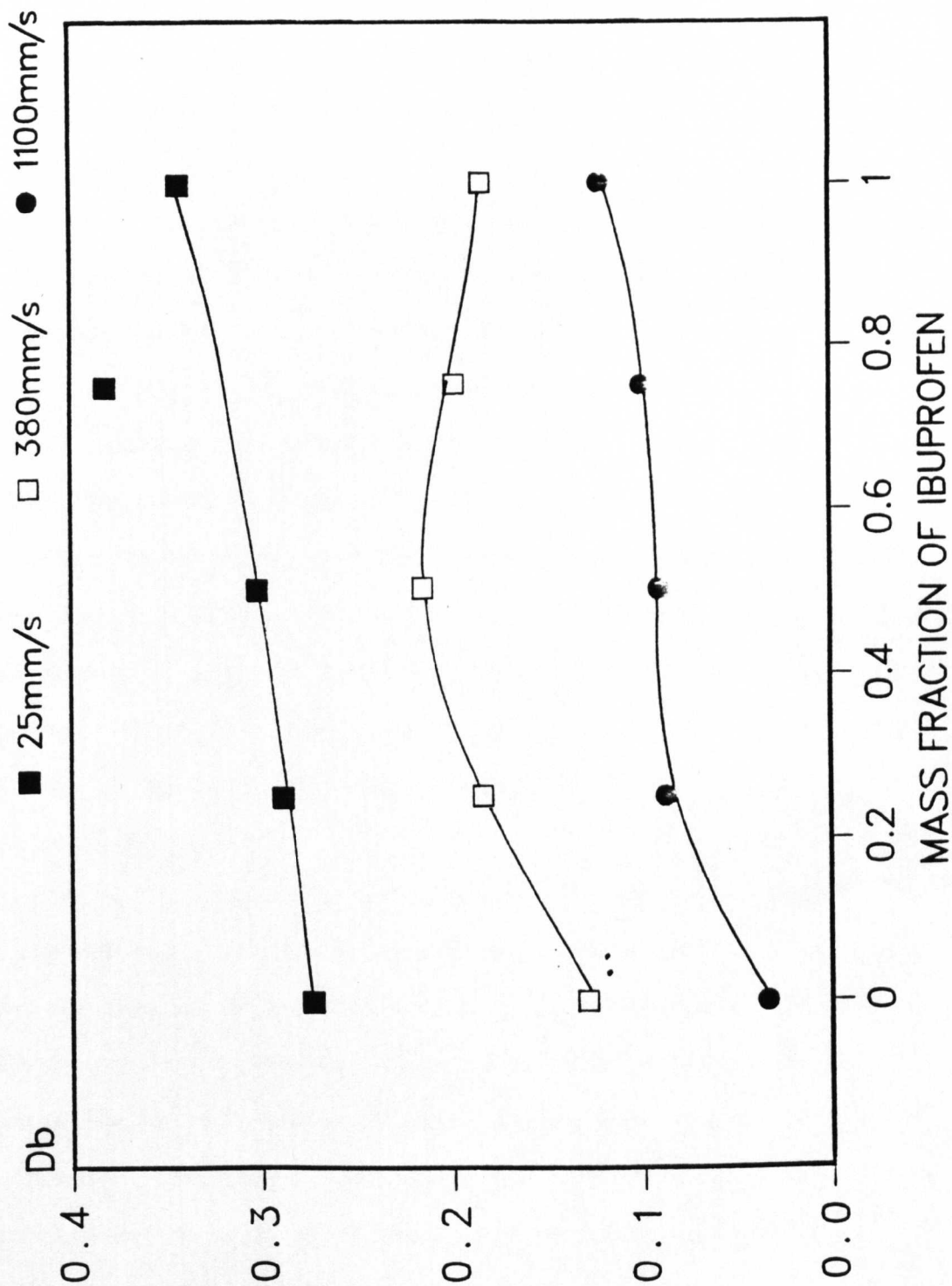


**FIG 6.1g**

THE EFFECT OF COMPRESSION SPEED ON THE EXTENT OF PARTICLE REARRANGEMENT FOR IBUPROFEN LACTOSE MIXTURES.



particles will tend to pack closer forming a more stable structure, while the ibuprofen crystals will form irregular loose regions. When the pressure is applied the ibuprofen crystals will tend to move to more stable positions after which the lactose will fill the remaining voids. The same trend in the extent of particle rearrangement was seen for each compression speed. It was interesting to note that virtually no particle rearrangement occurred with lactose at the highest compression speed.

The tensile strengths of compacts prepared from ibuprofen lactose mixtures are shown in FIG 6.1h. The most important point shown by these graphs is that compacts of the powder mixtures possess the same tensile strength as the ibuprofen alone. This indicates that the ibuprofen interferes with the formation of the lactose-lactose bonds at all compression speeds. This could be due to the ibuprofen physically inhibiting the lactose-lactose bonds or due to the lactose preferentially forming weaker bonds with the ibuprofen. At the highest compression speed compacts could only be formed from lactose alone due to capping. This was probably the combined result of air entrapment and inability of the weak compact to withstand the stresses imposed during rapid decompression.

The elastic recovery of the compacts formed from mixtures are shown in FIG 6.1i. At the slowest compression speed there is little difference between the elastic recovery of the two materials and the behaviour of the mixtures appears to be proportional to the concentration of each component. With a compression speed of 380mm/s the elastic recovery increases due to the reduction in interparticulate bonding which previously resisted the recovery.

The net energy used to form compacts from the mixtures are shown in FIG 6.1j. At the slowest compression speed the energy required to form the compact was proportional to the concentration of each

**FIG 6-1h** RADIAL TENSILE STRENGTH FOR IBUPROFEN LACTOSE MIXTURES COMPRESSED AT THREE DIFFERENT SPEEDS

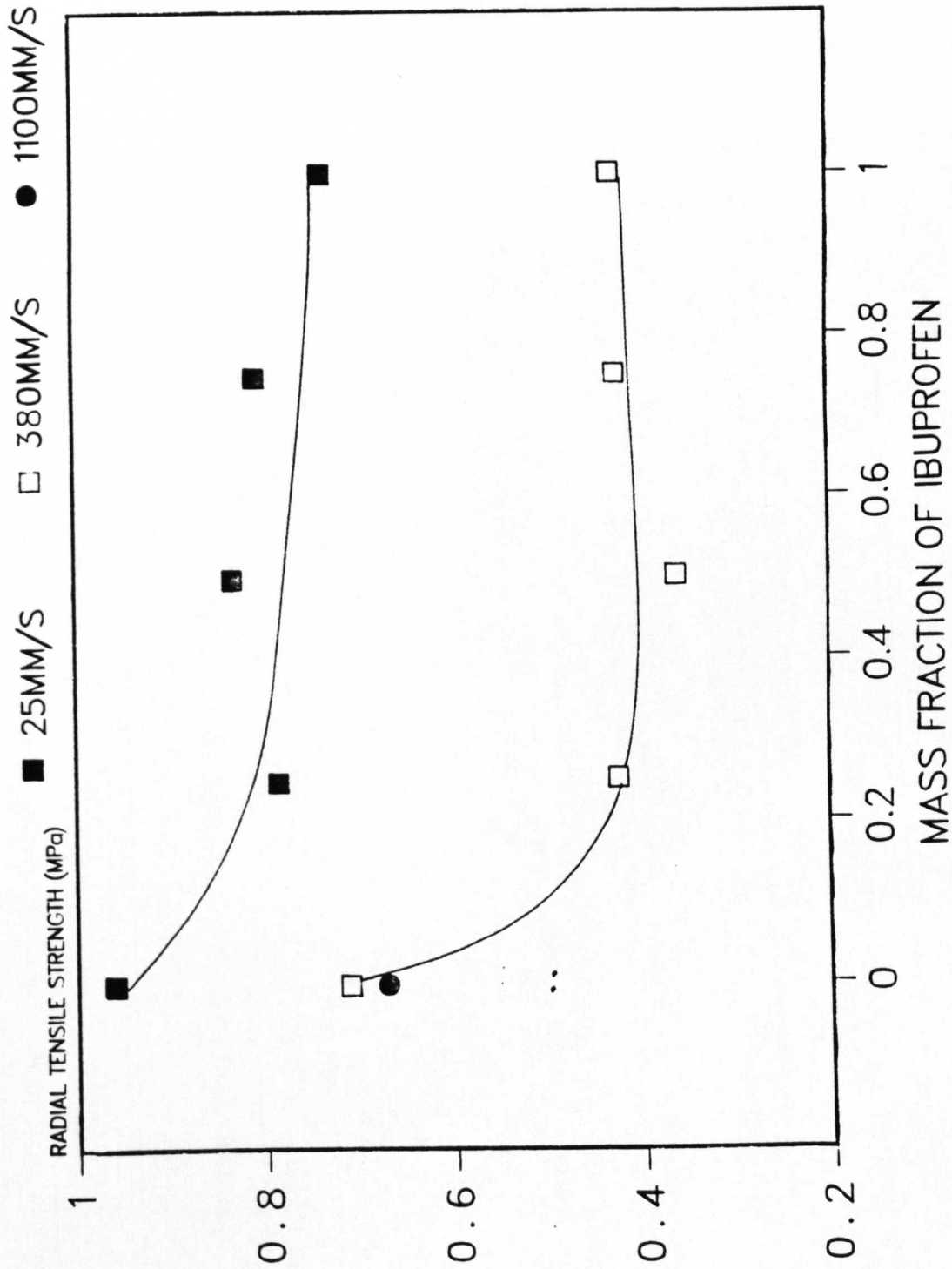


**FIG 6-1i** THE EFFECT OF COMPRESSION SPEED ON THE ELASTIC RECOVERY OF IBUPROFEN LACTOSE MIXTURES.

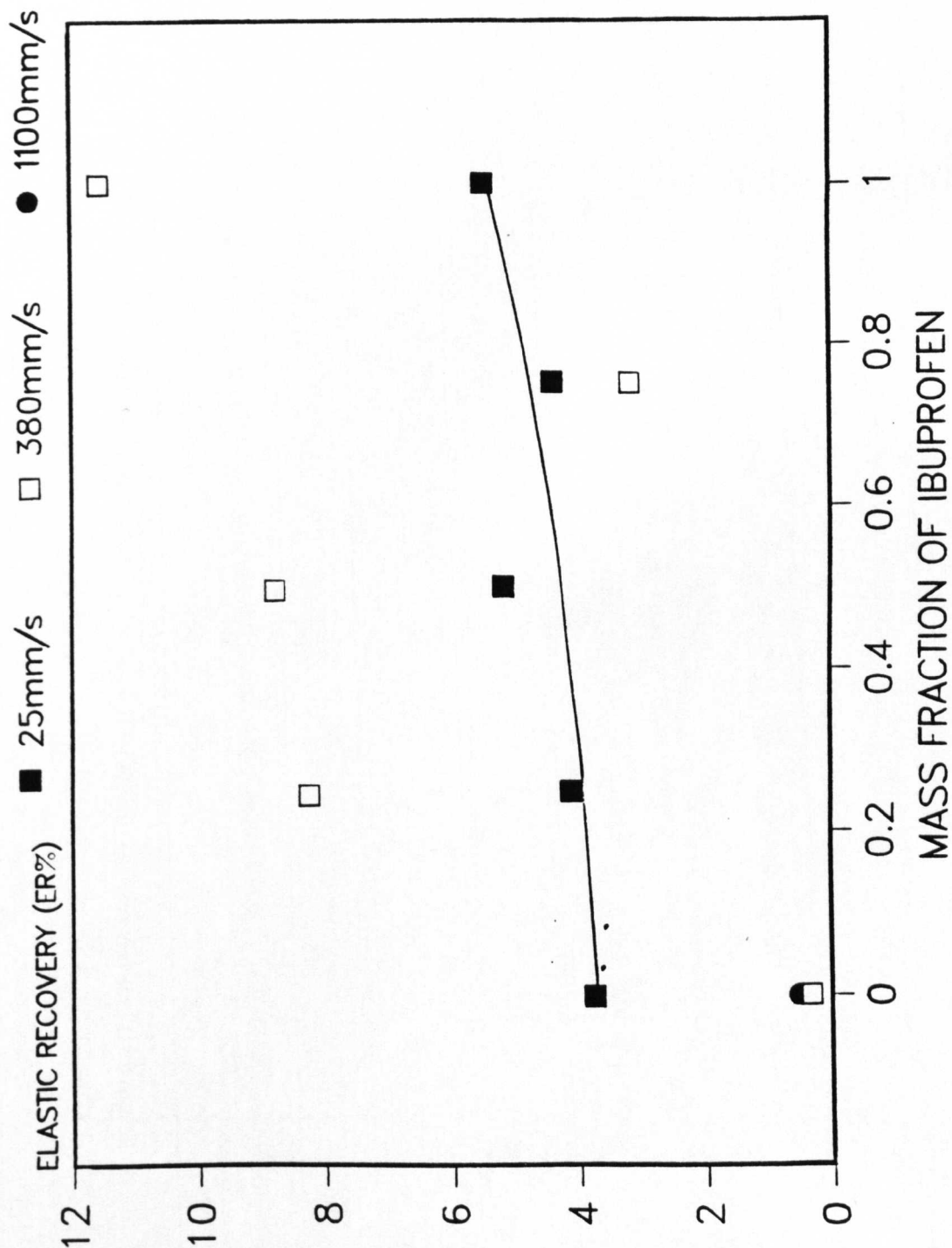
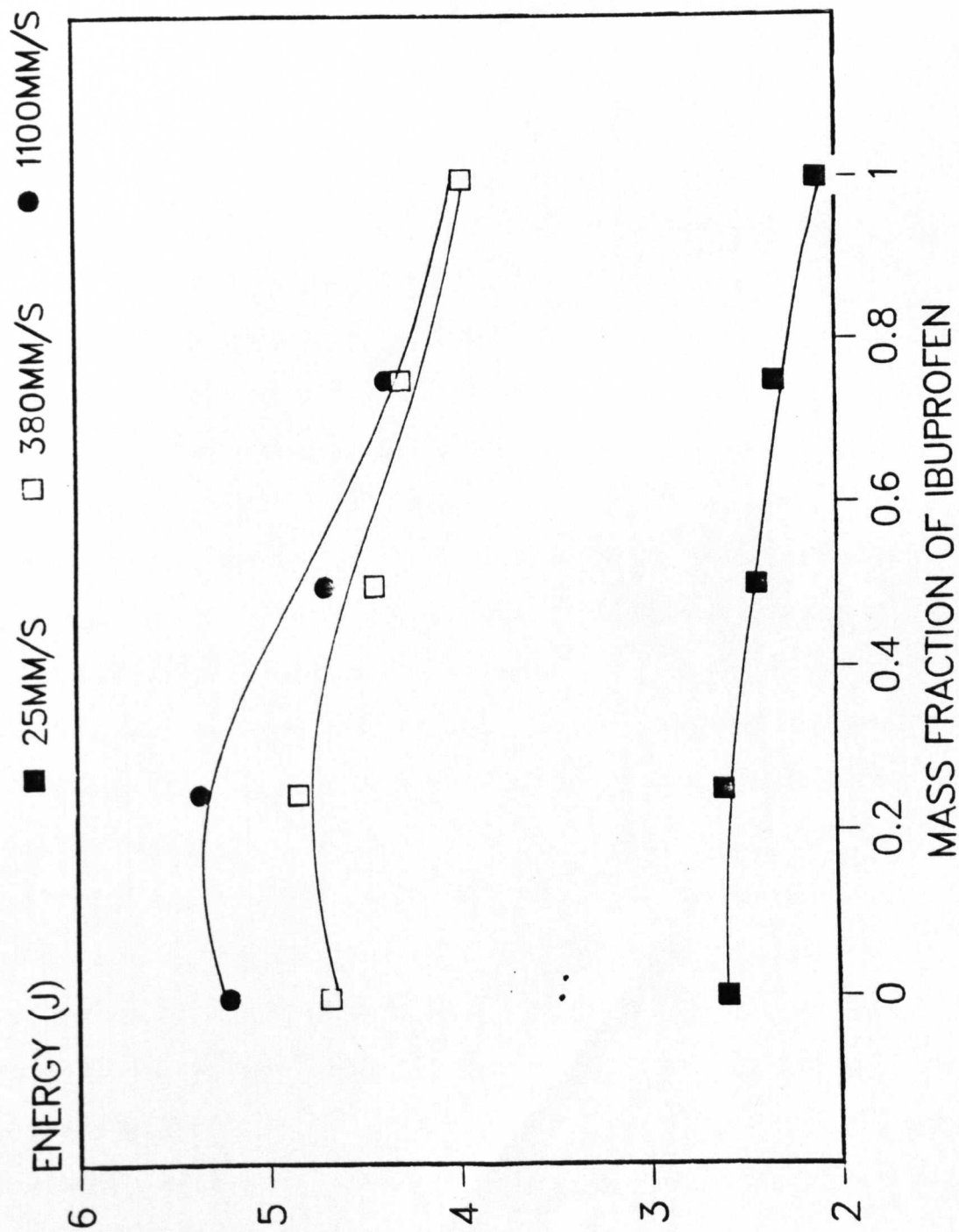


**FIGURE 1**  
 THE EFFECT OF COMPRESSION SPEED ON THE NET ENERGY OF  
 IBUPROFEN / LACTOSE MIXTURES.



component. When the compression speed was increased to 380mm/s the energy required to form compacts from each mixture was almost doubled in each case. This increase may again be accounted for by the increased cohesiveness of particles that occur at higher compression speeds combined with energy required for thermal changes, changes of state, and friction effects.

### Conclusions

Lactose was found to behave as a moderately hard brittle material at low compression speeds. An increase in the compression speed resulted in an apparent softening of the material and less brittle fracture. This somewhat surprising behaviour was thought due to an increase in the melting of asperities.

The more spherical shape of lactose compared to the needle shaped ibuprofen has been shown to reduce the extent of particle rearrangement during compression. Due to the time dependant nature of particle movement, the extent rearrangement for both materials was seen to decrease as the compression speed increased.

Both materials produced weak compacts. In the case of lactose this was explained by the formation of a large number of relatively small contact areas between particles with poor cohesion resulting in low bond strengths and a weak compact. An increase in the compression speed was seen to reduce the strength of lactose compacts. This was considered due to the increasing disruptive effects of escaping air, and the inability of the solid lactose bridges to withstand the stresses of decompression.

The elastic recovery of lactose was found to be relatively low and changed little with compression speed. The energy required to form the compacts increased with increasing compression speed which was accounted for by an increase in the cohesiveness of particles, energy required for thermal changes, changes of state, and friction effects.

When the ibuprofen and lactose were mixed some deviations from additive behaviour were seen. An increase in the speed of compression from 25mm/s to 380mm/s resulted in a change from additive behaviour to a positive interaction. This interaction was considered to be a balance between the plastic deformation by the ibuprofen relieving the applied load preventing the critical force required for fracture of the lactose being attained, and the lactose fragments bearing the applied load reducing plastic flow by ibuprofen. The latter was considered to dominate. When the compression speed was further increased and the consolidation mechanisms were considered to be similar the behaviour again became additive.

The needle shaped ibuprofen crystals tended to dictate the extent of particle rearrangement of the mixtures. At the highest compression speed very little rearrangement occurred especially with lactose.

The tensile strength of the compacts prepared from mixtures were determined by the ibuprofen present which was suggested to inhibit the formation of lactose-lactose bonds. An increase in compression speed reduced the strength of all compacts due to the disruptive effects of air escape and the inability of the weak compact to withstand the stresses imposed during rapid decompression. This reduction in strength influenced the extent of elastic recovery of the compacts. Generally the weaker the compact the more the materials were able to recover.

Slight positive deviations towards the proportion of lactose present in the mixture and the energy required to form the compacts were seen. This effect became more significant at high compression speeds.

## 7.1 Investigation of Compact Properties Prepared by Compression to Constant Thickness and to a Constant Force

### Introduction

Tablets today are manufactured by compression using high speed rotary tableting machines. Such machines compress a constant volume of powder between two rollers using an upper and lower punch. Once the compression weight of the tablet has been determined, the force used to compress the tablet may be adjusted by increasing or decreasing the separation between the two rollers. When the compression force has been set the position of the rollers remains fixed. Tablets manufactured under such conditions are usually considered compressed to a 'constant thickness'. Such a press is the Rotapress MkIII supplied by Manesty Machines Ltd. In practice there will be a small variation in the minimum punch separation during compression due to the slight differences in punch lengths and any eccentricity of the compression rollers. These variations will be more significant if the punches and compression rollers are worn.

The force exerted during compression will be determined by the separation between the punch tips and the weight of powder in the die. Therefore anything that can alter the die filling process can alter tablet weight, weight variation and the maximum compression force. Many variables may influence the die filling process including granule size and size distribution, poor flow and mixing of the formulation, variation in the lengths of the lower punches or, if the lower punch moves irregularly creating a die space of varying capacity. Variations in the ratio of small to large granules influence how the void spaces between particles are filled. Thus the apparent fill volume may remain constant but different proportions of large and small particles may

change the weight of fill in each die. If the granules are relatively large and the die cavity is small, the difference of only a few granules may significantly influence weight variation. The filling of the die is based on a continuous and uniform flow of granules from the hopper through the feed frame and into the die. If the formulation has poor flow properties or the machine speed exceeds the formulations flow capabilities the die will not be filled properly. Glidants may be added to the formulation to improve its flow properties. If the glidants and lubricants are not thoroughly distributed within the formulation, the flow of particles may be impaired causing variation of the fill weight. Small variations in the lengths of lower punches or irregular changes in their positions during the fill process can vary the fill weights as it is simply volumetric. Ridgway Watt and Rue (1980) have shown that variation of the fill weight may occur when using a Betapress due to partial compression of granules by the paddles of the mechanised feeder. A transparent Betapress turret was used by the same workers to show movement of the powders within the die as the turret rotates. They suggested part of the fill may be ejected by centrifugal forces prior to the compression stage.

Due to the reasons detailed above, the maximum compressive force experienced by the tablets during manufacture on a 'constant thickness' tableting machine are likely to vary from tablet to tablet. It has been shown that the compression force used to produce a compact has an effect on its hardness and disintegration time. Khan & Rhodes (1976) demonstrated the effect of compression force on the properties of six direct compression tablet formulations. An increase in the compression force was found to increase tablet hardness and either increase or decrease the disintegration time. These are important pharmaceutical parameters and must be controlled if uniformity of the dosage form is to be ensured. In order to maintain a

consistent dosage from one tablet to the next Pharmacopoeial tests have been introduced. These include uniformity of the tablet diameter, weight, content of the active ingredient, disintegration and dissolution rates. Thus if we enforce the uniformity of weight limits during tablet manufacture we may expect uniformity of the force used to compress the tablet.

The uniformity of weight test is carried out by removing a sample of twenty tablets from a batch, weighing them individually and calculating the mean weight, which in turn governs the permitted deviations from the mean. These are shown in Table 7.1a

Table 7.1a B.P. Uniformity of Tablet Weight

<u>Average Weight of Tablet</u>	<u>Percentage Deviation</u>
80mg or less	10.0
More than 80mg and less than 250mg	7.5
<u>250mg or more</u>	<u>5.0</u>

Not more than two tablets are permitted to differ from the mean by more than the stated percentage and no tablet by more than double that percentage. The effect of fill weight variation within these limits on the maximum compression force and subsequent tablet disintegration times will be determined during this investigation.

The effects of variation in fill weight would be less significant if the force used to compress the tablets could be kept constant. Ed Courtoy have developed a tablet press which is claimed to produce tablets under a constant force. This is achieved using a hydraulic system which supports the compression roller. This system would be expected to produce tablets of constant density exhibiting little variation in tablet strength and disintegration time. The maintenance of constant compression force would also be expected to be advantageous for the tableting of pressure sensitive materials such as ibuprofen.

Little data is available on tablets produced on such presses. This investigation has been designed to quantify the advantages or otherwise of compression under constant force compared to compression to a constant thickness under manufacturing conditions.

### Experimental

The methods used were as described earlier in 'Materials and Methods'. Any supplementary details have been detailed below.

A mixture of ibuprofen and Avicel was compressed using a haversine control profile applied to the upper and lower actuators with 16mm and 3mm peak displacement respectively. A compression speed (punch tip-powder impact velocity) of 113mms<sup>-1</sup> was maintained for all samples. This was thought to be representative of a rotary tableting machine (100-400mm/s) Roberts & Rowe (1985). The punch separation and mean punch force were monitored throughout the compression cycle via the transient recorder. After the ejection of the compact, the data was transferred digitally to the Apple IIe microcomputer where the peak force and minimum punch separation were identified and recorded. A displacement / time and force / time plot was produced for each tablet. A series of tablets were produced at a constant maximum force of 7.5KN. The weight of material compressed had a nominal weight of 500mg. The actual fill weights represented 500mg  $\pm$ 4% and  $\pm$ 8% which are within the  $\pm$ 5% and  $\pm$ 10% permitted by the B.P uniformity of weight limits. Seven tablets of each weight 460,480,500,520,540mg, were prepared. These compacts were representative of the output from the Ed Courtoy tablet press.

A series of tablets of similar fill weights were prepared by compression to a constant thickness to represent the more traditional fixed roller type machines. The minimum punch separation during

compression of these compacts was equivalent to that of the 500mg tablets prepared under constant force of 7.5kN.

The compacts were measured across their diameter and thickness using a digital micrometer ( $\pm 1\mu\text{m}$ ) within two minutes of ejection. The compacts were then allowed to stand for two hours after which they were re-measured. Four tablets were subjected to the B.P disintegration test and the time taken for each tablet to disintegrate was recorded. Three compacts were subjected to a crushing test. An Instron Testing Machine was used with a crosshead speed of  $0.83\text{mm/s}$ . Radial tensile strength was then calculated to enable comparison between tablets of different thickness.

This procedure was executed using the ibuprofen/Avicel 1:1w/w mixture and the commercial ibuprofen granulation. Ibuprofen was selected for the investigation due to its poor compressibility and sensitivity to compression pressure. Due to the hydrophobic nature of ibuprofen, compacts of the pure drug would not disintegrate. To overcome this problem the ibuprofen was mixed with microcrystalline cellulose (Avicel<sup>™</sup>). Avicel was selected as it is one of the most commonly used tableting excipients. The commercial ibuprofen granulation was used to make the investigation more representative of a real production situation.

Results

Table 7.1b The Maximum Force, Minimum Punch Separation, Disintegration Time and Tensile Strength for Tablets Prepared from an Ibuprofen Granulation Compressed to Constant Force  
Codes: IG=Ibuprofen Granulation, 460=Tablet weight, L=Constant Force

Tablet Code	Maximum Force/kN	Minimum Punch Separation mm	Disintegration Time /S	Radial Tensile Strength /MPa
IG460LT1	7.087	3.355	-	0.7887
IG460LT2	7.482	3.358	-	0.7857
IG460LT3	7.126	3.355	-	0.7778
IG460LT4	7.205	3.395	42	-
IG460LT5	7.680	3.350	48	-
IG460LT6	7.441	3.358	47	-
IG460LT7	7.197	3.356	45	-
x	7.317	3.362	45.5	0.7841
$\sigma_{n-1}$	0.220	0.0145	2.6	0.00564
IG480LT1	7.166	3.514	-	0.7377
IG480LT2	7.166	3.514	-	0.7661
IG480LT3	7.562	3.517	-	0.6976
IG480LT4	8.003	3.481	46	-
IG480LT5	7.047	3.513	37	-
IG480LT6	7.364	3.515	42	-
IG480LT7	7.166	3.514	46	-
x	7.353	3.509	42.7	0.7338
$\sigma_{n-1}$	0.333	0.013	4.3	0.0344
IG500LT1	7.759	3.638	-	0.6877
IG500LT2	7.957	3.600	-	0.8290
IG500LT3	7.561	3.637	-	0.8513
IG500LT4	7.324	3.635	54	-
IG500LT5	7.047	3.672	45	-
IG500LT6	7.839	3.639	55	-
IG500LT7	7.403	3.635	40	-
x	7.556	3.637	48.5	0.7893
$\sigma_{n-1}$	0.321	0.089	7.2	0.0208
IG520LT1	7.601	3.756	-	0.8166
IG520LT2	7.839	3.758	-	0.9036
IG520LT3	8.155	3.760	-	0.7806
IG520LT4	7.601	3.756	40	-
IG520LT5	7.997	3.759	45	-
IG520LT6	7.986	3.759	45	-
IG520LT7	7.522	3.795	45	-
x	7.814	3.763	43.7	0.8336
$\sigma_{n-1}$	0.244	0.014	2.5	0.0141
IG540LT1	7.918	3.917	-	0.7513
IG540LT2	7.957	3.918	-	0.7918
IG540LT3	7.126	3.991	-	0.7387
IG540LT4	7.403	3.913	47	-
IG540LT5	7.680	3.916	47	-
IG540LT6	8.036	3.918	48	-
IG540LT7	7.720	3.916	45	-
x	7.691	3.916	46.7	0.7608
$\sigma_{n-1}$	0.327	0.003	1.3	0.0277

Table 7.1c The Maximum Force, Minimum Punch Separation, Disintegration Time and Tensile Strength for Tablets Prepared from an Ibuprofen Granulation Compressed to Constant Thickness.

Codes: IG=Ibuprofen Granulation, 460=Tablet weight, T=Constant Thickness

Tablet Code	Maximum Force/kN	Minimum Punch Separation mm	Disintegration Time /S	Radial Tensile Strength /MPa
IG460TT1	4.078	3.610	-	0.2982
IG460TT2	4.236	3.571	-	0.3422
IG460TT3	3.761	3.648	-	0.3263
IG460TT4	3.721	3.607	31	-
IG460TT5	4.078	3.610	35	-
IG460TT6	3.880	3.609	40	-
IG460TT7	3.642	3.642	25	-
x	3.971	3.615	32.7	0.3222
$\sigma_{n-1}$	0.283	0.026	6.3	0.0223
IG480TT1	4.988	3.657	-	0.4847
IG480TT2	5.305	3.659	-	0.4522
IG480TT3	5.701	3.582	-	0.5542
IG480TT4	5.463	3.621	33	-
IG480TT5	5.463	3.621	38	-
IG480TT6	5.701	3.582	40	-
IG480TT7	5.146	3.658	35	-
x	5.395	3.626	36.5	0.4970
$\sigma_{n-1}$	0.268	0.034	3.1	0.0521
IG500TT1	7.759	3.638	-	0.6877
IG500TT2	7.957	3.600	-	0.8290
IG500TT3	7.561	3.637	-	0.8513
IG500TT4	7.324	3.635	54	-
IG500TT5	7.047	3.672	45	-
IG500TT6	7.839	3.639	55	-
IG500TT7	7.403	3.635	40	-
x	7.556	3.637	48.5	0.7893
$\sigma_{n-1}$	0.321	0.089	7.2	0.0208
IG520TT1	9.185	3.649	-	0.7835
IG520TT2	9.106	3.688	-	0.9314
IG520TT3	9.858	3.654	-	0.9594
IG520TT4	9.660	3.653	55	-
IG520TT5	9.897	3.655	57	-
IG520TT6	9.620	3.652	55	-
IG520TT7	9.304	3.650	54	-
x	9.518	3.657	55.2	0.8914
$\sigma_{n-1}$	0.321	0.013	1.2	0.0945
IG540TT1	13.32	3.681	-	1.1651
IG540TT2	13.52	3.682	-	1.4358
IG540TT3	13.22	3.680	-	1.4571
IG540TT4	13.52	3.682	85	-
IG540TT5	13.52	3.682	94	-
IG540TT6	13.03	3.678	92	-
IG540TT7	14.02	3.686	96	-
x	13.45	3.682	91.7	1.3527
$\sigma_{n-1}$	0.31	0.002	4.8	0.1628

Table 7.1d The Maximum Force, Minimum Punch Separation, Disintegration Time and Tensile Strength for Tablets Prepared from an Ibuprofen Avicel Mixture Compressed to Constant Force  
 Codes: IA=Ibuprofen Avicel Mix,460=Tablet weight,L=Constant Force

Tablet Code	Maximum Force/kN	Minimum Punch Separation mm	Disintegration Time /S	Radial Tensile Strength /MPa
IA460LT1	7.245	2.988	-	0.9886
IA460LT2	7.205	2.988	-	1.1304
IA460LT3	7.284	2.989	-	1.1316
IA460LT4	7.878	2.953	1950	-
IA460LT5	7.363	2.989	1146	-
IA460LT6	7.561	2.951	2216	-
IA460LT7	7.324	2.949	1507	-
x	7.408	2.972	1704	1.0835
$\sigma_{n-1}$	0.236	0.020	473.5	0.0822
IA480LT1	7.522	3.101	-	0.9250
IA480LT2	7.363	3.100	-	1.0467
IA480LT3	7.680	3.103	-	1.0346
IA480LT4	7.126	3.138	1370	-
IA480LT5	7.522	3.101	2300	-
IA480LT6	7.126	3.138	1194	-
IA480LT7	7.324	3.140	2005	-
x	7.380	3.117	1717.2	1.0021
$\sigma_{n-1}$	0.209	0.020	521.8	0.0670
IA500LT1	7.443	3.253	-	1.0211
IA500LT2	7.641	3.254	-	1.2649
IA500LT3	7.522	3.253	-	1.1591
IA500LT4	7.759	3.215	2120	-
IA500LT5	7.799	3.216	2876	-
IA500LT6	7.403	3.252	2015	-
IA500LT7	7.403	3.291	1995	-
x	7.567	3.248	2251.5	1.1484
$\sigma_{n-1}$	0.167	0.026	419.9	0.1220
IA520LT1	7.245	3.366	-	0.8885
IA520LT2	7.838	3.370	-	1.0486
IA520LT3	7.403	3.367	-	1.0103
IA520LT4	7.594	3.369	1744	-
IA520LT5	7.561	3.369	2160	-
IA520LT6	7.284	3.407	1853	-
IA520LT7	7.482	3.368	1655	-
x	7.487	3.374	1853	0.9825
$\sigma_{n-1}$	0.203	0.015	269.5	0.0836
IA540LT1	7.522	3.528	-	0.8770
IA540LT2	7.443	3.527	-	0.9493
IA540LT3	7.007	3.524	2375	-
IA540LT4	7.324	3.526	-	0.9419
IA540LT5	7.047	3.524	2280	-
IA540LT6	7.126	3.525	2353	-
IA540LT7	7.126	3.525	2402	-
x	7.228	3.526	2352	0.9227
$\sigma_{n-1}$	0.202	0.002	64.1	0.0398

Table 7.1e The Maximum Force, Minimum Punch Separation, Disintegration Time and Tensile Strength for Tablets Prepared from an Ibuprofen Avicel Mixture Compressed to Constant Thickness.  
Codes: IA=Ibuprofen Avicel Mix, 460=Tablet weight, T=Constant Thickness

Tablet Code	Maximum Force/kN	Minimum Punch Separation mm	Disintegration Time /S	Radial Tensile Strength /MPa
IA460TT1	4.829	3.125	-	0.6094
IA460TT2	4.829	3.164	-	0.6857
IA460TT3	4.829	3.164	-	0.6706
IA460TT4	4.711	3.164	235	-
IA460TT5	4.711	3.163	115	-
IA460TT6	4.751	3.163	192	-
IA460TT7	4.711	3.163	229	-
x	4.767	3.158	192.7	0.6552
$\sigma_n-1$	0.059	0.015	55.2	0.0404
IA480TT1	6.069	3.173	390	-
IA480TT2	5.899	3.212	290	-
IA480TT3	5.957	3.172	479	-
IA480TT4	5.780	3.171	195	-
IA480TT5	5.978	3.173	-	0.6331
IA480TT6	6.255	3.175	-	0.7057
IA480TT7	5.741	3.210	-	1.0465
x	5.958	3.184	338.5	0.7951
$\sigma_n-1$	0.178	0.019	122.9	0.2207
IA500TT1	7.443	3.253	-	1.0211
IA500TT2	7.641	3.254	-	1.2649
IA500TT3	7.522	3.253	-	1.1591
IA500TT4	7.759	3.215	2120	-
IA500TT5	7.799	3.216	2876	-
IA500TT6	7.403	3.252	2015	-
IA500TT7	7.403	3.291	1995	-
x	7.567	3.248	2251.5	1.1484
$\sigma_n-1$	0.167	0.026	419.9	0.1220
IA520TT1	9.699	3.241	1638	-
IA520TT2	9.581	3.280	1504	-
IA520TT3	9.620	3.240	2432	-
IA520TT4	9.858	3.242	3651	-
IA520TT5	9.858	3.242	-	1.2154
IA520TT6	9.659	3.281	-	1.1106
IA520TT7	9.541	3.280	-	1.1986
x	9.688	3.258	2306.2	1.1749
$\sigma_n-1$	0.127	0.021	985.6	0.0560
IA540TT1	11.25	3.293	-	1.0680
IA540TT2	11.69	3.256	-	0.8405
IA540TT3	12.42	3.262	-	1.3534
IA540TT4	12.01	3.299	3090	-
IA540TT5	12.06	3.299	2043	-
IA540TT6	12.12	3.299	2000	-
IA540TT7	12.12	3.259	3100	-
x	11.96	3.281	2558.2	1.0873
$\sigma_n-1$	0.376	0.021	620	0.257

## Discussion

In order to perform a true comparison between the two types of presses, all of the conditions experienced by the formulation on the actual presses should be reproduced during the simulation. Actual time displacement profiles were not used to control the movement of the punches. The effects of powder flow, die fill and centripetal force were absent. However we are interested in the principles of compression to a 'constant thickness' and to a 'constant force'. As such the Simulator enabled quantification of the two compression methods at realistic compression speeds with accuracy and reproducibility of fill weights, peak compression force and minimum punch separation not available on actual presses. The actual fill weight was maintained within  $\pm 1\text{mg}$  of the target weight.

### Mean Punch Force

The maximum mean punch force detected during the compression has been plotted against the weight of material placed into the die and is shown in FIGS 7.1a,b. The maximum force mean for each batch in the 'constant force' series for the mixture and the granulation was maintained between 7.228kN and 7.814kN. This represents a relatively narrow variation of force and would be expected to be similar to that attainable by the constant force press. As the fill weight increased in order to form a compact of apparent constant thickness, an increase in the applied force was required. A non linear increase in the maximum mean punch force of 153.9%, was seen for the mixture between fill weights of 460mg and 540mg. A similar increase of 269.3% was seen for the granulation. The increase in compression force was more significant in the range 500-540mg than 460-500mg as the compact was approaching zero porosity. These dramatic increases in the maximum applied force due to the fill weight variation would be expected to have a significant effect on the physical properties of the tablets.

FIG 7-1a

GRAPH OF APPLIED FORCE VESUS TABLET WEIGHT FOR AN IBUPROFEN GRANULATION COMPRESSED TO A CONSTANT THICKNESS AND A CONSTANT FORCE

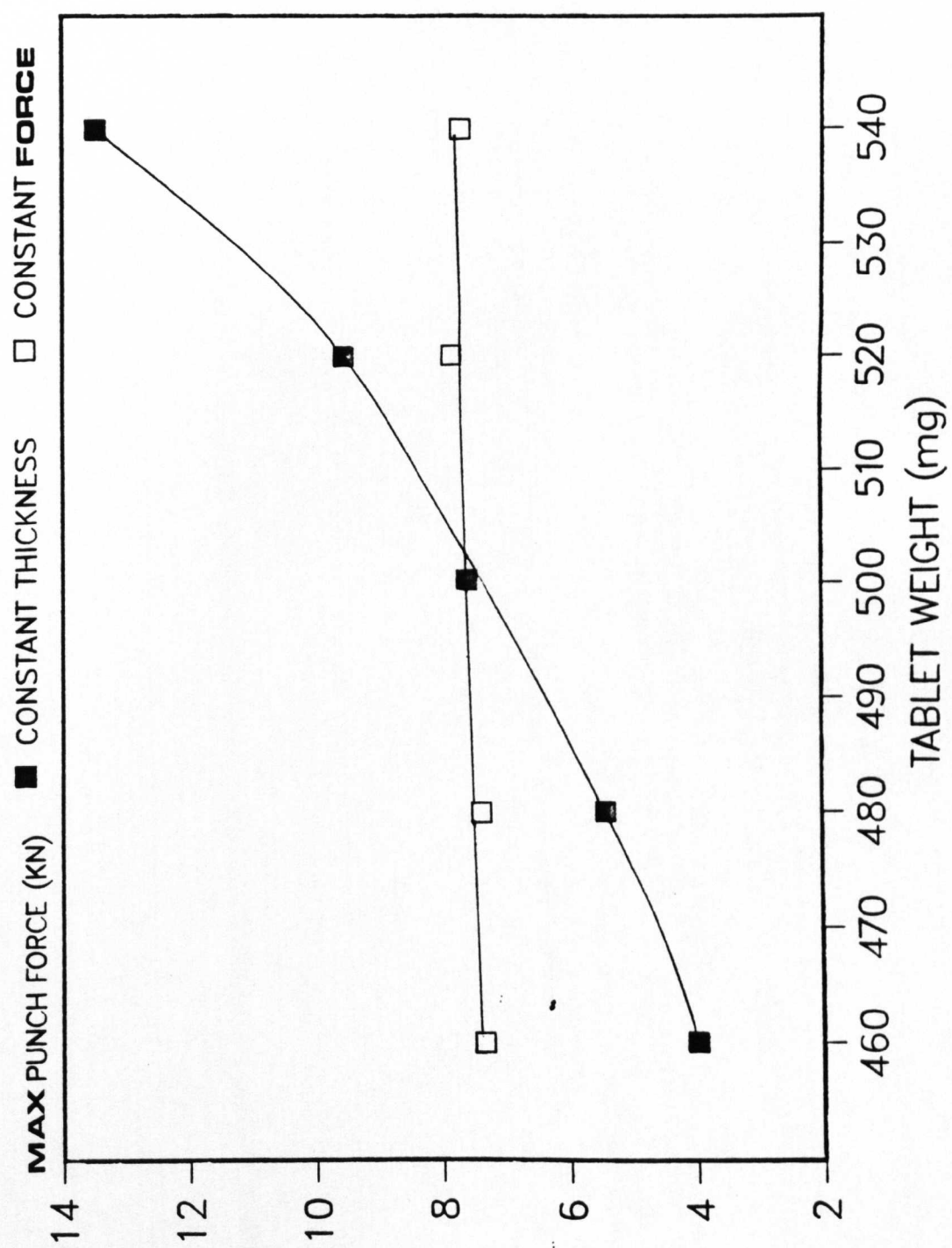
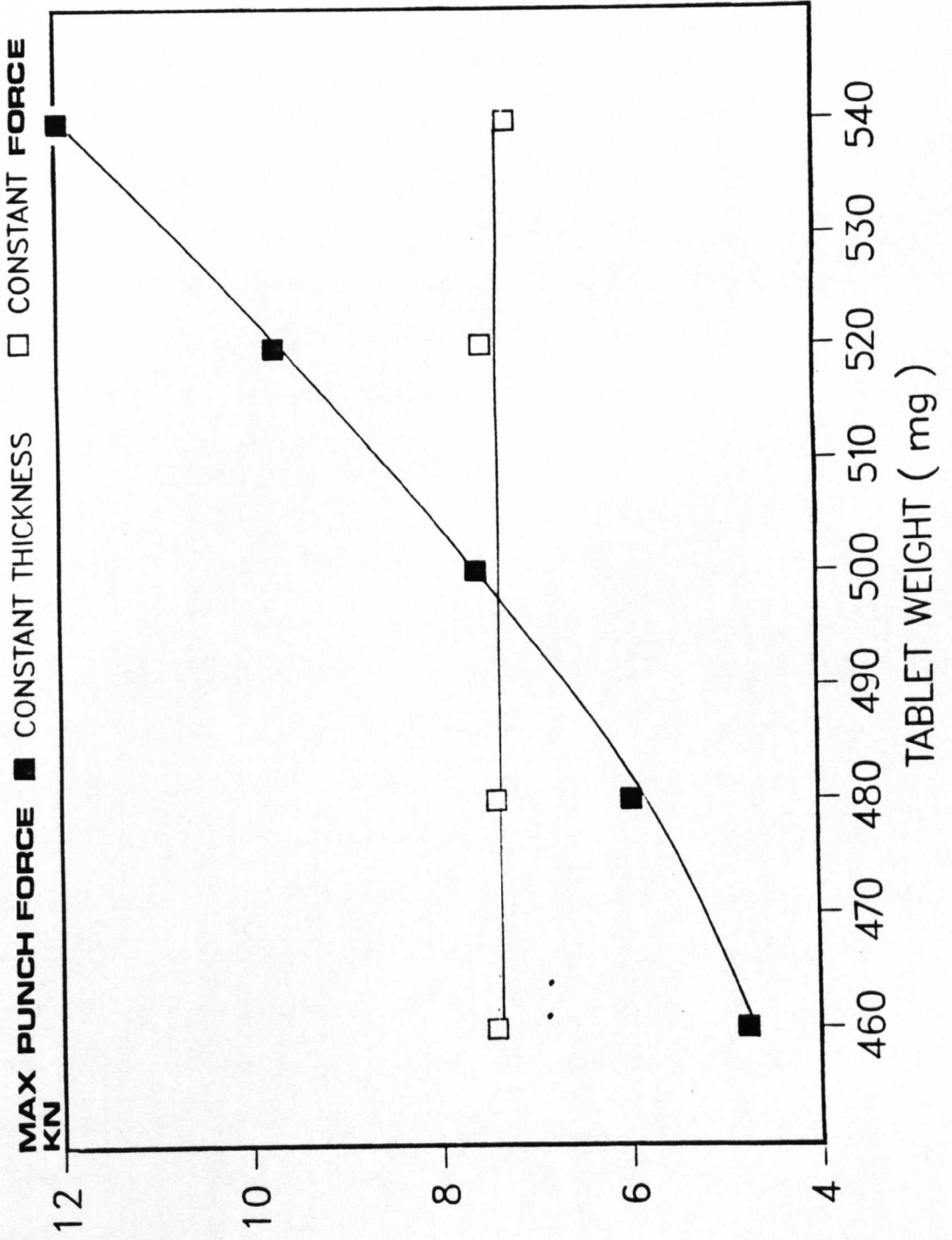


FIG 7.1b

GRAPH OF APPLIED FORCE VERSUS TABLET WEIGHT FOR IBUPROFEN : AVICEL  
1 : 1 MIXTURE COMPRESSED TO A CONSTANT THICKNESS AND A CONSTANT FORCE



### Minimum Punch Separation

The minimum punch separation for the 'constant thickness' series was maintained between 3.539mm and 3.619mm for the granulation; a change of only 2.26%. For the mixture, a similar displacement range between 3.155mm and 3.619mm was maintained; a change of only 2.54%. This control of minimum punch separation would be expected to be similar to that seen on a production 'constant thickness' tablet press. However this represents the apparent minimum punch separation. To obtain the actual punch separation a correction for distortion of the system must be made under force. The corrected figures are listed in tables 7.1b-e and plotted in FIGS 7.1c,d. The minimum punch separation was found to increase linearly with tablet weight for all tablets as shown in FIGS 7.1c,d. In the case of the constant thickness series this was due to distortion of the Simulator and punches under the applied force. Most of the distortion which occurs during the tableting cycle on the Simulator may be attributed to the punches and to a lesser extent the load cell. The load frame itself was constructed to minimise distortion and has little effect on displacement measurements due to the location of the measurement LVDTs. A similar phenomenon would be expected to occur using tableting machines, although the extent of distortion could differ. The deformation and taking up of slack in the bearings of the tablet press was described by Kennerley *et al* (1981) and Mueller and Caspar (1984). These effects would be machine and tooling specific. For rotary machines the tooling is much longer than the 'F' machine tooling used on the Simulator and would be expected to undergo proportionally more distortion. The rollers and their supports would also deform under load, contributing to a significantly greater distortion than seen with the Simulator. Consequently, tablets with weight variations within the B.P limits prepared using a 'constant

**FIG 7-1c** GRAPH OF TABLET THICKNESS VERSUS TABLET WEIGHT FOR AN IBUPROFEN GRANULATION COMPRESSED TO A CONSTANT THICKNESS AND TO A CONSTANT FORCE

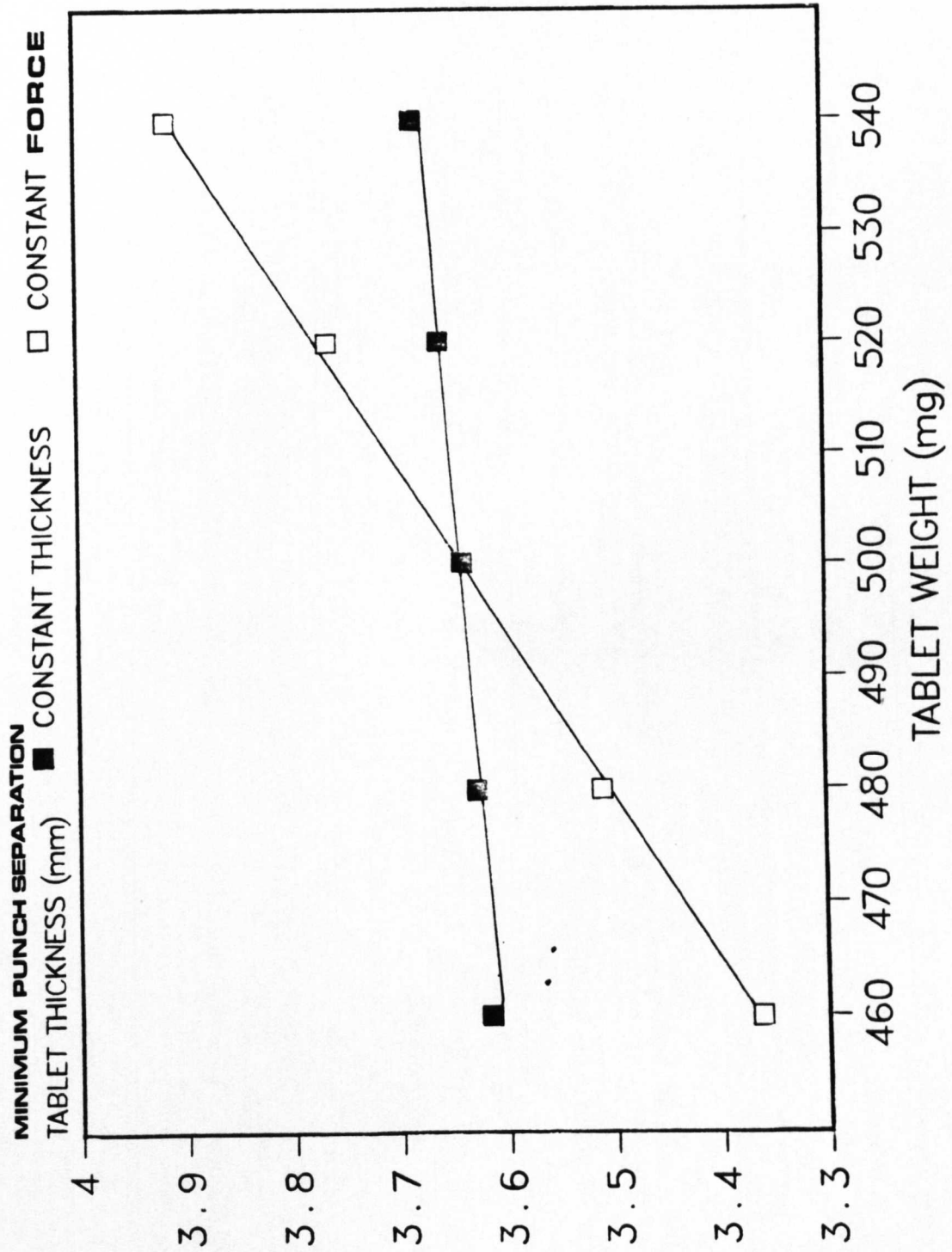
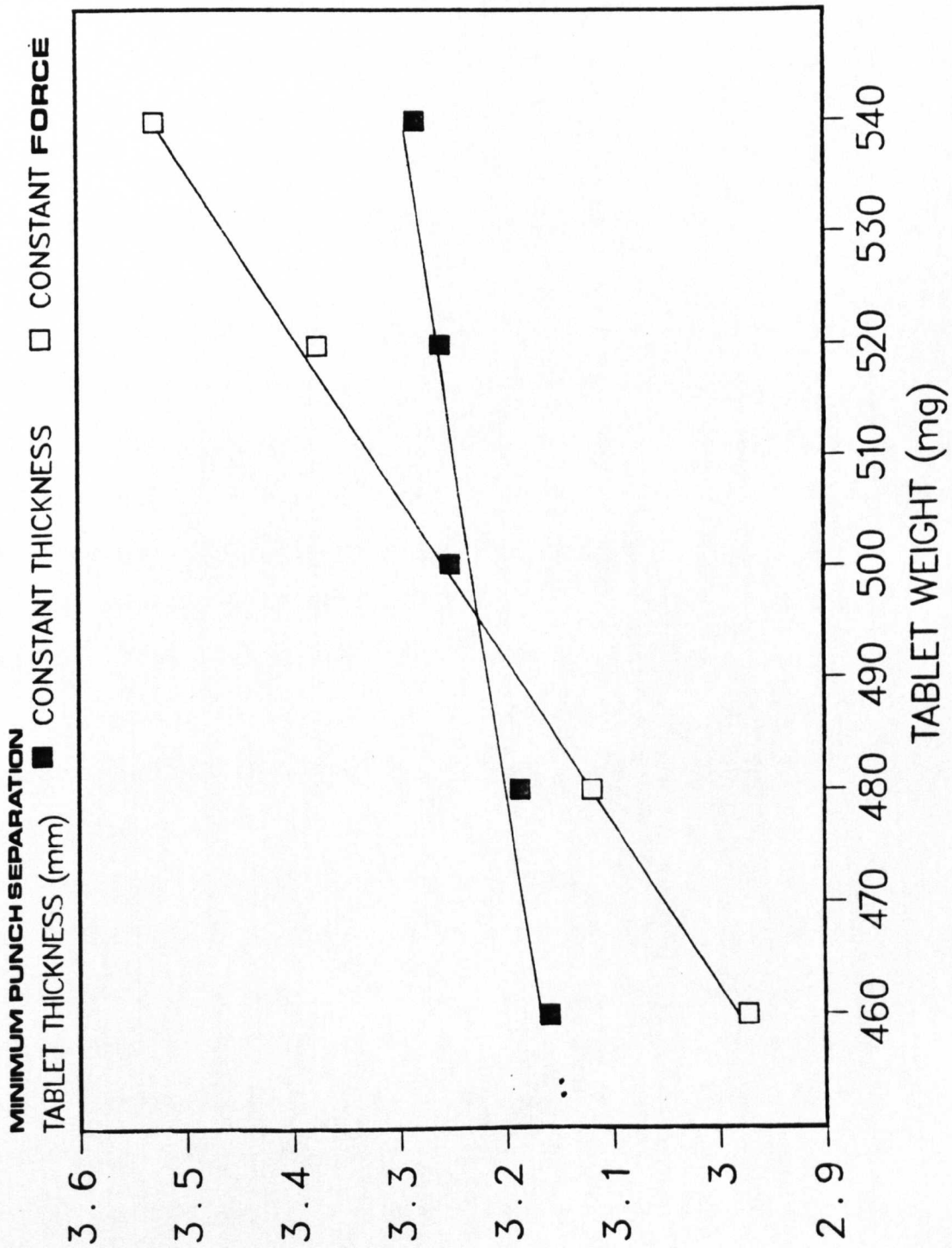


**FIG 7.1d** GRAPH OF TABLET THICKNESS VERSUS TABLET WEIGHT FOR IBUPROFEN:AVICEL 1:1 MIXTURE COMPRESSED TO A CONSTANT THICKNESS AND TO A CONSTANT FORCE



thickness' press will not actually be compressed to the same thickness due to the increased machine distortion with increased fill weight. Considerably greater increases in minimum punch separation were seen for the mixture and the granulation under 'constant force' conditions. Compression of the increasing fill weights by a constant force would be expected to produce tablets of the same density. The increase in tablet volume of the tablet would then be governed by:

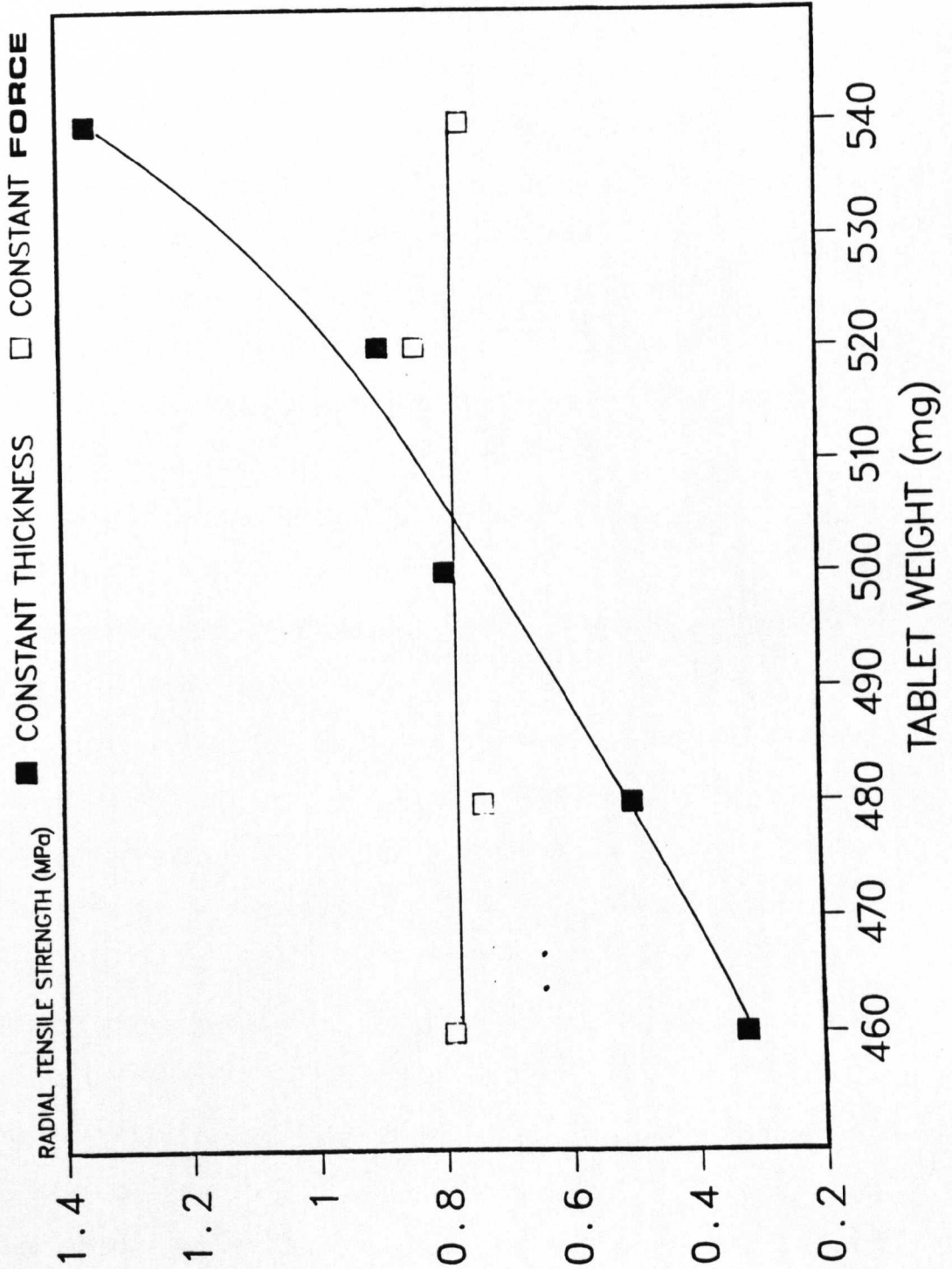
$$\rho = m / v$$

Where  $\rho$  is the density of the compact of volume  $v$  formed from a mass of material  $m$ . These large increases in the tablet volume and associated thickness may cause problems during further processing of the tablets, such as irregular handling by guide rails on blister packing machinery. The tablets formed by compression to 'constant force' would be expected to have similar densities, while the tablets prepared to 'constant thickness' show a considerable increase in density with increasing fill weight. The tablet density would be expected to influence the physical properties of the tablet.

#### Tensile Strength

The most important mechanical quality associated with compressed tablets is their strength. The tensile strength of tablets formed from the granulation to a constant force and constant thickness are shown in FIG 7.1e. Fell and Newton (1970) found that the tensile strength of crystalline lactose was directly proportional to the compressional force. A similar relationship was found to exist for the ibuprofen granulation. The failure of a tablet prepared from granules may be along the granule boundaries or through the granules. This depends on the relative strengths of the inter and intra granular bonds. The mechanism of consolidation of ibuprofen has been described earlier. These mechanisms will be combined with those of the other constituents in the granules. The extent of elastic and plastic deformation and

**FIG 7.1e** GRAPH OF RADIAL TENSILE STRENGTH VERSUS TABLET WEIGHT FOR AN IBUPROFEN GRANULATION COMPRESSED TO CONSTANT THICKNESS AND FORCE



brittle fracture of the granule constituents will be dependent on the compression force used to form the tablet. At lower forces the elastic and plastic deformation would be expected to be more significant while brittle fracture may occur at higher forces. The integrity of the granules during the compression process is difficult to determine. Rubinstein (1976) investigated the consolidation of granules during compaction. It was found that granules of dibasic calcium phosphate maintained their cylindrical shape even at high compression forces. Deformation occurred by changes in granule thickness and diameter. The ibuprofen granules were irregular in shape as shown in FIGS 3.2d,e and would thus be expected to behave in a different manner due to the change in distribution of the compressional forces. The tablets prepared to 'constant force' show tensile strengths proportional to the applied force. That is the strength of the tablets remained constant with increasing fill weight due to the uniformity of the applied force.

The tensile strength of tablets prepared from the ibuprofen Avicel mixture to 'constant thickness' and 'constant force' are shown in FIG 7.1f. Considering the tablets prepared to a 'constant force'. Although each tablet was prepared under similar forces the tensile strength shows considerable variability between batches. This could be due to use of a non homogeneous mixture which would be expected to produce tablets with strengths corresponding to the relative proportions of each ingredient. The mixture was prepared by tumbling the materials within a glass jar held by a cranked arm rotated using a stirrer motor. The mixture was tumbled for a further five minutes prior to the start of each days work to prevent settling and segregation of the two materials. The mixture and a resultant tablet can be seen as viewed using the electron microscope in FIGS 7.1g,h. The two materials appear well mixed although it is possible that the

**FIG 7-1f**

**GRAPH OF RADIAL TENSILE STRENGTH VERSUS TABLET WEIGHT FOR IBUPROFEN : AVICEL  
1 : 1 MIXTURE COMPRESSED TO A CONSTANT THICKNESS AND TO A CONSTANT FORCE**

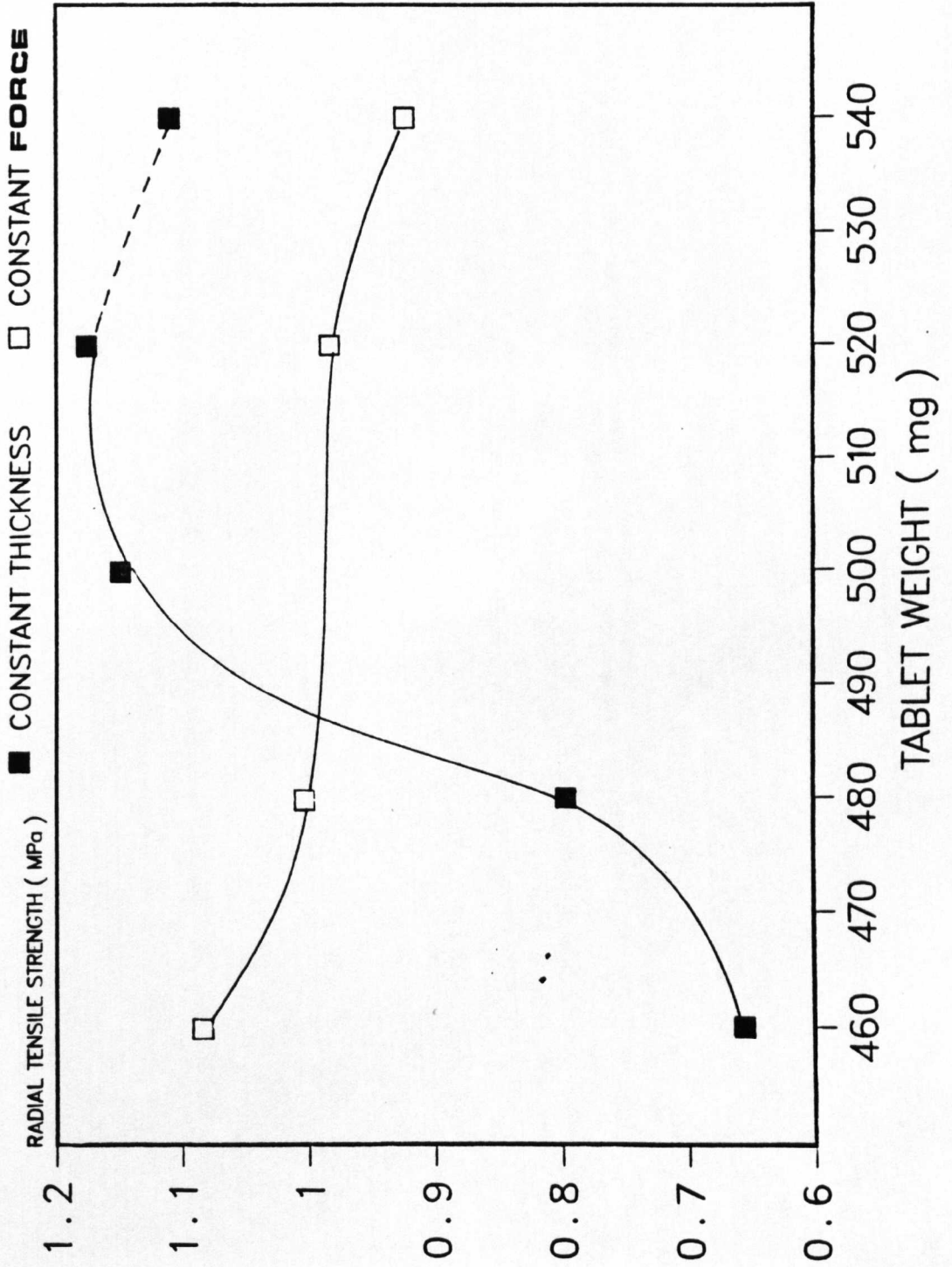




FIG 7.1g Scanning Electron Micrograph at Magnification X100  
Ibuprofen Avicel Mixture 1:1.

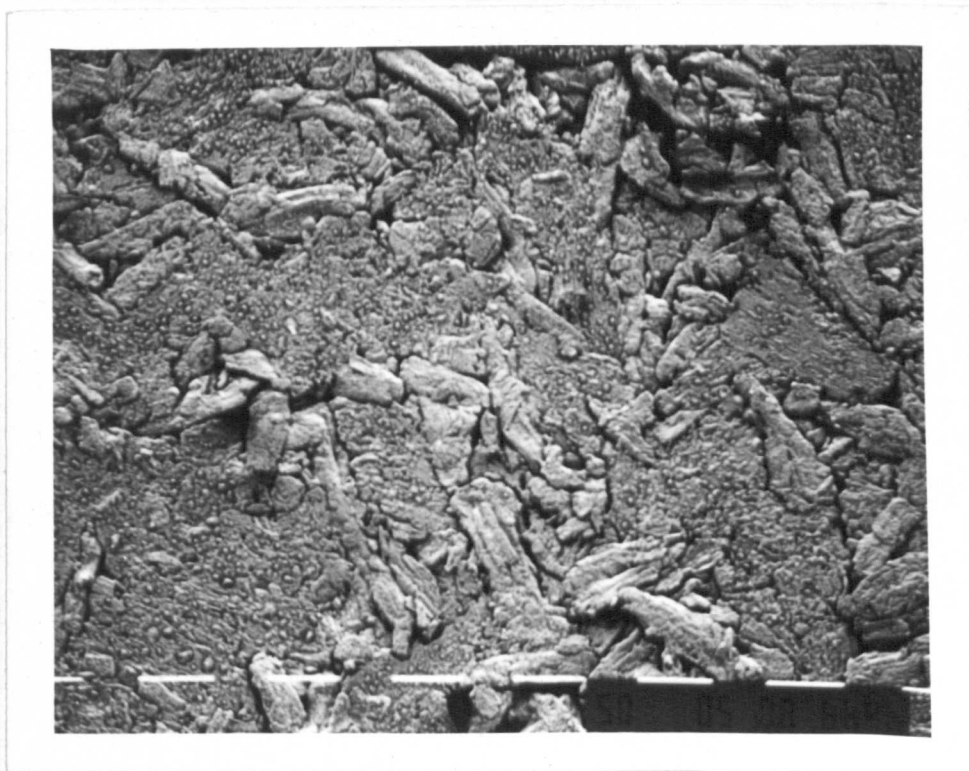


FIG 7.1h Scanning Electron Micrograph at Magnification X100  
Ibuprofen Avicel Mixture 1:1 Tablet.  
Upper Punch Contact Surface

tablets contain areas which contain higher concentrations of ibuprofen. The ibuprofen-ibuprofen bonds would be expected to be a great deal weaker than the Avicel-Avicel bonds, thus if the tablet is placed under stress these weaker ibuprofen areas would propagate the fractures. The distribution of the ibuprofen within the tablet combined with the inherent variability of the tensile strength test probably accounts for the range of tensile strengths observed. The strength of the tablets prepared at constant force from the mixture are higher than those prepared at constant force from the granulation. This may be attributed to relatively high proportion of Avicel in the mixture ie 50% compared to 35.1% of other than drug materials in the granulation. Avicel may be regarded as a special form of cellulose fibril in which the crystals are compacted close enough for hydrogen bonding, as proposed by Reier and Shangraw (1966). Mashadi and Newton (1987) proposed a mechanism for the failure of Avicel when compressed into beams. They found that it was polymeric in terms of rigidity but behaved like a ceramic material in terms of crack propagation. When compacted, Avicel contains mainly open pores which gradually reduce in size as pressure is applied, thus requiring greater energy to cause failure. As the compact becomes less porous, more resistance is offered to crack propagation.

The tensile strength of 'constant thickness' tablets increases in an irregular fashion with the applied force. Beyond 7.5kN the strength appears to reach a maximum after which capping occurred. The 7.5kN applied force which corresponds to the start of the tensile strength plateau has previously been shown to be the point at which the melting of ibuprofen becomes significant. Lamination and capping occur when the applied force exceeds 9.6kN. The mechanisms for these phenomena with respect to ibuprofen have been described previously.

It is interesting to note that the tablets prepared from the granulation under applied forces in excess of 13.4kN showed no signs of lamination. This could be due to several factors. Firstly, the origin of the ibuprofen is different and probably differs in its particle size distribution, purity and may be to some extent its crystal habit and melting point. The constituents of the granulation may to some extent mask the disruptive properties of the ibuprofen by forming stronger bonds at higher forces more able to withstand the stresses of decompression and ejection. The granulation may also permit the escape of air from the die cavity to a greater extent than the powder mixture by virtue of its particle size.

### Disintegration

It is generally accepted that for a drug to be readily available to the body, it must be in solution. For most tablets, the first important step towards solution is breaking down of the tablet into smaller particles or granules, a process called disintegration. Ibrahim (1985) found that the dissolution time was related to the disintegration time for hydrochlorothiazide and phenylbutazone formulations. The research work of others has shown that one should not automatically expect a correlation between disintegration and dissolution. However disintegration time provides a useful guide for the formulator in optimising a tablet formulation. Three of the variables in this investigation would be expected to have an effect on the disintegration time; the formulation, the maximum applied force used to form the tablet and weight of the tablet.

The mechanism of disintegration will depend on the first two variables. A number of disintegration mechanisms have been previously reported in the literature including, swelling, wicking, deformation, heat of adsorption, and particle-particle repulsive forces. Fassihi (1986) stated that the compression force dictated the disintegration

**Fig 7.1i** GRAPH OF DISINTEGRATION TIME VERSUS TABLET WEIGHT FOR IBUPROFEN : AVICEL 1 : 1 MIXTURE COMPRESSED TO A CONSTANT THICKNESS AND TO A CONSTANT FORCE

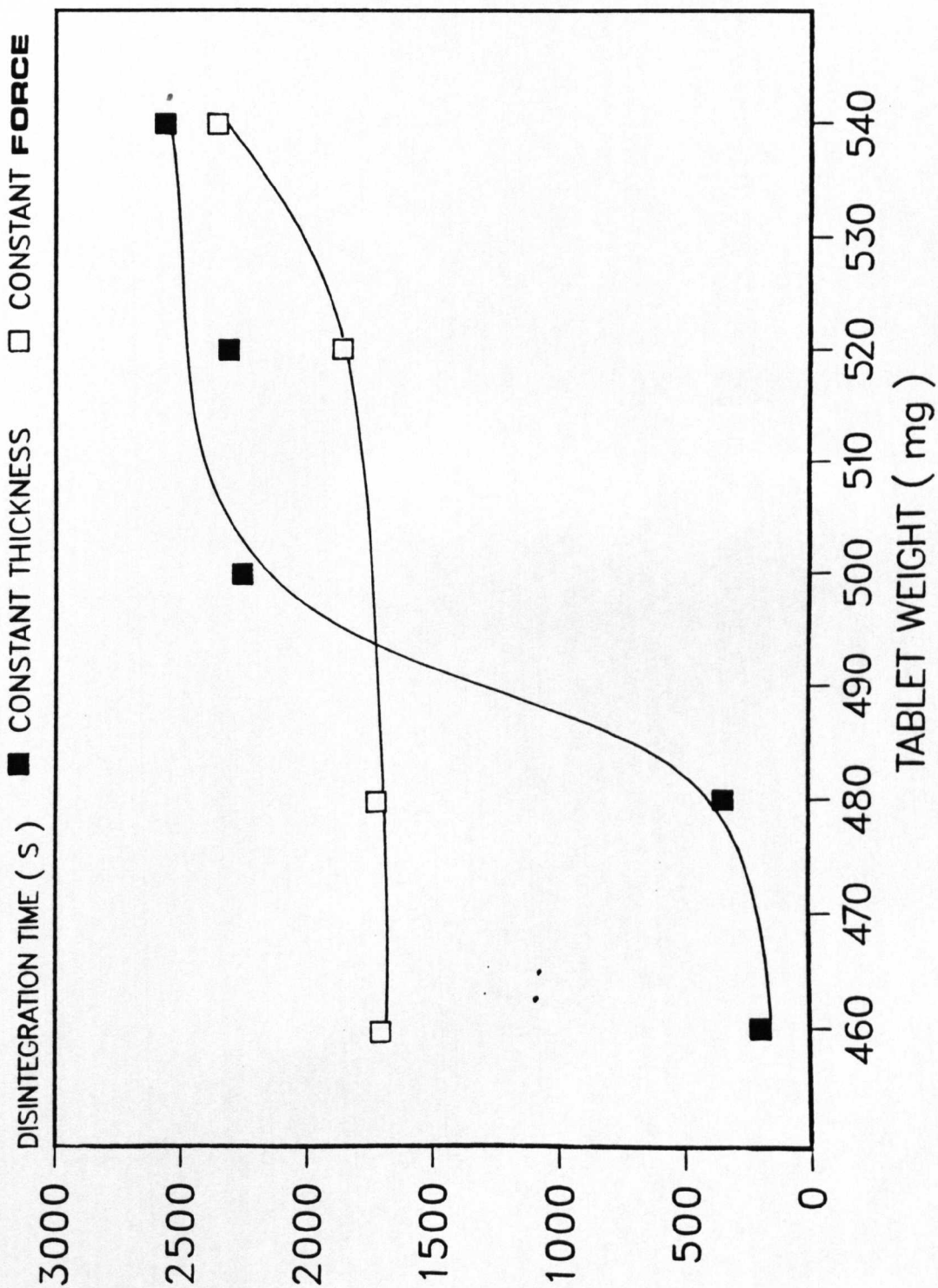
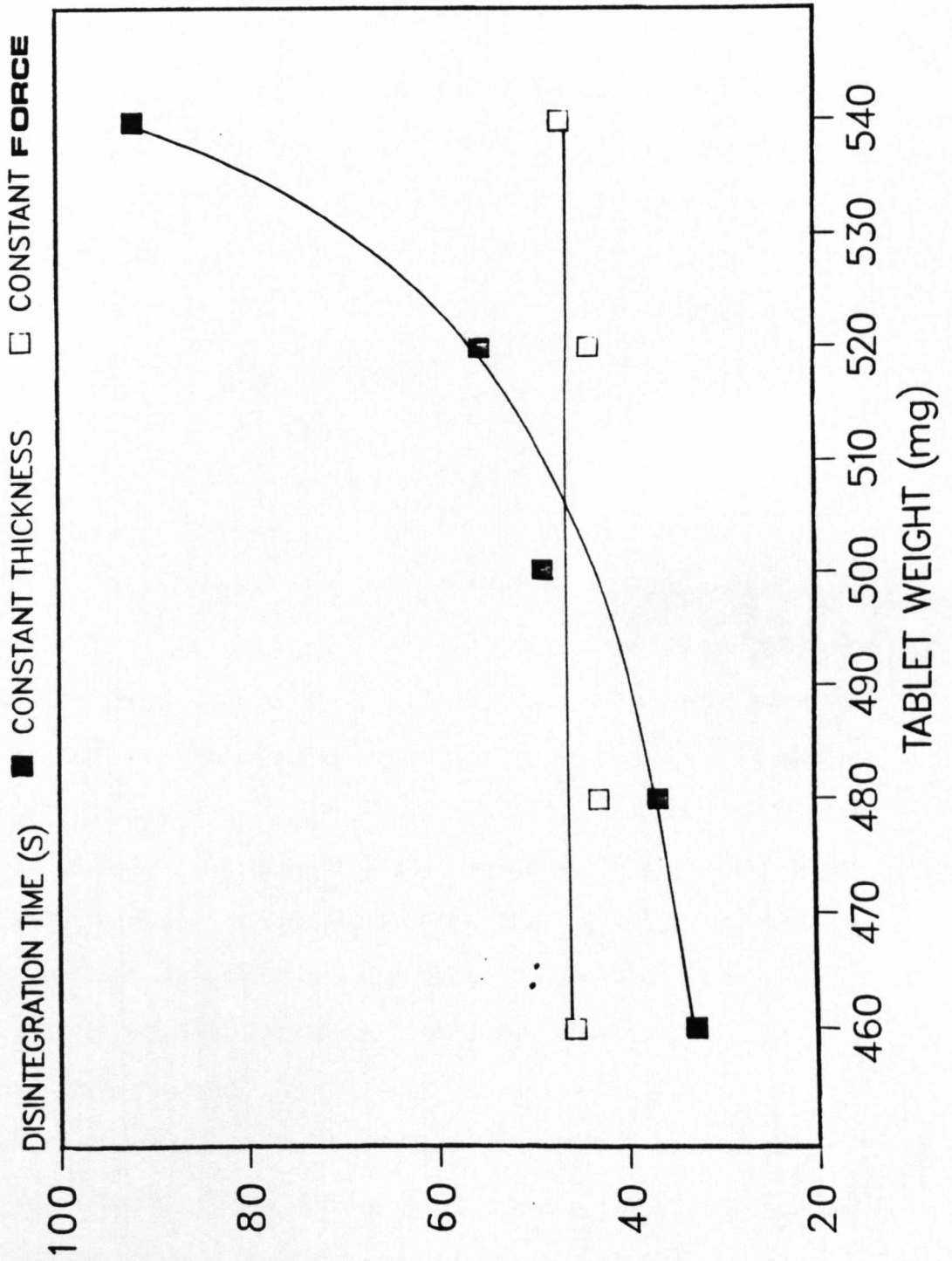


**Fig 7.1j** GRAPH OF DISINTEGRATION TIME VERSUS TABLET WEIGHT FOR AN IBUPROFEN GRANULATION COMPRESSED TO A CONSTANT THICKNESS AND TO A CONSTANT FORCE



mechanism more than the physicochemical properties of the disintegrant. This would tend to indicate that no simple theory satisfactorily explains the disintegration of a formulation. Distinct differences in the disintegration of the two formulations used in this investigation prepared under constant force and to a constant thickness can be seen in FIGS 7.1i,j.

Microcrystalline cellulose was suggested to be useful as a disintegrating agent when used in a proportion of at least 20% by Mendell (1972). The mixture used contains 50% of microcrystalline cellulose which will be responsible for the disintegration of these tablets. The disintegration times for the tablets compressed to a constant thickness increase proportionally with the applied force used to form them. The disintegration properties of microcrystalline cellulose were shown to be pressure dependent by Khan and Rhodes (1975b) and also by Lerk *et al* (1979). The latter workers found a linear relationship between time and the volumetric water up-take of microcrystalline cellulose tablets, indicating that the capillary forces driving the liquid into the tablet were opposed by a constant viscous resistance. They proposed that a constant volumetric penetration rate of fluid into the tablet was maintained by the breaking of hydrogen bonds immediately behind the penetration front which increased the pore volume. This fast aqueous penetration associated with microcrystalline cellulose was not observed with the ibuprofen microcrystalline cellulose mixture. This may be due to a combination of factors. Firstly, the high concentration of microcrystalline cellulose would have resulted in proportionally more hydrogen bonds being formed during the compression reflected by the high tensile strength. It would be expected that more time would be required by the penetrating fluid to overcome the greater number of hydrogen bonds. Secondly, and probably the more important effect is

due to the hydrophobic nature of ibuprofen. The widespread distribution of this material throughout the tablet would be expected to antagonize the capillary effects of the microcrystalline cellulose. Similar effects have been reported by Ganderton (1969) for tablets containing magnesium stearate, a hydrophobic lubricant. The increased penetration time was proportional to the magnesium stearate concentration. Thus the 50% concentration of hydrophobic ibuprofen accounts for the relatively long disintegration times observed for the mixture tablets.

The disintegration time was seen to increase dramatically once the applied force exceeded 7.5kN. This corresponds to the point at which the melting of ibuprofen becomes significant during compression. One possible mechanism for the prolonging of the disintegration times of such tablets is the presence of a hydrophobic outer skin of ibuprofen. This outer layer of ibuprofen probably forms when the melted ibuprofen is forced out of the interparticular voids within the tablet during compression. The melted ibuprofen collects at the surface restrained by the punches and die, it then solidifies during decompression. The constant density mixture tablets showed tablet size disintegration time dependence. The surface area to volume ratio decreased with increased tablet weight, consequently the disintegration time increased as the relative area available for disintegration decreased.

The tablets formed from the granulation all disintegrated rapidly indicating that the hydrophobic nature of ibuprofen, and the melting phenomena were not critical factors in this formulation. This is surprising as ibuprofen represents 64.9% of the granulation. However the ibuprofen present in the granulation differs in origin from that in the mixture and could differ in its physical properties. Alternatively the mechanism of the disintegration may account for the

rapid disintegration of the granulation. Swelling disintegrating agents such as starch may be incorporated into the granulation either mixed with the other ingredients prior to granulation or intra and inter granularly. The starch acts as a pathway for water penetration into the tablet and pushes apart granules due to the expansion of localized high concentrations of starch. The mechanism of disintegration for this granulation is probably a mixture of swelling and capillary action. The hydrophobic character of the ibuprofen may be masked by incorporation into the granules. The granules may then disintegrate relatively rapidly due to wicking and swelling.

The disintegration time was seen to increase with the maximum applied force. This was considered due to an increase in plastic deformation occurring at higher forces. This had the effect of increasing the particle-particle contact thereby increasing the number of bonds to be broken to cause disintegration. The plastic deformation would also be expected to occlude channels down which water may have passed during disintegration. Thus tablets formed under a higher maximum force with low porosity would experience a reduced ingress of water via fewer capillaries. The resultant slower expansion of the swelling agents would then have to rupture a more strongly bonded system.

The tablets prepared from the granulation under a constant force showed constant disintegration times irrespective of the tablet weight and volume.

#### Conclusions

The compression of both formulations to a constant thickness, with fill weights varied over the B.P uniformity of weight limits, produced a significant change in the maximum applied force required to form the tablets. This change in the applied force has been shown to

produce a dramatic effect on the physical properties of the resulting tablets.

The tensile strength of tablets prepared from the ibuprofen Avicel 1:1 mixture were seen to increase with the maximum applied force in an irregular manner. The mixture formed relatively strong tablets due to the high compressibility and extensive hydrogen bonding of Avicel. When the maximum applied force exceeded 7.5kN, the tablet tensile strength reached a maximum and tended to form laminated and capped tablets. This has been attributed to the melting of ibuprofen under pressure. A similar pattern was observed with the disintegration time of these tablets. Disintegration times were prolonged due to the hydrophobic nature of ibuprofen which inhibited the capillary action of Avicel. As the maximum applied force increased the disintegration time became extended. This was most noticeable at maximum applied forces above 7.5kN. This effect was again attributed to the melting of ibuprofen under pressure. At maximum applied forces in excess of 7.5kN the ibuprofen formed a hydrophobic outer layer which inhibited the ingress of water. The tablets formed under a constant force from different fill weights showed more uniform tensile strengths and disintegration times.

The tensile strength of tablets prepared from the ibuprofen granulation, was found to be proportional to the maximum applied force required to form the tablet. The disintegration time of these tablets showed a similar relationship. The increase of disintegration time with the maximum applied force was attributed to the extent of plastic deformation during compression. The tablets formed from the granulation under a constant force with increasing fill weights were found to exhibit more uniform tensile strengths and disintegration times.

These results indicate that tablets prepared under a constant maximum applied force, with fill weights varied over the B.P uniformity of weight limits, have relatively constant disintegration times and radial tensile strengths. This is an advantage over the tablets prepared to a constant thickness which showed considerable variation under the same conditions. The tablets prepared under a constant force were found to have increasing thickness with increasing fill weight. This was considered a disadvantage with regard to mechanical tablet handling and filling of containers. The tablets prepared to a constant thickness showed a similar trend. This was attributed to the distortion of the machine under load.

This investigation assumes that the Ed Courtoy machine produces tablets with the same degree of force variance as the Simulator. This may not be the case due to response time of the hydraulic systems of the two machines. In principle the compression to a constant force has been demonstrated to be superior to compression to a constant thickness. However these results are only valid for ibuprofen formulations. Other active ingredients and excipients would be expected to show different degrees of dependence on the maximum applied force. It would be expected that compression to a constant force would be more of an advantage with pressure sensitive materials such as ibuprofen.

### 8.1 Investigation of Compact Properties Prepared Using Combinations of Pre-compression and Main-compression.

#### Introduction

Precompression is the smaller preliminary compression force which may be applied immediately prior to the main-compression on some rotary tableting machines. Pre-compression is usually applied by a pair of small diameter rollers between which the upper and lower punches pass. The pre and main-compression pressure may be altered independently in order to optimise compression conditions. The magnitude of the pre-compression force is usually a fraction of the main-compression force, and may be as little as the weight of the punch alone, which is referred to as to as tamping. It has long been recognised that the use of pre-compression can reduce the incidence of capping and lamination.

Two mechanisms are thought to be responsible for this pre-compression effect. Gunsel and Kanig (1976) described the de-aeration effect. Here the tamping action of the pre-compression removed some or all of the air from the powder bed, the de-aerated compact was then subjected to the main-compression to form a robust tablet. If the air is not removed by pre-compression, then during decompression the entrapped air expands within the tablet developing internal faults resulting in lamination and capping.

An alternative explanation was proposed by Hiestand et al (1977). They explained the capping event as failure of the tablet to withstand the internal stresses of strain recovery. He proposed that pre-compression effectively extended the dwell time of the compression. As the compact was held under load for an increased period of time, the extent of stress relaxation was increased resulting in the formation of more particle-particle bonds and a stronger tablet.

Mann et al (1982) confirmed that the effects of pre-compression were in fact a combination of these two mechanisms. The extent of each depending on the powder bed porosity, the speed and the magnitude of the pre and main-compression pressures.

Armstrong et al (1982) investigated the effect of multiple compressions to the same thickness on a range of pharmaceutical materials. It was found that all materials experienced a decrease in the maximum force applied by the tablet press. This was attributed to the formation of a structure of decreasing porosity. When the time interval between the compressions was extended in stages from 1.3s up to 20min, the compacts formed offered less resistance to the punch. This was explained in terms of heat loss from the compact with time. As heat was lost from within the compact, the individual particles contracted reducing the size of the compact and increasing its porosity. These factors would be expected to weaken the compact. In the case of microcrystalline cellulose and directly compressible starch, the compact structure was strengthened as the time between compressions was increased. This was thought due to radial contraction combined with axial expansion to relieve the die wall pressure after removal of the upper punch. This was followed by the formation of interparticulate bonds which increased the resistance of the structure to further consolidation.

Vezin et al (1983) also recognised the significance of the separation of the two compression events. They stated that the separation of the pre and main-compression by relatively long times of about 0.2 seconds was a more significant factor in increasing the compact strength than the dwell or contact times. The time between the pre and main-compressions in this investigation will be maintained above 0.2 seconds.

However all of these investigations limited the pre-compression pressure to below 100MPa. The Kikusui tablet press originally developed for use with powder metals or ceramics, is capable of providing a pre and main-compression of 8 tons. A precompression of 8 tons may be considered excessive for pharmaceutical materials. Such high forces could not be used for increasing the capping pressure which is one of the main indications for pre-compression. It is claimed that two similar sized compressions such as 30kN pre followed by 40kN main-compression may produce tablets of an equivalent strength to a single compression at say 50kN. The main benefit of such a system is claimed to be a reduction in the tableting machine wear due to the lower maximum force employed.

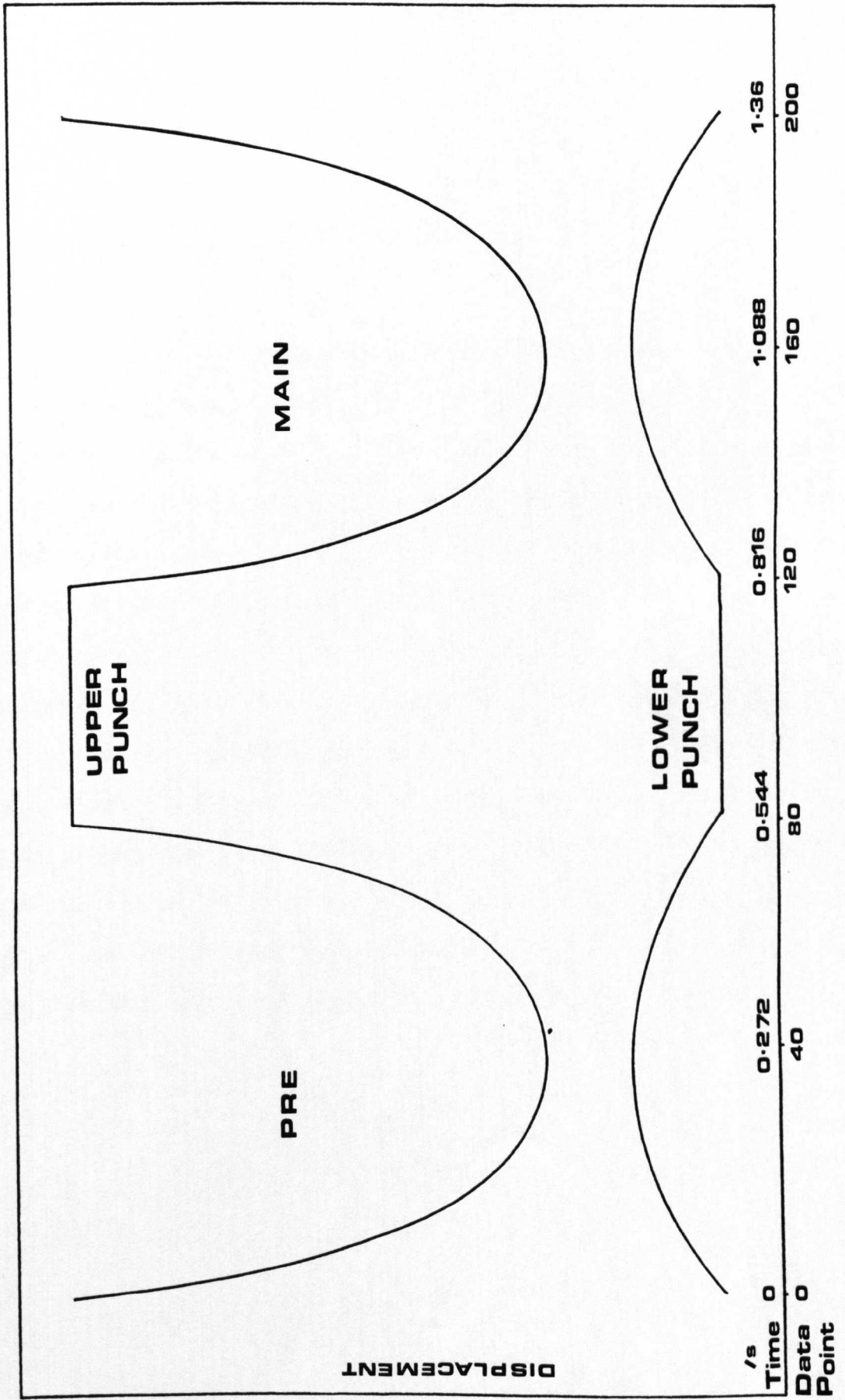
The benefits or otherwise for pharmaceutical materials of such high pre-compression pressures have yet to be established. This investigation has been designed to determine the effect of such conditions for a paracetamol formulation.

### Experimental

The methods used were as described earlier in the 'Preparation of Compacts'. Any supplementary details have been detailed below.

The Simulator was fitted with Manesty 12.5mm flat faced 'F' machine punches. Compression was achieved using double havasine control profiles applied to the upper and lower actuators as shown in FIG 8.1a. This profile would provide similar pre and main-compression forces. The maximum displacement of the pre and main-compressions were increased or decreased independently to give the required forces. Consequently a different control profile was required for each combination of pre and main-compression forces. The combinations of pre and main-compression forces used are shown below

FIG 8.1a Simulator Control Profile for Pre and Main - Compression



Pre / Main-Compression Forces

Pre-compression	Main-compression				
KN	KN				
0	10	20	30	40	50
10	10	20	30	40	50
20	10	20	30	40	50
30	10	20	30	40	50
40	10	20	30	40	50
50	10	20	30	40	50

A compression cycle time of 1.365 seconds was maintained for all samples. A displacement / time and force / time plot was produced for each tablet. The die was cleaned with acetone after each compression and lubricated with a suspension of 4% magnesium stearate in carbon tetrachloride. 500mg of a commercially available paracetamol granulation was accurately weighed out and poured into the die cavity using a powder boat (weighing accuracy  $\pm 1\text{mg}$ ). Four tablets were produced at each setting of pre and main-compression

Each of the tablets were measured across their diameter and thickness using a digital micrometer ( $\pm 1\mu\text{m}$ ) two minutes after ejection and then again two hours after ejection. After the later measurement the tablet was subjected to a crushing test using the Instron Testing Machine. The radial tensile strength was then calculated to enable comparison between tablets of different thickness.

Table 8.1a Pre and Main-compression Pressures and Contact Times for a Paracetamol Formulation

Codes: P = Precompression Force/kN M = Main Compression Force/kN

TABLET CODE	PRE-COMPRESSION		MAIN-COMPRESSION		TOTAL	RADIAL TENSILE
	PRESSURE	CONTACT	PRESSURE	CONTACT	CONTACT	STRENGTH
	MPa	TIME ms	MPa	TIME ms	TIME ms	MPa
P00M10T1	-	-	83.81	177.6	177.6	0.5809
P00M10T2	-	-	85.39	178.6	178.6	0.6452
P00M10T3	-	-	83.81	178.6	178.6	0.5984
P00M10T4	-	-	82.23	177.6	177.6	0.5986
x	-	-	83.81		178.10	0.6058
$\sigma_{n-1}$	-	-	1.290		0.58	0.0276
P00M20T1	-	-	167.64	215.5	215.5	1.1741
P00M20T2	-	-	167.64	217.4	217.4	1.2173
P00M20T3	-	-	162.89	215.5	215.5	1.0972
P00M20T4	-	-	167.64	217.4	217.4	1.1604
x	-	-	166.45		216.45	1.1623
$\sigma_{n-1}$	-	-	2.375		1.09	0.0497
P00M30T1	-	-	240.38	236.8	236.8	1.8732
P00M30T2	-	-	243.54	240.7	240.7	1.8229
P00M30T3	-	-	243.54	239.7	239.7	1.7680
P00M30T4	-	-	241.96	237.8	237.8	1.7052
x	-	-	242.35		238.76	1.7923
$\sigma_{n-1}$	-	-	1.515		1.76	0.0722
P00M40T1	-	-	321.03	271.8	271.8	2.1400
P00M40T2	-	-	319.45	269.8	269.8	2.0289
P00M40T3	-	-	317.87	265.9	265.9	2.0955
P00M40T4	-	-	319.45	262.1	262.1	2.0319
x	-	-	319.45		267.19	2.0741
$\sigma_{n-1}$	-	-	1.291		3.00	0.0536
P00M50T1	-	-	389.02	291.2	291.2	2.2727
P00M50T2	-	-	390.61	291.2	291.2	2.3989
P00M50T3	-	-	393.81	291.2	291.2	2.5011
P00M50T4	-	-	392.21	289.2	289.2	2.2558
x	-	-	391.41		290.70	2.3571
$\sigma_{n-1}$	-	-	2.061		1.00	0.1153

Table 8.1b Pre and Main-compression Pressures and Contact Times for a Paracetamol Formulation

Codes: P = Precompression Force/kN M = Main Compression Force/kN

TABLET CODE	PRE-COMPRESSION		MAIN-COMPRESSION		TOTAL	RADIAL TENSILE STRENGTH
	MPa	TIME ms	MPa	TIME ms	CONTACT TIME ms	
P10M10T1	79.83	184.4	85.39	145.6	330.0	0.5690
P10M10T2	79.83	189.3	86.97	140.7	330.0	0.5710
P10M10T3	79.83	184.4	90.13	140.7	325.2	0.6380
P10M10T4	79.83	184.4	82.23	145.6	330.0	0.6290
x	79.83	185.62	86.18	143.15	328.80	0.6017
$\sigma_{n-1}$	0.00	2.45	3.289	2.83	2.40	0.0368
P10M20T1	79.83	184.4	162.86	174.7	359.1	1.2951
P10M20T2	79.83	189.3	170.84	169.8	359.1	1.1639
P10M20T3	79.83	184.4	156.55	174.7	359.1	1.0849
P10M20T4	79.83	184.4	160.46	174.7	359.1	1.1100
x	79.83	185.62	162.67	173.47	359.10	1.1635
$\sigma_{n-1}$	0.00	2.45	6.030	2.45	0.00	0.0937
P10M30T1	79.83	184.4	226.16	194.1	378.5	1.5212
P10M30T2	79.83	184.4	219.85	194.1	378.5	1.5609
P10M30T3	79.83	184.4	216.66	194.1	378.5	1.4930
P10M30T4	79.83	184.4	216.66	194.1	378.5	1.5574
x	79.83	184.40	219.83	194.10	378.50	1.5331
$\sigma_{n-1}$	0.00	0.00	4.478	0.00	0.00	0.0322
P10M40T1	79.83	179.6	327.31	223.2	402.8	2.1820
P10M40T2	79.83	174.7	327.31	223.2	397.9	2.2850
P10M40T3	79.83	174.7	328.90	223.2	397.9	2.3010
P10M40T4	79.83	174.7	332.10	223.2	397.9	2.2640
x	79.83	175.92	328.90	223.20	399.12	2.2580
$\sigma_{n-1}$	0.00	2.45	2.259	0.00	2.45	0.0529
P10M50T1	79.83	184.4	376.40	242.6	427.1	2.4620
P10M50T2	79.83	184.4	403.07	247.5	431.9	2.4160
P10M50T3	79.83	184.4	399.95	247.5	431.9	2.6550
P10M50T4	79.83	179.6	404.26	247.5	427.1	2.5460
x	79.83	183.2	395.92	246.27	429.50	2.5198
$\sigma_{n-1}$	0.00	2.4	13.139	2.45	2.77	0.1050

Table 8.1c Pre and Main-compression Pressures and Contact Times for a Paracetamol Formulation

Codes: P = Precompression Force/kN M = Main Compression Force/kN

TABLET CODE	PRE-COMPRESSION		MAIN-COMPRESSION		TOTAL	RADIAL TENSILE STRENGTH
	PRESSURE MPa	CONTACT TIME ms	PRESSURE MPa	CONTACT TIME ms	CONTACT TIME ms	
P20M10T1	158.14	223.2	93.08	145.6	368.8	1.0888
P20M10T2	159.74	218.4	100.43	150.4	368.8	1.1564
P20M10T3	154.95	218.4	89.89	145.6	364.0	1.2761
P20M10T4	164.45	218.4	97.15	150.4	368.8	1.4004
x	159.32	219.60	95.14	148.00	367.60	1.2304
$\sigma_{n-1}$	3.957	2.40	4.612	2.77	2.40	0.1373
P20M20T1	159.66	223.2	175.54	179.6	402.8	1.4162
P20M20T2	159.66	223.2	175.54	174.7	397.9	1.3037
P20M20T3	159.66	218.4	173.95	174.7	393.1	1.3013
P20M20T4	159.66	218.4	175.54	179.6	398.0	1.1060
x	159.66	220.80	175.14	177.15	397.95	1.2818
$\sigma_{n-1}$	0.00	2.77	0.794	2.83	3.96	0.1289
P20M30T1	159.66	223.2	245.08	199.0	422.2	1.7378
P20M30T2	159.66	223.2	246.68	199.0	422.2	1.7325
P20M30T3	159.66	223.2	246.68	199.0	422.2	1.5998
P20M30T4	159.66	223.2	248.27	199.0	422.2	1.6284
x	159.66	223.2	246.68	199.0	422.2	1.6746
$\sigma_{n-1}$	0.00	0.00	1.304	0.00	0.00	0.0709
P20M40T1	159.66	223.2	316.29	218.4	441.6	2.1409
P20M40T2	159.66	218.4	311.50	218.4	436.8	1.9014
P20M40T3	159.66	223.2	311.50	223.2	446.4	1.9674
P20M40T4	159.66	218.4	313.10	218.4	436.8	1.9358
x	159.66	220.80	313.09	219.60	440.40	1.9864
$\sigma_{n-1}$	0.00	2.77	2.258	2.40	4.59	0.1065
P20M50T1	159.66	223.2	397.72	252.4	475.6	2.5388
P20M50T2	159.66	223.2	399.23	247.5	470.7	2.3258
P20M50T3	159.66	223.2	393.33	252.4	475.6	2.3895
P20M50T4	159.66	218.4	393.97	252.4	470.7	2.1157
x	159.66	222.00	396.04	251.17	473.15	2.3425
$\sigma_{n-1}$	0.00	2.40	2.868	2.45	2.83	0.1756

Table 8.1d Pre and Main-compression Pressures and Contact Times for a Paracetamol Formulation

Codes: P = Precompression Force/kN M = Main Compression Force/kN

TABLET CODE	PRE-COMPRESSION		MAIN-COMPRESSION		TOTAL	RADIAL TENSILE
	PRESSURE	CONTACT	PRESSURE	CONTACT	CONTACT	STRENGTH
	MPa	TIME ms	MPa	TIME ms	TIME ms	MPa
P30M10T1	249.79	242.7	84.22	135.9	378.5	1.9489
P30M10T2	246.68	247.5	70.41	140.7	388.2	1.8708
P30M10T3	251.39	247.5	84.22	135.9	383.4	1.9458
P30M10T4	241.97	247.5	71.21	140.7	388.2	1.9725
x	247.40	246.30	77.52	138.30	385.77	1.9345
$\sigma_{n-1}$	4.149	2.40	7.750	2.77	4.85	0.0441
P30M20T1	237.25	242.6	150.56	174.7	417.4	1.7644
P30M20T2	248.27	242.6	152.16	174.7	417.4	1.9234
P30M20T3	246.68	247.5	160.30	169.9	417.4	1.9087
P30M20T4	245.08	247.5	156.23	174.7	422.2	2.0062
x	244.32	245.05	154.81	173.50	418.60	1.9007
$\sigma_{n-1}$	4.886	2.83	4.368	2.40	2.40	0.1005
P30M30T1	239.49	242.7	245.08	199.0	441.6	1.952
P30M30T2	239.49	242.7	248.27	199.0	441.6	1.9797
P30M30T3	239.49	242.7	248.27	199.0	441.6	1.9452
P30M30T4	239.49	247.5	249.87	199.0	446.5	1.9398
x	239.49	243.90	247.88	199.00	442.82	1.9542
$\sigma_{n-1}$	0.00	2.40	2.009	0.00	2.45	0.0177
P30M40T1	239.49	242.7	324.19	223.2	465.9	2.1744
P30M40T2	239.49	242.7	314.69	218.4	461.0	2.1104
P30M40T3	239.49	242.7	313.10	223.2	465.9	2.1986
P30M40T4	239.49	242.7	321.00	223.2	465.9	2.2596
x	239.49	242.70	318.25	222.00	464.67	2.1858
$\sigma_{n-1}$	0.00	0.00	5.231	2.40	2.45	0.0617
P30M50T1	239.49	242.7	398.04	247.5	490.2	2.3213
P30M50T2	239.49	247.5	400.11	247.5	495.0	2.5364
P30M50T3	239.49	247.5	390.53	247.5	495.0	2.6945
P30M50T4	239.49	247.5	391.41	247.5	495.0	2.4061
x	239.49	246.30	395.02	247.50	493.80	2.4895
$\sigma_{n-1}$	0.00	2.40	4.767	0.00	2.40	0.1628

Table 8.1e Pre and Main-compression Pressures and Contact Times for a Paracetamol Formulation

Codes: P = Precompression Force/kN M = Main Compression Force/kN

TABLET CODE	PRE-COMPRESSSION		MAIN-COMPRESSSION		TOTAL	RADIAL TENSILE
	PRESSURE	CONTACT	PRESSURE	CONTACT	CONTACT	STRENGTH
	MPa	TIME ms	MPa	TIME ms	TIME ms	MPa
P40M10T1	317.88	262.1	79.33	140.7	402.8	2.3140
P40M10T2	319.40	266.9	89.01	145.6	412.5	2.3181
P40M10T3	327.30	262.1	93.88	145.6	407.7	2.4494
P40M10T4	322.59	266.9	87.42	140.7	407.7	2.2113
x	321.80	264.50	87.41	143.15	407.67	2.3232
$\sigma_{n-1}$	4.167	2.77	6.049	2.83	3.96	0.0976
P40M20T1	325.79	262.1	163.49	174.7	436.8	2.4910
P40M20T2	333.53	266.9	162.69	179.6	446.5	2.4475
P40M20T3	325.79	262.1	153.83	174.7	436.8	2.2545
P40M20T4	330.50	266.9	150.56	174.7	441.6	2.2874
x	328.90	264.50	157.65	175.92	440.42	2.3701
$\sigma_{n-1}$	3.800	2.77	6.440	2.45	4.64	0.1166
P40M30T1	330.50	262.1	257.38	203.8	465.9	2.4339
P40M30T2	317.88	266.9	250.91	203.8	470.8	2.3932
P40M30T3	322.59	266.9	257.46	208.7	475.6	2.2212
P40M30T4	314.69	266.9	257.46	203.8	470.8	2.3496
x	323.41	265.70	255.80	205.02	470.77	2.3495
$\sigma_{n-1}$	8.286	2.40	3.260	2.45	3.96	0.0922
P40M40T1	319.32	266.9	328.98	223.2	490.2	2.5396
P40M40T2	319.32	266.9	328.98	223.2	490.2	2.3740
P40M40T3	319.32	266.1	325.79	223.2	485.3	2.4256
P40M40T4	319.32	266.1	322.60	223.2	485.3	2.4961
x	319.32	266.50	326.59	223.20	487.75	2.4588
$\sigma_{n-1}$	0.00	0.46	3.058	0.00	2.83	0.0735
P40M50T1	319.32	262.1	398.52	257.2	519.3	2.5406
P40M50T2	319.32	266.9	397.48	252.4	519.3	2.4748
P40M50T3	319.32	266.9	397.07	252.4	519.3	2.5199
P40M50T4	319.32	262.1	394.84	252.4	514.4	2.5440
x	319.32	264.50	397.08	253.60	518.07	2.5198
$\sigma_{n-1}$	0.00	2.77	1.569	2.40	2.45	0.0390

Table 8.1f Pre and Main-compression Pressures and Contact Times for a Paracetamol Formulation

Codes: P = Precompression Force/kN M = Main Compression Force/kN

TABLET CODE	PRE-COMPRESSION		MAIN-COMPRESSION		TOTAL	RADIAL TENSILE STRENGTH
	PRESSURE MPa	CONTACT TIME ms	PRESSURE MPa	CONTACT TIME ms	CONTACT TIME ms	
P50M10T1	391.57	296.0	80.95	140.7	436.8	2.4521
P50M10T2	396.92	296.0	82.55	140.7	436.8	2.4337
P50M10T3	397.96	296.0	79.33	140.7	436.8	2.4666
P50M10T4	391.57	296.0	79.35	140.7	436.8	2.4867
x	394.51	296.00	80.55	140.70	436.80	2.4598
$\sigma_{n-1}$	3.414	0.00	1.537	0.00	0.00	0.0224
P50M20T1	401.71	296.0	166.69	174.7	470.8	2.5356
P50M20T2	396.92	296.0	157.03	174.7	470.8	2.5820
P50M20T3	396.92	291.2	156.23	174.7	465.9	2.6212
P50M20T4	396.92	296.0	161.89	174.7	470.8	2.6513
x	398.52	294.80	160.46	174.70	469.57	2.5975
$\sigma_{n-1}$	2.259	2.40	4.848	0.00	2.45	0.0501
P50M30T1	403.22	296.0	245.24	203.8	499.9	2.4874
P50M30T2	398.51	296.0	243.64	203.8	499.9	2.5549
P50M30T3	398.51	296.0	240.45	203.8	499.9	2.6214
P50M30T4	395.40	296.0	241.25	199.0	495.0	2.6857
x	398.92	296.00	242.65	202.60	498.67	2.5874
$\sigma_{n-1}$	3.225	0.00	2.199	2.40	2.45	0.0854
P50M40T1	396.92	296.0	313.26	223.2	519.3	2.6056
P50M40T2	393.80	296.0	315.65	228.1	524.1	2.6087
P50M40T3	396.92	296.0	322.20	223.2	519.3	2.6092
P50M40T4	398.51	300.9	323.80	223.2	524.1	2.6387
x	396.54	297.22	318.73	224.42	521.70	2.6155
$\sigma_{n-1}$	1.972	2.45	5.070	2.45	2.77	0.0155
P50M50T1	399.16	296.0	407.69	247.5	543.5	2.8811
P50M50T2	399.16	296.0	401.71	252.4	548.4	2.5445
P50M50T3	399.16	296.0	392.21	247.5	543.5	2.6770
P50M50T4	399.16	296.0	392.21	252.4	548.4	2.5581
x	399.16	296.00	398.46	249.95	545.95	2.6651
$\sigma_{n-1}$	0.00	0.00	7.616	2.83	2.83	0.1557

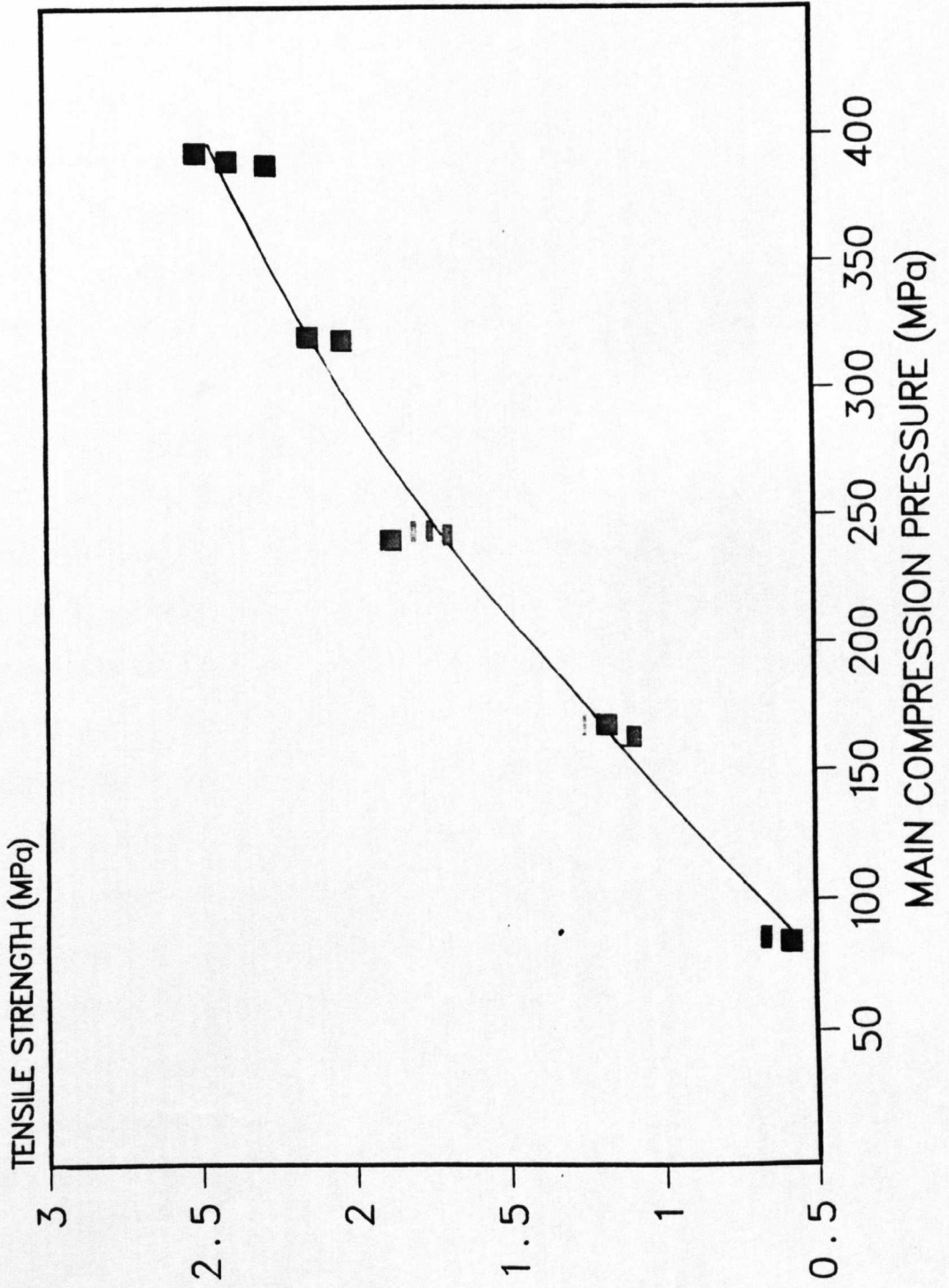
## Discussion

Granules should possess sufficient strength to withstand normal handling without breaking down and producing large amounts of fine powder. These granules did not break down during the mixing and handling operations employed during this investigation. Some size reduction of the granules during compression into tablets is desirable, to expose the areas of fresh clean surface necessary for optimum bonding to take place. The failure of the tablet may be propagated through the tablet along individual granule boundaries or through the granules themselves, depending on whether the granular bonding is weaker or stronger than that between the composite particles. Thus at low compression pressures the failure may occur along the granule boundaries, while at higher pressures the failure may propagate through the granules.

Since tablets are anisotropic and the conditions of crushing tests rarely provide well defined uniform stresses, exact interpretation of the results are often difficult. Only compacts which failed in tension, shown by the splitting of the tablet into two equal halves along a linear fracture were accepted for this investigation. Consequently the reproducibility within each batch was relatively good, the sample standard deviation for all batches remained below 0.17. This enforced confidence in the significance of these results.

The tensile strengths of tablets prepared under increasing compression pressures are shown in FIG 8.1b. The tablet tensile strength is directly proportional to the increasing compression pressure below 240MPa. Newton *et al* (1971) found a similar relationship for lactose monohydrate tablets up to 300MPa compression pressure. At compression pressures above 240MPa the tablet strength is less than expected. This is probably due to the compact approaching its minimum porosity between 240MPa and 320MPa. Thus beyond this

**FIG 8.1b** TENSILE STRENGTH VERSUS MAIN COMPRESSION PRESSURE FOR A PARACETAMOL FORMULATION.

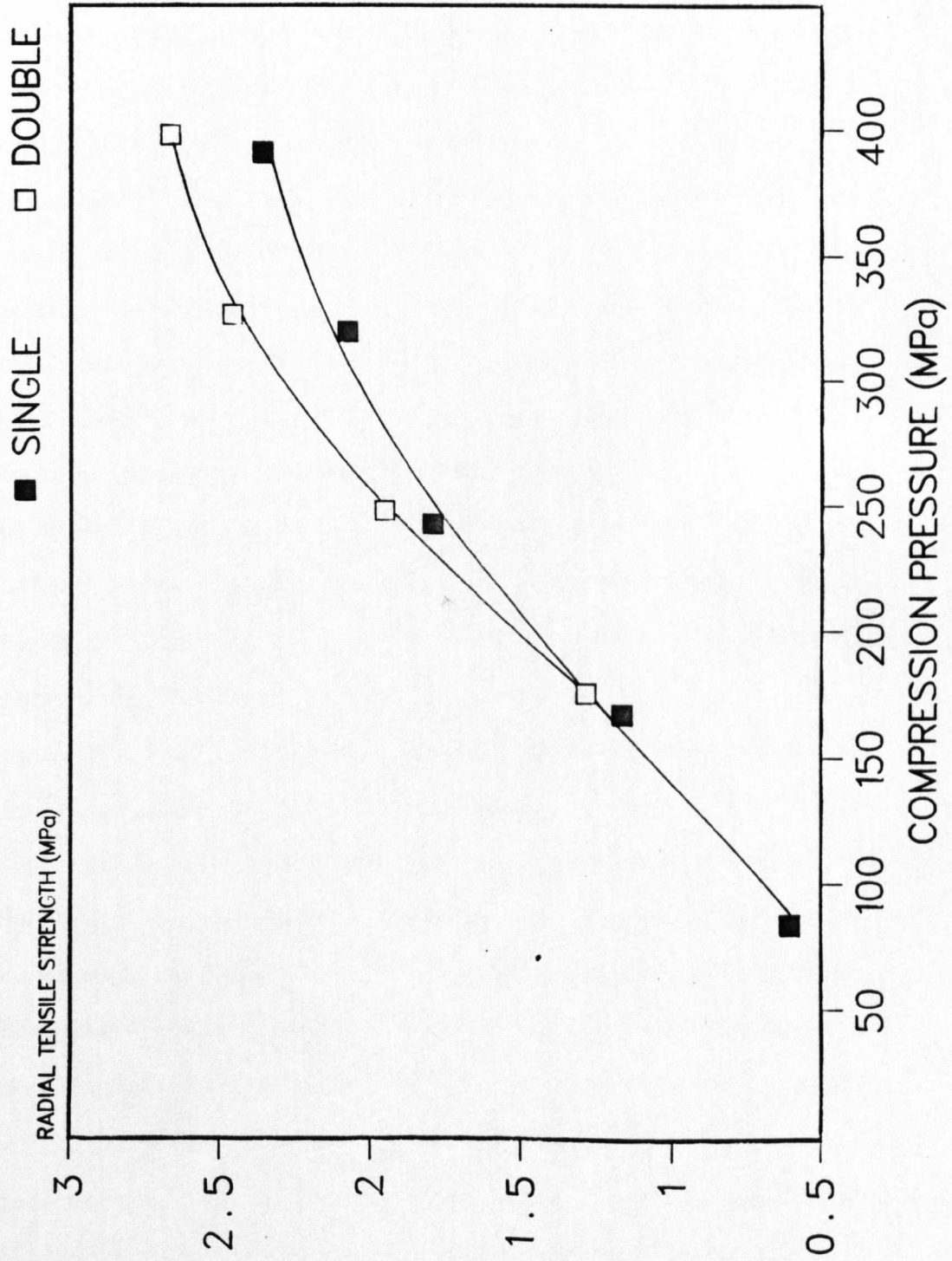


region, the true particle contact cannot be increased to the same extent and the tablet strength approaches a maximum.

The formulation contains 83.3% paracetamol. The consolidation mechanism of this material has been described in conflicting reports. Doelker and Shotten (1977) reported that plastic flow occurred during the compression of paracetamol as indicated by compression cycle plots. Humbert-Droz (1983) reported brittle behaviour, while Roberts and Rowe (1985) proposed a mixture of plastic flow and brittle fracture was the most probable method of consolidation. The later was supported by a mean yield pressure of approximately 110MPa which changed little with increasing compression speed, indicating that fragmentation was the main mechanism. Starch is also present and its mechanism of consolidation was also described by Roberts and Rowe (1985). Starch shows initial reluctance to deformation at low pressures. As the elastic deformation is overcome, as pressure increases, the material yields. It is probable then, that during compression of this formulation that consolidation occurs by a mixture of brittle fracture, plastic and elastic deformation. At low pressures the elastic and plastic deformation will be the main mechanism of consolidation while at higher pressures fragmentation will dominate.

FIG 8.1c shows the effect of single and double compressions at the same pressure. There is little difference in tablet strength between single and double compressions below pressures of 240MPa. Above this pressure tablet strength increased from single to double compressions. An increase in tablet strength of 18.51% occurs between a single compression to 320MPa and a double compression to the same pressure. Even considering the inherent variability of tensile strength measurements this represents a significant increase in tablet strength. From the graph it can be seen that a compact prepared by a single compression of 391MPa would be expected to have a similar

**FIG 8-1c** RADIAL TENSILE STRENGTH VERSUS COMPRESSION PRESSURE FOR A PARACETAMOL FORMULATION WITH A SINGLE AND DOUBLE COMPRESSION.



tensile strength to a tablet prepared by double compression to 312MPa. This would tend to confirm the claims of the Kikusui tablet press manufacturers in that a lower maximum compression pressure may be used if double compression is employed. This would effectively reduce tablet machine wear and contribute to the longevity of the machine. The mechanism responsible for the increase in tablet tensile strength is probably related to the extended dwell time generated by the second compression. When using double compression, the tablet will effectively remain under load for an extended period equal to the contact times shown in the tables 8.1a-f. This will enable further stress relaxation to take place by virtue of plastic deformation, which will increase the true area of contact between particles. Consequently bonding within the tablet increases providing a tablet of higher tensile strength. For this reason the significance of the effects of double compression would be expected to be dependent on the plastic nature of the formulation. The starch and to a lesser extent the paracetamol would be expected to contribute to the increase in tablet strength in this formulation.

It is interesting to note that during the second compression the tablet was compressed to the same thickness as during the first compression within the resolution of the displacement measuring system. According to the work of de Blaey and Polderman (1970) the second compression represents only the work stored in the tablet as elastic deformation. The increase in tensile strength observed after a second compression during this investigation would tend to indicate otherwise. It is probable that some of the work done by the second compression is used for permanent deformation bond formation and raising the temperature of the compact. The validity of using a second compression and to a greater extent using multiple compressions to estimate the elastic deformation of a material is thus questionable.

If the maximum compression pressure, whether it be the pre or main compression is plotted against the tensile strength of the resultant tablet then a clear relationship may be seen as shown in FIG 8.1d. This indicates that it is the maximum compression pressure which is the most important factor in determining the tensile strength of the tablet. However as we have already seen this is an over simplification of the situation. The effect of varying the pre and main-compression pressure can be seen in FIG 8.1e. This graph consists of a number of different series with a common magnitude of pre-compression plotted against the tensile strength. If we consider the open squares which represent a pre-compression force of 160MPa, the tensile strength increases slightly initially as the smaller main-compression pressure increases. When the main-compression pressure increases to 240MPa which exceeds the pre-compression pressure, the tablet strength increases along the 'main stream' which corresponds to the maximum compression pressure curve. A similar trend is observed for all pre-compression series. The initial slight increase in tensile strength indicates that the second smaller compression does contribute to bonding processes within the already formed tablet. The mechanism involved will be similar to that already described, the second compression effectively extends the dwell time during which further bonding takes place.

It may also be argued that a certain amount of bond rupture will occur during a second compression which should weaken the compact. However as the strength actually increases it is clear that the proportion of bonds formed exceeds the number of bonds ruptured. It should be remembered that the formation and breaking of bonds during both compressions will be dynamic processes. Any factor which favours either process will have an effect on the strength of the tablet. The temperature within the compact will increase during compression and

**FIG 8-1d** RADIAL TENSILE STRENGTH VERSUS MAXIMUM COMPRESSION PRESSURE FOR A PARACETAMOL FORMULATION.

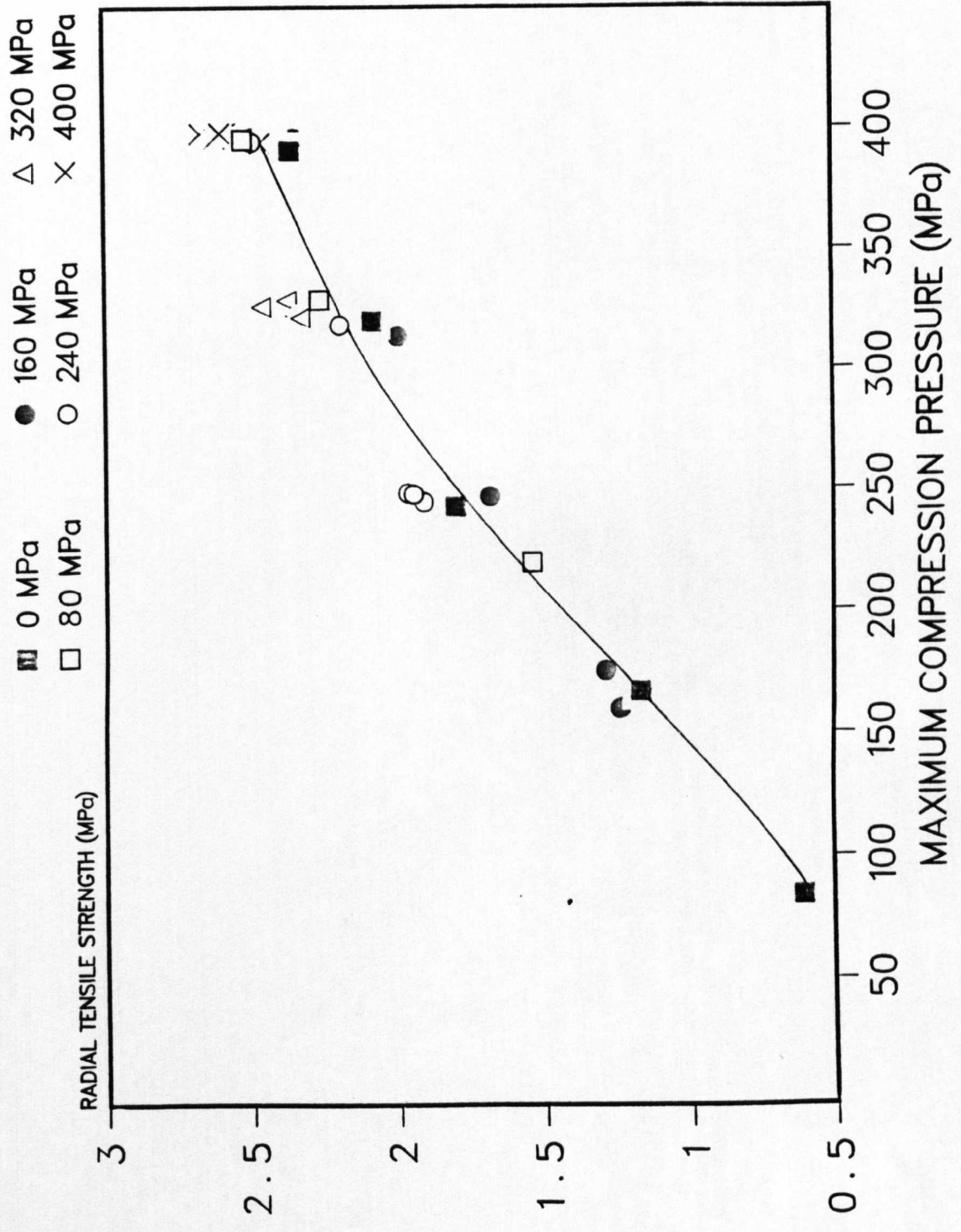
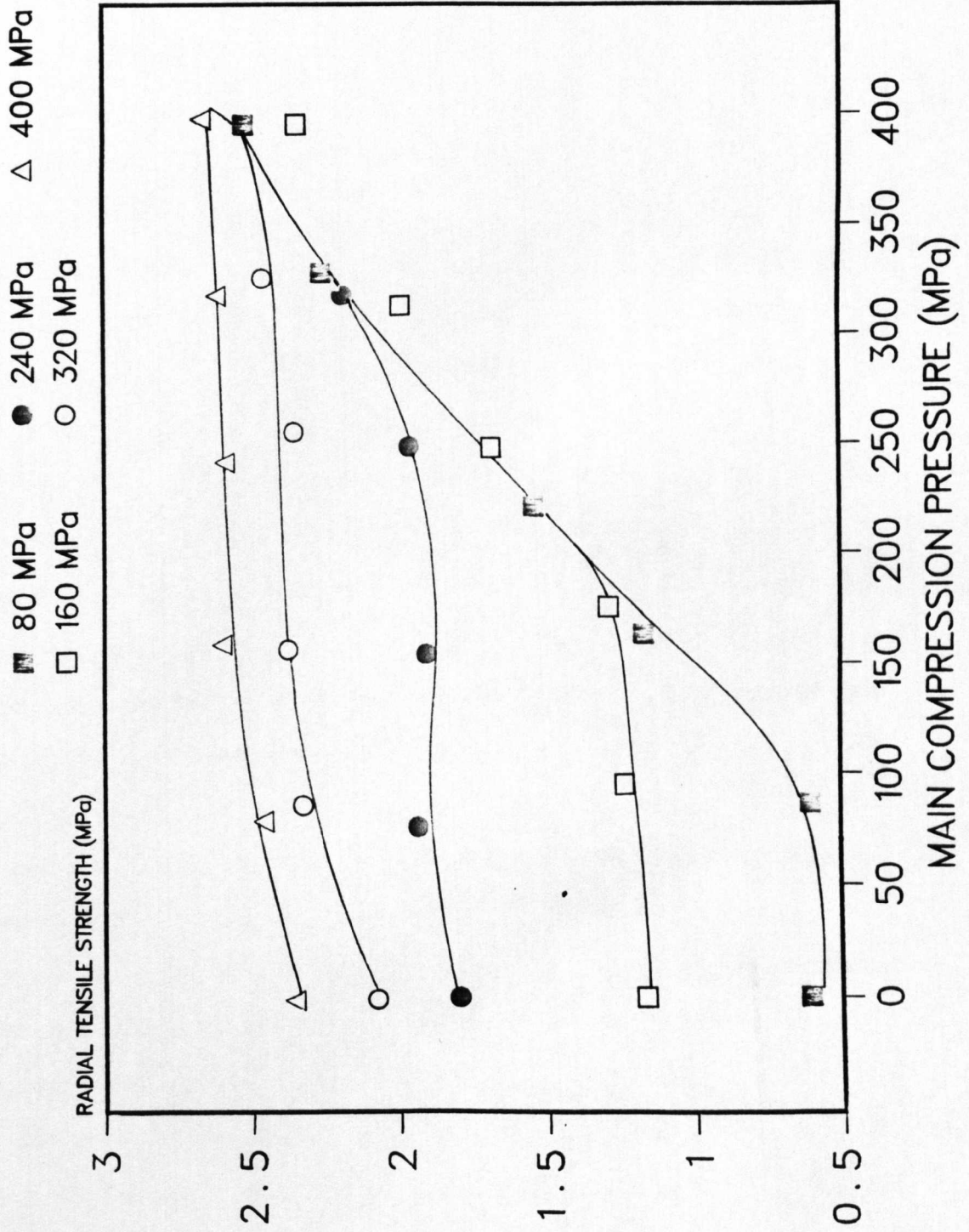


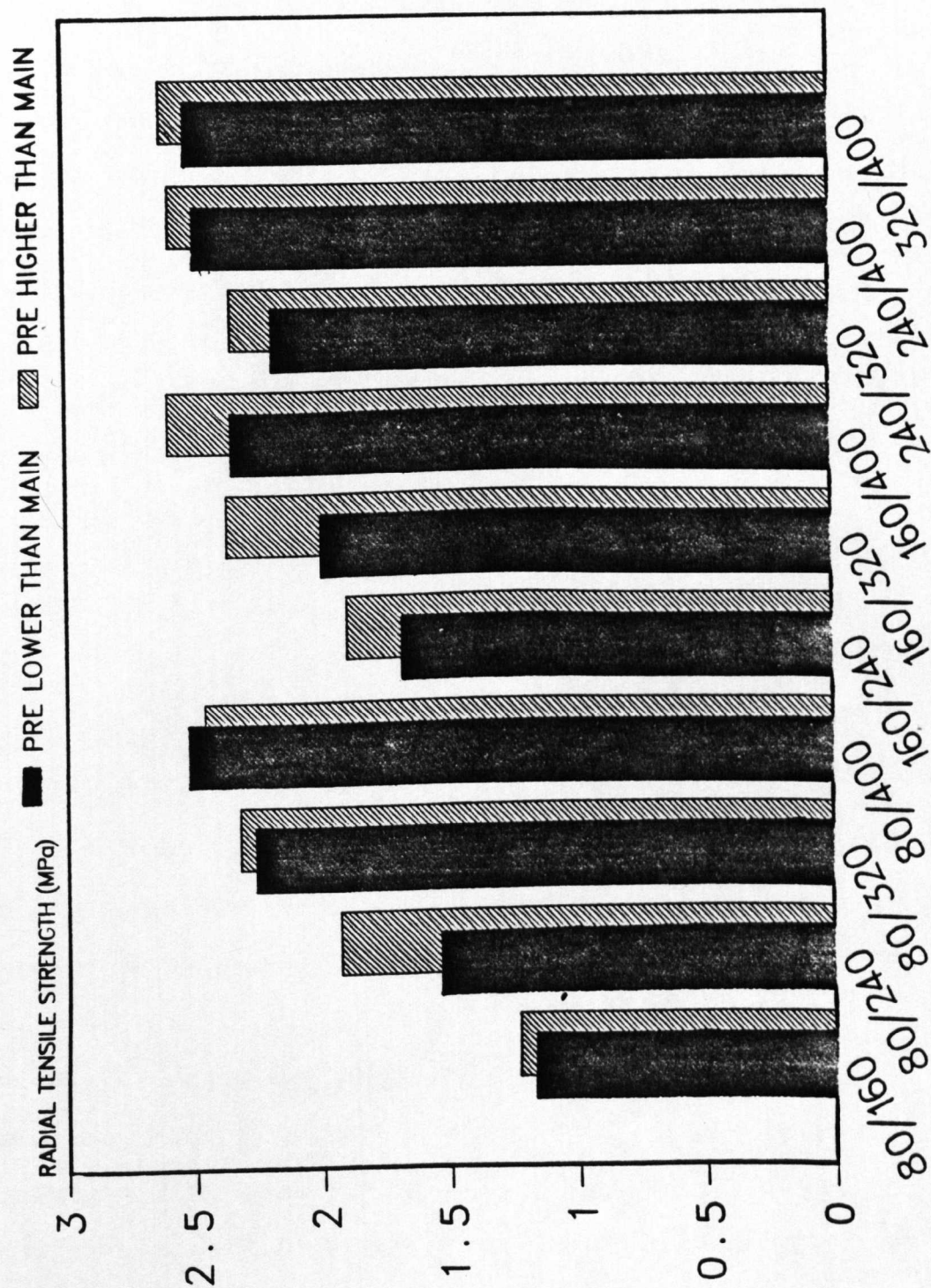
**FIG 8-1e** RADIAL TENSILE STRENGTH VERSUS MAIN COMPRESSION PRESSURE FOR A PARACETAMOL FORMULATION WITH VARYING PRECOMPRESSION PRESSURE.



again during recompression according to the findings of Hanus and King (1968). These temperature changes would be expected to influence the cohesion, deformation and flowability of the formulation. Esezobo and Pilpel (1986) found that as temperature within the tablet was increased, the extent of plasticity and stress relaxation increased while the elasticity decreased. The temperature increase generated by the first compression will be dissipated with time to the die and other parts of the Simulator which act as a heat sink. The rate of this heat transfer will be dependent on the specific heat and thermal conductivity of the formulation. Armstrong *et al* (1982) increased the time between multiple compressions from 1.3s to 1.5, and 20min in order to allow the elevated temperatures within the tablet to dissipate. As the second compression in this investigation occurs only 0.272s after the first compression, the temperature of tablet will remain elevated until the start of the second compression. The recompression of this warm, more ductile material would be expected to produce further plastic deformation and stress relaxation to produce stronger tablets. This process could contribute to the increase in strength seen earlier between single and double compressions of the same pressure. It would also be expected to influence the strength of all of the tablets prepared by multiple compression depending on the magnitude and orientation of the pre and main-compression pressures. The greater the pre-compression pressure the greater the effect.

If the orientation of the pre and main compression pressures are considered as shown in FIG 8.1f it can be seen that the orientation is significant. For example if we consider a pre-compression pressure of 80MPa and a main-compression pressure of 240MPa then the tensile strength of the tablet will be 1.533MPa. If we reverse the magnitude of the pre and main-compression pressures then the tensile strength increases to 1.935MPa. This is the trend for all but one combination

**FIG 81f** RADIAL TENSILE STRENGTH FOR A PARACETAMOL FORMULATION PREPARED WITH VARYING PRE AND MAIN COMPRESSION PRESSURES.



of pressures 80MPa and 400MPa which represents the largest difference between pre and main-compression pressures. The increase in tablet strength observed when using the larger compression pressure first could be a result of temperature changes within the tablet. The larger the first compression pressure the warmer and more ductile the tablet presented to the second compression. The warm ductile tablet would deform more readily increasing particle-particle contact and increasing the tablet strength. If the smaller compression pressure is used first then this effect is reduced resulting in a weaker tablet. The effects of temperature would be expected to be combined with the extent of bond disruption during the second compression.

If the greater compression pressure follows a lesser compression pressure more of the initial bonds formed will be disrupted. However if the first compression is greater, then the second smaller compression would disrupt fewer bonds forming a stronger tablet.

### Conclusions

The paracetamol granulation was found to consolidate mainly by elastic and plastic deformation at lower compression pressures and mainly by brittle fracture at higher pressures. The maximum compression pressure exerted during the tableting cycle was found to be the major factor contributing to the tensile strength of the tablets.

The use of a second compression either before or after the main compression was found to produce a significant increase in tablet tensile strength. The greater the magnitude of the second compression, the greater its effect on tensile strength. The contribution of a second compression towards the tablet tensile strength was attributed to the effective increase in dwell time it generated. The increased time of the tablet under load permitted further stress relaxation by

plastic deformation which increased the tensile strength of the tablet.

It was considered probable that some of the work done by the second compression was used for permanent deformation, bond formation and raising the temperature of the compact.

The orientation of the higher and lower compression pressures during tableting was found to influence the tablet tensile strength. Stronger tablets resulted if the greater pressure was exerted first. This was considered to be a function of temperature increases within the tablet and the disruptive effects of the second compression.

For this formulation the use of high pre and main-compression pressures would be beneficial in that more robust tablets may be manufactured. Two smaller compressions may be used in preference to a single larger compression to produce tablets of equivalent strength. This would be expected to reduce tableting machine wear.

Conclusions

A high speed hydraulic press has been developed into a computer controlled high speed compression Simulator, capable of reproducing displacement time profiles seen on any production tableting machine. The system has been validated to monitor punch displacements to  $\pm 12\mu\text{m}$  and loads to  $\pm 0.05\%$  of full scale. Confidence in the results obtained using the Simulator was enforced by comparison with other operational Simulators. The established Simulator was then used to investigate the effects of compression on ibuprofen.

Ibuprofen was found to consolidate mainly by plastic deformation with a lesser contribution from the melting of asperities. A significant amount of pressure induced melting and subsequent fusion bonding occurred at higher pressures. Ibuprofen was found to be sensitive to the magnitude and rate of application of the compression pressure. The extent of plastic flow exhibited by ibuprofen during compression was found to decrease as the compression speed increased. Lamination and capping of ibuprofen compacts at high compression speeds was considered to be due to a combination of air entrapment and the inability of the compact to withstand the stresses of decompression.

When ibuprofen was mixed with a second material and compressed, the consolidation mechanism and properties of the compacts formed were found to follow a complex relationship. With respect to mean yield pressures, at low compression speeds there was a positive interaction which was explained by bonding between the ibuprofen and the microcrystalline cellulose. While at high compression speeds, there was a negative deviation from additive behaviour probably due to melting of the ibuprofen. The affinity between the two components of the mixture resulted in adhesion of the particles which reduced the extent of particle slippage and rearrangement towards a minima between

50% and 75% of ibuprofen. This became less significant as the compression speed increased. As the bonds between the ibuprofen and microcrystalline cellulose were weaker than the hydrogen bonds that would otherwise have formed between the microcrystalline cellulose particles, the tensile strength of the mixtures showed negative deviation from additive behaviour. The tensile strength of compacts prepared from the mixtures decreased with increasing compression speed due to the reduced time available for plastic flow. At higher compression speeds more energy was required to form the compacts due to the utilization of more energy to overcome the increased cohesiveness of particles that occur at higher compression speeds. The elastic recovery of compacts prepared from mixtures of these two components was found to be a balance between two factors; the strength of the bonds between the particles and secondly the elasticity of the particles. The elastic recovery increased with compression speed due to the reduced number of bonds formed which resisted the recovery.

The behaviour of ibuprofen was investigated further by the introduction of another excipient; lactose. Lactose was found to behave as a moderately hard brittle material at low compression speeds. An increase in the compression speed resulted in an apparent softening of the material and less brittle fracture. This somewhat surprising behaviour was thought due to an increase in the melting of asperities.

When the ibuprofen and lactose were mixed some deviations from additive behaviour were seen. These interactions were considered to be a balance between the plastic deformation by the ibuprofen relieving the applied load preventing the critical force required for fracture of the lactose being attained, and the lactose fragments bearing the applied load reducing plastic flow by ibuprofen. The needle shaped ibuprofen crystals tended to dictate the extent of particle

rearrangement of the mixtures. At the highest compression speed very little rearrangement occurred especially with lactose. The tensile strength of the compacts prepared from mixtures were determined by the ibuprofen present which was suggested to inhibit the formation of lactose-lactose bonds. An increase in compression speed reduced the strength of all compacts due to the disruptive effects of air escape and the inability of the weak compact to withstand the stresses imposed during rapid decompression. This reduction in strength influenced the extent of elastic recovery as with microcrystalline cellulose mixtures. Slight positive deviations towards the proportion of lactose present in the mixture and the energy required to form the compacts were seen. This effect became more significant at high compression speeds.

The Simulator was then employed to investigate different aspects of tableting machine design. The first aspect concerned the advantages or otherwise of compression to a constant load over the more traditional compression to a constant thickness. A simple ibuprofen Avicel mixture and a commercial ibuprofen formulation were selected for this part of the study.

These results indicated that tablets prepared under a constant maximum applied load, with fill weights varied over the B.P uniformity of weight limits, had relatively constant disintegration times and radial tensile strengths. This was considered an advantage over the tablets prepared to a constant thickness which showed considerable variation under the same conditions. The tablets prepared under a constant load were found to have increasing thickness with increasing fill weight. This was considered a disadvantage with regard to mechanical tablet handling and filling of containers. The tablets prepared to a constant thickness showed a similar trend to a lesser extent. This was attributed to the distortion of the machine under

load. In principle the compression to a constant load was demonstrated to be superior to compression to a constant thickness.

The second aspect of tableting machine design to be investigated was the use of relatively high precompression pressures using a commercially available paracetamol granulation. The paracetamol granulation was found to consolidate mainly by elastic and plastic deformation at lower compression pressures and mainly by brittle fracture at higher pressures. The maximum compression pressure exerted during the tableting cycle was found to be the major factor contributing to the tensile strength of the tablets. The use of a second compression either before or after the main compression was found to produce a significant increase in tablet tensile strength. The greater the magnitude of the second compression, the greater its effect on tensile strength. The contribution of a second compression towards the tablet tensile strength was attributed to the effective increase in dwell time it generated. The increased time of the tablet under load permitted further stress relaxation by plastic deformation which increased the tensile strength of the tablet. It was considered probable that some of the work done by the second compression was used for permanent deformation, bond formation and raising the temperature of the compact. The orientation of the greater and lesser compression pressures during tableting was found to influence the tablet tensile strength. Stronger tablets resulted if the greater pressure was exerted first. This was considered to be a function of temperature increases within the tablet and the disruptive effects of the second compression.

1) That the simulation of the tableting process be improved by the measurement and utilization of actual displacement-time profiles from production tableting machines. The displacement-time profile could then be modelled to produce the optimum tableting cycle. The effects of mechanically filling the die could be simulated by development of automated die filling. The effects of centrifugal force experienced by a powder on a tableting machine could be added to the Simulator.

2) That the effects of compression speed on compact properties other than those elucidated in this study be investigated. These could include changes in the density distribution, surface hardness, temperature , and acoustic emissions.

3) That the work initiated here into the effects of compression speed on mixtures be extended to include further excipients and be developed to assess real formulations.

4) That the advantages of compression to a constant load and the use of relatively high precompression be confirmed by an investigation using such machines.

5) That the use of other methods of analysis be used to further quantify the effects of compression speed. The use of power required to form compacts may provide interesting results. Such work has already been initiated using the SK&F Simulator, but a great deal more research will be required before we may confidently predict compression behaviour from this parameter.

## References

- Abu-Taleb, A.E., Aly, S.A.S., 1985, Drug Dev. & Ind. Pharm. 11 1971-1987
- Alderborn, G., Nyström, C., Pasanen, K., Duberg., 1982, J. Pharm. Pharmacol. 34 suppl. 51P
- Alderborn, G., Nyström, C., 1985, Powder Tech. 44 37-42
- Alderborn, G., 1986, Acta. Pharm. Suec. 23 60
- Alderborn, G., Börjesson, E., Glazer, M., Nyström, C., 1988, Acta. Pharm. Suec. 25 31-40
- Al-Hassani, S.T.S., Es-Saheb, M., 1984, Inst. Phys. Conf. Ser. No 70 Mech. Prop. High Rates of Strain, Oxford 421-426
- Armstrong, N.A., Griffiths, R.V., 1970, Pharm. Acta. Helv. 45 583-588
- Armstrong, N.A., Haines-Nutt, R.F., 1972, J. Pharm. Pharmacol. 24 suppl. 135P
- Armstrong, N.A., Lowndes, D.H.L., 1984, Int. Pharm. Tech. & Prod. Mfr. 5 (3) 11-14
- Armstrong, N.A., Blundell, L.P., 1985, J. Pharm. Pharmacol. 37 suppl. 28P
- Armstrong, N.A., Palfrey, L.P., 1987, J. Pharm. Pharmacol. 39 497-501
- Athy, L.F., 1930, Bull. Am. Assoc. Petrol Geologist 14 1
- Aulton, M.E., 1981, Pharm. Acta. Helv. 56 332-336
- Aulton, M.E., Tebby, H.G., White, P.J.P., 1974, J. Pharm. Pharmacol. 26 suppl. 59-60P
- Aulton, M.E., Tebby, H.G., 1975, J. Pharm. Pharmacol. 27 suppl. 4P
- Bangudu, A.B., Pilpel, N., 1984, J. Pharm. Pharmacol. 36 712-722
- Bangudu, A.B., Pilpel, N., 1985, J. Pharm. Pharmacol. 37 289-293
- Barton, D., 1978, "Investigation into Compaction of Pharmaceutical Powders". M.Sc Dissertation, University of Manchester
- Bateman, S.D., Rubinstein, M.H., 1987, J. Pharm. Pharmacol. 39 suppl. 66P
- Bhatia, R.P., Lordi, N.G., 1979, J. Pharm. Sci. 68 896-899
- Burlinson, H., 1954, J. Pharm. Pharmacol. 6 1055
- Carless, J.E., Leigh, S., 1974, J. Pharm. Pharmacol. 26 289-297
- Carstensen, J.T., Touré, 1980, Powder Technol. 26 199-204
- Chan, S.Y., Pilpel, N., Cheng, D.C.H., 1983, Powder Technol. 34 173-189
- Charlton, B., Newton, J.M., 1984, J. Pharm. Pharmacol. 36 645-651

Cheng, D.C.H., 1968, Chem.Eng.Sci. 23 1405-1420

Chowhan, Z.T., Palagyi, L., 1978, J.Pharm.Sci. 67 1385-1389

Chowhan, Z.T., 1980, J.Pharm.Sci. 69 1-4

Church, M.S., Kennerley, J.W., 1982, J.Pharm.Pharmacol. 34 suppl. 50P

Church, M.S., Kennerley, J.W., 1983, J.Pharm.Pharmacol. 35 suppl. 43P

Church, M.S., Kennerley, J.W., 1984, J.Pharm.Pharmacol. 36 suppl. 44P

Cole, E.T., Rees, J.E., Hersey, J.A., 1975, Pharm.Acta.Helv. 50 28-32

Cooper, A.R., Eaton, L.E., 1962, J.Am.Ceram.Soc. 45 97-101

Cook, G.D., Summers, M.P., 1985, J.Pharm.Pharmacol. suppl. 29P

Danielson, D.W., Morehead, W.T., Rippie, E.G., 1983, J.Pharm.Sci. 72 342-345

David, S.T., Augsburg, L.L., 1977, J.Pharm.Sci. 66 2 155-159

De Blaey, C.J., Polderman, J., 1970, Pharm.Weekblad. 105 241-250

De Blaey, C.J., Polderman, J., 1971a, Pharm.Weekblad. 106 57-65

De Blaey, C.J., van Outdshoorn, M.C.D., Polderman, J., 1971b, Pharm.Weekblad. 106 589-599

De Blaey, C.J., Weekers-Andersen, A.B., Polderman, J., 1971c, Pharm.Weekblad. 106 893

De Blaey, C.J., 1972, Pharm.Weekblad. 107 236-242

Depraetère, P., Seiller, M., Puisieux, F., 1978, International Conference on Powder Technology and Pharmacy, Basel Switzerland, "Laser Measurements of Velocities of Tablet Punches".

Doelker, E., Shotton, E., 1977, J.Pharm.Pharmacol. 29 193-198

Doelker, E., Gurny, R., Mordier, D., Hart, J.P., Rees, J.E., Aulton, M.E., 1987, Acta Pharm.Suec. 24 68

Down, G.R.B., 1983, Powder Tech. 35 167-169

Down, G.R.B., McMullen, J.N., 1983, Powder Tech. 42 169-174

Duberg, M., Nyström, C., 1985, Int.Pharm.Tech.& Prod.Mfr. 6 (2) 17-25

Duberg, M., Nyström, C., 1986, Powder Tech. 46 67-75

Eaves, T., Jones, T.M., 1971, J.Pharm.Pharmacol. 23 suppl. 259S

Ejiofor, O., Esezobo, O.E., Pilpel, N., 1986, J.Pharm.Pharmacol. 38 1-7

Esezobo, S., Pilpel, N., 1986, J.Pharm.Pharmacol. 38 409-413

Fell, J.T., Newton, J.M., 1970a, J.Pharm.Sci. 59 689-691

Fell, J.T., Newton, J.M., 1970b, J.Pharm.Pharmacol. 22 247-248

Fell, J.T., Newton, J.M., 1971, J.Pharm.Sci. 60 1866

FMC Excipients for Pharmaceutical Tablets & Capsules, 1987

Ganderton, D., 1969, J.Pharm.Pharmacol. 21 suppl.9S

German, R.M., Ham, V., 1979, Powder Technology, 22 283-285

Gerritsen, A.H., Stemerding, S., 1980, Powder Technology, 27 183-188

Gregory, H.R., 1962, Trans.Inst.Chem.Eng. 40 241-251

Griffith, A.A., 1920, The Phenomena of Rupture and Flow in Solids 163-198

Gunsel, W.C., Kanig, J.L., 1976, Theory and Practice of Industrial Pharmacy. Second Edition 321-358

Hanus, E.J., King, L.D., 1968, J.Pharm.Sci. 57 677-684

Hardman, J.S., Lilley, B.A., 1970, Nature 228 353-355

Heckel, R.W., 1961a, Trans.Met.Soc. A.I.M.E. 221 671-675

Heckel, R.W., 1961b, Trans.Met.Soc. A.I.M.E. 221 1001-1008

Heng, P.W.S., Staniforth, J.N., 1988, J.Pharm.Pharmacol. 40 360-362

Hersey, J.A., Rees, J.E., 1970, Particle Size Analysis Conference, Bradford, England

Hersey, J.A., Rees, J.E., 1971, Nature Physical science 230 96

Hersey, J.A., Cole, E.T., Rees, J.E., 1973, Proceedings of the First International Conference on the Compaction and Consolidation of Particulate Mater. 165-172

Hiestand, E.N., Smith D.P., 1984, Powder Tech. 38 145-159

Hiestand, E.N., 1985, J.Pharm.Sci. 74 768-770

Hiestand, E.N., Wells, J.E., Peot, C.B., Ochs, J.F., 1977, J.Pharm.Sci. 66 510-519

Higuchi, T., Elowe, L.N., Busse, L.W., 1954, J.Amer.Pharm.Ass.(sci.Ed) 43 685

Higuchi, T., Rao, A.N, Busse, L.W., Swintosky, J.V., 1953, J.Amer.Pharm.Ass.(sci.Ed) 42 194

Ho, A.Y.K, Greer, H., Clare, D., 1978, J.Pharm.Pharmacol. 30 suppl.95P

Ho, A.Y.K., 1986, "Time Dependent Characteristics in Tablet Compaction", PhD Thesis, University of London

Hoblitzell, J.R., Rhodes, C.T., 1986, Drug Dev.Ind.Pharm. 12 507-525

Houwink, R., 1958, Elasticity, plasticity and structure of matter. second edition. New York: Dover Publications.

Humbert-Droz, P., Gurny, R., Mordier, D., Doelker, E., 1983, Int.J.Pharm.Tech.& Prod.Mfr. 4 29-35

Hunter, B.M., 1974, J.Pharm.Pharmacol. 25 suppl. 58P

Hunter, B.M, Fisher, D.G, Pratt, R.M, Rowe, R.C., 1976, J.Pharm.Pharmacol.28 suppl. 65P

Hüttenrauch, R., 1978, Acta Pharm.Technol.suppl 6 24, 55

Ibrahim, H.G., Pisano, F., Bruno, A., 1977, J.pharm.Sci. 66 669-673

Ibrahim, H.G., 1985, J.Pharm.Sci. 74 575-577

Irono, C.I., Pilpel, N., 1982, J.Pharm.Pharmacol. 34 146-151

Jackson, I.M., 1984, "Compact Characteristics of Powder Mixtures." Ph.D Thesis Liverpool Polytechnic

Jaffe, J., Foss, N.E., 1959, J.Am.Pharm.Ass.Sci.Ed. 48 26

Järvinen, M.J., Juslin, M.J, 1974, Farm.Aikak. 83 1-8

Jayashinghe, S.S., Pilpel, N., Harwood, C.F., 1969/70, Mater.Sci.Eng 5 287-294

Jetzer, W.E., 1986a, J.Pharm.Pharmacol. 38 254-258

Jetzer, W.E., 1986b, Int.J.Pharm. 31 201-207

Jones, T.M., 1977, in . Polderman.J. (ed) Formulation and Preparation of Dosage Forms, Elsevier. Holland, 29-44

Jones, T.M., 1981, Int.J.Pharm.Tech.Prod.Mfr. 2 17-24

Kawakita, K., 1956, Science (Japan) 26 149-153

Kawakita, K., Ludde, K.H., 1970, Powder Technol. 4 61

Kendall, K., (1978), The Impossibility of Comminuting Small Particles by Compression. Nature (London). 272 710-711

Kennerley, J.W., Newton, J.M., Stanley, P., 1981, Acta.Pharm.Suec. 18 106-107

Kerridge, J.C., Newton J.M., 1986, J.Pharm.Pharmacol. 38 suppl 79P

Khan, F., Pilpel, N., 1986, Powder Tech. 48 145-150

Khan, K.A., Musikabhumma, P., Warr, J.P., 1981, Drug Dev.& Ind.Pharm. 7 525-538

Khan, K.A., Rhodes, C.T., 1975a, J.Pharm.Sci. 64 444-447

Khan, K.A., Rhodes, C.T., 1975b, Can.J.Pharm.Sci. 10 62

Khan, K.A., Rhodes, C.T., 1976, J.Pharm.Sci. 65 1835-1837

- Kitamori, N., Shimamoto, T., 1976, Chem.Pharm.Bull. 24 1789
- Kolbuszewski, J., 1950, Research (London) 3. 478-483
- Krycer, I., Pope, D.G., Hersey, J.A., 1982a, Int.J.Pharm.Tech & Prod.Mfr 3 4 93-99
- Krycer, I., Pope, D.G., Hersey, J.A., 1982b, Drug Dev.Ind.Pharm. 8 307-342
- Krycer, I., Pope, D.G., 1982, Powder Tech. 33 101-111
- Lamberson, R.L., Raynor, G.E., 1976, Man.Chem.Aerosol News June 55-61
- Lammens, R.F., Liem, T.B., Polderman, J., De Blaey, C.J., 1980, Powder tech. 26 169-185
- Lammens, R.F., Struyk, F.A., Varkevisser, F.A., Polderman, J., De Blaey, C.J., 1981, Powder Technology 28 147-165
- Lerk, C.F., Bolhuis, G.K., Boer, A.H., 1979, J.Pharm.Sci. 68 205-211
- Lerk, C.F., Zuurman, K., Kussendrager, K., 1984, J.Pharm.Pharmacol. 36 399
- Leuenerger, H., Hiestand, E., Sucker, H., 1981, Chem.Ingenieur Techn. 53 45-47
- Leuenerger, H., 1982, Int.J.Pharm. 12 41-45
- Leuenerger, H., 1985, Int.J.Pharm. 27 127-138
- Leuenerger, H., Jetzer, W.E., 1984, Powder Technology 37 209-218
- Long, W.M., Alderton, J.R., 1960, Powder Metallurgy 6 52
- Long, W.M., 1960, Powder Metallurgy 6 73-86
- Lordi, N., Shiromani, P., 1984, Drug.Dev.Ind.Pharm. 10 729
- Malamataris, S., Pilpel, N., 1981, Powder Tech. 28 35-42
- Malamataris, S., Pilpel, N., 1983, J.Pharm.Pharmacol. 35 1-6
- Mann, S.C., Bowen, D.B., Hunter, B.M., Roberts, R.J., Rowe, R.C., Tracy, R.H.T., 1981, J.Pharm.Pharmacol. 33 suppl. 25P
- Mann, S.C., Roberts, R.J., Rowe, R.C., Hunter, B.M., 1982, J.Pharm.Pharmacol. 34 suppl. 49P
- Mann S.C, Roberts R.J, Rowe R.C, Hunter B.M, Rees J.E, 1983, J.Pharm.Pharmacol. 35 suppl. 44P
- Mann, S.C., 1984, "An Investigation into Factors Effecting the Capping of Pharmaceutical Tablets.", MSc Thesis, University of Bath.
- Mann, S.C., 1987, Acta.Pharm.Suec. 24 54-55
- Marshall, K., Sixsmith, D., Stanleywood, N.G., 1972, J.Pharm.Pharmacol. 24 705-785

- Marshall, P.V., York, P., Richardson, R., 1986, J.Pharm.Pharmacol. 38 suppl. 47P
- Mashadi, A.B., Newton, J.M., 1987, J.Pharm.Pharmacol. 39 961-965
- Mendell, E.J., 1972, Manuf.Chem.Aerosol News 43 31
- Morimoto, Y., Hayashi, T., Nakanishi, A., 1984, Inst.Phys.Conf.Ser.No 70 Mech.Prop.High Rates of Strain, Oxford 427-434
- Moschos, A.E., Rees, J.E., 1985, J.Pharm.Pharmacol. 37 suppl. 32P
- Mueller, F., Caspar, U., 1984, Pharm. Ind. 46 1049-1056
- Nelson, E., Busse, L.W., Higuchi, T., 1955, J.Am.Pharm.Assoc. (Sci.Ed) 44 223-225
- Newton, J.M., Rowley, G., Fell, J.T., Peacock, D.G., Ridgway, K., 1971, J.Pharm.Pharmacol. 23 suppl. 195-201S
- Newton, J.M., Cook, D.T., Hollebbon, C.E., 1977, J.Pharm.Pharmacol. 29 247
- Nyström, C., Karehill, P.G., 1986, Powder Tech. 47 201-209
- Nyqvist, H., Nicklasson, M., 1981, Acta.Pharm.Suec. 18 305-314
- O'Neil, E., Greenwood, H.J., 1932, J.Inst.Metals, 48 47-67
- Onyekweli, A.O., Pilpel, N., 1981, J.Pharm.Pharmacol. 33 377-381
- Panaggio, A., Rhodes, C.T., Schwartz, J.B., 1984, Pharm.Acta.Helv. 59 37-39
- Patel, C.I., Staniforth, J.N., Hart, J.P., 1985, J.Pharm.Pharmacol. 37 suppl. 30P
- Patel, C.I., Staniforth, J.N., 1987, J.Pharm.Pharmacol. 39 647-650
- Pitt, K.G., Newton, J.M., Richardson, R., 1987, J.Pharm.Pharmacol. 39 suppl. 65P
- Ragnarsson, G., Sjögren, J., 1983, J.Pharm.Pharmacol. 35 201-204
- Ramaswamy, C.M., Varma, Y.B.G., Venkateswarlu, D., 1971, Chem.Eng.J. 1 168-171
- Rankell, A.S., Higuchi, T., 1968, J.Pharm.Sci. 57 574
- Rees, J.E., Hersey, J.A., Cole, E.T., 1970, J.Pharm.Pharmacol. 22 suppl. 64-69S
- Rees, J.E., Hersey, J.A., Cole, E.T., 1972, J.Pharm.Sci. 61 1313-1315
- Rees, J.E., Rue, P.J., 1978a, J.Pharm.Pharmacol. 30 601-607
- Rees, J.E., Rue, P.J., 1978b, International Conference on Powder Technology and Pharmacy, Basel Switzerland, "Time Dependent Deformation of Some Direct-Compression Tablet Excipients".

Rees, J.E., 1980, Postgraduate School on the Theory and Practice of Solid Dosage Forms and Manufacture. School of Pharmacy, University of London. 197-213

Reier, G.E., Shangraw, R.E., 1966, J.Pharm.Sci. 55 510-514

Ridgway, K., Scotton, J.B., 1970, J.Pharm.Pharmacol. 22 suppl. 24S-28S

Ridgway, K., Aulton, M.E., Rosser, 1970, J.Pharm.Pharmacol. 22 suppl. 70S-78S

Ridgway-Watt, P., 1981, J.Pharm.Pharmacol 33 suppl 114P

Ridgway-Watt, P., Rue, P.J., 1980, J.Pharm.Pharmacol 32 suppl 22P

Rippie, E.G., Danielson, D.W., 1981, J.Pharm.Sci. 70 476-482

Ritter, A., Sucker, H.B., 1980, Pharm. Tech. 4 56-65 & 128

Roberts, R.J., Rowe, R.C., 1985, J.Pharm.Pharmacol. 37 377-384

Roberts, R.J., Rowe, R.C., 1986a, J.Pharm.Pharmacol. 38 526-528

Roberts, R.J., Rowe, R.C., 1986b, J.Pharm.Pharmacol. 38 567-571

Roberts, R.J., Rowe, R.C., 1987a, Int.J.Pharm. 36 205-209

Roberts, R.J., Rowe, R.C., 1987b, Int.J.Pharm. 37 15-18

Roberts, R.J., Rowe, R.C., 1987c, Chem.Eng.Sci. 42 903-911

Roberts, R.J., Rowe, R.C., 1987d, J.Pharm.Pharmacol. 39 suppl. 70P

Rubinstein, M.H., 1976, J.Pharm.Sci 65 376-379

Sagawa, Y., Sakamoto, T., Maekawa, H., 1977, Yakuzaigaku 37 15

Sakr, F.M., Pilpel, N., 1982, Int.J.Pharm. 10 57-65

Sanyo, Y., 1977, Int.J.Powder Met.Powder.Tech. 13 81-98

Seelig, R.P., Wulff, J., 1946, Trans.Am.Min.Metall.Engr.166 492-505

Selkirk, A.B., 1985, Powder Tech. 43 285

Sheikh-Salem, M., Fell, J.T., 1981, J.Pharm.Pharmacol. 33 491-494

Shlanta, S., Milosovich, G., 1964, J.Pharm.Sci. 53 562-564

Shotton, E., Rees, J.E., 1966, J.Pharm.Pharmacol. 18 suppl. 160S

Sixsmith, D., 1980, J.Pharm.Pharmacol. 32 854-855

Sixsmith, D., 1982, J.Pharm.Pharmacol. 34 345-346

Sixsmith, D., McCluskey, D., 1981, J.Pharm.Pharmacol. 33 79-81

Skotnicky, J., 1953, Czechoslov.J.Phys. 3 225

Spriggs, R., 1961, J.Amer. Ceram.Soc. 44 628-629

- Stanley-Wood, N.G., Johansson, M.E., 1986, Acta.Pharm.Suec. 23 271-278
- Summers, M.P., Enever, R.P., Carless, J.E., 1977, J.Pharm.Sci. 66 1172-1175
- Travers, D.M., Merriman, M.P.H., 1970, J.Pharm.Pharmacol. 22suppl. 11S-16S
- Tuladhar, M.D., Carless, J.E., Summers, M.P., 1983, J.Pharm.Pharmacol. 35 269-274
- van der Watt, J.G., 1987, Int.J.Pharm. 36 51-54
- Van Kamp, H.V., Bolhuis, G.K., Lerk, C.F., 1986 Acta Pharm.Suec. 23 217-230
- Vezin, W.R., Pang, H.M., Khan, K.A., Malkowska, S., 1983, Drug Dev.Ind.Pharm. 9 1465-1474
- Vromans, H., Bolhuis, G.K., Lerk, C.F., Kussendrager, K.D., Bosch, H., 1986, Acta.Pharm.Suec, 23 231-240
- Waring, M.J., Rubinstein, M.H., Howard, J.R., (1987), Int.J.Pharm. 36 29-37
- Waring, M.J., Rubinstein, M.H., Howard, J.R., Cole, P., (1987), J.Pharm.Pharmacol. 39 suppl. 131P
- Woodhead, P.J., Newton, J.M., 1983, J.Pharm.Pharmacol. 35 133-137
- Woodhead, P.J., Chapman, S.R., Newton, J.M., 1983, J.Pharm.Pharmacol. 35 621-626
- York, P., 1978, J.Pharm.Pharmacol 30 11-14
- York, P., Pilpel, N., 1972, Mater.Sci.Eng. 9 281-291
- York, P., Pilpel, N., 1973, J.Pharm.Pharmacol 25 suppl. 1P

APPENDIX 1

SOFTWARE : Applesoft Simulator loading program

APPENDIX 2

SOFTWARE : Applesoft Simulator Control Program

```

5 HOME
20 REM BOTH STRAIGHT LINE AND SINEWAVE FACILITIES ARE AVAIL
TABLE
30 REM PROFILES MAY BE STORED AND RETRIEVED FROM DISK.
40 REM DATA POINT OUTPUT IS VIA M/C SUBROUTINE ,RATE IS US
ER DEFINABLE
50 REM EJECTION IS PROGRAM DEFINED AND IS CONTROLLED BY BA
SIC
60 REM RECOMPRESSION ,COMPRESSION WITH EJECTION ,EJECTION
,OR ZEROING
70 REM ARE AVAILABLE FROM THE DRIVER MENU
80 REM DATA TRANSFER IS ACCESSIBLE FROM THE DRIVER MENU ,I
T USES A M/C
90 REM SUBROUTINE AND SAVES DATA FROM DL902 TO DISK.
100 HIMEM: 32767
110 DIM A%(4096)
120 RECEIVE = 32768:SECT = 32882
130 KB = - 16384:KS = - 16368
150 VTAB (12): HTAB (14)
160 PRINT "PLEASE WAIT!"
170 D$ = CHR$ (4)
180 PRINT D$"BLOADMEL.OBJO"
190 PRINT D$"BLOAD BLOG.1"
200 REM *****
210 REM ***** DATA POINT SIMULATION *****
220 REM ***** FOR ESH SIMULATOR 50KN *****
230 REM ***** 3MS-1 *****
240 REM *****
250 REM ***** SETTING POKE VALUES *****
260 REM DE,DL1=DELAY
270 REM S=NUMBER OF DATA POINTS
280 REM H,M,L=HIGH,MID,LOW NIBBLE UPPER ACTUATOR
290 REM HL,ML,LL=HIGH,MID,LOW NIBBLE FOR LOWER ACTUATOR
300 REM OC,OL=UPPER,LOWER ACTUATOR ADDRESS
310 DIM W(202)
320 DIM WW(202)
330 DIM V(202)
340 DIM VV(202)
350 DE = 37001
360 DL1 = 37002
370 S = 37003
380 H = 37004
390 M = 37204
400 L = 37404
410 HL = 37604
420 ML = 37804
430 LL = 38004
440 OC = 49332
450 OL = 49336
460 PRE O: NORMAL
470 REM ***** SET OUTPUTS TO ZERO *****
480 FOR Z = 1 TO 4
490 OC = 49276 + (16 * 3) + (4 * Z)
500 VO = 0 / 12.8: POKE OC + 2,VO
510 VO = (VO - INT (VO)) * 16: POKE OC + 1,VO
520 POKE OC,VO * 16
530 POKE OC + 3,0
540 NEXT Z
550 FOR I = 1 TO 200: REM ZERO THE BINARY VALUES
560 POKE H + I - 1,0: POKE M + I - 1,0: POKE L + I - 1,0

```

```

570 POKE HL + I - 1,0: POKE ML + I - 1,0: POKE LL + I - 1,0
580 NEXT I
590 REM ***** SCREEN SET UP *****
600 HOME
610 VTAB (4)
620 ES$ = "ESH 50KN COMPACTION SIMULATOR"
630 EH$ = "*****"
640 HTAB (6)
650 PRINT ES$
660 HTAB (6)
670 PRINT EH$
680 PRINT : PRINT
690 PRINT "          MASTER MENU."
700 PRINT "          *****"
710 PRINT
720 PRINT "      1) CREATE A COMPRESSION PROFILE."
730 PRINT
740 PRINT "      2) RUN A COMPRESSION PROFILE."
750 PRINT
760 PRINT "      3) ESCAPE FROM PROGRAM."
770 PRINT
780 PRINT "      A) ABORT "
790 PRINT : PRINT
800 PRINT "      Please make your selection (1,2 or 3)"
810 GET A$
820 IF A$ = "A" THEN STOP
830 IF A$ = "1" THEN 990
840 IF A$ = "2" THEN 1920
850 IF A$ = "3" THEN 870
860 GOTO 810
870 HOME
880 HTAB (13)
890 VTAB (11)
900 PRINT "Are you sure !"
910 PRINT
920 HTAB (10)
930 FLASH
940 PRINT " PROGRAM DESTRUCT (Y/N)"
950 GET A$
960 IF A$ = "Y" THEN NEW
970 IF A$ = "N" THEN 460
980 GOTO 950
990 REM ***** CREATE A COMPRESSION PROFILE ***
1000 HOME
1010 HTAB (6)
1020 PRINT ES$
1030 HTAB (6)
1040 PRINT EH$
1050 PRINT
1060 PRINT "      CREATING A COMPRESSION PROFILE."
1070 PRINT "      *****"
1080 PRINT
1090 PRINT "Input stroke displacement MAX = 25mm."
1100 PRINT "Input '222' for straight line entry."
1110 PRINT "Input '333' for havasine curve entry."
1120 PRINT "Input '9999' to finish."
1130 PRINT
1140 N = 1
1150 UA$ = "          UPPER ACTUATOR"
1160 UU$ = "*****"
1170 PRINT UA$

```

```

1180 PRINT UU$
1190 LA$ = "                LOWER ACTUATOR"
1200 REM
1210 PRINT N")";
1220 INPUT V(N)
1230 IF V(N) = 9999 THEN V(N) = 0: GOTO 1540
1240 IF V(N) = 222 THEN 1440
1250 IF V(N) = 333 THEN 1320
1260 IF V(N) > 25 THEN 1300
1280 N = N + 1
1285 IF N > 200 THEN 1540
1290 GOTO 1200
1300 PRINT : PRINT "THE MAXIMUM VALUE IS 25mm!"
1310 GOTO 1220
1320 HTAB (7): PRINT "HAVASINE CURVE ENTRY:-"
1330 HTAB (7): PRINT "*****"
1340 INPUT "Enter the first data point ";IP
1350 INPUT "Enter the last data point ";LP
1360 INPUT "Enter first data point value ";XI
1370 INPUT "Enter peak data point value ";XL
1380 PI = 3.141592654:DP = LP - IP:VP = XL - XI:I = 0
1390 FOR N = IP TO LP
1400 V(N) = VP * SIN (I) + XI
1410 I = I + (PI / DP)
1415 IF N > 199 THEN 1540
1420 NEXT N
1430 GOTO 1150
1440 HTAB (7): PRINT "STRAIGHT LINE ENTRY:-"
1450 HTAB (7): PRINT "*****"
1460 INPUT "Enter the first data point ";IP
1470 INPUT "Enter the last data point ";LP
1480 INPUT "Enter first data point value ";V(IP)
1490 INPUT "Enter peak data point value ";V(LP)
1500 FOR N = IP + 1 TO LP
1510 V(N) = V(N - 1) + ((V(LP) - V(IP)) / (LP - IP))
1515 IF N > 199 THEN 1540
1520 NEXT N
1530 GOTO 1150
1540 V(N) = 0:N = 1
1550 PRINT LA$
1560 PRINT UU$
1570 PRINT
1580 PRINT N")";: INPUT W(N)
1590 IF W(N) = 9999 THEN 1900
1600 IF W(N) = 222 THEN 1770
1610 IF W(N) = 333 THEN 1650
1620 IF W(N) > 25 THEN 1880
1630 N = N + 1
1635 IF N > 200 THEN 1900
1640 GOTO 1580
1650 HTAB (7): PRINT "HAVASINE CURVE ENTRY:-"
1660 HTAB (7): PRINT "*****"
1670 INPUT "Enter the first data point ";IP
1680 INPUT "Enter the last data point ";LP
1690 INPUT "Enter first data point value ";YI
1700 INPUT "Enter last data point value ";YL
1710 PI = 3.141592654:DP = LP - IP:WP = YL - YI:I = 0
1720 FOR N = IP TO LP
1730 W(N) = WP * SIN (I) + YI
1740 I = I + (PI / DP)
1745 IF N > 199 THEN 1900
1750 NEXT N

```

```

1760 GOTO 1550
1770 HTAB (7): PRINT "STRAIGHT LINE ENTRY:-"
1780 HTAB (7): PRINT "*****"
1790 INPUT "Enter the first data point ";IP
1800 INPUT "Enter the last data point ";LP
1810 INPUT "Enter first data point value ";W(IP)
1820 INPUT "Enter last data point value ";W(LP)
1830 FOR N = IP + 1 TO LP
1840 W(N) = W(N - 1) + ((W(LP) - W(IP)) / (LP - IP))
1845 IF N > 199 THEN 1900
1850 NEXT N
1860 GOTO 1550
1870 GOTO 1580
1880 PRINT : PRINT " THE MAXIMUM VALUE IS 25mm!"
1890 GOTO 1580
1900 W(N) = 0
1910 N = 200
1920 HOME
1930 HTAB (6): PRINT ES$
1940 HTAB (6): PRINT EH$
1950 PRINT " CREATING A COMPRESSION PROFILE."
1960 PRINT " *****"
1970 PRINT
1980 PRINT " 1) TO REVIEW DECIMAL DATA"
1990 PRINT
2000 PRINT " 2) TO EDIT DECIMAL DATA"
2010 PRINT
2020 PRINT " 3) TO SAVE A FILE"
2030 PRINT
2040 PRINT " 4) TO LOAD A FILE"
2050 PRINT
2060 PRINT " 5) TO RUN A PROFILE"
2070 PRINT
2080 PRINT " 6) TO RETURN TO THE MASTER MENU"
2090 PRINT
2100 PRINT " 7) TO CALCULATE SPEED FROM TRACE"
2110 PRINT
2120 PRINT " Please make your selection (1-8)";
2130 GET A$
2140 IF A$ = "1" THEN 2220
2150 IF A$ = "2" THEN 2510
2160 IF A$ = "3" THEN 2820
2170 IF A$ = "4" THEN 3110
2180 IF A$ = "5" THEN 3580
2190 IF A$ = "6" THEN 590
2200 IF A$ = "7" THEN 4430
2210 GOTO 2130
2220 REM ***** REVIEW DATA *****
2230 HOME
2240 IF N < = 1 THEN 2850
2250 PRINT
2260 PRINT " REVEIHING PROFILE DATA"
2270 PRINT " *****"
2280 PRINT : PRINT
2290 PRINT "To reveiw data press 'R'"
2300 PRINT : PRINT "To return to the profile menu during
reveiw press 'P'"
2310 PRINT " UPPER LOWER"
2320 PRINT "*****"
2330 PRINT
2340 X = 0

```

```

2350 GET A$
2360 IF A$ = "R" THEN 2390
2370 IF A$ = "P" THEN 1920
2380 GOTO 2350
2390 X = X + 1
2400 PRINT "(";X;")=";V(X);
2410 HTAB (26)
2420 PRINT W(X)
2430 IF X = N THEN 2460
2440 GOTO 2350
2450 PRINT
2460 PRINT "          END OF DATA !"
2470 PRINT "To return to menu press 'P'"
2480 GET A$
2490 IF A$ = "P" THEN 1920
2500 GOTO 2480
2510 REM ***** CORRECT DATA *****
2520 REM ***** IN BASIC *****
2530 IF N < = 1 THEN 2850
2540 HOME
2550 PRINT "          EDDITING PROFILE DATA."
2560 PRINT "          *****"
2570 PRINT : PRINT
2580 PRINT "Which data point do you wish to correct?"
2590 INPUT Y
2600 IF Y > N THEN 2620
2610 GOTO 2700
2620 PRINT : PRINT "The highest value in memory is ";N
2630 PRINT "To increase this value press 'I'.          To cont
inue editing          press 'E' ."
2640 GET A$
2650 IF A$ = "E" THEN 2570
2660 IF A$ = "I" THEN 2680
2670 GOTO 2640
2680 INPUT "Please enter the new maximum value ";N
2690 GOTO 2570
2700 PRINT "The presant value of data points ";Y;" are "
2710 PRINT "UPPER :- ";V(Y);"          LOWER :- ";W(Y)
2720 PRINT "Please enter the correct values "
2730 PRINT "UPPER          LOWER "
2740 INPUT V(Y)
2750 HTAB (25)
2760 INPUT W(Y)
2770 PRINT : PRINT "Press 'C' to correct further values or
press 'R' to return to the profile menu"
2780 GET A$
2790 IF A$ = "C" THEN 2580
2800 IF A$ = "R" THEN 1920
2810 GOTO 2780
2820 REM ***** SAVING DATA ON DISK *****

2830 IF N < = 1 THEN 2850
2840 GOTO 2910
2850 HOME : VTAB (10)
2860 PRINT "          NO DATA IN MEMORY !"
2870 PRINT : PRINT "Please create a profile or load one fro
m"
2880 HTAB (18)
2890 PRINT "disk"
2900 FOR Q = 1 TO 3000: NEXT Q: GOTO 1920
2910 HOME
2920 HTAB (6): PRINT ES$

```

```

2930 HTAB (6): PRINT EH$
2940 PRINT
2950 PRINT "          SAVING DATA ON DISK"
2960 PRINT "          *****"
2970 PRINT :
2980 INPUT "What is the name of this file ?";N$
2990 VTAB (10): HTAB (10): PRINT "Saving ";N$;" on disk."
3000 PRINT D$"OPEN";N$
3010 PRINT D$"WRITE";N$
3020 PRINT N
3030 FOR Z = 1 TO 200
3040 PRINT V(Z)
3050 NEXT Z
3060 FOR Z = 1 TO 200
3070 PRINT W(Z)
3080 NEXT Z
3090 PRINT D$"CLOSE"
3100 GOTO 1920
3110 REM ***** LOAD PROFILE FROM DISK *****
**
3120 HOME
3130 HTAB (6): PRINT ES$
3140 HTAB (6): PRINT EH$
3150 PRINT
3160 PRINT "          DISK PROFILES AVAILABLE"
3170 PRINT "          *****"
3190 PRINT "          1) 0 - 0 PRE 16 - 3 MAIN."
3200 PRINT "          2) 16 - 3 PRE 16 - 3 MAIN."
3210 PRINT "          3) 16 - 3 PRE 17 - 3 MAIN."
3220 PRINT "          4) 16 - 3 PRE 18 - 3 MAIN."
3230 PRINT "          5) 16 - 3 PRE 18.2 - 3 MAIN."
3240 PRINT "          6) 16 - 3 PRE 16.2 - 3 MAIN."
3250 PRINT "          7) 16 - 3 PRE 16.7 - 3 MAIN."
3260 PRINT "          8) 16 - 3 PRE 17.7 - 3 MAIN."
3270 PRINT "          9) 16 - 3 PRE 15.8 - 3 MAIN"
3280 PRINT "          10) 16 - 3 PRE 16.5 - 3 MAIN."
3290 PRINT "          11) 16 - 3 PRE 16.9 - 3 MAIN."
3300 PRINT "          12) 16 - 3 PRE 17.5 - 3 MAIN."
3302 PRINT "          13) 16 - 3 PRE 16.1 - 3 MAIN."
3304 PRINT "          14) 16 - 3 PRE 17.2 - 3 MAIN."
3306 PRINT "          15) 16 - 3 PRE 17.1 - 3 MAIN."
3308 PRINT "          16) 16 - 3 PRE 15.5 - 3 MAIN."
3309 PRINT "          17) 16 - 3 PRE - 3 MAIN."
3310 PRINT "Please select the option required ";
3320 INPUT N
3330 IF N = 1 THEN N$ = "PRE1": GOTO 3450
3340 IF N = 2 THEN N$ = "PRE2": GOTO 3450
3350 IF N = 3 THEN N$ = "PRE3": GOTO 3450
3360 IF N = 4 THEN N$ = "PRE4": GOTO 3450
3370 IF N = 5 THEN N$ = "PRE5": GOTO 3450
3380 IF N = 6 THEN N$ = "PRE6": GOTO 3450
3390 IF N = 7 THEN N$ = "PRE7": GOTO 3450
3400 IF N = 8 THEN N$ = "PRE8": GOTO 3450
3410 IF N = 9 THEN N$ = "PRE9": GOTO 3450
3415 IF N = 10 THEN N$ = "PRE10": GOTO 3450
3418 IF N = 11 THEN N$ = "PRE11": GOTO 3450
3420 IF N = 12 THEN N$ = "PRE12": GOTO 3450
3422 IF N = 13 THEN N$ = "PRE13": GOTO 3450
3424 IF N = 14 THEN N$ = "PRE14": GOTO 3450
3426 IF N = 15 THEN N$ = "PRE15": GOTO 3450
3428 IF N = 16 THEN N$ = "PRE16": GOTO 3450
3429 IF N = 17 THEN N$ = "PRE17": GOTO 3450

```

```

3430 GOTO 3320
3440 PRINT : PRINT "      NOT AVAILABLE PLEASE RESELECT ": F
OR E = 1 TO 1000: NEXT E: GOTO 3110
3450 HTAB (8): PRINT "Loading ";N$;" from disk."
3460 D$ = CHR$ (4)
3470 PRINT D$"OPEN";N$
3480 PRINT D$"READ";N$
3490 INPUT N
3500 FOR Z = 1 TO 200
3510 INPUT V(Z)
3520 NEXT Z
3530 FOR Z = 1 TO 200
3540 INPUT W(Z)
3550 NEXT Z
3560 PRINT D$"CLOSE"
3570 GOTO 1920
3580 REM *****
3590 GOTO 3740
3600 REM ***** PRINT OUT DATA POINTS *****
3610 PRE 1
3620 PRINT "PROFILE :- ";N$: PRINT : PRINT
3630 HTAB (17): PRINT "UPPER PUNCH ";: HTAB (40): PRINT "LO
WER PUNCH"
3640 PRINT
3650 FOR RA = 1 TO 200
3660 PRINT "DATA POINT (";RA;" ) ";
3670 HTAB (19)
3680 PRINT V(RA);
3690 HTAB (40)
3700 PRINT W(RA)
3710 NEXT RA
3720 PRE 0
3730 REM ***** END OF PRINT ROUTINE *****
3740 HOME
3750 HTAB (6): PRINT ES$
3760 HTAB (6): PRINT EH$
3770 VTAB (12): HTAB (12)
3780 PRINT "Converting data "
3790 POKE S,(199 + 1)
3800 FOR I = 1 TO 200
3810 V(I) = V(I) * 4
3820 W(I) = W(I) * 4
3830 VO = V(I) / 12.8: POKE (H + I - 1),VO
3840 VO = (VO - INT (VO)) * 16: POKE (M + I - 1),VO
3850 VO = VO * 16: POKE (L + I - 1),VO
3860 VO = W(I) / 12.8: POKE (HL + I - 1),VO
3870 VO = (VO - INT (VO)) * 16: POKE (ML + I - 1),VO
3880 VO = VO * 16: POKE (LL + I - 1),VO
3890 NEXT I
3900 REM *****
3910 REM ***** SET RATE *****
3920 HOME
3930 HTAB (6)
3940 VTAB (3)
3950 PRINT "   ESH COMPACTION SIMULATOR"
3960 HTAB (6)
3970 PRINT "   *****": PRINT : PRINT
3980 IF S < = 1 THEN 2850
3990 HTAB (3)
4000 PRINT "Profile :- ";N$
4010 PRINT "   Setting compaction variables :-"
4020 PRINT

```

```

4030 PRINT "*****"
4040 PRINT : PRINT " Delay between data points (1-255)";
4050 INPUT "DELAY = ";DA
4060 DB = DA
4070 GOTO 4170
4080 REM ***** RECOMPRESSION ROUTINE *****
4090 HOME
4100 HTAB (6): PRINT ES$
4110 HTAB (6): PRINT EH$
4120 VTAB (12)
4130 HTAB (8): PRINT " Compression in progress "
4140 POKE 37001,DA
4150 POKE 37002,DB
4160 CALL 768
4170 HOME
4180 HTAB (6): PRINT ES$
4190 HTAB (6): PRINT EH$
4200 VTAB (6): HTAB (11)
4210 PRINT "Profile      :- ";N$
4220 VTAB (8): HTAB (11)
4230 PRINT "Present delay:- ";DA
4240 PRINT
4250 PRINT "To repeat cycle - - - - -press 'R'"
4260 PRINT
4270 PRINT "To compress with ejection - -press 'C'"
4280 PRINT
4290 PRINT "To reset speed- - - - -press 'S'"
4300 PRINT : PRINT "To return to menu - - - - -press 'P'"

4310 PRINT : PRINT "To return acctuators to zero press 'Z'"

4320 PRINT : PRINT "To eject tablet from -7mm - -press 'E'"

4330 PRINT : PRINT "To transfer data and store- -press 'T'"
;
4340 INPUT A$
4350 IF A$ = "P" THEN 1920
4360 IF A$ = "C" THEN 5030
4370 IF A$ = "S" THEN 3920
4380 IF A$ = "R" THEN 4080
4390 IF A$ = "Z" THEN 4720
4400 IF A$ = "E" THEN 4810
4410 IF A$ = "T" THEN GOSUB 5130: GOTO 4170
4420 GOTO 4340
4430 REM ***** SPEED CALCULATION *****
*
4440 HOME
4450 HTAB (9)
4460 PRINT "CALCULATION OF VELOCITY"
4470 HTAB (9)
4480 PRINT "*****"
4490 PRINT : PRINT "VERTICLE AXIS :- DISTANCE"
4500 PRINT "*****"
4510 INPUT "Distance travelled by actuators (mm) ";DI
4520 INPUT "What is the hieght of the trace (mm) ";TH
4530 PRINT "Each verticle mm of trace=";DI / TH" mm"
4540 PRINT : PRINT "HORIZONTAL AXIS :- TIME "
4550 PRINT "*****"
4560 INPUT "What is the length of the trace (mm)";LT
4570 INPUT "Transient setting 'A' (mS)";TA
4580 PRINT
4590 PRINT "Each horizontal mm of trace=";(2048 * TA) / LT;

```

```

"mS"
4600 PRINT : PRINT "GRADIENT OF SLOPE"
4610 PRINT "*****"
4620 INPUT "What is the triangle verticle(mm)";TV
4630 INPUT "What is the triangle horizontal(mm)";HT
4640 DD = TV * (DI / TH)
4650 TT = HT * ((TA * 2048) / LT)
4660 PRINT : HTAB (8)
4670 PRINT "SPEED=";DD / TT;" M/S"
4680 HTAB (7): PRINT "Press 'R' to return to menu.";
4690 GET A$
4700 IF A$ = "R" THEN 1920
4710 GOTO 4690
4720 REM *****ACTUATOR RETURN*****
4730 FOR Z = 1 TO 4
4740 OC = 49276 + (16 * 3) + (4 * Z)
4750 VO = 0 / 12.8: POKE OC + 2,VO
4760 VO = (VO - INT (VO)) * 16: POKE OC + 1,VO
4770 POKE OC,VO * 16
4780 POKE OC + 3,0
4790 NEXT Z
4800 GOTO 4170
4810 REM ***** EJECTION ROUTINE *****
*
4820 HOME
4830 HTAB (6): PRINT ES$
4840 HTAB (6): PRINT EH$
4850 VTAB (12)
4860 HTAB (8): PRINT " Ejection in progress "
4870 FOR YY = 1 TO 200
4880 OL = 49336
4890 FOR VJ = 0 TO 60 STEP 1
4900 EJ = VJ / 12.8: POKE OL + 2,EJ
4910 EJ = (EJ - INT (EJ)) * 16: POKE OL + 1,EJ
4920 POKE OL,EJ * 16
4930 POKE OL + 3,0
4940 NEXT VJ
4950 FOR YY = 1 TO 1000: NEXT YY
4960 FOR VJ = 60 TO 0 STEP - 1
4970 EJ = VJ / 12.8: POKE OL + 2,EJ
4980 EJ = (EJ - INT (EJ)) * 16: POKE OL + 1,EJ
4990 POKE OL,EJ * 16
5000 POKE OL + 3,0
5010 NEXT VJ
5020 GOTO 4170
5030 REM ***** COMPRESSION WITH EJECTION *****
5040 HOME
5050 HTAB (6): PRINT ES$
5060 HTAB (6): PRINT EH$
5070 VTAB (12)
5080 HTAB (8): PRINT " Compression in progress "
5090 POKE 37001,DA
5100 POKE 37002,DB
5110 CALL 768
5120 GOTO 4810
5130 REM SUBROUTINE TO RECEIVE
5140 REM DATA FROM THE LOGGER
5150 B9 = 2: REM DEFAULT OF 2 BLOCKS
5160 REM
5170 REM ARRAY
5180 REM
5190 HOME : PRINT " Data Capture to APPLE Disc"

```

```

5200 PRINT " -----"
5210 PRINT
5220 INVERSE
5230 REM AS DEFAULT SETTING
5240 HTAB 6
5250 PRINT "PROGRAM SET FOR ";B9;" BLOCK XFER"
5260 NORMAL
5270 PRINT
5280 PRINT "1 : PRINT TO SCREEN ONLY (FOR TESTING)"
5290 PRINT
5300 PRINT "2 : RECEIVE/SAVE DATA TO NEW FILE"
5310 PRINT
5320 PRINT "3 : VIEW CURRENT DATA
5330 PRINT
5340 PRINT "4 : CATALOG/FREE SECTORS"
5350 PRINT : PRINT "5 : SET SINGLE/DOUBLE BLOCK XFER"
5360 PRINT : PRINT "6 : MINIMUM MAXIMUM DATA."
5370 PRINT : PRINT "7 : RETURN TO SIMULATOR."
5380 VTAB 22: INPUT "WHICH MODE ? :";R$
5390 IF R$ = "" THEN 5380
5400 N9 = ASC (R$):N9 = N9 - 48
5410 IF N9 < 1 OR N9 > 7 THEN 5380
5420 IF N9 = 7 THEN RETURN
5430 ON N9 GOSUB 5460,5660,5840,5990,6050,6100
5440 GOTO 5190
5450 END
5460 HOME
5470 VTAB 5
5480 PRINT "TO OBTAIN DATA, PRESS RETURN"
5490 VTAB 7
5500 PRINT "ENSURE THAT BLOG.1 IS LOADED, AND"
5510 VTAB 9
5520 PRINT "THE DATA LOGGER IS CORRECTLY SET UP"
5530 VTAB 12
5540 INPUT "PRESS RETURN TO START";R$
5550 CALL RECEIVE
5560 HOME : PRINT "RECEIVING DATA..."
5570 M = 2048 * B9
5580 FOR I = 1 TO M: PRINT A%(I);" ";
5590 X = PEEK (KB): IF X > 127 THEN POKE KS,0:I = M
5600 NEXT
5610 PRINT : PRINT : PRINT
5620 PRINT "PRESS RETURN FOR MAIN MENU"
5630 INPUT "ANY KEY AND THEN RETURN TO REPEAT :";R$
5640 IF R$ = "" THEN RETURN
5650 GOTO 5460
5660 HOME : VTAB 5
5670 PRINT "DATA WILL BE SAVED TO A FILE"
5680 VTAB 7: INPUT "WHAT FILENAME ? :";NN$
5690 IF R$ = "" THEN 5680
5700 VTAB 10: INPUT "PRESS RETURN TO OBTAIN DATA ";R$
5710 CALL RECEIVE
5720 VTAB 15
5730 PRINT "SAVING TO DISC..."
5740 PRINT CHR$ (4)"OPEN";NN$
5750 PRINT CHR$ (4)"WRITE";NN$
5760 M = 2048 * B9
5770 FOR I = 1 TO M: PRINT A%(I): NEXT
5780 PRINT CHR$ (4)"CLOSE
5790 VTAB 18
5800 PRINT "PRESS RETURN FOR MAIN MENU"

```

```

5810 INPUT "ANY KEY AND THEN RETURN TO REPEAT :";R$
5820 IF R$ = "" THEN RETURN
5830 GOTO 5660
5840 HOME
5850 M = 2048 * B9
5860 VTAB 3: INPUT "START VALUE :";N1
5870 IF N1 > 2048 * B9 THEN PRINT "INVALID START VALUE": G
OTO 5860
5880 VTAB 6: INPUT "END VALUE :";N2
5890 IF N2 > M OR N2 < N1 THEN PRINT "INVALID END VALUE":
GOTO 5880
5900 FOR I = N1 TO N2 STEP 3
5910 PRINT "VAL "I"="A%(I);
5920 IF I + 1 > M THEN I = M: GOTO 5960
5930 HTAB 14: PRINT "VAL "I + 1"="A%(I + 1);
5940 IF I + 2 > M THEN I = M: GOTO 5960
5950 HTAB 28: PRINT "VAL "I + 2"="A%(I + 2)
5960 NEXT I
5970 PRINT : PRINT : INPUT "PRESS RETURN FOR MAIN MENU";R$
5980 RETURN
5990 PRINT D$"CATALOG"
6000 PRINT "THERE ARE ";
6010 CALL SECT
6020 PRINT " SECTORS FREE"
6030 PRINT : PRINT : INPUT "PRESS RETURN TO CONTINUE";R$
6040 RETURN
6050 HOME
6060 VTAB 5: PRINT "SINGLE/DOUBLE BLOCK XFER (1 OR 2)"
6070 VTAB 8: INPUT "WHICH ?";B9
6080 IF B9 < > 1 AND B9 < > 2 THEN GOTO 6070
6090 RETURN
6100 REM ***** MIN MAX *****
6110 REM SELECTS THE MINIMUM AND MAXIMUM LU FOR LOAD AND D
ISP RESPECTIVELY
6115 REM DM=MINIMUM DISPLACEMENT LU NO
6116 REM LM=MAXIMUM LOAD LU NO
6120 HOME
6130 HTAB (6)
6140 PRINT ES$
6150 HTAB (6)
6160 PRINT EH$
6162 VTAB (12): HTAB (5):
6164 PRINT " Calculating data please wait."
6170 DN = A%(5)
6180 FOR N = 5 TO 2048
6190 IF N = 2048 THEN 6240
6200 IF A%(N + 1) = < DN THEN NEXT N
6210 IF A%(N + 1) > DN THEN DN = A%(N + 1)
6220 DM = N + 1
6230 NEXT N
6240 LN = A%(2053)
6250 FOR N = 2053 TO 4095
6260 IF N = 4095 THEN 6437
6270 IF A%(N + 1) = > LN THEN NEXT N
6280 IF A%(N + 1) < LN THEN LN = A%(N + 1)
6290 LM = N + 1
6300 NEXT N
6301 GOTO 6437
6310 REM CALIBRATION
6311 PRINT
6312 INPUT "LU DISPLACEMENT REF K1: ";K1

```

```

6314 INPUT "LU DISPLACEMENT OFFSET K3: ";K3
6315 GOTO 6437
6316 INPUT "LU LOAD ZERO           K5: ";K5
6330 LET K2 = 1.59347E - 5
6350 LET K4 = 7.63E - 9
6370 LET K6 = 39.59
6380 REM LOAD
6390 L1 = (K5 - A%(DM + 2048)) * K6
6400 L2 = (K5 - A%(LM)) * K6
6410 REM DISPLACEMENT
6420 D1 = (K1 - A%(DM)) * K2 + K3 + (K4 * L1)
6430 D2 = (K1 - A%(LM - 2048)) * K2 + K3 + (K4 * L2)
6431 HOME
6432 VTAB (12)
6434 PRINT "@ Peak load : ";L2;" N AT ";D2;" M"
6435 PRINT
6436 PRINT "@ Min sep   : ";L1;" N AT ";D1;" M"
6437 REM
6438 INPUT " Enter the tablet code :- ";TC$
6440 PR# 1
6442 PRINT "*****
****": PRINT
6443 PRINT "TABLET CODE :- ";TC$: PRINT
6445 HTAB (24): PRINT "DISPLACEMENT LOAD"
6446 PRINT "@ PEAK LOAD           ";A%(LM - 2048);: HTAB
(39): PRINT A%(LM): PRINT
6447 PRINT "@ MINIMUM DISP           ";A%(DM);: HTAB (39): P
RINT A%(DM + 2048): PRINT
6448 PRINT "*****
****"
6449 GOTO 6500
6450 PRINT "PEAK LOAD= ";L2;" N AT ";D2;" M"
6460 PRINT
6470 PRINT "MIN SEP   = ";L1;" N AT ";D1;" M"
6480 PRINT
6500 PR# 0
6600 RETURN

```

### APPENDIX 3

SOFTWARE :     Machine Code Subroutine For The Simulator Control  
                  Program To Output Data points From The Apple IIe  
                  Microcomputer To The Electronic Control Console

## SOURCE FILE: MEL

9089:	1	DELO	EQU	37001
908A:	2	DEL1	EQU	37002
908B:	3	S	EQU	37003
908C:	4	H	EQU	S+1
9154:	5	M	EQU	H+200
921C:	6	L	EQU	M+200
92E4:	7	HL	EQU	L+200
93AC:	8	ML	EQU	HL+200
9474:	9	LL	EQU	ML+200
COB4:	10	OC	EQU	49332
COB8:	11	OL	EQU	49336

----- NEXT OBJECT FILE NAME IS MEL.OBJO

0300:	12		ORG	\$300
0300:18	13	START		CLC
0301:A2 00	14		LDX	£0
0303:BD 8C 90	15	LOOP	LDA	H,X
0306:8D B6 C0	16		STA	OC+2
0309:BD 54 91	17		LDA	M,X
030C:8D B5 C0	18		STA	OC+1
030F:BD 1C 92	19		LDA	L,X
0312:8D B4 C0	20		STA	OC
0315:BD E4 92	21		LDA	HL,X
0318:8D BA C0	22		STA	OL+2
031B:BD AC 93	23		LDA	ML,X
031E:8D B9 C0	24		STA	OL+1
0321:BD 74 94	25		LDA	LL,X
0324:8D B8 C0	26		STA	OL
0327:A9 00	27		LDA	£0
0329:8D BB C0	28		STA	OL+3
032C:8D B7 C0	29		STA	OC+3
032F:20 39 03	30		JSR	DLLY
0332:E8	31			INX
0333:EC 8B 90	32		CPX	S
0336:DO CB	33		BNE	LOOP
0338:60	34			RTS
0339:48	35	DLLY		PHA
033A:8A	36			TXA
033B:48	37			PHA
033C:98	38			TYA
033D:48	39			PHA
033E:AC 8A 90	40		LDY	DEL1
0341:AE 89 90	41	DL1	LDX	DELO
0344:CA	42	DL2		DEX
0345:DO FD	43		BNE	DL2
0347:88	44			DEY
0348:DO F7	45		BNE	DL1
034A:68	46			PLA
034B:A8	47			TAY
034C:68	48			PLA
034D:AA	49			TAX
034E:68	50			PLA
034F:60	51			RTS

\*\*\* SUCCESSFUL ASSEMBLY: NO ERRORS

#### APPENDIX 4

SOFTWARE : Machine Code Subroutine For The Simulator Control  
Program To Transfer Data From The Transient Recorder  
To The Apple IIe Microcomputer.

```

1 */   LOGGER LINK TO APPLE ][
2 *
3 *       VIA 6522 PARALLEL CHIP
4 *
5 * CHIP DEFINES ASSUMING SLOT 4
6 *
7 ORA      EQU   $C401      ;I/O REG A
8 ORB      EQU   $C400      ;I/O REG B
9 DDRA     EQU   $C403      ;DATA DIRECTION REGS
10 DDRB    EQU   $C402
11 ACR      EQU   $C40B      ;AUX CONTROL - NOT USED
12 IFR      EQU   $C40D      ;INTERRUPT FLAG REGISTER
13 IER      EQU   $C40E      ;INTERRUPT ENABLE REGISTER
14 *
6502      *
15 *
16 PCR      EQU   $C40C      ;NOT USED INITIALLY HERE
17 *
18 8
19 *
20 * KEYBOARD AND KEYBOARD STROBE FOR TEST PURPOSES.
21 KEY      EQU   $C000
22 KEYSTR   EQU   $C010
23 *
24 *
25 COUNT    EQU   $FE        ;USED AS POINTER FOR STORING DATA
26 *
27 *
28 *
29 *
30 CONFIG   LDA   £0          ;SET ORA FOR INPUT
31          STA   DDRA
32          TAY
33          LDA   £$FF        ;SET ORB FOR OUTPUT
34          STA   DDRB        ;USED TO RESET CB1 ONLY
35 *
36 * ADDRESS OF AZ( ) INTO COUNT
37 *
38          LDA   $6B
39          STA   COUNT
40          LDA   $6C
41          STA   COUNT+1
42 *
43 * ADD 9+1 TO POINT TO LO BYTE OF AZ(1)
44 *
45          CLC
46          LDA   COUNT        ;INTEGERS ARE STORED AS
47          ADC   £$0A        ;LO-HI,LO-HI,LO-HI ETC
48          STA   COUNT        ;AND SAVE IT BACK
49          BCC   OK1
50          INC   COUNT+1
51 *
52 * NOW REQUEST O/P BY SENDING +VE PULSE ON CB2
53 *
54 OK1      LDA   £$C0        ;1100 0000

```

```

55          STA  PCR          ;1ST SET CB2 TO LO
56 *
57 * NOW FORCE CB2 TO '1', IE +VE PULSE
58 *
59          LDA  £$F0        ;1111 0000
60 *
61 * BITS 5,6,7 FORCE CB2 TO '1'. BIT 4 ENSURES THAT
62 * A LO-HI TRANSITION ON CB1 WILL SET BIT 4 OF IFR
63 *
64 * NOW WAIT FOR RESPONSE.....
65 *
66 LOOP1    LDA  £$10        ;0001 0000
67          BIT  IFR
68          BEQ  LOOP1       ;WAIT FOR BIT 4 ON IFR
69 *
70 * THE LO-HI TRANSITION ON CB1 IS THE DIGITAL OUTPUT FLAG
71 * WHEN DETECTED, DATA IS READY TO FLOW
72 *
73          STA  ORB         ;AN ALTERNATIVE HERE IS STA IFR
74 *
75 *
76 RECBLK   LDA  £1          ;CB1 TRIGGER FLAG ON HI-LO
77          STA  PCR         ;CA1 TRIGGER FLAG ON LO-HI
78 *
79 LOOP2    LDA  £$02        ;0000 0010 :CA1 FLAG
80          BIT  IFR
81          BNE  SAVE        ;SAVE DATA
82 *
83          LDA  £$10        ;0001 0000 :CB1 FLAG
84          BIT  IFR         ;SHOWS HI-LO ON CB1
85          BNE  END         ;IF SO, END OF BLOCK
86 *
87          LDA  KEY         ;FINALLY TEST FOR KEYPRESS
88          BPL  LOOP2       ;AS A LAST RESORT
89          LDA  KEYSTR      ;RESET KB STROBE
90 *
91 END      LDA  £$C0        ;SET CB2 TO ZERO
92          STA  PCR         ;BEFORE SIGNING OFF
93          RTS            ;AND RETURN TO CALLER
94 *
95 *   THE SAVE ROUTINE
96 *
97 SAVE     LDA  ORA         ;READ PORT A
98          STA  (COUNT),Y ;AND SAVE IT
99 *
100 *
101 *
102 * NOW INCREMENT ADDRESS BY 2
103 *
104          CLC
105          LDA  COUNT
106          ADC  £2
107          STA  COUNT      ;AND SAVE IT BACK
108          BCC  OK2
109          INC  COUNT+1
110 *
111 * NOW USE PCR TO SEND WORD REQUEST ,CA1

```

```

112 * WHILE MAINTAINING BIT 0 EQUAL TO 1, AS
113 * AT THE START OF RECBLK
114 *
115 * BITS 1,2,3 SEND CA2 HI
116 *
117 OK2      LDA  £$OF      ;0000 1111
118          STA  PCR
119 *
120 * BITS 2,3 SEND CA2 LO
121 *
122          LDA  £$OD      ;0000 1101
123          STA  PCR
124          BNE  RECBLK
125 *
126 *
127 *
128 *
129 *
130 *      TAKEN FROM APPLE USER, VOL6,NO5 MAY 1986,P54
131 *      ROUTINE TO OBTAIN FREE SECTORS
132 *
133 *          APPLE DOS
134 *
135 *
136 VTOC     EQU  $B3F2
137 *
138 START    LDX  £0
139          STX  $D3
140          STX  $D4      ;INITIALISE FREE SECTOR COUNT
141          LDY  £$C8      ;LOAD OFFSET INTO VTOC
142 NXTMAP   LDA  VTOC,Y
143          BEQ  NONFR
144 AGAIN    ASL
145          BCC  AGAIN
146          PHA          ;SAVE REMAINING BIT MAP
147          INC  $D3
148          BNE  NOINC
149          INC  $D4
150 NOINC    PLA
151          BNE  AGAIN      ;IF NOT 0 GET NEXT FREE SECTOR
152 NONFR    DEY          ;DEC INDEX INTO BITMAP
153          BNE  NXTMAP
154          LDX  $D3
155          LDA  $D4
156          JSR  $ED24      ;OUTPUT FREE SECTORS AS DECIMAL
157          JSR  $DB57      ;OUTPUT LINEFEED
158          RTS

```

## APPENDIX 5

CONTROL PROFILE : An Example Of The Data Points Used To Generate A  
Displacement / Time profile With Pre and Main  
Compression.

PROFILE :- PRE5

	UPPER PUNCH	LOWER PUNCH
DATA POINT (1)	0	0
DATA POINT (2)	.636104242	.119269545
DATA POINT (3)	1.27120267	.238350501
DATA POINT (4)	1.90429107	.357054575
DATA POINT (5)	2.53436839	.475194073
DATA POINT (6)	3.16043835	.592582191
DATA POINT (7)	3.78151102	.709033316
DATA POINT (8)	4.39660433	.824363312
DATA POINT (9)	5.00474571	.938389821
DATA POINT (10)	5.60497356	1.05093254
DATA POINT (11)	6.19633879	1.16181352
DATA POINT (12)	6.77790634	1.27085744
DATA POINT (13)	7.34875664	1.37789187
DATA POINT (14)	7.90798702	1.48274757
DATA POINT (15)	8.45471326	1.58525873
DATA POINT (16)	8.98807086	1.68526329
DATA POINT (17)	9.50721647	1.78260309
DATA POINT (18)	10.0113292	1.87712423
DATA POINT (19)	10.499612	1.96867725
DATA POINT (20)	10.9712927	2.05711739
DATA POINT (21)	11.4256256	2.1423048
DATA POINT (22)	11.8618922	2.22410479
DATA POINT (23)	12.2794027	2.30238801
DATA POINT (24)	12.677497	2.37703068
DATA POINT (25)	13.0555455	2.44791478
DATA POINT (26)	13.4129505	2.51492822
DATA POINT (27)	13.7491469	2.57796504
DATA POINT (28)	14.0636031	2.63692557
DATA POINT (29)	14.3558218	2.69171658
DATA POINT (30)	14.625341	2.74225144
DATA POINT (31)	14.8717345	2.78845023
DATA POINT (32)	15.0946128	2.8302399
DATA POINT (33)	15.2936234	2.86755439
DATA POINT (34)	15.4684516	2.90033468
DATA POINT (35)	15.618821	2.92852894
DATA POINT (36)	15.7444939	2.95209261
DATA POINT (37)	15.8452715	2.9709884
DATA POINT (38)	15.9209944	2.98518645
DATA POINT (39)	15.971543	2.99466431
DATA POINT (40)	15.9968373	2.99940699
DATA POINT (41)	15.9968373	2.99940699
DATA POINT (42)	15.971543	2.99466431
DATA POINT (43)	15.9209944	2.98518645
DATA POINT (44)	15.8452715	2.9709884
DATA POINT (45)	15.7444939	2.9520926
DATA POINT (46)	15.618821	2.92852894
DATA POINT (47)	15.4684516	2.90033467
DATA POINT (48)	15.2936234	2.86755438
DATA POINT (49)	15.0946128	2.8302399
DATA POINT (50)	14.8717345	2.78845022
DATA POINT (51)	14.625341	2.74225143
DATA POINT (52)	14.3558218	2.69171658
DATA POINT (53)	14.063603	2.63692557
DATA POINT (54)	13.7491469	2.57796504
DATA POINT (55)	13.4129505	2.51492822
DATA POINT (56)	13.0555455	2.44791477

DATA POINT (57)	12.6774969	2.37703068
DATA POINT (58)	12.2794027	2.30238801
DATA POINT (59)	11.8618922	2.22410479
DATA POINT (60)	11.4256256	2.1423048
DATA POINT (61)	10.9712927	2.05711739
DATA POINT (62)	10.499612	1.96867725
DATA POINT (63)	10.0113292	1.87712423
DATA POINT (64)	9.50721648	1.78260309
DATA POINT (65)	8.98807089	1.68526329
DATA POINT (66)	8.45471328	1.58525874
DATA POINT (67)	7.90798706	1.48274757
DATA POINT (68)	7.34875668	1.37789188
DATA POINT (69)	6.77790638	1.27085745
DATA POINT (70)	6.19633885	1.16181353
DATA POINT (71)	5.60497362	1.05093255
DATA POINT (72)	5.00474578	.938389834
DATA POINT (73)	4.39660441	.824363326
DATA POINT (74)	3.7815111	.709033331
DATA POINT (75)	3.16043845	.592582208
DATA POINT (76)	2.53436849	.475194092
DATA POINT (77)	1.90429117	.357054595
DATA POINT (78)	1.27120277	.23835052
DATA POINT (79)	.636104351	.119269566
DATA POINT (80)	0	0
DATA POINT (81)	0	0
DATA POINT (82)	0	0
DATA POINT (83)	0	0
DATA POINT (84)	0	0
DATA POINT (85)	0	0
DATA POINT (86)	0	0
DATA POINT (87)	0	0
DATA POINT (88)	0	0
DATA POINT (89)	0	0
DATA POINT (90)	0	0
DATA POINT (91)	0	0
DATA POINT (92)	0	0
DATA POINT (93)	0	0
DATA POINT (94)	0	0
DATA POINT (95)	0	0
DATA POINT (96)	0	0
DATA POINT (97)	0	0
DATA POINT (98)	0	0
DATA POINT (99)	0	0
DATA POINT (100)	0	0
DATA POINT (101)	0	0
DATA POINT (102)	0	0
DATA POINT (103)	0	0
DATA POINT (104)	0	0
DATA POINT (105)	0	0
DATA POINT (106)	0	0
DATA POINT (107)	0	0
DATA POINT (108)	0	0
DATA POINT (109)	0	0
DATA POINT (110)	0	0
DATA POINT (111)	0	0
DATA POINT (112)	0	0
DATA POINT (113)	0	0
DATA POINT (114)	0	0
DATA POINT (115)	0	0
DATA POINT (116)	0	0
DATA POINT (117)	0	0
DATA POINT (118)	0	0

DATA POINT (119)	0	0
DATA POINT (120)	0	0
DATA POINT (121)	.714528647	.117779447
DATA POINT (122)	1.42795554	.235377287
DATA POINT (123)	2.13918063	.352612192
DATA POINT (124)	2.84710727	.469303395
DATA POINT (125)	3.55064386	.585270966
DATA POINT (126)	4.24870563	.700336091
DATA POINT (127)	4.94021619	.81432135
DATA POINT (128)	5.6241093	.927050983
DATA POINT (129)	6.29933044	1.03835117
DATA POINT (130)	6.96483848	1.1480503
DATA POINT (131)	7.61960724	1.25597921
DATA POINT (132)	8.2626271	1.3619715
DATA POINT (133)	8.89290661	1.46586373
DATA POINT (134)	9.50947389	1.56749569
DATA POINT (135)	10.1113782	1.6667107
DATA POINT (136)	10.6976916	1.76335576
DATA POINT (137)	11.2675099	1.85728185
DATA POINT (138)	11.8199545	1.94834414
DATA POINT (139)	12.3541736	2.03640224
DATA POINT (140)	12.8693434	2.12132034
DATA POINT (141)	13.3646697	2.20296753
DATA POINT (142)	13.8393886	2.2812179
DATA POINT (143)	14.2927681	2.35595079
DATA POINT (144)	14.7241093	2.42705098
DATA POINT (145)	15.1327469	2.49440884
DATA POINT (146)	15.518051	2.55792049
DATA POINT (147)	15.8794273	2.61748802
DATA POINT (148)	16.2163187	2.67301957
DATA POINT (149)	16.5282058	2.72442952
DATA POINT (150)	16.8146075	2.7716386
DATA POINT (151)	17.0750823	2.81457401
DATA POINT (152)	17.3092286	2.85316955
DATA POINT (153)	17.5166853	2.88736571
DATA POINT (154)	17.6971326	2.91710976
DATA POINT (155)	17.8502921	2.94235584
DATA POINT (156)	17.9759278	2.96306502
DATA POINT (157)	18.0738459	2.97920537
DATA POINT (158)	18.1438955	2.990752
DATA POINT (159)	18.1859685	2.99768711
DATA POINT (160)	18.2	3
DATA POINT (161)	18.1859685	2.99768711
DATA POINT (162)	18.1438955	2.990752
DATA POINT (163)	18.0738459	2.97920537
DATA POINT (164)	17.9759278	2.96306502
DATA POINT (165)	17.8502921	2.94235584
DATA POINT (166)	17.6971325	2.91710976
DATA POINT (167)	17.5166853	2.88736571
DATA POINT (168)	17.3092286	2.85316955
DATA POINT (169)	17.0750823	2.814574
DATA POINT (170)	16.8146075	2.77163859
DATA POINT (171)	16.5282057	2.72442952
DATA POINT (172)	16.2163187	2.67301957
DATA POINT (173)	15.8794273	2.61748802
DATA POINT (174)	15.518051	2.55792049
DATA POINT (175)	15.1327469	2.49440883
DATA POINT (176)	14.7241093	2.42705098
DATA POINT (177)	14.2927681	2.35595078
DATA POINT (178)	13.8393885	2.28121789
DATA POINT (179)	13.3646696	2.20296752

DATA POINT (180)	12.8693434	2.12132033
DATA POINT (181)	12.3541735	2.03640223
DATA POINT (182)	11.8199544	1.94834413
DATA POINT (183)	11.2675098	1.85728184
DATA POINT (184)	10.6976915	1.76335574
DATA POINT (185)	10.1113782	1.66671068
DATA POINT (186)	9.50947378	1.56749568
DATA POINT (187)	8.8929065	1.46586371
DATA POINT (188)	8.262627	1.36197148
DATA POINT (189)	7.61960713	1.25597919
DATA POINT (190)	6.96483836	1.14805028
DATA POINT (191)	6.29933032	1.03835115
DATA POINT (192)	5.62410918	.927050964
DATA POINT (193)	4.94021607	.81432133
DATA POINT (194)	4.24870549	.70033607
DATA POINT (195)	3.55064373	.585270945
DATA POINT (196)	2.84710712	.469303372
DATA POINT (197)	2.13918049	.352612169
DATA POINT (198)	1.42795539	.235377262
DATA POINT (199)	.714528498	.117779423
DATA POINT (200)	0	0

## APPENDIX 6

SOFTWARE : Control Subroutine To Execute Heckel Analysis Using The  
Minitab Spreadsheet.

```
LET C3 = (C2/(K200*((0.012714/2)*(0.012714/2)))/1000000)
LET C4 = K1/(K200 * 0.404114 * (C1 * 100))
LET C5 = LOGE (1/(1-(C4/K2)))
CHOO 20 35 C3,CORR.C5,PUT INTO C8 C9
NAME C1 'sep m'
name c2 'load KN'
NAME C3 'P MPa'
name c4 'gcm-3'
name c5 'loge'
NAME C8 'R MPa'
NAME C9 'R LOGE'
REGRESS C9 ON 1 PARAMETER C8
DESC C1-C5 C8 C9
plot c5 c3
plot c9 c8
```

## APPENDIX 7

SOFTWARE : Fortran 'Energy' program Used To Calculate The Areas  
Under The Force Displacement Curves.

c78

```
PROGRAM Energy
PARAMETER (Nmax = 2048)
REAL X(1:Nmax),Y(1:Nmax),Work(1:Nmax),Xoc(1:Nmax),Yoc(1:Nmax),
1   XCopy(1:Nmax),Xco(1:Nmax),Yco(1:Nmax)
INTEGER IP(1:Nmax),IST(1:Nmax),IND(1:Nmax),INDW(1:Nmax),
1   Nx(1:Nmax)
CHARACTER *13,Outfil
REAL K1,K2,K3,K4,K5,K6,K7
COMMON /Kvals/K1,K2,K3,K4,K5,K6,K7
5   CALL Serisk
* Data input from nominated file
10  print *
    PRINT *, '*****'

    N = 2048
    CALL DATAIN(X,Y,Nmax,n,Outfil,IP,IST)
* X range for energy loop determined
    CALL Procl(X,Y,Work,Xoc,Yoc,Xcopy,Xco,Yco,IP,IST,IND,INDW,Nx,
1     n,Nmax,nel,xa,xb,xc,xd,Iyb,Iyc,Iyd,Outfil)
    CALL Calibr(X,Y,Xco,Yco,Nmax,nel,Outfil,IP,IST)
    CALL Proc2(X,Y,Work,Xoc,Yoc,Xcopy,Xco,Yco,IP,IST,IND,INDW,Nx,
1     nel,Nmax,nel,xa,xb,xc,xd,Iyb,Iyc,Iyd,Outfil
2     ,nab,numb)
*
*   PRINT *, ' n nel nab ',n,nel,nab
*   PRINT *, ' Results in ',Outfil,' hopefully!!'
    OPEN (Unit = 31, File = Outfil, Status = 'UNKNOWN')
    CALL FILOUT(Xco,Yco,Numb,Nab,Nmax,Outfil)
    CALL Restr(Iopt)
    IF (Iopt.eq.2) THEN
* New parameters and data
        GOTO 5
    ELSEIF (Iopt.eq.3) THEN
* New data same parameters
        GOTO 10
    ENDIF
50  STOP
1000 Format('0Peak force is           ',E11.4,' at ',E11.4/
1     ' Zero force is           ',E11.4,' at ',E11.4/
2     ' Minimum punch separation is ',E11.4,' at ',E11.4)
1100 Format(I)
1200 FORMAT(' Compression energy estimate = ',E11.4,' error = ',
1     E11.4,/
2     ' Corrected energy = ',E11.4,' compression power = '
3     ,E11.4)
1300 FORMAT(' Decompression energy estimate = ',E11.4,' error = ',
1     E11.4/
2     ' Corrected energy = ',E11.4,' compression power = '
3     ,E11.4)
    END

    SUBROUTINE FILOUT(X,Y,nel,nab,nmax,Outfil)
*
* a routine to produce an output file of ordered and compressed
* data for either the full cycle, (xa,xb) or none.
*
    REAL X(1:nmax), Y(1:nmax)
    CHARACTER*13 Outfil
5   WRITE(5,1000)
    READ *,k
```

```

IF ( (1.le.k) .AND. (k.le.3) ) THEN
  IF (k.eq.1) THEN
    n = nel
  ELSEIF (k.eq.2) THEN
    n = nab
  ELSE
    n = 0
  ENDIF
ELSE
  PRINT *, 'Selected option invalid TRY AGAIN!'
  GOTO 5
ENDIF
OPEN (Unit = 31, File = Outfil, Status = 'Unknown')
DO 10 i = 1,n
  WRITE(31,*) x(i),y(i)
10 CONTINUE
CLOSE (Unit = 31)
RETURN
1000 FORMAT(/' Filing options are 1 - all, 2 - (xa,xb) 3 - none. ',
1 'Your choice is ', $)
END

```

```

SUBROUTINE SETKS(K1,K2,K3,K4,K5,K6)

```

```

*
* A routine to establish the batch and machine constants.

```

```

* Batch constants are :

```

```

* K1 Lu displacement reference

```

```

* K3 Lu displacement reference offset

```

```

* K5 Lu load 'zero'

```

```

* Machine constants are :

```

```

* K2 Lu conversion to metres

```

```

* K4 Distortion

```

```

* K6 Lu conversion to Newtons

```

```

REAL K1,K2,K3,K4,K5,K6

```

```

C K2 = 1.59347E-5

```

```

C K6 = 39.59

```

```

C K4 = 7.63E-9

```

```

RETURN

```

```

END

```

```

SUBROUTINE DATAIN(X,Y,Nmax,n,Outfil,Ip,IST)

```

```

*
* Subroutine to read all data pairs from a nominated data file.

```

```

REAL X(1:Nmax),Y(1:Nmax),Loadn

```

```

INTEGER IP(1:nmax),IST(1:nmax)

```

```

CHARACTER *4 Ext

```

```

CHARACTER*9 Dfile

```

```

CHARACTER *13 Outfil,Dfil

```

```

REAL K1,K2,K3,K4,K5,K6,K7

```

```

COMMON /Kvals/K1,K2,K3,K4,K5,K6,K7

```

```

Ext = '.Dat'

```

```

PRINT *, 'Name of data file is ? - ''e'' to stop'

```

```

* Dfile = 'GLX980T3.DAT'

```

```

READ '(A)',Dfile

```

```

IF (Dfile.EQ.'e' .OR. Dfile.EQ.'E') STOP
Dfil = Dfile//Ext
Outfil = Dfil(3:)
Print *, 'Output file name will be ', Outfil
OPEN (UNIT=30, FILE=Dfile, STATUS='OLD')
READ (30,*,END=20) (X(i),i=1,n),(Y(j),j=1,n)
*
* Data is calibrated, the first four data values are ignored.
* n is reset to be n-4!!
*
CLOSE (UNIT=30)
*
CALL SETKS(K1,K2,K3,K4,K5,K6)
CALL Findxa(X,Y,nmax,n,IP,IST,xa,Iya)
DO 40 i = Iya,n
*
Loadn = (K5 - Y(i))*K6
j = i - Iya + 1
*
Y(j) = Loadn
Y(j) = K5 - Y(i)
^
X(j) = (K1 - X(i))*K2 + K3 + K4*Loadn
X(j) = K1 - X(i)
*
PRINT *, X(j),Y(j)
40 CONTINUE
n = n - Iya + 1
*
OPEN (UNIT = 40, FILE='Data.dat', STATUS = 'unknown')
*
DO 50 i = 1,n
*
WRITE(40,*) i,Y(i),X(i)
*50 CONTINUE
*
CLOSE (UNIT=40)
RETURN
20 PRINT *, 'Data input error file end reached'
STOP
END

SUBROUTINE xrange(X,Y,IP,IST,Nmax,n,xa,xb,xc,xd,Iyb,Iyc,Iyd)
*
* Determines the x ranges from the supplied data.
*
REAL X(1:Nmax),Y(1:Nmax)
INTEGER IP(1:Nmax), IST(1:Nmax)
IFAIL = 0
CALL M0LABF(Y,1,n,IP,IST,Ifail)
IF (Ifail .NE. 0) THEN
PRINT *, 'M0labf fails in Xrange calculation'
STOP
ENDIF
* Locate Ymax
DO 10 j = 1,n
IF (IP(j).EQ.1) THEN
Iyb = j
GOTO 20
ENDIF
10 CONTINUE
20 xa = X(1)
xb = X(Iyb)
*
PRINT *, 'Maximum y at x,i: ',xb,Iyb
* Locate minimum value of x
CALL M0laaf(X,1,n,IP,IST,IFAIL)
IF (IFAIL .NE. 0) THEN
PRINT *, 'M0laaf fails in Xrange calculation'
STOP

```

```

ENDIF
DO 30 j=1,n
  IF (IP(j) .EQ. 1 ) THEN
    Iyc = j
    xc = X(Iyc)
    PRINT *, 'min x at x,i :',xc,Iyc
    *
    GOTO 40
  ENDIF
30 CONTINUE
* Locate zero value of Y
40 DO 50 j = Iyb,n
  IF (Y(j) .LE. 0) THEN
    Iyd = j

    GOTO 60
  ENDIF
50 CONTINUE
60 xd = X(Iyd)
* PRINT *, 'zero y at x,i: ',xd,Iyd
RETURN
END

SUBROUTINE Dataab(X,Xcopy,Nx,Iyb,Nmax,IND,INDW,Xoc,Yoc,Y,Nab
1
,Work)
*
* Determines the data set for the range (xa,xb).
*
REAL X(1:Nmax),Xcopy(1:Nmax),Y(1:Nmax),Work(1:Nmax)
REAL Xoc(1:Nmax),Yoc(1:Nmax)
INTEGER IND(1:Nmax), INDW(1:Nmax), Nx(1:Nmax)
CALL F01CMF(X,Iyb,Xcopy,Iyb,Iyb,1)
CALL M01AKF(Xcopy,WORK,IND,INDW,Iyb,Nmax,IFAIL)
C OPEN (UNIT = 78, FILE='xabbef.dat',STATUS = 'unknown')
C WRITE (78,1000) (i,Xcopy(i),Xcopy(i),i=1,Iyb)
1000 FORMAT (' ',I3,1x,E14.7,1x,E14.7)
IF (IFAIL.NE. 0) THEN
  PRINT *, 'M01akf fails in Dataab'
  STOP
ENDIF
Is = 0
CALL Cmpdat(Xoc,Yoc,Y,Xcopy,Nx,Iyb,Is,Nmax,Ind,Nab)
C OPEN (UNIT = 77, FILE='xaxb.dat',STATUS = 'unknown')
C WRITE (77,1000) (i,Xoc(i),Yoc(i),i=1,Nab)
C PRINT *, 'CHECK Xoc(Nab) ',Xoc(Nab),Nab,Yoc(Nab)
RETURN
END

SUBROUTINE Dataac(X,Xcopy,Nx,Iyc,Nmax,IND,INDW,IP,IST,
1
Xoc,Yoc,Y,Nab,Nbc,Nac,xb,xc,Work)
*
* Determines the data set for the range (xa,xc).
*
REAL X(1:Nmax),Xcopy(1:Nmax),Y(1:Nmax),Work(1:Nmax)
REAL Xoc(1:Nmax),Yoc(1:Nmax)
INTEGER IND(1:Nmax), INDW(1:Nmax), Nx(1:Nmax), IP(1:Nmax),
1
IST(1:Nmax)
CALL F01CMF(X,Iyc,Xcopy,Iyc,Iyc,1)
CALL M01AKF(Xcopy,WORK,IND,INDW,Iyc,Nmax,IFAIL)
IF (IFAIL.NE. 0) THEN
  PRINT *, 'M01akf fails in Dataac'

```

```

        STOP
    ENDIF
    Is = 0
    CALL Cmpdat(Xoc,Yoc,Y,Xcopy,Nx,Iyc,Is,Nmax,Ind,Nac)
    IFAIL = 0
    CALL M01ABF(Yoc,1,Nac,IP,IST,Ifail)
    IF (IFAIL.NE. 0) THEN
        PRINT *, 'M01abf fails in Dataac'
        STOP
    ENDIF
    DO 10 ij=1,Nac
        IF (IP(ij).EQ.1) THEN
            Nab = ij
            GOTO 20
        ENDIF
10    CONTINUE
20    xb = x(Nab)
    Nbc = Nac - Nab + 1
    xc = x(Nac)
    PRINT *, 'RESULTS in dataac: xb ',xb,' xc ',xc,' nab,nbc '
    C      1      ,nab,nac
    *      OPEN (UNIT = 78, FILE='xacbef.dat',STATUS = 'unknown')
    *      WRITE (78,1000) (i,Xcopy(i),Xcopy(i),i=1,Iyc)
1000    FORMAT (' ',I3,lx,E14.7,lx,E14.7)
    C      Is = 0
    C      CALL Cmpdat(Xoc,Yoc,Y,Xcopy,Nx,Iyb,Is,Nmax,Ind,Nab)
    *      OPEN (UNIT = 77, FILE='xaxc.dat',STATUS = 'unknown')
    *      WRITE (77,1000) (i,Xoc(i),Yoc(i),i=1,Nac)
    *      PRINT *, 'CHECK Xoc(Nab) ',Xoc(Nab),Nab,Yoc(Nab)
    *      PRINT *, 'CHECK Xoc(Nac) ',Xoc(Nac),Nac,Yoc(Nac)
    *      RETURN
    *      END

```

```

SUBROUTINE Cmpdat(Xoc,Yoc,Y,Xcopy,Nx,Iy,Is,Nmax,Ind,k)

```

```

*
* Routine to compress data into Xoc and Yoc
*

```

```

REAL Xoc(1:Nmax), Yoc(1:Nmax), Y(1:Nmax), Xcopy(1:Nmax)
INTEGER NX(1:Nmax), Ind(1:Nmax)
DO 10 j=1,Iy
    IF (j.EQ.1) THEN
        k=1
        Nx(1) = 1
        Xoc(1) = Xcopy(1)
        Yoc(1) = Y(IND(j) + Is)
    ELSE
        IF (Xcopy(j).EQ.Xcopy(j-1)) THEN
            Yoc(k) = Yoc(k) + Y(IND(j) + Is)
            Nx(k) = Nx(k) + 1
        ELSE
            k = k+1
            Xoc(k) = Xcopy(j)
            Nx(k) = 1
            Yoc(k) = Y(IND(j) + Is)
        ENDIF
    ENDIF
10 CONTINUE
* Data averaged
DO 20 l=1,k
    Yoc(l) = Yoc(l)/Nx(l)

```

```

20 CONTINUE
C PRINT *, 'k = ', k, ' VALUES entered'
RETURN
END

SUBROUTINE Datacd(X,Xcopy,Nx,Npts,Nmax,IND,INDW,Xoc,Yoc,Y,Ncd
1 ,Work,Iyc,Iyd)
*
* Determines data for the range (xc,xd).
*
REAL X(1:Nmax),Xcopy(1:Nmax),Y(1:Nmax),Work(1:Nmax)
REAL Xoc(1:Nmax),Yoc(1:Nmax)
INTEGER IND(1:Nmax), INDW(1:Nmax), Nx(1:Nmax)
DO 5 j=Iyc,Iyd
Xcopy(j-Iyc+1) = X(j)
CONTINUE
IFAIL = 1
CALL M01AJF(Xcopy,WORK,IND,INDW,Npts,Nmax,IFAIL)
IF (IFAIL.NE. 0) THEN
PRINT *, 'M01ajf fails in Datacd'
STOP
ENDIF
Is = Iyc-1
CALL Cmpdat(Xoc,Yoc,Y,Xcopy,Nx,Npts,Is,Nmax,Ind,Ncd)
RETURN
END

SUBROUTINE XYCOMP(X,Y,XC,YC,nmax,n,nstart,nel)
REAL X(1:nmax),Y(1:nmax),XC(1:nmax),YC(1:nmax)
*
* Routine to form a single array of compressed and ordered data.
* Contents of arrays X and Y placed in XC and YC, beginning at the
* nstart'th element.
* If nstart = 1 the whole array is stored.
*
IF (nstart.EQ.1) THEN
XC(1) = X(1)
YC(1) = Y(1)
nel = n
ELSE
nel = nstart + n - 1
ENDIF
DO 10 i = nstart+1, nstart+n-1
XC(i) = X(i - nstart + 1)
YC(i) = Y(i - nstart + 1)
10 Continue
RETURN
END

SUBROUTINE Databc(X,Xcopy,Nx,Npts,Nmax,IND,INDW,Xoc,Yoc,Y,nbc
1 ,Work,Iyb,Iyc)
*
* Determines data for the range (xb,xc).
*
REAL X(1:Nmax),Xcopy(1:Nmax),Y(1:Nmax),Work(1:Nmax)
REAL Xoc(1:Nmax),Yoc(1:Nmax)
INTEGER IND(1:Nmax), INDW(1:Nmax), Nx(1:Nmax)
DO 5 j=Iyb,Iyc
Xcopy(j-Iyb+1) = X(j)
CONTINUE
CALL M01AKF(Xcopy,WORK,IND,INDW,Npts,Nmax,IFAIL)

```

```

IF (IFAIL.NE. 0) THEN
  PRINT *, 'Molakf fails in Databc'
  STOP
ENDIF
Is = Iyb-1
CALL Cmpdat(Xoc,Yoc,Y,Xcopy,Nx,Npts,Is,Nmax,Ind,nbc)
RETURN
END

```

```

SUBROUTINE ANSWER (STRING,TRUTH)

```

```

*
* A SUBROUTINE TO ASK A QUESTION SUPPLIED IN A STRING
* AND TO OBTAIN A YES/NO RESPONSE
* THE QUESTION IS WRITTEN TO THE ASSIGNED INPUT FILE
* THE RESPONSE IS EXPECTED THROUGH THE USER'S TERMINAL

```

```

* ARGUMENTS ARE:
* STRING - A STRING OF ANY LENGTH
* TRUTH - A LOGICAL VARIABLE

```

```

LOGICAL TRUTH

```

```

CHARACTER*(*) STRING
CHARACTER*1 CHAR,YES,NO,YES2,NO2

```

```

DATA YES,YES2,NO,NO2/'Y','y','N','n'/

```

```

5 PRINT *,STRING,'? ANSWER Y/N'
  READ (5,1000) CHAR
  IF (CHAR.EQ.YES .OR. CHAR.EQ.YES2) THEN
    TRUTH = .TRUE.
    RETURN
  ELSEIF (CHAR.EQ.NO .OR. CHAR.EQ.NO2) THEN
    TRUTH = .FALSE.
    RETURN

```

```

  ELSE
    WRITE (5,1100)
    GO TO 5

```

```

  ENDIF
1000 FORMAT (A1)
1100 FORMAT (' Your response must be Y,y,N or n.'
1      ' Give your reply again')

```

```

  END
SUBROUTINE Serisk

```

```

* Routine to read the values of K1,K3 and K5 for a series calculation

```

```

*
REAL K1,K2,K3,K4,K5,K6,K7
COMMON /Kvals/K1,K2,K3,K4,K5,K6,K7
PRINT *
PRINT *, '+++++'
PRINT *, 'Enter the values of K1, K3 and K5 as prompted'
WRITE (5,1000)
* K1 = 244
  READ *,K1
  WRITE (5,1100)

```

```

*      K3 = 1.662E-3
      READ *,K3
      WRITE (5,1200)
      READ *,K5
*      K5 = 249
      WRITE (5,1300)
      READ *,K7
*      K7 = 1
      PRINT *
      RETURN
1000  Format (' Lu displacement reference           = ', '$)
1100  FORMAT (' Lu displacement reference offset (m) = ', '$)
1200  Format (' Lu load at zero                   = ', '$)
1300  Format (' Sample rate - A, time interval    = ', '$)
      END

```

```

BLOCK DATA
REAL K1,K2,K3,K4,K5,K6,K7
COMMON /Kvals/K1,K2,K3,K4,K5,K6,K7
c      DATA K2,K4,K6/3.9768E-5,0.0,198.64/
c      DATA K2,K4,K6/3.9768E-5,7.63E-9,39.59/
      DATA K2,K4,K6/1.59347E-5,7.63E-9,39.59/
      END

```

```

SUBROUTINE Findxa(X,Y,nmax,n,IP,IST,xa,Iya)

```

```

*
* A subroutine to determine the location of xa that is the latest
* X point before a positive load (Y)
*

```

```

      REAL X(1:nmax),Y(1:nmax)
      INTEGER IP(1:nmax),IST(1:nmax)
      REAL K1,K2,K3,K4,K5,K6,K7
      COMMON /Kvals/K1,K2,K3,K4,K5,K6,K7

```

```

*
* Locate minimum Y i.e. xb
*

```

```

      IFAIL = 0
      CALL M01aaf(Y,5,n,IP,IST,IFAIL)
      IF (IFAIL.NE.0) THEN

```

```

          STOP
      ENDIF
      DO 10 j=5,n
          IF(IP(j).EQ.1) THEN
              Iyb = j
              GOTO 20
          ENDIF

```

```

10      CONTINUE

```

```

*
* Locate first Y >= K5
*

```

```

20      Continue
      DO 30 j = Iyb,5,-1
          IF (Y(j).GE.K5) THEN
              Iya = j
              xa = X(Iya)
              RETURN
          ENDIF

```

```

30      CONTINUE
      PRINT *, 'No sensible xa locatable in Findxa'
      STOP
      END

```

```

SUBROUTINE TIME(point,I1,I2,x,y,Timec)
* Prints time between points
CHARACTER*(*) point
REAL K1,K2,K3,K4,K5,K6,K7
COMMON /Kvals/K1,K2,K3,K4,K5,K6,K7
Timec = K7*(I2-I1)*1E-6
Write (5,1000) point,x,y,Timec
RETURN
1000 FORMAT(' ',A,' = ',E13.7,' load = ',G13.7,' time = ',E12.5)
END

SUBROUTINE Restrtr(i)
*
* Restarting options chosen STOP, new parameters and dat or new data
* same parameters.
*
10 WRITE(5,1000)
READ *,j
IF ( (1.le.j) .AND. (j.le.3) ) THEN
  IF (i.eq.1) THEN
    STOP
  ELSE
    i = j
  ENDIF
ELSE
  PRINT *,'Response invalid, TRY AGAIN!'
  GOTO 10
ENDIF
RETURN
1000 FORMAT(/' Next case options 1 - STOP, 2 - New parameters, ',
1 '3 - data only. Option? ', $)
END

SUBROUTINE Proc2(X,Y,Work,Xoc,Yoc,Xcopy,Xco,Yco,IP,IST,IND,
1 INDW,nx,nn,Nmax,nel,xa,xb,xc,xd,Iyb,Iyc,Iyd,Outfil
2 ,nab,numb)
REAL X(1:Nmax),Y(1:Nmax),Work(1:Nmax),Xoc(1:Nmax),Yoc(1:Nmax),
1 XCopy(1:Nmax),Xco(1:Nmax),Yco(1:Nmax)
INTEG ER Nx(1:Nmax),IP(1:Nmax),IST(1:Nmax),IND(1:Nmax),
1 INDW(1:Nmax)
Character *13,Outfil
REAL K1,K2,K3,K4,K5,K6,K7
COMMON /Kvals/K1,K2,K3,K4,K5,K6,K7
n=nn
CALL Xrange(X,Y,IP,IST,Nmax,n,xa,xb,xc,xd,Iyb,Iyc,Iyd)
PRINT *
PRINT *,'Xrange answers:'
WRITE (5,*) ' xa = ',xa,' load = ',Y(1)
CALL TIME('xb',1,Iyb,xb,Y(Iyb),Tab)
CALL TIME('xc',Iyb,Iyc,xc,Y(Iyc),Timebc)
CALL TIME('xd',Iyc,Iyd,xd,Y(Iyd),Tcd)
Write (5,1000) Y(Iyb),xb,Y(Iyd),xd,Y(Iyc),xc
* Data in (xa,xb) is ordered and compressed.
CALL Dataac(X,Xcopy,Nx,Iyc,Nmax,IND,INDW,Ip,IST,
1 Xoc,Yoc,Y,Nab,Nbc,Nac,xb,xc,Work)
C CALL Dataab(X,Xcopy,Nx,Iyb,Nmax,IND,INDW,Xoc,Yoc,Y,Nab,Work)
CALL XYCOMP(Xoc,Yoc,Xco,Yco,Nmax,Nac,1,Nel)
PRINT *,'Data points in (xb,xa) = ',Nab
* PRINT *,'Data points in (xc,xa) = ',Nac

```

```

*      PRINT *, 'Data points in (xc,xb) = ', Nbc
*      WRITE (5,*) (Xoc(i),Yoc(i),i=1,Nab)
      Ifail = 0
*      Integration over (xa,xb) is performed.
      CALL D0lgaf(Xoc,Yoc,Nab,Totab,Erab,Ifail)
      IF (Ifail .ne. 0) THEN
        WRITE (5,'0Xrange answers:')
        STOP
      ENDIF
      Ttab = - Totab
      TT= Ttab + Erab
      Powrab = TT/Tab
      WRITE (5,1200) Ttab,Erab,TT,Powrab
      IF (Iyb.NE.Iyc) THEN
C
*
*      Data in (xb,xc) ordered and compressed
*
C      Np = Iyc - Iyb + 1
C      CALL Databc(X,XCopy,Nx,Np,Nmax,IND,INDW,Xoc,Yoc,Y,Nbc,Work,
C      1      Iyb,Iyc)
C      PRINT *, 'Data points in (xb,xc) = ', Nbc
C      CALL XYCOMP(Xoc,Yoc,Xco,Yco,Nmax,Nbc,Nel,Nel)
C      ENDIF
*      Data in (xc,xd) ordered and compressed.
      Np = Iyd - Iyc + 1
      IF (Y(Iyc).LT.0) RETURN
      CALL Datacd(X,Xcopy,Nx,Np,Nmax,IND,INDW,Xoc,Yoc,Y,Ncd,Work,
      1      Iyc,Iyd)
      CALL XYCOMP(Xoc,Yoc,Xco,Yco,Nmax,Ncd,Nel,Nel)
      PRINT *, 'Data points in (xc,xd) = ', Ncd
*      WRITE (5,*) (Xoc(i),Yoc(i),i=1,Ncd)
      Ifail = 0
*      Integration over (xc,xd)
      CALL D0lgaf(Xoc,Yoc,Ncd,Totcd,Erzd,Ifail)
      IF (Ifail .ne.0) THEN
        PRINT *, 'Error in D0lgaf over bd'
        STOP
      ENDIF
      Np = n - Iyd + 1
      IF (Np .NE. 1) THEN
        CALL Datacd(X,Xcopy,Nx,Np,Nmax,IND,INDW,Xoc,Yoc,Y,Nda,Work,
      1      Iyd,n)
        CALL XYCOMP(Xoc,Yoc,Xco,Yco,Nmax,Nda,Nel,Nel)
      ENDIF
      numb = nac + ncd - 1
      TT = totcd + erzd
      Powrcd = Totcd/tcd
      WRITE (5,1300) Totcd,Erzd,TT,Powrcd
      RETURN
1000  Format('0Peak force is          ',E11.4,' at ',E11.4/
      1      ' Zero force is          ',E11.4,' at ',E11.4/
      2      ' Minimum punch separation is ',E11.4,' at ',E11.4)
1100  Format(I)
1200  F'ORMAT(/' Compression energy estimate = ',E11.4,' error = ',
      1      E11.4,/
      2      ' Corrected energy = ',E11.4,' compression power = '
      3      ',E11.4)
1300  F'ORMAT(' Decompression energy estimate = ',E11.4,' error = ',
      1      E11.4/
      2      ' Corrected energy = ',E11.4,' compression power = '

```

3

,F11.4)

END

SUBROUTINE Calibr(X,Y,Xco,Yco,Nmax,n,Outfil,Ip,IST)

\*  
\* Subroutine to read all data pairs from a nominated data file.  
\*

REAL X(1:Nmax),Y(1:Nmax),Loadn,Xco(1:nmax),Yco(1:nmax)

INTEGER IP(1:nmax),IST(1:nmax)

CHARACTER \*13 Dfile,Outfil

REAL K1,K2,K3,K4,K5,K6,K7

COMMON /Kvals/K1,K2,K3,K4,K5,K6,K7

PRINT \*,'Name of data file is ? - 'e' to stop'

Dfile = 'GLX980T3.DAT'

READ \*,Dfile

IF (Dfile.EQ.'e' .OR. Dfile.EQ.'E') STOP

Outfil = Dfile(4:)

Print \*,'Output file name will be ',Outfil

OPEN (UNIT=30, FILE=Dfile, STATUS='OLD')

READ (30,\*,END=20) (X(i),i=1,n),(Y(j),j=1,n)

\* Data is calibrated, the first four data values are ignored.

\* n is reset to be n-4!!

CLOSE (UNIT=30)

CALL SETKS(K1,K2,K3,K4,K5,K6)

CALL Findxa(X,Y,nmax,n,IP,IST,xa,Iya)

Iya = 1

DO 40 i = Iya,n

Loadn = (K5 - Y(i))\*K6

Loadn = Yco(i)\*K6

j = i - Iya + 1

Y(j) = Loadn

X(j) = (K1 - X(i))\*K2 + K3 + K4\*Loadn

X(j) = Xco(i)\*K2 + K3 + K4\*Loadn

PRINT \*, X(j),Y(j)

CONTINUE

n = n - Iya + 1

OPEN (UNIT = 40, FILE='Data.dat', STATUS = 'unknown')

DO 50 i = 1,n

WRITE(40,\*) 1,Y(i),X(i)

CONTINUE

CLOSE (UNIT=40)

RETURN

PRINT \*,'Data input error file end reached'

STOP

END

SUBROUTINE Procl(X,Y,Work,Xoc,Yoc,Xcopy,Xco,Yco,IP,IST,IND,

1 INDW,nx,n,Nmax,nel,xa,xb,xc,xd,Iyb,Iyc,Iyd,Outfil)

REAL X(1:Nmax),Y(1:Nmax),Work(1:Nmax),Xoc(1:Nmax),Yoc(1:Nmax),

1 XCopy(1:Nmax),Xco(1:Nmax),Yco(1:Nmax)

INTEGER Nx(1:Nmax),IP(1:Nmax),IST(1:Nmax),IND(1:Nmax),

1 INDW(1:Nmax)

Character \*13,Outfil

REAL K1,K2,K3,K4,K5,K6,K7

COMMON /Kvals/K1,K2,K3,K4,K5,K6,K7

CALL Xrange(X,Y,IP,IST,Nmax,n,xa,xb,xc,xd,Iyb,Iyc,Iyd)

PRINT \*,'Xrange answers:'

**DAMAGED**

**TEXT**

**IN**

**ORIGINAL**

```

*      WRITE (5,*) 'i= 1', ' xa = ',xa, ' load = ',Y(1)
*      CALL TIME('xb',1,Iyb,xb,Y(Iyb),Tab)
*      CALL TIME('xc',Iyb,Iyc,xc,Y(Iyc),Timebc)
*      CALL TIME('xd',Iyc,Iyd,xd,Y(Iyd),Tcd)
*      Write (5,1000) Y(Iyb),xb,Y(Iyd),xd,Y(Iyc),xc
* Data in (xa,xb) is ordered and compressed.
*      CALL Dataac(X,Xcopy,Nx,Iyc,Nmax,IND,INDW,Ip,IST,
1          Xoc,Yoc,Y,Nab,Nbc,Nac,xb,xc,Work)
C      CALL Dataab(X,Xcopy,Nx,Iyb,Nmax,IND,INDW,Xoc,Yoc,Y,Nab,Work)
*      CALL XYCOMP(Xoc,Yoc,Xco,Yco,Nmax,Nac,1,Nel)
*      PRINT *, 'Data points in (xb,xa) = ',Nab
*      PRINT *, 'Data points in (xc,xa) = ',Nac
*      PRINT *, 'Data points in (xc,xb) = ',Nbc
*      WRITE (5,*) (Xoc(i),Yoc(i),i=1,Nab)
*      Ifail = 0
* Integration over (xa,xb) is performed.
*      CALL D01gaf(Xoc,Yoc,Nab,Totab,Erab,Ifail)
*      IF (Ifail .ne. 0) THEN
*          WRITE (5,'0Xrange answers:')
*          STOP
*      ENDIF
*      Ttab = - Totab
*      TT= Ttab + Erab
*      Powrab = TT/Tab
*      WRITE (5,1200) Ttab,Erab,TT,Powrab
C      IF (Iyb.NE.Iyc) THEN
*
* Data in (xb,xc) ordered and compressed
*
C          Np = Iyc - Iyb + 1
C          CALL Databc(X,Xcopy,Nx,Np,Nmax,IND,INDW,Xoc,Yoc,Y,Nbc,Work,
C      1          Iyb,Iyc)
C          PRINT *, 'Data points in (xb,xc) = ',Nbc
C          CALL XYCOMP(Xoc,Yoc,Xco,Yco,Nmax,Nbc,Nel,Nel)
C      ENDIF
* Data in (xc,xd) ordered and compressed.
*      Np = Iyd - Iyc + 1
*      IF (Y(Iyc).LT.0) RETURN
*      CALL Datacd(X,Xcopy,Nx,Np,Nmax,IND,INDW,Xoc,Yoc,Y,Ncd,Work,
1          Iyc,Iyd)
*      CALL XYCOMP(Xoc,Yoc,Xco,Yco,Nmax,Ncd,Nel,Nel)
*      PRINT *, 'Data points in (xc,xd) = ',Ncd
*      WRITE (5,*) (Xoc(i),Yoc(i),i=1,Ncd)
*      Ifail = 0
* Integration over (xc,xd)
*      CALL D01gaf(Xoc,Yoc,Ncd,Totcd,Er cd,Ifail)
*      IF (Ifail .ne.0) THEN
*          PRINT *, 'Error in D01gaf over bd'
*          STOP
*      ENDIF
*      Np = n - Iyd + 1
*      IF (Np .NE. 1) THEN
1          CALL Datacd(X,Xcopy,Nx,Np,Nmax,IND,INDW,Xoc,Yoc,Y,Nda,Work,
              Iyd,n)
*      CALL XYCOMP(Xoc,Yoc,Xco,Yco,Nmax,Nda,Nel,Nel)
*      ENDIF
*      TT = totcd + ercd
*      Powrcd = Totcd/tcd
*      WRITE (5,1300) Totcd,Er cd,TT,Powrcd
*      RETURN

```

```
1000   Format('0Peak force is           ',E11.4,' at ',E11.4/  
      1     ' Zero force is           ',E11.4,' at ',E11.4/  
      2     ' Minimum punch separation is ',E11.4,' at ',E11.4)  
1100   Format(I)  
1200   FORMAT(' Compression energy estimate = ',E11.4,' error = ',  
      1     E11.4,/  
      2     ' Corrected energy = ',E11.4,' compression power = '  
      3     ',E11.4)  
1300   FORMAT(' Decompression energy estimate = ',E11.4,' error = ',  
      1     E11.4/  
      2     ' Corrected energy = ',E11.4,' compression power = '  
      3     ',E11.4)  
      END
```